

3. Summary of Western North Pacific and North Indian Ocean Tropical Cyclones

3.1 Western North Pacific Ocean Tropical Cyclones

The year of 1997 was an El Niño year, and by some measures (e.g., the magnitude of the warming of the Sea Surface Temperature (SST) in the eastern equatorial Pacific), the El Niño episode of 1997 was one of the strongest in recorded history (Climate Prediction Center (CPC) 1997). El Niño had a large influence on the distribution of western North Pacific (WNP) TCs during 1997. The signature characteristics of the distribution, character and behavior of the tropical cyclones (TCs) of the WNP during 1997 (some known to be related to El Niño) include:

- (1) a very high number of super typhoons;
- (2) an early start of WNP TC activity with a higher than average number during the early season (01 January to 15 July);
- (3) a tendency -- especially during the first half of the year -- for the TC tracks to be north oriented;
- (4) a substantial eastward displacement of the mean genesis location for all TCs and for many of the individual TCs;
- (5) the formation, east of the international dateline, of two TCs which moved into the WNP and became super typhoons -- Oliwa (02C) and Paka (05C) (these are Hawaiian names given to them by the Central Pacific Hurricane Center (CPHC));
- (6) the landfall of only one TC in the Philippines;
- (7) the formation in the monsoon trough of all but one of the TCs -- (Scott (07W) formed in direct association with a cyclonic circulation (cell) in the tropical upper tropospheric trough (TUTT)); and,
- (8) the simultaneous existence in the Philippine Sea of 2 super typhoons -- Ivan (28W) and Joan (29W) -- each possessing an extreme intensity of 160 kt (82 m/sec).

Some of these unusual characteristics of the distribution and behavior of the TCs in the western North Pacific during 1997 are likely related to the large-scale atmospheric and oceanic circulation anomalies associated with 1997's strong El Niño/Southern Oscillation (ENSO) event. Of the items in this list, (2), (4) and (7) are typical features of El Niño years.

The annual number of significant TCs in the WNP during 1997 (Table 3-1) was almost normal: 33 versus the climatological average of 32 (Table 3-2). The year of 1997 included 11 super typhoons, 12 lesser typhoons, 8 tropical storms and 2 tropical depressions. The calendar-year total of 31 TCs (of at least tropical storm intensity) was one higher than the climatological average (Figure 3-1). The calendar-year total of 23 typhoons was five above the long-term average, and is the highest annual number of typhoons recorded in the WNP basin since 1971 when there were 24. The 11 super typhoons is an unprecedented value. Since 1970, as best-track wind and intensities became ever more constrained to conform to standardized TC wind-pressure relationships (e.g., Atkinson and Holiday 1977), the highest annual number of super typhoons is 7. (Figure 3-2). The high number of super typhoons in the WNP was one of the most significant highlights of 1997. The annual number of super typhoons may be weakly related to El Niño: the El Niño years of 1972, 76, 82, 87, 91, 93 and 94 had 2, 5, 5, 7, 7, 3, and 6 super typhoons respectively (for an average of 5.0); and, the La Niña years of 1973, 83, 88, 89, 95, and 96 had 3, 4, 3, 7, 5 and 6 super typhoons respectively (for an average of 4.7). A suggested physical mechanism for the increase in super typhoons during El Niño years is the longer over-water, low-latitude trajectories of the TCs which, because of El Niño, form well to the east of normal. The

annual number of super typhoons during 1997 is unprecedented, and its association with one of the strongest recorded El Niño events may be more than just a coincidence.

During the Boreal Spring of 1997, El Niño (i.e., very warm SST in the central and eastern equatorial Pacific) developed rapidly, coupled with a drop in the magnitude of the Southern Oscillation Index (Figure 3-3). Unusually persistent low-level westerly wind flow became established at low latitudes in the WNP. This westerly wind flow was also displaced eastward from its normal domain

(Figure 3-4). The set-up of low-level, low-latitude westerly wind flow early in the year led to the establishment of a near-equatorial trough across Micronesia from the western Caroline Islands eastward into the Marshall Islands. This trough supported the development of several TCs early season. According to Lander (1994), the only statistic of numbers of TCs in the WNP which is significantly correlated with any ENSO index is an increase in the number of cyclones from 01 January to 15 July.

Table 3-1 WESTERN NORTH PACIFIC SIGNIFICANT TROPICAL CYCLONES FOR 1997

TROPICAL CYCLONE	PERIOD OF WARNING	NUMBER WARNING ISSUED	ESTIMATED MAXIMUM INTENSITY KT (M/SEC)	ESTIMATED MSLP (MB)
01W TS HANNAH	19 JAN - 24 JAN	17	50 (26)	987
02W STY ISA	11 APR - 23 APR	47	145 (75)	892
03W TS JIMMY	22 APR - 25 APR	15	55 (28)	984
04W TS KELLY	07 MAY - 10 MAY	14	45 (23)	991
05W TS LEVI	25 MAY - 30 MAY	19	45 (23)	991
06W TY MARIE	26 MAY - 02 JUN	27	90 (46)	954
07W STY NESTOR	06 JUN - 15 JUN	37	140 (72)	898
08W TY OPAL	15 JUN - 21 JUN	26	90 (46)	954
09W TY PETER	23 JUN - 29 JUN	24	65 (33)	976
10W STY ROSIE	18 JUL - 28 JUL	38	140 (72)	898
11W TS SCOTT*	24-25 JUL/27-02 AUG	30	55 (28)	984
12W TY TINA	29 JUL - 09 AUG	44	90 (46)	954
13W TY VICTOR	30 JUL - 03 AUG	15	65 (33)	976
14W STY WINNIE	08 AUG - 19 AUG	44	140 (72)	898
15W TY YULE	16 AUG - 23 AUG	27	65 (33)	976
16W TD	18 AUG - 19 AUG	5	30 (15)	1000
17W TY ZITA	21 AUG - 23 AUG	10	75 (39)	967
18W TY AMBER	21 AUG - 30 AUG	36	110 (57)	933
19W STY BING	27 AUG - 05 SEP	36	135 (69)	904
20W TS CASS	28 AUG - 30 AUG	11	45 (23)	991
02C STY OLIWA#	02 SEP - 17 SEP	53(6)	140 (72)	898
21W TY DAVID	11 SEP - 20 SEP	35	95 (49)	949
22W TY FRITZ	20 SEP - 25 SEP	21	75 (39)	968
23W TS ELLA	21 SEP - 25 SEP	14	40 (21)	994
24W STY GINGER	22 SEP - 30 SEP	31	145 (75)	892
25W TS HANK	03 OCT - 04 OCT	7	40 (21)	994
26W TD	04 OCT - 07 OCT	10	30 (15)	1000
27W STY IVAN	13 OCT - 24 OCT	46	160 (82)	872
28W STY JOAN	13 OCT - 24 OCT	44	160 (82)	872
29W STY KEITH	27 OCT - 08 NOV	48	155 (80)	878
30W TY LINDA	31 OCT - 09 NOV	35	65 (33)	976
31W TY MORT	10 NOV - 16 NOV	23	65 (33)	976
05C STY PAKA#	02 DEC - 21 DEC	61(17)	160 (82)	901**
JTWC TOTAL		950		
#NPMOC TOTAL		(23)		
GRAND TOTAL		973		

* REGENERATED

** ATLANTIC INTENSITY - MSLP RELATIONSHIP USED

WARNINGS ISSUED BY NPMOC

Table 3-2 DISTRIBUTION OF WESTERN NORTH PACIFIC TROPICAL CYCLONES FOR 1959 - 1997

YEAR	JAN	FEB	MAR	APR	MAY	JUN	JUL	AUG	SEP	OCT	NOV	DEC	TOTALS
1959	0	1	1	1	0	1	3	8	9	3	2	2	31
	000	010	010	100	000	001	111	512	423	210	200	200	17 7 7
1960	1	0	1	1	1	3	3	9	5	4	1	1	30
	001	000	001	100	010	210	210	810	041	400	100	100	19 8 3
1961	1	1	1	1	4	6	5	7	6	7	2	1	42
	010	010	100	010	211	114	320	313	510	322	101	100	20 11 11
1962	0	1	0	1	3	0	8	8	7	5	4	2	39
	000	010	000	100	201	000	512	701	313	311	301	020	24 6 9
1963	0	0	1	1	0	4	5	4	4	6	0	3	28
	000	000	001	100	000	310	311	301	220	510	000	210	19 6 3
1964	0	0	0	0	3	2	8	8	8	7	6	2	44
	000	000	000	000	201	200	611	350	521	331	420	101	26 13 5
1965	2	2	1	1	2	4	6	7	9	3	2	1	40
	110	020	010	100	101	310	411	322	531	201	110	010	21 13 6
1966	0	0	0	1	2	1	4	9	10	4	5	2	38
	000	000	000	100	200	100	310	531	532	112	122	101	20 10 8
1967	1	0	2	1	1	1	8	10	8	4	4	1	41
	010	000	110	100	010	100	332	343	530	211	400	010	20 15 6
1968	0	1	0	1	0	4	3	8	4	6	4	0	31
	000	001	000	100	000	202	120	341	400	510	400	000	20 7 4
1969	1	0	1	1	0	0	3	3	6	5	2	1	23
	100	000	010	100	000	000	210	210	204	410	110	010	13 6 4
1970	0	1	0	0	0	2	3	7	4	6	4	0	27
	000	100	000	000	000	110	021	421	220	321	130	000	12 12 3
1971	1	0	1	2	5	2	8	5	7	4	2	0	37
	010	000	010	200	230	200	620	311	511	310	110	000	24 11 2
1972	1	0	1	0	0	4	5	5	6	5	2	3	32
	100	000	001	000	000	220	410	320	411	410	200	210	22 8 2
1973	0	0	0	0	0	0	7	6	3	4	3	0	23
	000	000	000	000	000	000	430	231	201	400	030	000	12 9 2
1974	1	0	1	1	1	4	5	7	5	4	4	2	35
	010	000	010	010	100	121	230	232	320	400	220	020	15 17 3
1975	1	0	0	1	0	0	1	6	5	6	3	2	25
	100	000	000	001	000	000	010	411	410	321	210	002	14 6 5
1976	1	1	0	2	2	2	4	4	5	0	2	2	25
	100	010	000	110	200	200	220	130	410	000	110	020	14 11 0
1977	0	0	1	0	1	1	4	2	5	4	2	1	21
	000	000	010	000	001	010	301	020	230	310	200	100	11 8 2
1978	1	0	0	1	0	3	4	8	4	7	4	0	32
	010	000	000	100	000	030	310	341	310	412	121	000	15 13 4
1979	1	0	1	1	2	0	5	4	6	3	2	3	28
	100	000	100	100	011	000	221	202	330	210	110	111	14 9 5
1980	0	0	1	1	4	1	5	3	7	4	1	1	28
	000	000	001	010	220	010	311	201	511	220	100	010	15 9 4
1981	0	0	1	1	1	2	5	8	4	2	3	2	29
	000	000	100	010	010	200	230	251	400	110	210	200	16 12 1
1982	0	0	3	0	1	3	4	5	6	4	1	1	28
	000	000	210	000	100	120	220	500	321	301	100	100	19 7 2
1983	0	0	0	0	0	1	3	6	3	5	5	2	25
	000	000	000	000	000	010	300	231	111	320	320	020	12 11 2
1984	0	0	0	0	0	2	5	7	4	8	3	1	30
	000	000	000	000	000	020	410	232	130	521	300	100	16 11 3
1985	2	0	0	0	1	3	1	7	5	5	1	2	27
	020	000	000	000	100	201	100	520	320	410	010	110	17 9 1
1986	0	1	0	1	2	2	2	5	2	5	4	3	27
	000	100	000	100	110	110	200	410	200	320	220	210	19 8 0
1987	1	0	0	1	0	2	4	4	7	2	3	1	25
	100	000	000	010	000	110	400	310	511	200	120	100	18 6 1
1988	1	0	0	0	1	3	2	5	8	4	2	1	27
	100	000	000	000	100	111	110	230	260	400	200	010	14 12 1
1989	1	0	0	1	2	2	6	8	4	6	3	2	35
	010	000	000	100	200	110	231	332	220	600	300	101	21 10 4
1990	1	0	0	1	2	4	4	5	5	5	4	1	31
	100	000	000	010	110	211	220	500	410	230	310	100	21 9 1
1991	0	0	2	1	1	1	4	8	6	3	6	0	32
	000	000	110	010	100	100	400	332	420	300	330	000	20 10 2

(TABLE CONTINUED ON TOP OF NEXT PAGE)

Table 3-2 (CONTINUED FROM PREVIOUS PAGE)

YEAR	JAN	FEB	MAR	APR	MAY	JUN	JUL	AUG	SEP	OCT	NOV	DEC	TOTALS
1992	1	1	0	0	0	3	4	8	5	6	5	0	33
	100	010	000	000	000	210	220	440	410	510	311	000	21 11 1
1993	0	0	2	2	1	2	5	8	5	6	4	3	38
	000	000	011	002	010	101	320	611	410	321	112	300	21 9 8
1994	1	0	1	0	2	2	9	9	8	7	0	2	41
	001	000	100	000	101	020	342	630	440	511	000	110	21 15 5
1995	1	0	0	0	1	2	3	7	7	8	2	3	34
	001	000	000	000	010	020	210	421	412	512	020	012	15 11 8
1996	0	1	0	2	2	0	7	10	7	5	6	3	43
	000	001	000	011	110	000	610	433	610	212	132	111	21 12 10
1997	1	0	0	2	3	3	4	8	4	6	1	1	33
	010	000	000	110	120	300	310	611	310	411	100	100	23 8 2
(1959-1996)													
MEAN	0.6	0.3	0.6	0.8	1.3	2.1	4.6	6.5	5.8	4.8	3.0	1.5	31.9
CASES	22	11	23	29	48	79	175	248	219	182	113	57	1206

The criteria used in TABLE 3-2 are as follows:

- 1) If a tropical cyclone was first warned on during the last two days of a particular month and continued into the next month for longer than two days, then that system was attributed to the second month.
- 2) If a tropical cyclone was warned on prior to the last two days of a month, it was attributed to the first month, regardless of how long the system lasted.
- 3) If a tropical cyclone began on the last day of the month and ended on the first day of the

next month, that system was attributed to the first month. However, if a tropical cyclone began on the last day of the month and continued into the next month for only two days, then it was attributed to the second month.

TABLE 3-2 LEGEND

Total for the month/year	→	33
Typhoons	→	23 8 2
Tropical Storms	→	
Tropical Depressions	→	

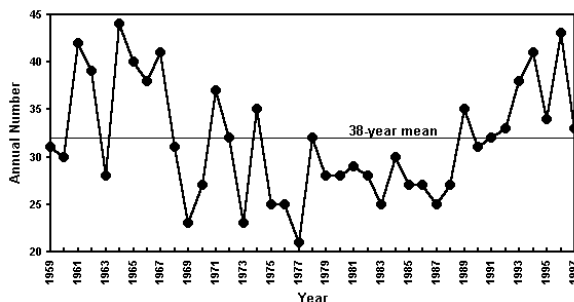


Figure 3-1 Tropical cyclones of tropical storm or greater intensity in the western North Pacific (1960-1997).

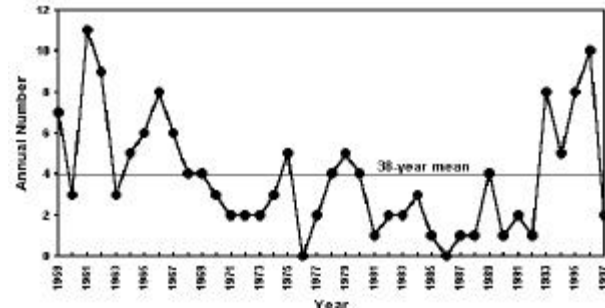


Figure 3-2 Number of western North Pacific super typhoons (1960-1997).

The annual mean genesis location of TCs which form in the WNP is related to the status of ENSO: it tends to be east of normal during El Niño years and west of normal during those years characterized by large-scale climatic anomalies opposite to those of El Niño, years known as La Niña or ENSO cold phase. Consistent with the TC distribution typically associated with El Niño (or an ENSO warm phase), the annual mean genesis location for all TCs during 1997 was substantially east of normal (Figure 3-5a). This was a pronounced

change from the TC distributions during 1995 and 1996 (both weak La Niña years) when this statistic was west of normal. A breakdown of the genesis locations of the individual WNP TCs of 1997 (Figure 3-5b) shows that most formed east of 140E. Eleven formed east of 160E, while only two -- two below normal -- formed in the South China Sea. Through the period of 1960 to 1991, the five years with the highest annual average of the Southern Oscillation Index (SOI) (i.e., 1988, 1975, 1974, 1973,

and 1971) had an average of 2.4 TCs east of 160E, and the five years with the lowest annual average SOI (i.e., 1991, 1987, 1982, 1977, and 1972) had an average of 7.4 TCs east of 160E. (Note: all El Niño years have below normal values of the SOI.) During 1996, only one TC formed within the region designated as the "El Niño" box on Figure 3-5b, while 10 TCs formed there during 1997 (including those TCs that originated east of the International Date Line).

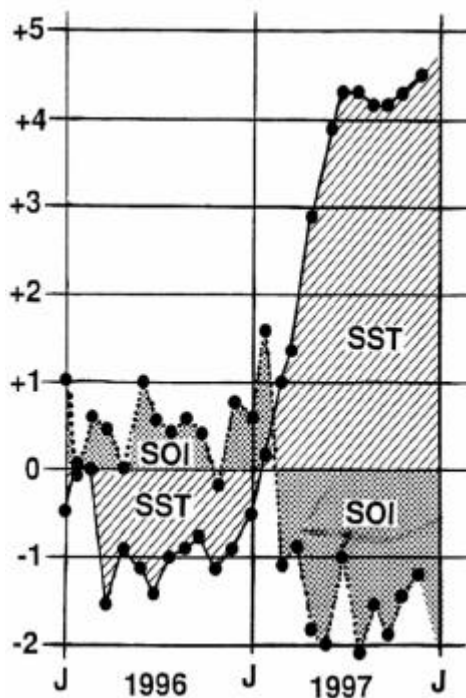


Figure 3-3 Anomalies from the monthly mean for eastern equatorial Pacific Ocean sea-surface temperature (hatched) in degrees Celsius and the Southern Oscillation Index (SOI) (shaded) for the period 1996 through 1997. (Adapted from Climate Prediction Center, 1997).

The annual number of TCs which form in this "El Niño" box has been shown by Lander (1994) to be dramatically affected by El Niño: far more TCs form within it during EL Niño years than during normal and La Niña years. Only one TC during 1997 -- Scott (07W) -- formed north of 20N in direct

association with a TUTT cell. All other TCs of 1997 formed at low latitudes in the monsoon trough. There was a tendency during 1997 for low-level monsoon winds to persist at low latitudes and for the axis of the monsoon trough to remain near 10N across Micronesia (Figure 3-6).

Low-level westerly wind anomalies persisted throughout Micronesia with the largest westerly wind anomalies located at low latitudes near and to the east of the international dateline. Corresponding anomalies in the upper troposphere consisted of easterly wind anomalies over most of the low latitudes of the WNP. These large-scale atmospheric flow-pattern anomalies of 1997 were nearly everywhere the reverse of those that persisted for most of 1995 and 1996. The atmospheric flow anomalies of 1997 over the WNP are typical of those expected during an El Niño year.

Monsoon westerlies and the axis of the monsoon trough frequently stretched across all of Micronesia as far as the international dateline (and occasionally beyond) during most of 1997. Despite the nearly continuous presence of the monsoon trough and abundant deep convection, the number of TCs (of at least tropical storm intensity) was near normal; and, compared with 1995 and 1996, the number of TCs which failed to mature and remained only at tropical depression intensity was much reduced. The TCs of 1997 tended to emerge one-by-one from the eastern portion of the basin and then recurve or move north; each subsequent development at low latitude tended to occur after the prior TC had exited the tropics; and, the TCs emerging from the eastern end of the monsoon trough tended to be large, very intense and slow-moving. There were few cases of multiple TCs (i.e., the simultaneous occurrence of two or more) in the WNP during 1997. The most noteworthy case of multiple TCs was the simultaneous formation and development in October of Ivan (28W) and Joan (29W).

These two TCs formed simultaneously along a segment of the monsoon trough axis, which stretched across the Marshall Islands and eastward beyond the international dateline. Moving west-northwestward, these two TCs intensified and, while in the Philippine Sea, they simultaneously attained an extreme intensity of 160 kt (82 m/sec) -- the first time in the JTWC archives that two TCs of such extreme intensity co-existed in the WNP. The westernmost of these TCs, Ivan (28W), was the first and only TC of 1997 to make landfall in the Philippine archipelago. It grazed the northern tip of Luzon before recurving behind Joan (29W). The low number of landfalling TCs in the Philippines and along the coast of Asia (excluding Japan) may be partly related to El Niño (e.g., Dong 1988). Despite the low number of TCs to make landfall in eastern Asia, two that did, Winnie (10W) and Linda (31W), were significant natural disasters which caused much loss of life and great destruction at their respective landfall sites in China and Vietnam. Mainland Japan, the Ryukyu Islands, the Bonin Islands, and the Mariana Islands were each affected by several typhoons. The last TC of 1997 in the WNP, Paka (05C), affected the Marshall Islands and the island of Guam and Rota.

The tracks of the TCs, which formed in the WNP during 1997, indicate a below-normal number of TCs in the South China Sea, and a below-normal number of straight-moving tracks. By contrast, there were a large number of TCs that moved northward, either on north-oriented tracks or conventional recurving tracks. Of the 33 significant TCs in the WNP during 1997, 8 (24%) were straight moving, 15 (46%) were recurvers, 6 (18%) moved on north-oriented tracks, and 4 (12%) were designated as "other".

In summary, a chronology of all the TC activity in the JTWC AOR during 1997 is provided in Figure 3-7. Composite best tracks for the WNP TCs are provided for the

periods: 01 January to 02 August (Figure 3-8a), 21 July to 22 September (Figure 3-8b), and 17 September to 22 December (Figure 3-8c). Table 3-3 includes: a climatology of typhoons, and tropical storms/typhoons for the WNP for the period 1945-1997.

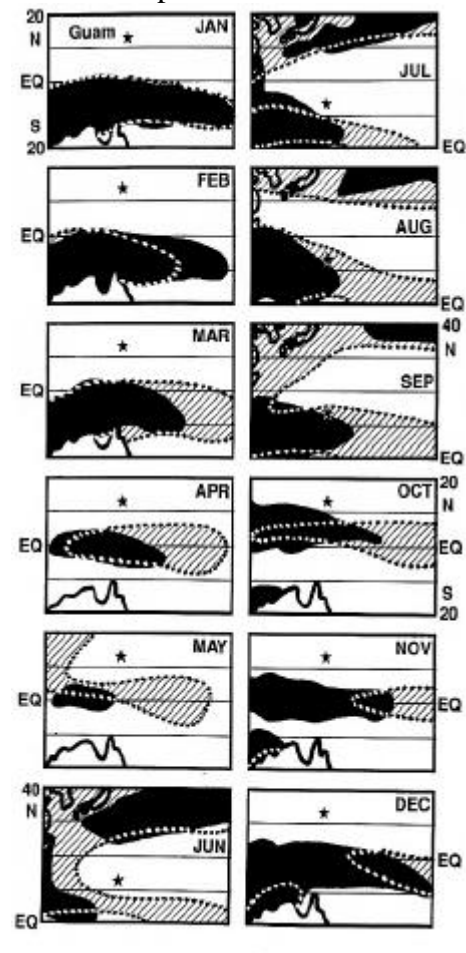


Figure 3-4 Comparison between climatological (black) and analyzed (shaded) mean monthly winds with a westerly component for the WNP in 1997. For June, July, and August the area of coverage is shifted northward to include the subtropics. For reference, the star indicates Guam's location. The outline of Australia appears in the lower left of each panel except for June, July and August where the Korean peninsula and Japan appear in the upper left. The climatology is adapted from Sadler et al. (1987). The 1997 monthly mean winds were adapted from the CPC (1997).

3.1.1 Monthly Activity Summary

JANUARY

Beginning during November of 1996, episodes of strong low-level monsoon westerlies began to occur in the low latitudes of the WNP. Most of the WNP TCs of November and December 1996 were associated with these episodes of enhanced low-level westerly wind flow. The simultaneous occurrence of TCs in the Southern Hemisphere -- some of them twins to the WNP TCs -- was a signature characteristic of the TC distribution as 1996 came to a close. Although the monsoon trough of the southern hemisphere became the dominant site of TC development by January of 1997, there were some episodes of enhanced westerly wind flow along the equator associated with a concurrent establishment of a near-equatorial trough in the WNP.

During just such time of enhanced westerly flow along the equator, the tropical disturbance which became **Hannah (01W)** formed in the near-equatorial trough south of the Marshall Islands. Moving on a long westward track for over two weeks, it reached a peak intensity of 50 kt (26m/s), and then dissipated in the Philippine Sea. Many of TCs of 1997 (including Hannah) shared the unusual characteristic of forming well to the east of normal: a typical behavior of TC's during an El Niño year. Although Tropical Storm Hannah was in most aspects relatively unremarkable, it was, in retrospect, an early manifestation of an unusual large-scale tropical circulation pattern which would see many of the TC's of 1997 form well east of normal in the Marshall Islands. We now know that the weather events over the low latitudes of the western Pacific during the late 1996 and early 1997 may be looked upon as the antecedent (or onset) conditions leading to the development of strong El Niño conditions by April of 1997. An eastward displacement

of the mean genesis location of TCs in the WNP is a hallmark signature of El Niño.

FEBRUARY

In keeping with February's climatology as the month of lowest TC frequency in the WNP, there were no significant TCs in the WNP basin during February.

MARCH

There were no significant tropical cyclones in the WNP basin during March.

APRIL

During most of April, a monsoon trough stretched across Micronesia and westerly low-level winds persisted at low latitudes. During the final week of the month, sea-level pressure fell across the eastern Caroline Islands, abundant deep convection increased, and a monsoon depression developed. This monsoon depression moved westward and became **Super Typhoon Isa (02W)** -- the first of 11 super typhoons, the most ever in a single year -- to occur in 1997. Passing to the south of Guam on 16 April, Isa produced up to 10 inches (250 mm) of rain and wind gusts to near 60 kt (31 m/sec). Moving into the Philippine Sea late in the month, the typhoon turned to the north, intensified to a super typhoon, and then recurved over water to the southeast of Japan.

As Isa was recurving, monsoon westerlies persisted in low levels of Micronesia, and extended to the international dateline. **Tropical Storm Jimmy (03W)** formed a low latitude in a near-equatorial trough which extended across the southern Marshall Islands. This small TC moved northwest and intensified, reaching a peak of 55 kt (28 m/sec) as it made a turn to the northeast. It then encountered a shear line and dissipated over water during the final week of April.

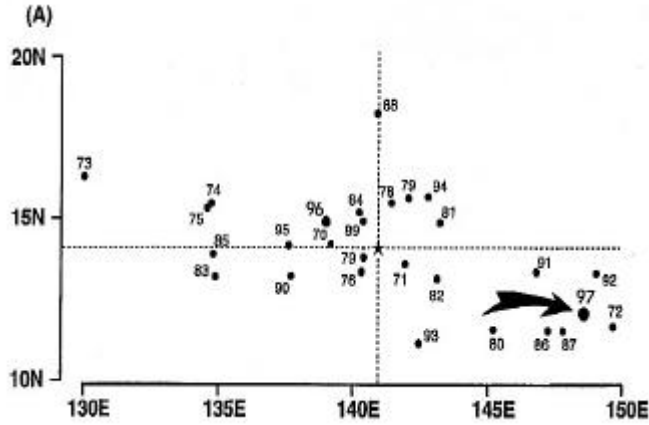


Figure 3-5a Mean annual genesis locations for the period 1970-1997. 1997's location is indicated by the arrow. The star lies at the intersection of the 28-year average latitude and longitude of genesis for statistical purposes, genesis is defined as the first 25 kt (13 m/sec) intensity on the best track.

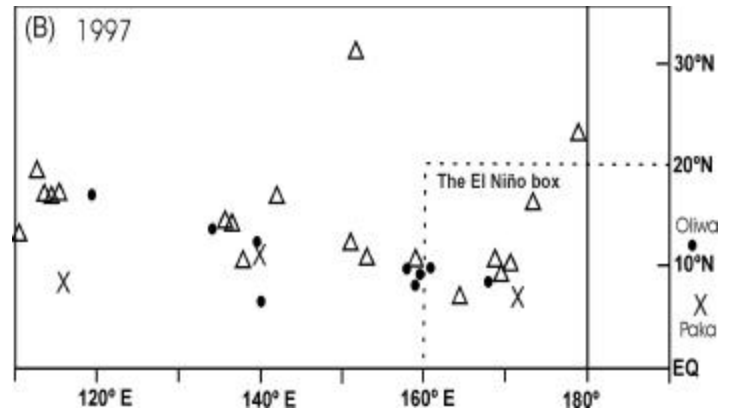


Figure 3-5b Point of formation of significant tropical cyclones in 1997 as indicated by the initial intensity of 25 kt (13 m/sec) on the best track. The symbols indicate: solid dots = 16 July to 15 October; and, X = 16 October to 31 December.

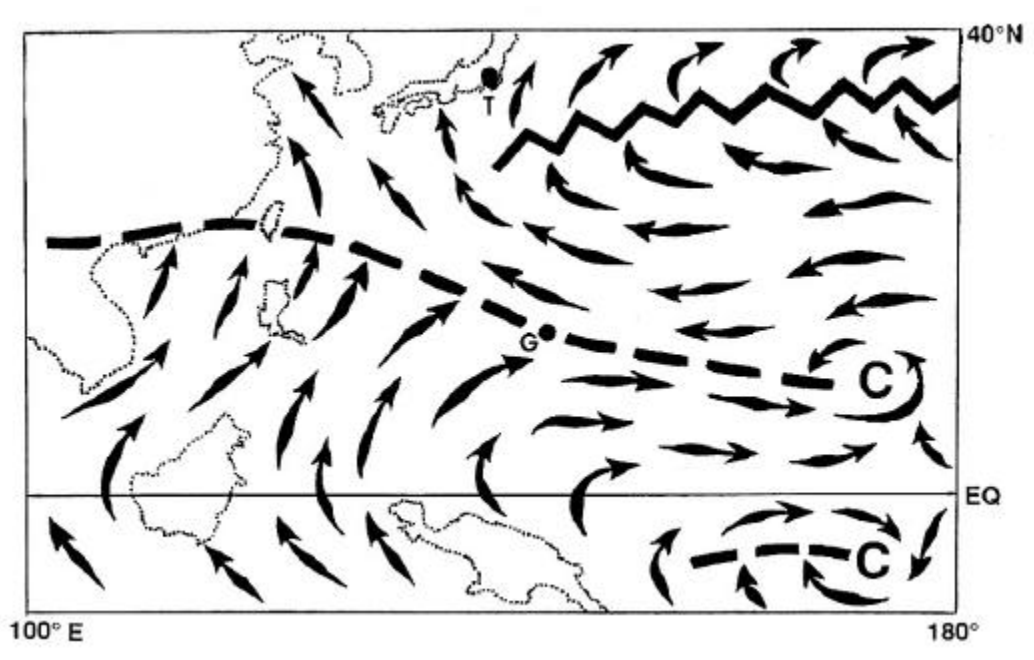


Figure 3-6 Schematic illustration of the low-level circulation pattern which dominated the WNP during August. Arrows indicate wind direction, dashed line indicates the axis of the monsoon trough, C indicates LLCCs, A= anticyclone center, G=Guam, and T=Tokyo.

MAY

As the month of May began, monsoon westerlies persisted across the low latitudes of the eastern half of Micronesia. **Tropical Storm Kelly (04W)**, like Jimmy (03W) two weeks earlier, formed at low latitude in the southern Marshall Islands. It was a relatively weak TC, which moved slowly to the northwest, then after heeling over to a faster westward track, it dissipated over water. During mid-May, the tropics of the WNP became inactive.

The next episode of TC development commenced during the final week of May when two TCs -- **Tropical Storm Levi (05W)** and **Typhoon Marie (06W)** -- formed at opposite ends of the basin: Levi in the South China Sea and Marie at low latitude near 160E. While still a depression, Levi moved eastward across Luzon where it caused severe flooding in Metro-Manila. Ivan (27W) was the only mature system to hit the Philippines. After entering the Philippine Sea, it turned to the north, reached its maximum intensity of 45 kt (23 m/sec), and eventually recurved on 28 May, merging with the Mei-Yu front south of Japan. Marie initially moved westward, then turned to the north and maintained a northward track for several days. While intensification was initially slow, Marie eventually reached a maximum intensity of 90 kt (47 m/sec). Shortly thereafter, Marie recurved and eventually became extratropical.

JUNE

Levi and Marie were still active in early June as they accelerated into midlatitudes, became extratropical, and crossed the international dateline to become mid-latitude lows northwest of Hawaii. Low-latitude monsoon westerlies continued to persist across Micronesia during June, and three TCs -- Nestor (07W), Opal (08W) and Peter (09W) -- formed in the monsoon trough.

Super Typhoon Nestor (07W) began as a monsoon depression in the Marshall Islands. It moved toward the west-northwest and slowly intensified. After becoming a tropical storm, it jogged to the north-northwest passing to the east and over the top of the Mariana Island chain. It became the second super typhoon of the season when located about 200 nm (370 km) northeast of Saipan (WMO 91232). Undergoing another synoptic-scale meander, it swung back to a northwesterly track before undergoing recurvature to the east of Japan.

As Nestor (07W) recurved, another monsoon depression -- originating in the eastern Caroline Islands -- consolidated and became **Typhoon Opal (08W)**. Opal moved on a north oriented track and began to rapidly intensify, but ran into westerly shear as it reached its maximum intensity of 90 kt (47 m/sec). It then turned to the northeast and became the first TC of the season to hit Japan, making landfall in southern Honshu. Opal then accelerated north of Tokyo, entered the Pacific Ocean, and became extratropical.

After Opal (08W) recurved, another monsoon depression, originating again in the eastern Caroline Islands, consolidated and became **Typhoon Peter (09W)**. During the last week of June, Peter approached Luzon, but then turned north and became a minimal typhoon of 65 kt (34 m/sec) as it neared the Ryukyu Island Chain. After Peter reached 30N, it turned to the northeast, made landfall in Kyushu, and traversed nearly the entire length of Honshu. Exiting Honshu and moving over water, the TC reintensified to become a typhoon once again as it passed to the south of the Kamchatka peninsula.

JULY

During the first few days of July, Typhoon Peter (09W) moved eastward at high latitude and slowly weakened. It crossed the international dateline and became a weak

extratropical low on 04 July. During the first half of July there was a break in TC activity.

There wasn't another named TC in the WNP basin until 19 July when **Super Typhoon Rosie (10W)** was upgraded from a tropical depression to a tropical storm. Rosie formed as a monsoon depression at low latitudes to the south of Guam. It moved on a north-oriented track and became the year's third super typhoon while it was moving toward the north approximately 600 nm (1110 km) east-northeast of Luzon. During the last week of July, Rosie made landfall on the south coast of Shikoku, and then passed across Honshu into the Sea of Japan where it stalled and weakened. The remnants of Rosie, drifted southeastward back across Honshu and dissipated over water southwest of Tokyo.

While most of the tropical cyclones had developed in the monsoon trough in the eastern and western parts of the basin, the birth of **Tropical Storm Scott (11W)** occurred north of 20N in direct association with a cyclonic circulation in the Tropical Upper Tropospheric Trough. As TD 11W, the system interacted with the outflow of Super Typhoon Rosie (10W), and was steered to the southeast for a few days. It eventually turned to the northwest for 24 hours, then recurved and reached its maximum intensity of 55 kt (29 m/sec). Scott spent its entire life over water.

Like so many other 1997 tropical cyclones, the disturbance that became **Typhoon Tina (12W)** developed in the El Niño-induced monsoon trough in the eastern Caroline Islands. Organization was very slow for over a week as the disturbance moved to the northwest. On 29 July, the system became TD 12W and on 05 August it reached its 90 kt (47 m/sec) maximum intensity. Tina then turned to the north, passed between Taiwan and Okinawa, made landfall in southern Korea, and dissipated in the Sea of Japan on 10 August.

As Tina was developing in the eastern part of the basin, the cloud system that became **Typhoon Victor (13W)** was consolidating together west of Luzon in the South China Sea. The system moved on a northward track and intensified slowly against northerly upper-level shear. It finally reached minimal typhoon intensity just prior to making landfall near Waglan Island, Hong Kong on 02 August.

AUGUST

August was an extremely busy with a total of ten TCs spending some part of their life in the month. As Tina (12W) and Victor (13W) were maturing in the western portion of the WNP basin, yet another monsoon depression was developing in association with El Niño-induced westerlies in the Marshall Islands. The new monsoon depression soon reached tropical storm intensity, and then intensified into **Super Typhoon Winnie (14W)**, the fourth of the eleven super typhoons. Winnie was unique in that as it moved toward Okinawa, a large rain band completely encircled the eye wall cloud, producing an outer eye wall cloud with a diameter of nearly 200 nm (370 km), one of the largest ever observed. Doppler radar at Kadena AB (Okinawa) clocked winds of 100 kt (52 m/sec) in the outer eye wall cloud. Winnie later made landfall south of Shanghai, China and dissipated rapidly. Torrential rains associated with Winnie caused considerable death and destruction in China.

As Winnie was forming its unusual concentric eye wall clouds, **Typhoon Yule (15W)** and **Tropical Depression 16 (TD 16W)** were organizing in the prolific monsoon trough that extended from east of the international dateline westward to the Caroline Islands. The disturbance that became Yule began at the extremely low latitude of 03N, while the system that became 16W started east of the Date Line. The two systems engaged in a direct interaction, with

Yule moving to the north-northeast and TD16W moving to the west. The two systems eventually merged with Yule becoming the dominant circulation. Yule briefly attained typhoon intensity, and after a long north-oriented track, it became an intense tropical-extratropical hybrid system with typhoon-force winds. The weakened system finally recurved at almost 50N.

Typhoon Zita (17W) was one of the three TCs to reach typhoon intensity in the South China Sea, and one of four TCs to develop in the monsoon trough in a 8-day period. It developed in the monsoon trough about 300 nm (560 km) to the west of Luzon and moved in a northward direction. The system rapidly moved into easterly steering flow and turned to the west. Despite its proximity to the China mainland, it intensified significantly, reaching a maximum intensity of 75 kt (39 m/sec) over the Luichow Peninsula. Zita maintained this strength across the Gulf of Tonkin, and made landfall in Vietnam on the morning of 23 August.

The pre-**Typhoon Amber (18W)** disturbance developed southwest of Guam and took a slow westward, then northwestward track toward Taiwan. Amber intensified slightly faster than the normal Dvorak one T-number per day, and had reached 100 kt (52 m/sec) on the morning of 25 August. At this time, **Tropical Storm Cass (20W)** began to form southwest of Amber in the South China Sea, about 160 nm (296 km) south of Hong Kong. Shear from the outflow from Typhoon Amber inhibited Cass' intensification. On 28 August, the two TCs underwent a binary interaction, which accelerated Amber toward Taiwan and caused Cass to move slowly to the east. After some vacillation in intensity, Amber reached its peak of 110 kt (57 m/sec) just prior to hitting Taiwan on 29 August. Amber weakened over the mountainous island, and later made landfall on mainland China. Tropical Storm Cass (20W) was very short-lived, spending

only 2.5 days in warning. Once Amber move over Taiwan, Cass moved to the north and intensified to its peak of 45 kt (23 m/sec). Cass made landfall in mainland China, 150 nm (278 km) west of Taiwan, and later dissipated over the mountains of southern China.

While Amber (18W) was developing southwest of Guam, the disturbance destined to become **Super Typhoon Bing (19W)** was developing near the eastern extent of the monsoon trough in the Marshall Islands. The system was upgraded to TD 19W on 27 August and tracked westward at 13-15 kt (24-28 km/hr) toward the Mariana Islands. On the afternoon of 29 August, Tropical Storm Bing passed through the channel that separates Guam and Rota with 40-kt (21-m/sec) sustained winds. After passing Guam, Bing began to rapidly intensify, and 54 hours later, it reached its peak intensity of 135 kt (70 m/sec), becoming the fifth super typhoon of the season. Near 143E, Bing slowed its forward motion and turned to the north. Shortly thereafter, it accelerated to a speed of 11-13 kt (20-24 km/hr), maintaining northward motion for three days, until it recurved to the northeast about 300 nm (555 km) south of eastern Japan. Bing's forward speed accelerated to 30 kt (56 km/hr) as it transitioned into a 55-kt (29 m/sec) extratropical cyclone on 05 September.

SEPTEMBER

September was also a busy month with five TCs. At the end of August, a tropical disturbance formed to the southwest of Hawaii in the monsoon trough displaced far to the east as a result of the intense El Niño event. The disturbance would eventually become **Super Typhoon Oliwa (02C)** (a Hawaiian name -- pronounced "Oh'-lee-vah") after it crossed the international dateline. Oliwa reached tropical storm intensity in the Central North Pacific and proceeded on a westward track, crossing the dateline on 04

September. In the WNP, Oliwa intensified slowly to typhoon intensity, then explosively deepened, with its winds increasing from 75 kt (39 m/sec) to its peak of 140 kt (72 m/sec) in only 24 hours. Super Typhoon Oliwa (02C) continued its west-northwest motion, slowly weakening. At mid-month, it recurved northeast of the Ryukyu Islands and made landfall in southern Kyushu with an intensity of 70 kt (36 m/sec), causing some deaths and considerable destruction. Oliwa dissipated in the Sea of Japan.

The disturbance that became **Typhoon David (21W)**, initially developed east of the dateline in the active monsoon trough. TD 21W moved to the northwest, intensifying at a normal one T-number/day rate. The system was large, and the northward component was attributed to the "Beta effect" of its large size. David attained its maximum intensity of 95 kt (49 m/sec) on the morning of 15 September. Typhoon David recurved, passed south of Japan, and became extratropical on 21 September en route to the Gulf of Alaska.

While David (21W) was recurving southeast of Japan, the disturbance that became **Super Typhoon Ginger (24W)**, was consolidating near the international dateline as one of 10 TCs which formed east of 160E and south of 20N -- within the El Niño box (See Figure 3-3a). Ginger moved on a north-oriented track in the eastern portion of the WNP basin. Ginger underwent a 24-hour period of explosive deepening, and as it neared its peak intensity of 145 kt (75 m/sec), the typhoon possessed an extensive system of primary and peripheral rain bands. When Ginger reached 30N, it accelerated within the mid-latitude westerlies where it transitioned into a vigorous extratropical low.

Typhoon Fritz (22W) was first seen as an area of enhanced convection in the South China Sea. As the system moved away from the coast of Vietnam, it slowly intensified. After a few days of eastward movement, Fritz turned back to the west toward Vietnam and

continued to intensify. It reached its peak intensity of 75 kt (39 m/sec), which it maintained until it made landfall in Vietnam on 25 September. The system dissipated over land, but torrential rains triggered landslides that took the lives of many gold prospectors.

Tropical Storm Ella (23W) developed as a very small circulation east of the dateline. By 21 September, convection had become well-organized, albeit small (30 nm (56 km), over the system center. Ella sped to the west-northwest at 18-25 kt (33-46 km/hr), reached its maximum intensity of 40 kt (21 m/sec) on 22 September, recurved and dissipated on 24 September near 40N 170E.

OCTOBER

Tropical Storm Hank (25W) was the shortest-lived tropical cyclone of the season, with warnings issued for only 36 hours. The disturbance that became Hank, was first observed on 27 September in the South China Sea, but the first warning was not issued until 03 September. The system moved erratically, and upper-level wind shear prevented it from intensifying beyond 40 kt (21 m/sec). Hank made landfall in northern Vietnam on 05 September and dissipated soon thereafter.

As Hank was developing in the South China Sea, **Tropical Depression 26W (TD 26W)** formed southeast of Guam. The disturbance initially moved northward, then healed over to the west and passed north of Guam on 03 October, where it attained its maximum intensity of 30 kt (16 m/sec). TD 26W maintained this intensity for three more days, but strong westerly upper level shear never allowed it to intensify. As an exposed low level circulation, TD 26W merged with a frontal boundary over the Philippine Sea.

Super Typhoon Ivan (27W) and Super Typhoon Joan (28W) were two of three TCs in the WNP during 1997 to attain an extreme intensity of 160 kt (82 m/sec), and were the 8th and 9th of 1997's unprecedented number of 11 super typhoons. An equatorial westerly

wind burst associated with the El Niño preceeded the formation of Ivan, Joan and a Southern Hemisphere twin -- Tropical Cyclone Lusi (02P). After developing, Ivan moved to the west-northwest and eventually passed 55 nm (102 km) south of Guam. From 150600Z to 171800Z, Ivan intensified from 65 kt (34 m/sec) to 160 kt (83 m/sec). The typhoon continued its westward movement, becoming the first and only named TC in 1997 to hit the Philippines. Ivan recurved in the Luzon Strait, and after weakening, became extratropical south of Japan. Joan developed just east of Ivan, and took a similar track to the west, but passed 155 nm (287 km) north of Guam. Joan explosively deepened, intensifying from 70 kt (36 m/sec) to 160 kt (83 m/sec) in 36 hours -- a deepening rate of 2.8 mb per hour. Joan remained at or above the super typhoon threshold (130 kt, 68 m/sec) for 4.5 days -- a record. Joan and Ivan were the two most intense TCs ever seen to exist simultaneously. Joan slowly weakened, finally recurved, and while traveling eastward along 30N, became an intense extratropical cyclone.

As Ivan and Joan began to recurve, yet another disturbance was developing in the El Niño-induced monsoon trough in the eastern Caroline and Marshall Islands. This disturbance would become the tenth of eleven 1997 super typhoons -- **Super Typhoon Keith (29W)**. After several days of westward movement and difficulty in organizing, the system finally consolidated and began to intensify at a normal rate of one Dvorak "T-number" per day. Once it reached 105 kt (55 m/sec), the typhoon began to rapidly intensify, peaking at 155 kt (81 m/sec) in just 24 hours. The small eye and narrow wall cloud of Keith passed between the islands of Saipan and Rota in the Mariana Islands, and no island endured the full force of the typhoon. Keith remained a super typhoon for 3.5 days as it moved to the northwest at the end of the month. On 04 November, **Super**

Typhoon Keith's (29W) forward motion slowed, and the typhoon began to weaken and recurve. A few days later, a weakened Keith was speeding at 45 kt (83 km/hr) to the east-northeast and becoming extratropical.

NOVEMBER

The disturbance that became **Typhoon Linda (30W)**, developed near the end of October near 10N about 200 nm (370 km) east of the Philippines. The system moved westward and reached tropical storm intensity within 24 hours of moving into the South China Sea. The system continued to intensify as it approached the Ca Mau province of Vietnam on 02 November, and reached typhoon intensity in the Gulf of Thailand. The typhoon weakened while crossing the Malay Peninsula, but reintensified in the Bay of Bengal. Linda was the first TC since Typhoon Forrest (30W) in 1992 to successfully make this low latitude trek. After attaining typhoon intensity in the Bay of Bengal on 06 November, Linda ran into progressively more severe wind shear, and four days later, it dissipated over the Bay. Linda caused considerable damage and loss of life in Vietnam.

Typhoon Mort (31W) was the last TC of November and the last 1997 TC to form west of the international dateline. Mort began in a weak monsoon trough south of Guam. The system moved to the west and reached its maximum intensity of 65 kt (34 m/sec) in the Philippine Sea on 12 November. Mort peaked at 55 kt (29 m/sec), before it again ran into strong shear, which pushed the convection to the south at the low-level circulation center. On 16 November, Mort made landfall on the east coast of Luzon as a tropical depression.

DECEMBER

No TCs originated in the WNP during December 1997, and were it not for the entry of **Super Typhoon Paka (05C)** into the basin from the central North Pacific, it is probable

that there would have been no TCs in the WNP during December.

Trade winds dominated the tropics of the WNP for most of December. Anomalous easterly wind flow became established at low latitudes, except at eastern longitudes near the international dateline where El Niño-related low-level westerly wind flow persisted. The majority of monsoon-related deep convection had moved to the east of the international dateline, and twin near equatorial troughs extended along 8N and 5S from near 160E to the south of Hawaii at about 160W. A tropical storm -- Paka (05C) -- which had formed south of Hawaii during late November, moved steadily westward during December. It crossed the International Date Line on 07 December, and became a typhoon in the Marshall Islands. Continuing on a west-northwestward track, it intensified into a super typhoon and passed over Guam on 16 December, where the 600 million dollar level of destruction resulted in a Presidential declaration of Guam as a disaster area. Reliable measurements of wind gusts on Guam were as high as 149 kt (77 m/sec) and

storm total rainfall amounts in excess of 15 inches (635 mm) occurred. Paka continued to move west-northwestward into the Philippine Sea where it eventually dissipated over water after reaching an extreme estimated intensity of 160 kt (82 m/sec).

With the dissipation of Paka, the "year of the super typhoon" in the western North Pacific came to a close. At the end of December, high pressure, persistent easterly winds, and reduced amounts of deep convection prevailed in the tropics of the basin. ENSO-related drought conditions worsened to record proportions in Micronesia, and TC activity shifted into the Southern Hemisphere with a classical El Niño shift to the east.

During 1997 for the western North Pacific, JTWC issued 950 warnings. Super Typhoons Paka (05C) and Oliwa (02C) were the longest lived TCs of the year, requiring 78 and 59 warnings respectively, even after moving from their genesis regions in the central North Pacific across the international dateline into the JTWC area of responsibility.

Table 3-3 WESTERN NORTH PACIFIC TROPICAL CYCLONES

TYPHOONS (1945-1959)													
	JAN	FEB	MAR	APR	MAY	JUN	JUL	AUG	SEP	OCT	NOV	DEC	TOTALS
MEAN	0.3	0.1	0.3	0.4	0.7	1	2.9	3.1	3.3	2.4	2	0.9	16.4
CASES	5	1	4	6	10	15	29	46	49	36	30	14	245
TYPHOONS (1960-1997)													
	JAN	FEB	MAR	APR	MAY	JUN	JUL	AUG	SEP	OCT	NOV	DEC	TOTALS
MEAN	0.3	0.1	0.2	0.4	0.7	1.1	2.8	3.5	3.4	3.3	1.7	0.7	18
CASES	10	2	8	16	27	41	107	132	129	124	63	26	685
TROPICAL STORMS AND TYPHOONS (1945-1959)													
	JAN	FEB	MAR	APR	MAY	JUN	JUL	AUG	SEP	OCT	NOV	DEC	TOTALS
MEAN	0.4	0.1	0.5	0.5	0.8	1.6	2.9	4	4.2	3.3	2.7	1.2	22.2
CASES	6	2	7	8	11	22	44	60	64	49	41	18	332
TROPICAL STORMS AND TYPHOONS (1960-1997)													
	JAN	FEB	MAR	APR	MAY	JUN	JUL	AUG	SEP	OCT	NOV	DEC	TOTALS
MEAN	0.5	0.2	0.4	0.7	1.2	1.8	4.3	5.7	5.1	4.3	2.7	1.2	28.1
CASES	20	9	17	25	44	70	163	215	193	164	101	47	1068

TABLE 3-4 TROPICAL CYCLONE FORMATION ALERTS FOR THE WESTERN NORTH PACIFIC OCEAN FOR 1976-1997

YEAR	INITIAL TCFAS	TROPICAL CYCLONES WITH TCFAS	TOTAL TROPICAL CYCLONES	PROBABILITY OF TCFA WITHOUT WARNING*	PROBABILITY OF TCFA BEFORE WARNING
1976	34	25	25	26%	100%
1977	26	20	21	23%	95%
1978	32	27	32	16%	84%
1979	27	23	28	15%	82%
1980	37	28	28	24%	100%
1981	29	28	29	3%	96%
1982	36	26	28	28%	93%
1983	31	25	25	19%	100%
1984	37	30	30	19%	100%
1985	39	26	27	33%	96%
1986	38	27	27	29%	100%
1987	31	24	25	23%	96%
1988	33	26	27	21%	96%
1989	51	32	35	37%	91%
1990	33	30	31	9%	97%
1991	37	29	31	22%	94%
1992	36	32	32	20%	100%
1993	50	35	38	30%	92%
1994	50	40	40	20%	100%
1995	54	33	35	39%	94%
1996	41	39	43	5%	91%
1997	36	30	33	17%	91%
(1976- 1997)					
MEAN:	37	29	30	22%	97%
TOTALS:	818	635	670		

* Percentage of initial TCFA's not followed by warnings.

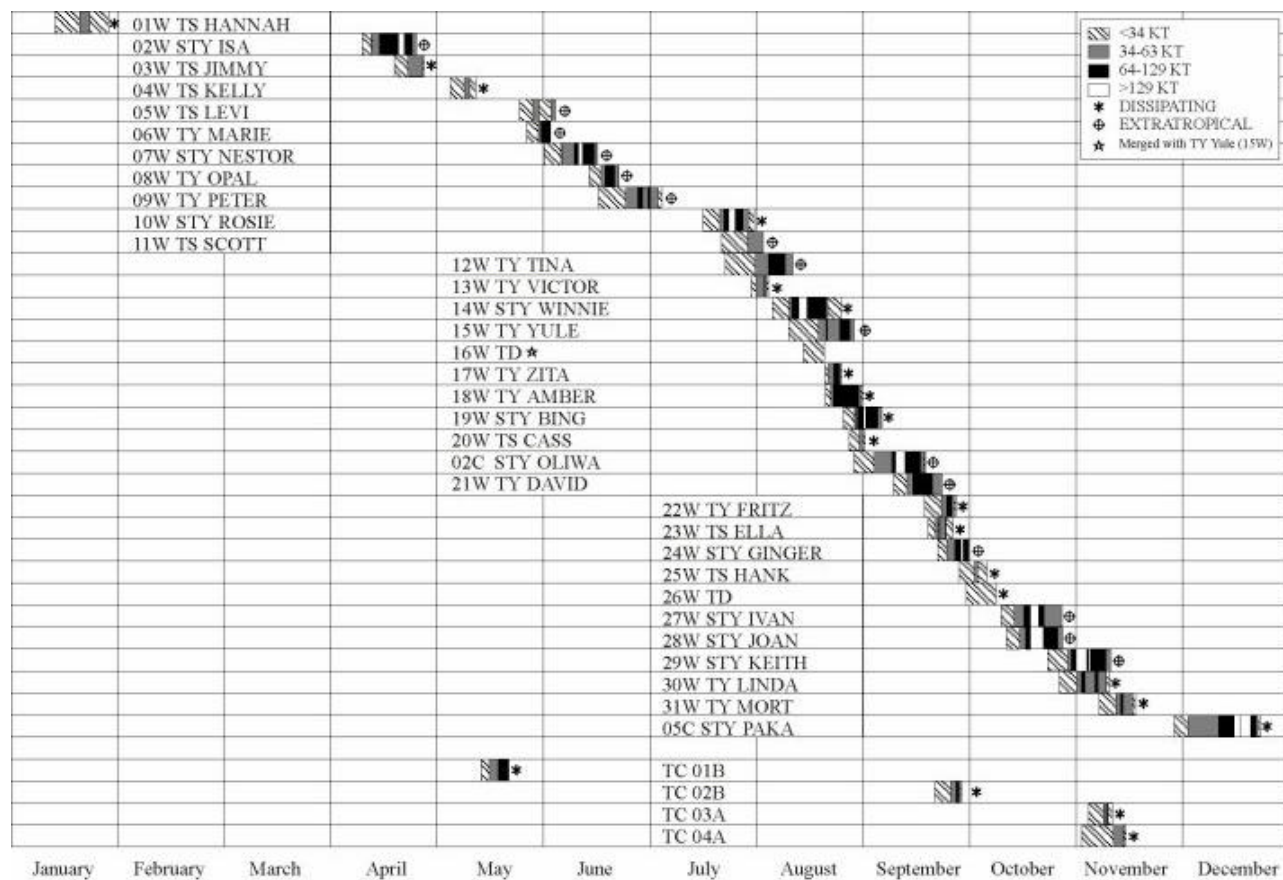


Figure 3-7 Chronology of western North Pacific and North Indian Ocean tropical cyclones for 1997 .

TABLE 3-5 NORTH INDIAN OCEAN SIGNIFICANT TROPICAL CYCLONES FOR 1997				
TROPICAL CYCLONE	PERIOD OF WARNING	NUMBERS OF WARNINGS ISSUED	ESTIMATED MAX INTENSITY KT (M/SEC)	EST MSLP (MB)
01B	14 MAY - 20 MAY	22	115 (59)	927
02B	24 SEP - 27 SEP	10	65 (33)	976
03A	08 NOV - 09 NOV	7	35 (18)	997
04A	10 NOV - 14 NOV	17	55 (28)	984
TOTAL		56		

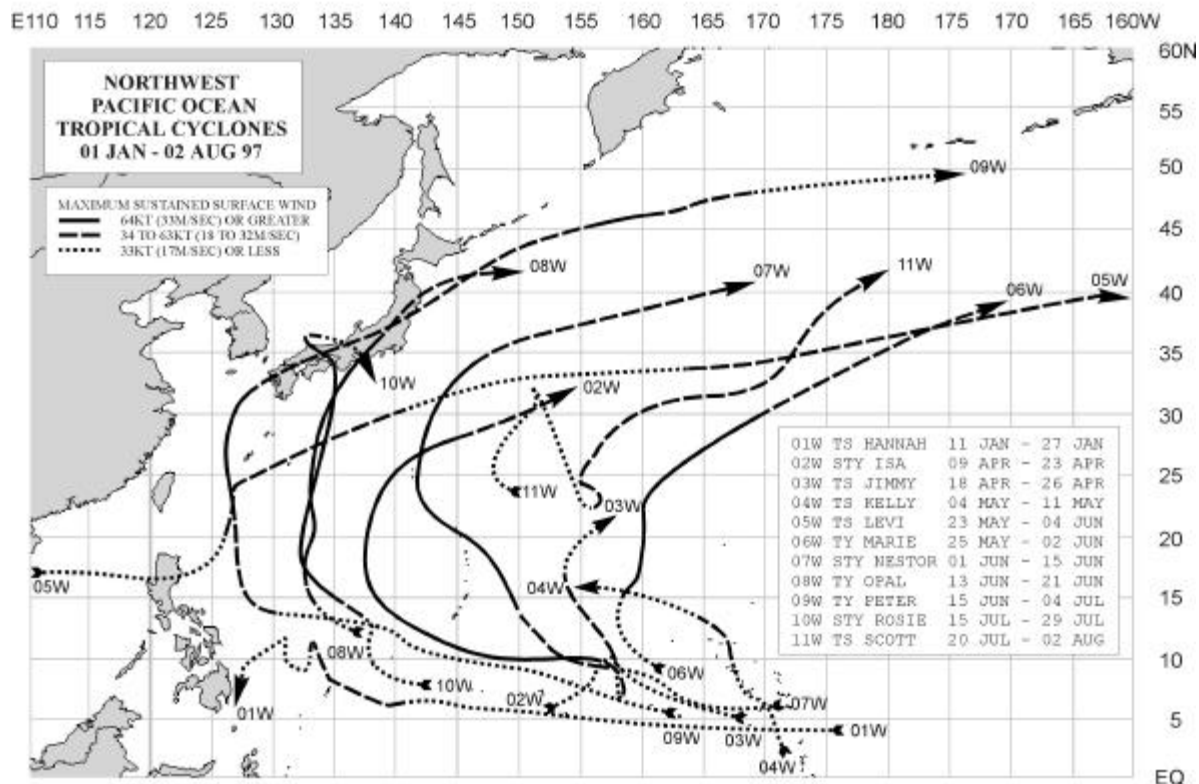


Figure 3-8a Composite best tracks for the western North Pacific Ocean tropical cyclones for the period 01 January to 02 August 1997

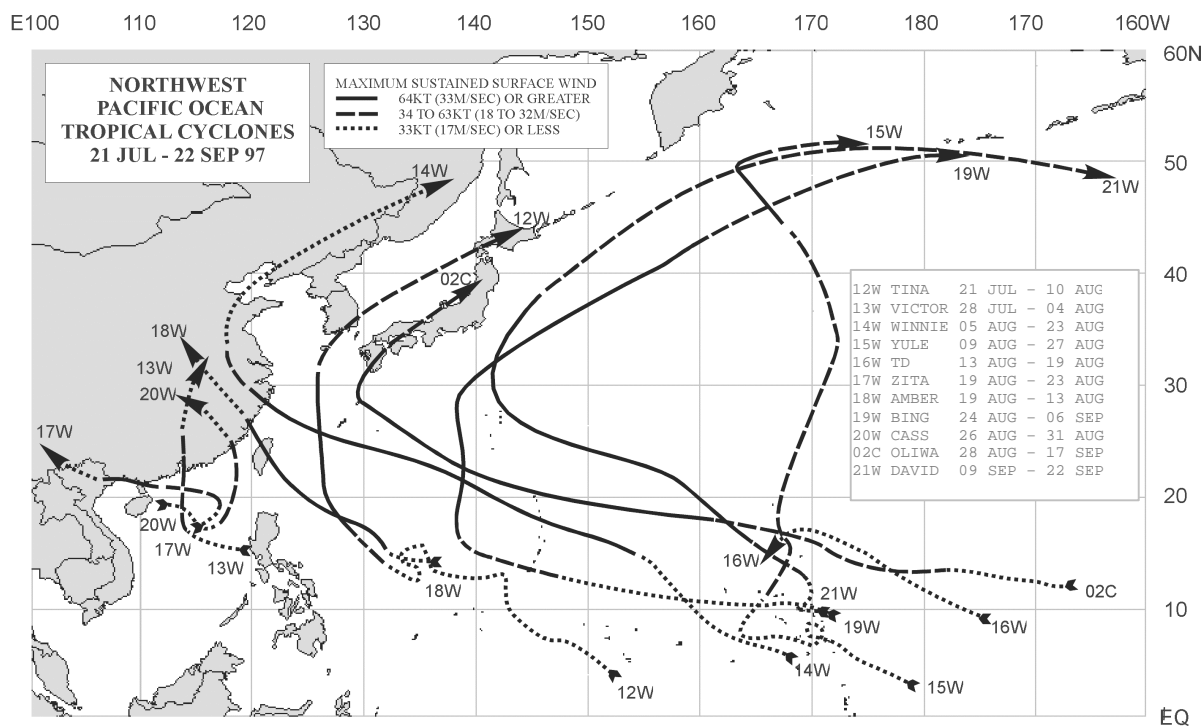


Figure 3-8b Composite best tracks for the western North Pacific Ocean tropical cyclones for the period 21 July to 22 September 1997

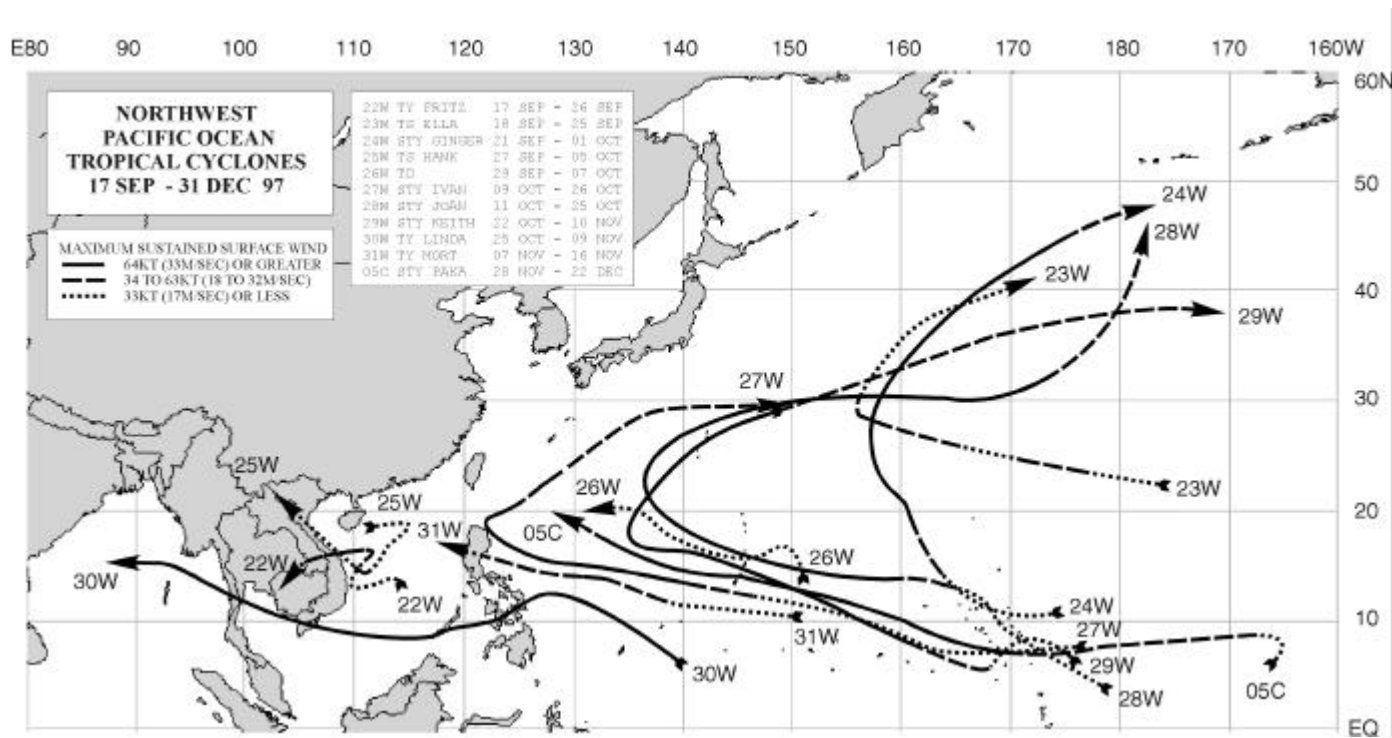


Figure 3-8c Composite best tracks for the western North Pacific Ocean tropical cyclones for the period 17 September to 22 December 1997

TROPICAL STORM HANNAH (01W)

I. HIGHLIGHTS

The first named tropical cyclone of 1997, Hannah, developed from a tropical disturbance in a near-equatorial trough south of the Marshall Islands. Moving on a long westward track for over two weeks, it reached a peak intensity of 50 kt (26 m/sec), and then dissipated in the Philippine Sea. Many of the tropical cyclones of 1997 (including Hannah) shared the unusual characteristic of forming well to the east of normal; a typical behavior of tropical cyclones during an El Niño year.

II. TRACK AND INTENSITY

The tropical disturbance which became Hannah was first described on the 11 January significant tropical weather advisory as an area of persistent deep convection located at very low latitude (4°N) and just to the west of the International Date Line (IDL). The disturbance remained poorly organized for several days as it moved steadily westward along 4°N. After a westward journey covering over 2000 nm (3700 km) in a period of one week, it began to show signs of development. On 19 January,

when the system was south-southwest of Guam, an increase in the amount of deep convection and the presence of a low-level circulation center were detected by multi-spectral satellite imagery (Figure 3-01-1) and synoptic data. This prompted JTWC to issue a Tropical Cyclone Formation Alert valid at 00Z on 19 January. The first warning on Tropical Depression (TD) 01W was issued valid at 0600Z on the nineteenth based on a blend of synoptic data, scatterometer data, and satellite intensity estimates, which indicated that the winds in the system had increased to at least 25 kt (13 m/sec). Twelve hours later, at 191800Z, TD 01W was upgraded to Tropical Storm Hannah. This was based, once again, on a blend of synoptic data, scatterometer data, and satellite intensity estimates which indicated intensification to 35 kt (18 m/sec). Hannah reached peak intensity of 50 kt (26m/sec) at 0600Z on 20 January based on conventional satellite intensity estimates, and special sensor microwave imagery (SSM/I). These sources all indicated

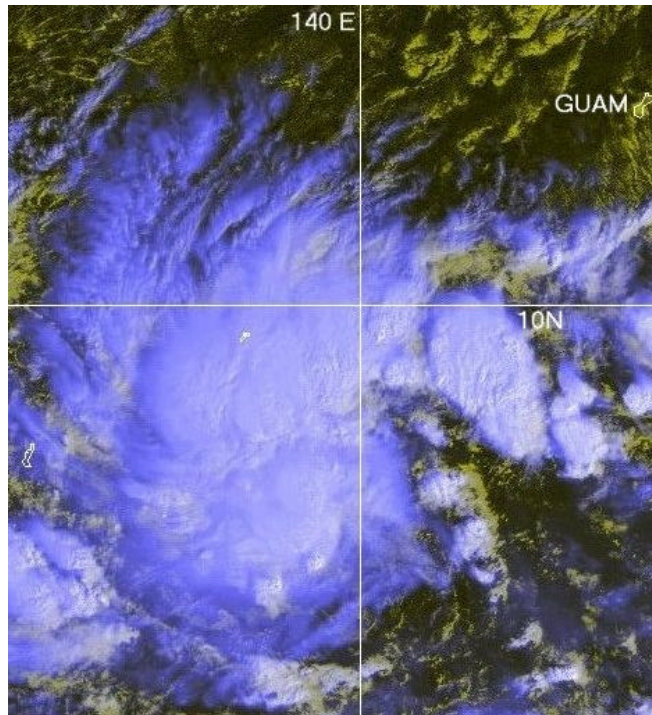


Figure 3-01-1 The deep convection associated with the pre-Hannah tropical disturbance becomes better organized, and JTWC responds by issuing a Tropical Cyclone Formation Alert. Note the large extent of low-level westerly winds along the equator and at low latitudes in both hemispheres implied by the distribution and pattern of the deep convection (182333Z January infrared GMS imagery).

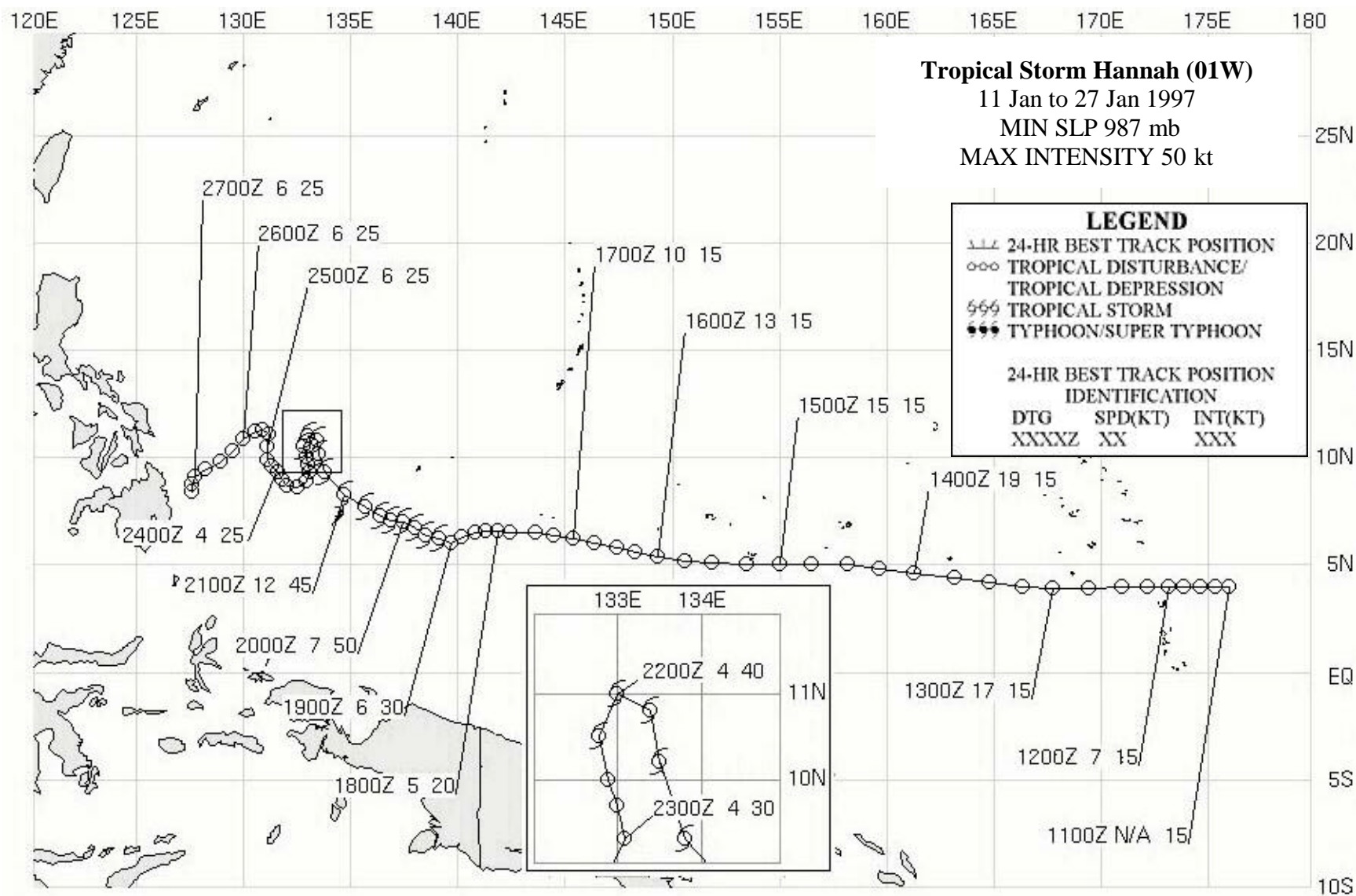
that the deep convection and the low-level cloud lines had become organized into well-defined cyclonic bands. After 0600Z the cyclone approached a region of low-level northeasterly flow overlaid by upper level southeasterly winds. Weakening ensued as vertical wind shear forced the dwindling amounts of deep convection to the northern quadrant. Hannah's motion became erratic on 21 January as the system began to interact with a shear line that trailed into the tropics from a large and vigorous extratropical low moving eastward off the coast of Japan. Trapped at the end of the shear line, the areal extent of Hannah's deep convection began to rapidly diminish, and the final warning was issued valid at 1800Z on the 24th when the intensity had fallen to 25 kt (13 m/sec) and further weakening was expected. Post analysis revealed that the remains of Hannah maintained an intensity of about 25 kt (13m/sec) for the next three days as it moved slowly toward Mindanao.

III. DISCUSSION

Although Tropical Storm Hannah was in most respects unremarkable, in retrospect it's development can be seen as part of the unusual large-scale tropical circulation pattern associated with El Niño, which would cause many of the tropical cyclones of 1997 to form well east of normal. We now know that the weather events over the Pacific warm pool during late 1996 and early 1997 may be looked upon as the antecedent (or onset) conditions leading to the development of strong El Niño conditions by April of 1997. An eastward displacement of the mean genesis location of tropical cyclones in the western North Pacific is a signature of El Niño.

IV. IMPACT

No reports of significant damage or injuries were received at JTWC.



SUPER TYPHOON ISA (02W)

I. HIGHLIGHTS

The first of eleven super typhoons to occur in the western North Pacific during 1997, Isa formed at a low latitude in the Caroline Islands along the axis of the near equatorial trough. On the night of 16 April, Isa passed 140 nm (260 km) to the south of Guam. There was no significant damage reported (the peak wind gust on island was 61 kt (31 m/sec)), though peripheral rainbands of the typhoon produced rainfall of 6 to 10 inches (15 to 25 cm) across the island. Most of the objective track guidance available to JTWC turned Isa to the north well before it happened; a common model bias that is identified and explained in the model-traits knowledge base of the "Systematic Approach".

II. TRACK AND INTENSITY

The tropical disturbance that became Isa developed in a near-equatorial trough that had become established across Micronesia. On 09 April, a large cloud cluster with the characteristics of a monsoon depression formed in the Caroline Islands, and was subsequently described in the 09 April 0600Z Significant Tropical Weather Advisory (ABPW). Synoptic data and animated satellite imagery indicated that a large, weak, low-level cyclonic circulation accompanied this cloud cluster. After several cycles of mesoscale cloud cluster growth, dissipation and regeneration, the system acquired a persistent and well-organized area of deep convection on 11 April, prompting JTWC to issue a Tropical Cyclone Formation Alert (TCFA), valid at 0000Z. The first warning on Tropical Depression (TD) 02W was issued valid at 1800Z on 11 April, based on satellite intensity estimates of 30 kt (15 m/sec), cooling cloud tops, and increased organization of the outflow aloft.

TD 02W was a large tropical cyclone that intensified slowly. The strong, deep monsoonal westerlies to its south prevented much movement from 0000Z on 10 April to 0000Z on 12 April. Based on satellite intensity estimates of 35 kt (18 m/sec), 02W was upgraded to Tropical Storm Isa (02W) on the warning valid at 0600Z on 12 April. After becoming a tropical storm, intensification occurred more rapidly, and the system began to move toward the west-northwest. Isa was upgraded to a typhoon on the 13 April 1800Z warning. At this point, the motion of the system became more westward, and the rate of intensification slowed. During the six-day period from 0000Z on the 14th to 0000Z on the 20th, the intensity of the typhoon steadily increased from 65 kt (33 m/sec) to its peak of 145 kt (75 m/sec) (Figure 3-02-1). This rate of intensification (approximately one-half a T-number per day) is defined by Dvorak (1975, 1984) as slow. Approximately 36 hours prior to reaching peak intensity, Isa turned to the north, a major track change indicated by most of the numerical guidance for several days (although the models made the turn far too early). Moving slowly north along 137E during the 24-hour period from 20 April 0000Z to 21 April 0000Z, Isa began to weaken. At 0000Z, on 21 April, the typhoon turned to the north-northeast and doubled its forward speed to approximately 12 kt (22 km/hr) while continuing to weaken. At 0000Z on the 22nd, the typhoon, having weakened to 80 kt (41 m/sec), began to accelerate in the midlatitude flow and the speed of translation increased from 12 kt (22

km/hr) to 17 kt (32 km/hr) at 0000Z on the 23rd, and to 24 kt (44 km/hr) at 1200Z on the 23rd. The final warning on Isa was issued valid at 0600Z on the 23rd, as the system accelerated to the northeast and its cloud system became sheared. The remnants of Isa later merged with the cloud band on the northeast side of a vigorous extratropical low that had developed and moved eastward into the Pacific from northern Japan.

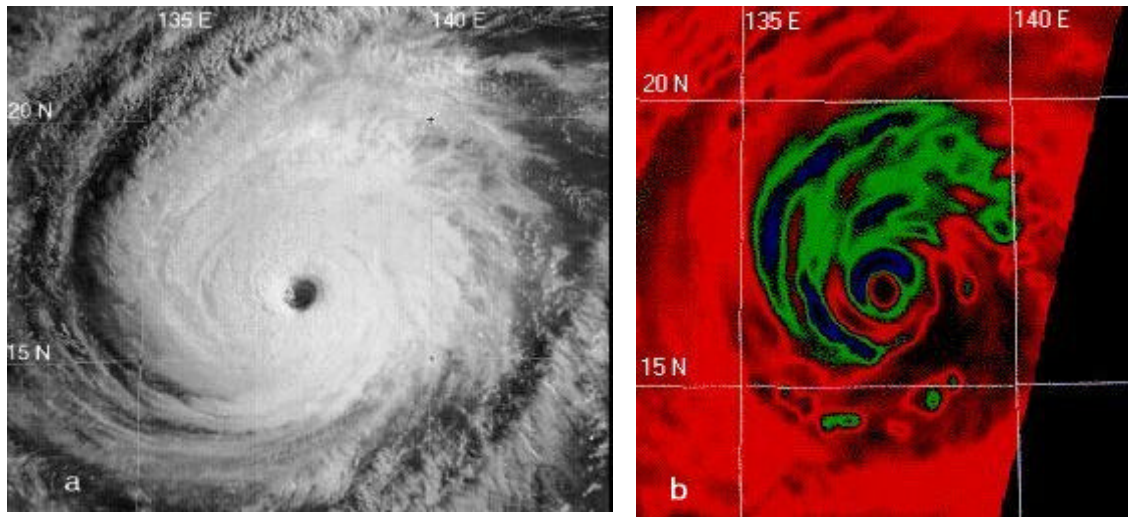


Figure 3-02-1 Isa near the time of its peak intensity. (a) Visible imagery within three hours of its best track peak (192131Z April visible GMS imagery) and (b) microwave imagery within two hours of the peak (200146Z April 85 GHz horizontally polarized microwave DMSP imagery).

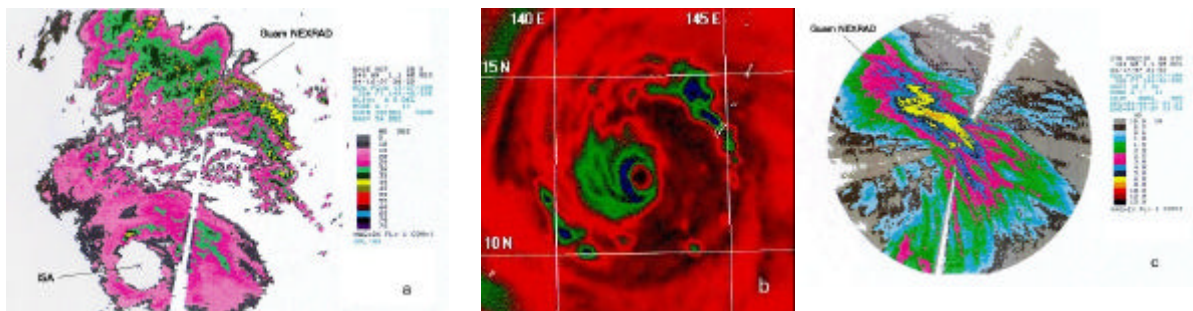


Figure 3-02-2 A peripheral rainband on the northeast side of Isa remained in a fixed position over Guam for over 12 hours resulting in rainfall totals of up to 10 inches. (a) As Isa's eye moved westward away from Guam, heavy showers and thunderstorms embedded in an outer rainband were directed over the island for an extended period (162029Z April NEXRAD base reflectivity). (b) The rainband as it appeared in microwave imagery (170805Z April 85 GHz horizontally polarized microwave DMSP imagery). (c) The narrowness of the ribbon of high amounts of rainfall is apparent on NEXRAD integrations of precipitation (NEXRAD storm-total precipitation ending at 172154Z April).

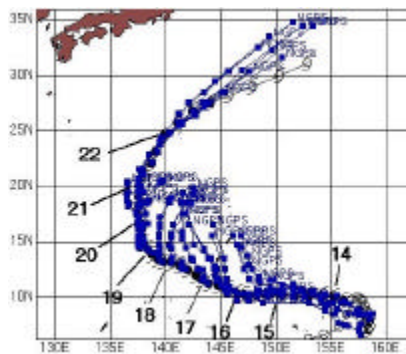


Figure 3-02-3 Most of the objective guidance available at the JTWC had a persistent and strong northward bias for much of Isa's track. (NOGAPS forecasts out to 72 hours are superimposed over Isa's best track).

III. DISCUSSION

a. A Next-generation Radar (NEXRAD) view of Isa as it passed Guam

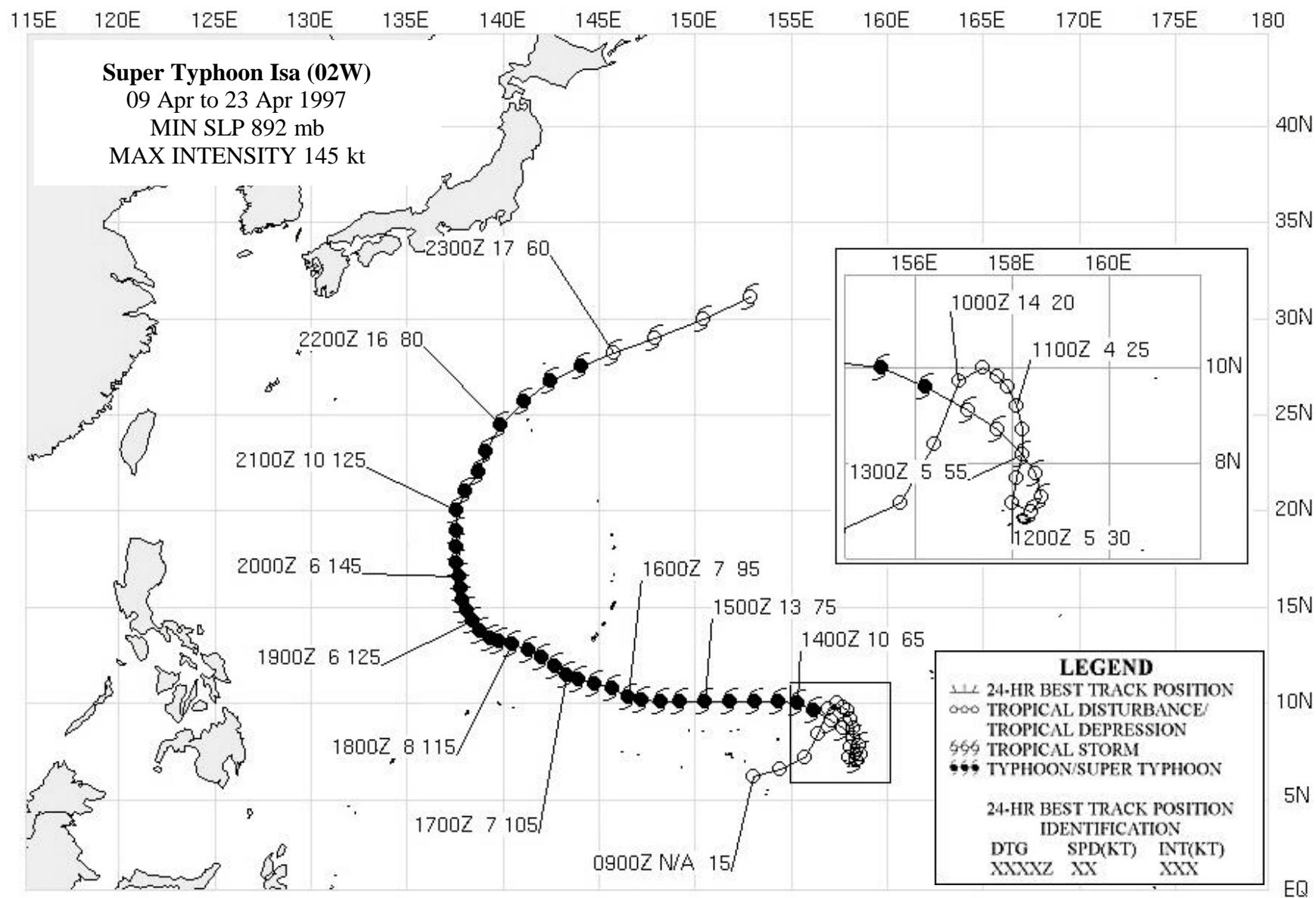
Isa passed closest to Guam during the early morning of 17 April. Most of the rainfall and the highest winds associated with the typhoon, however, occurred after Isa began moving away from the island, and was associated with a peripheral rainband (see the NEXRAD display of Figure 3-02-2a and the microwave imagery of Figure 3-02-2b). Twenty-four hour rainfall measurements on Guam approached 10 inches in some places. The NEXRAD storm-total precipitation product (Figure 3-02-2c) shows the narrow ribbon of very high rainfall produced over Guam (and adjacent ocean) by the nearly stationary typhoon rainband. Although the rainband was stationary, the convective elements within the band were moving rapidly northwestward in deep-layer southeasterly flow of 45-50 kt (23-26 m/sec).

b. Model biases

Numerical track prediction biases (predominantly those of the NOGAPS model), as described in the "Systematic and Integrated Approach" to tropical cyclone forecasting (Carr and Elsberry 1994), were observed in Typhoon Isa, particularly the NOGAPS tendency to prematurely turn a westward moving tropical cyclone to the north. Although JTWC forecasters were aware of the model bias and delayed forecasting the turn, the actual delay was longer than anticipated. JTWC forecast Isa's northward turn to occur near its actual closest point of approach to Guam, leading to over-forecasting of wind on the island. While the "Systematic Approach" deserves credit for alerting the forecaster's to the model's bias, and for correctly identifying that the northward turn would eventually occur, the turn was delayed for a very long time relative to other examples of this type, as illustrated in Carr and Elsberry (1994) and in training materials devised for the JTWC forecasters. Recent work by Carr (personal communication) on the problem of premature recurvature in model guidance (e.g., NOGAPS and GFDN) has led to new findings. In the early formulations of the "Systematic Approach", there were only two scenarios in which the numerical guidance tended to turn a westward moving tropical cyclone towards the north too early: 1) During cases of Indirect Tropical Cyclone Interaction, and 2) during cases of westward motion equatorward of a Dominant Subtropical Ridge when the model analysis of the tropical cyclone was too large. An additional scenario has recently been identified, and applies to Isa: Premature recurvature forecasts also occur in the transition seasons (spring; and late fall through early winter) when the subtropical ridge is meridionally thin, particularly if the tropical cyclone is intense. Presumably the intense tropical cyclone in the model is too large and drives through a weakness in the thin ridge sooner than its real-world counterpart (as was the case with Isa) or indicates a false recurvature in the case of a straight runner (as was the case with 05C, Paka).

IV. IMPACT

No reports of significant damage or injuries were received at JTWC. Welcome dry-season rainfall of up to 10 inches (25 cm) was recorded on Guam as Isa passed near.



TROPICAL STORM JIMMY (03W)

The tropical disturbance that was to become Tropical Storm Jimmy (03W) formed in mid-April from the same low-level equatorial westerly wind system that produced Super Typhoon Isa (02W) and Tropical Cyclone 34P (Ian) a week earlier. First mention of the pre-Jimmy disturbance appeared on the 0600Z Significant Tropical Weather Advisory (ABPW) on 18 April. After three days of tracking slowly to the west-northwest, the pre-Jimmy disturbance separated from the low-latitude maximum cloud zone and began its intensification. JTWC issued a Tropical Cyclone Formation Alert (TCFA) at 0400Z on 22 April. The system developed very rapidly and the first warning, valid at 0600Z on 22 April, was for Tropical Storm Jimmy (03W). By this time, Isa had already broken through the subtropical ridge, leaving the ridge weakened to non-

existent west of 150E. Water vapor wind data showed southerly and southwesterly winds aloft over the Philippine Sea, preventing movement west of 150E. Jimmy tracked around the western periphery of the maritime subtropical ridge reaching 153E before recurving. Jimmy peaked just after its recurvature at 55 kt (28 m/sec) in the low-shear environment near the subtropical ridge axis. After moving north of the subtropical ridge, Jimmy quickly weakened due to increased southwesterly winds aloft. JTWC issued the final warning, valid at 1800Z, on 25 April, as the low-level circulation center became completely exposed and it was clear that the remnants of Jimmy would soon merge with an approaching frontal boundary.

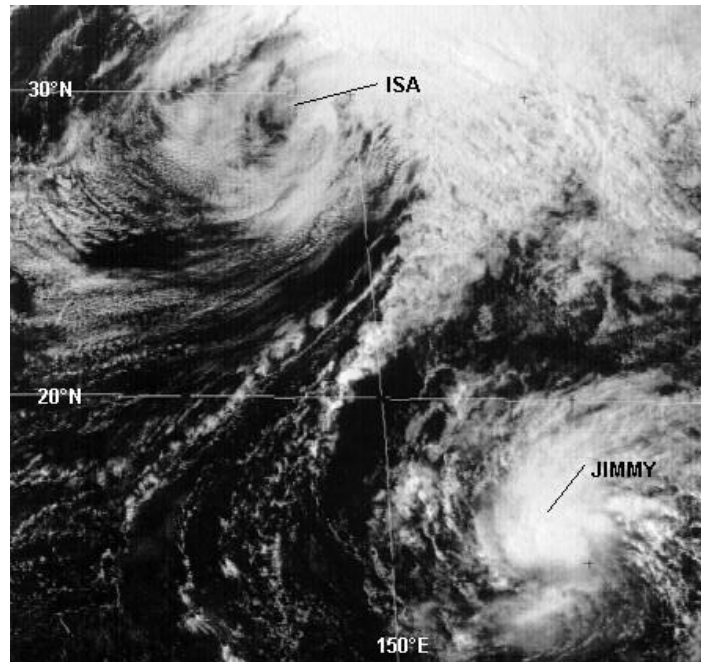
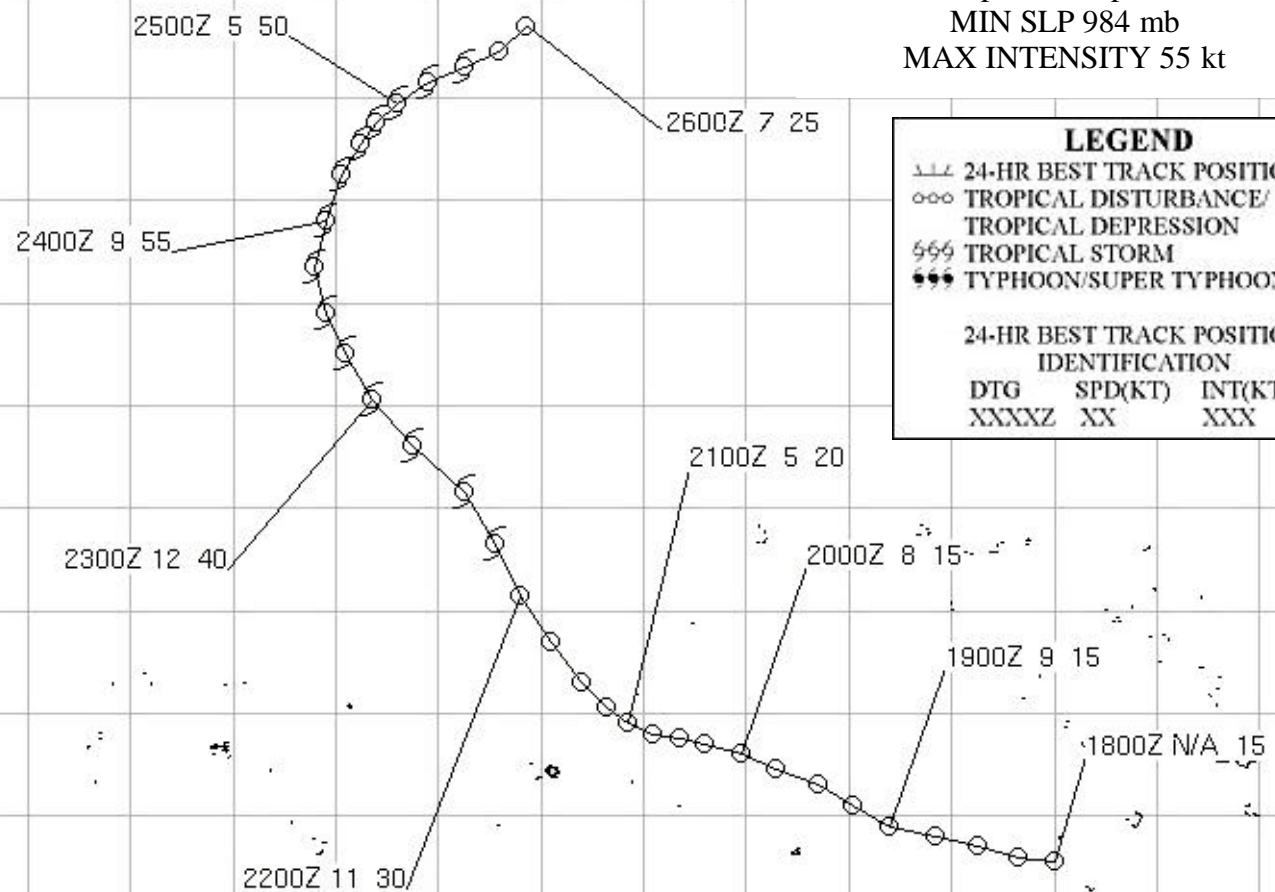


Figure 3-03-1 Tropical Storm Jimmy intensifies as it follows the remnants of Isa (02W) through the weakened subtropical ridge (230531Z April visible GMS imagery).

142E 144E 146E 148E 150E 152E 154E 156E 158E 160E 162E 164E 166E 168E 170E 172E 174E

Tropical Storm Jimmy (03W)
 18 Apr to 26 Apr 1997
 MIN SLP 984 mb
 MAX INTENSITY 55 kt



LEGEND

--- 24-HR BEST TRACK POSITION
 ooo TROPICAL DISTURBANCE/
 TROPICAL DEPRESSION
 555 TROPICAL STORM
 888 TYPHOON/SUPER TYPHOON

24-HR BEST TRACK POSITION
 IDENTIFICATION
 DTG SPD(KT) INT(KT)
 XXXXZ XX XXX

22N
 20N
 18N
 16N
 14N
 12N
 10N
 8N
 6N
 4N
 2N

TROPICAL STORM KELLY (04W)

On 4 May, as Tropical Cyclone 35P (June) moved southeastward across Fiji, a band of convection flared up (Figure 3-04-1) north of the equator. The Significant Tropical Weather Advisory (ABPW) was reissued at 0200Z on the 5th to mention that this convection was associated with a low-level circulation in the near-equatorial trough. The convection persisted, prompting JTWC to issue a Tropical Cyclone Formation Alert (TCFA) at 2300Z on the 6th, and, as convection organization continued to improve, a warning for Tropical Depression (TD) 04W, valid at 0000Z on the 7th. TD 04W continued to intensify, developing a small, central dense overcast feature (CDO) that contributed to a 35 kt (18 m/sec) satellite intensity estimate at 0000Z on the 8th. The system peaked at 45 kt (23 m/sec) on 08 May at 1200Z. On 9 May, increased vertical wind shear began displacing Kelly's persistent deep central convection to the east of the low-level circulation center (LLCC). As the circulation weakened, the exposed LLCC separated from the convection and tracked to the west-northwest in the low-level flow. Kelly continued to weaken and JTWC issued the final warning, valid at 1800Z on 10 May. No reports of damage or injuries were received. During Kelly's passage through the southern Marshall Islands, Majuro received nearly 8 inches (20 cm) of rain in 24 hours from an outer rainband.

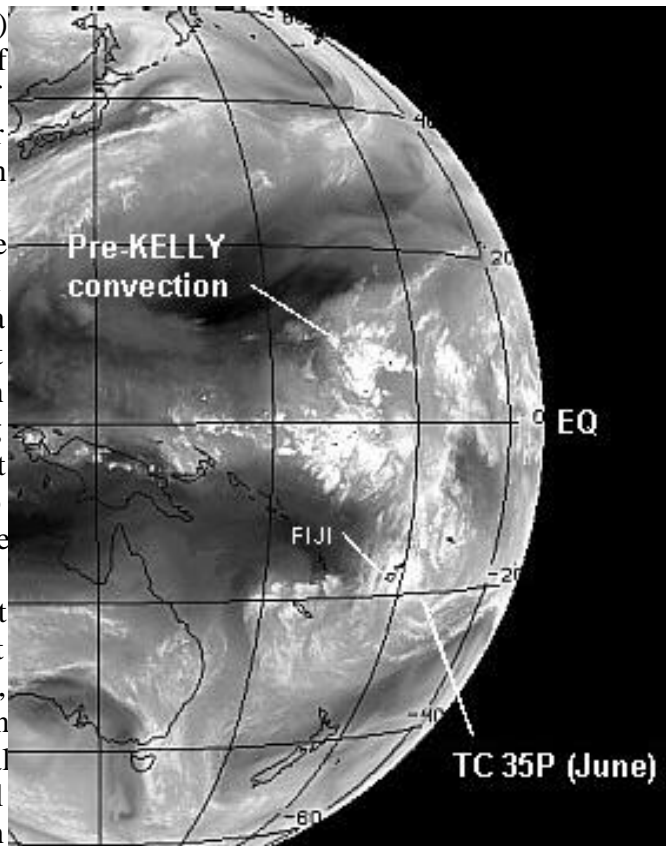
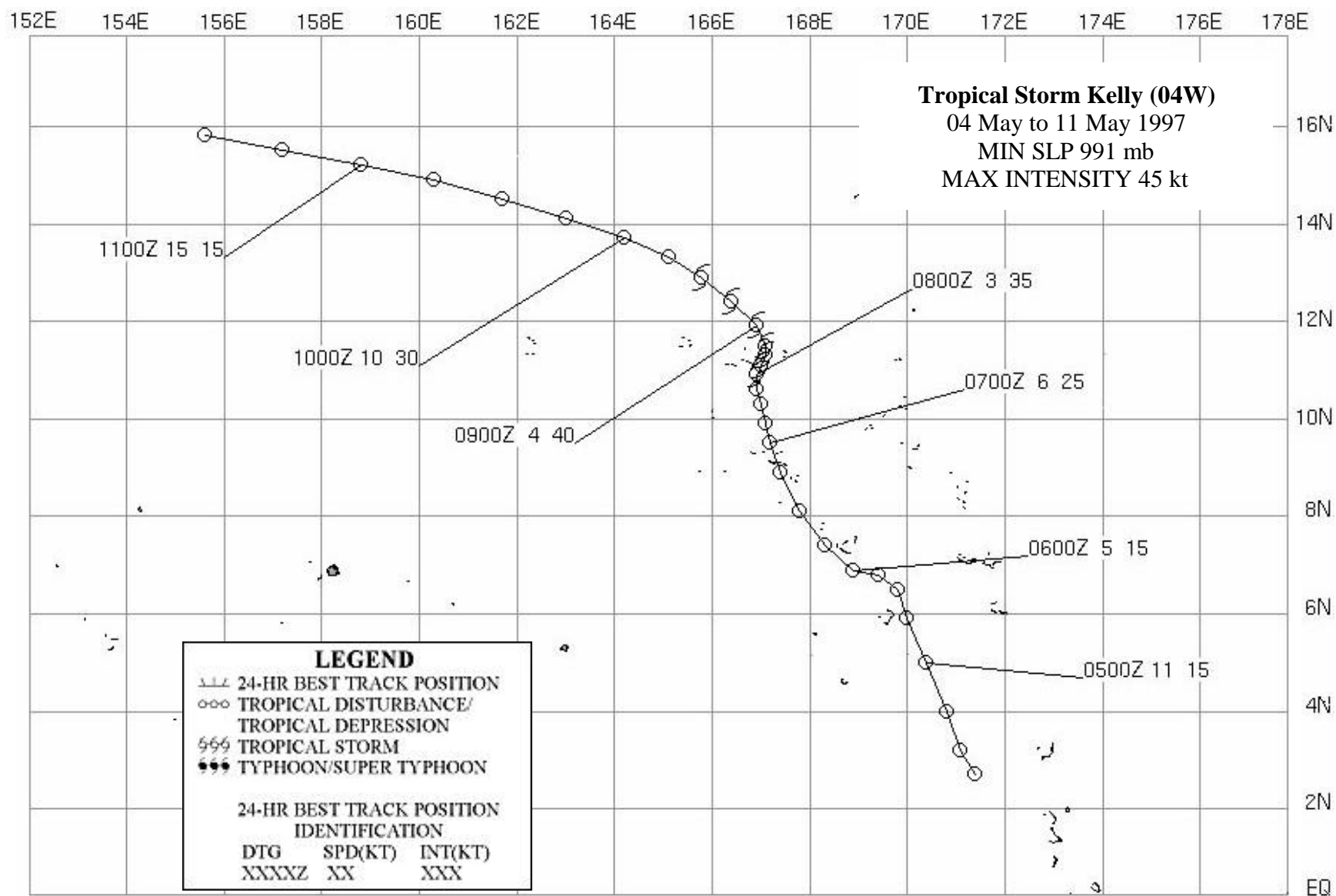


Figure 3-04-1 Cloudiness associated with the pre-Kelly tropical disturbance appears north of the equator as Tropical Cyclone 35P (June) tracks southeastward across Fiji (042233Z May visual GMS imagery).



TROPICAL STORM LEVI (05W)

Tropical Storm Levi (05W), one of three tropical cyclones to develop in May, formed in the monsoon trough in the center of the South China Sea, between central Vietnam and Luzon. A low-level circulation center (LLCC) was first analyzed at 0000Z on 23 May. It was mentioned on the Significant Tropical Weather Advisory (ABPW) 6 hours later. The system assumed the form of a monsoon depression, having deep convection on the eastern and

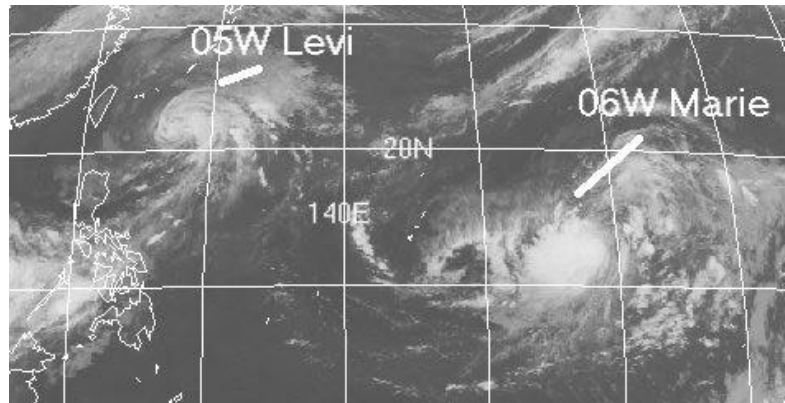
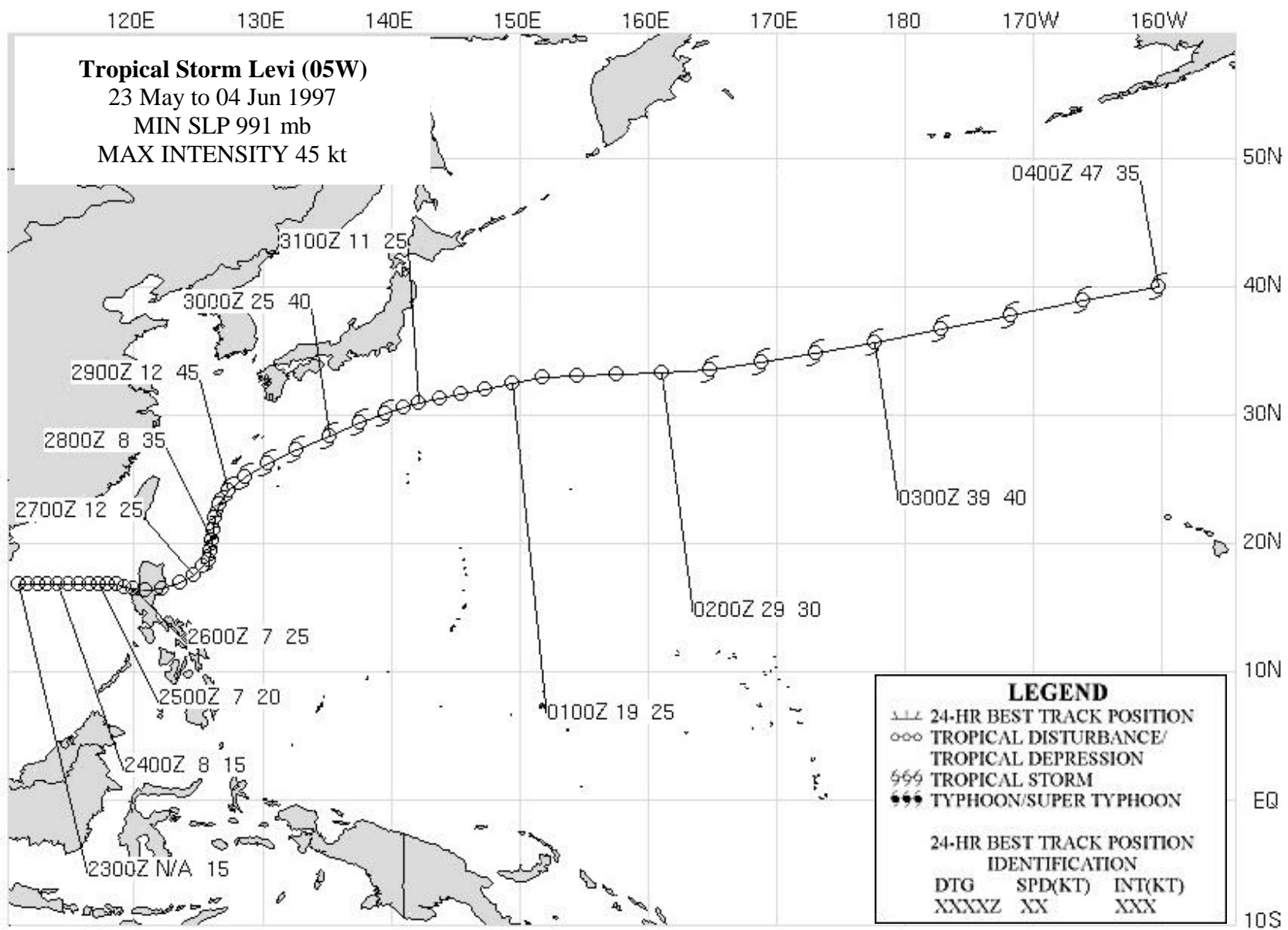


Figure 3-05-1. 281233Z May 1997 infrared imagery of Tropical Storm Levi (05W) as it moves on a northward track at its 45-kt (23-m/s) maximum intensity.

southern peripheries, with little consolidation near the center. On 24 May, convection began to organize near the LLCC, and a Tropical Cyclone Formation Alert (TCFA) was issued at 0600Z on the 25th. Twelve hours later, the first warning was released on Tropical Depression (TD) 05W. The depression moved eastward and crossed central Luzon on 26 May, producing copious amounts of rainfall which caused severe flooding. This forced the closure of government offices, schools, and the Philippine stock market in Manila. The main generator at the Ninoy Aquino International Airport in Manila was totally submerged by floodwater, shutting down the airport for several hours. A total of 33 people lost their lives in the Philippines, primarily from flooding and mudslides.

After emerging into the Philippine Sea late on 26 May, TD 05W began to move to the northeast and was soon upgraded to Tropical Storm Levi (05W). On 28 May, the tropical storm reached its maximum intensity of 45 kt (23 m/sec). At this point, the system began to move on a northward track, steered by the monsoonal mid-tropospheric flow which connected the southwest monsoon with the Mei-yu front south of the Ryukyu Islands. Levi maintained its 45-kt (23 m/sec) winds during recurvature until 29 May at 1800Z when upper level westerly shear began to weaken the cyclone. The final warning on Tropical Storm Levi (05W), valid at 0600Z on the 30th, was issued as the system raced off to the northeast.



TYPHOON MARIE (06W)

Typhoon Marie (06W) was the only of the three May tropical cyclones to develop into a typhoon. The disturbance that eventually became Marie developed much farther east than normal for a May tropical cyclone. An active monsoon trough extended to the Marshall Islands in response to strong low level equatorial westerly winds associated with the developing 1997 El Niño. The disturbance was first mentioned on the 26 May Significant Tropical Weather Advisory (ABPW) and was located about 250 nm (463 km) east of Kwajalien Atoll (WMO 91366). A Tropical Cyclone Formation Alert (TCFA) was issued at 1630Z on 26 May, and the first warning was produced soon thereafter at 1800Z. For the next two days, Tropical Depression 06W intensified

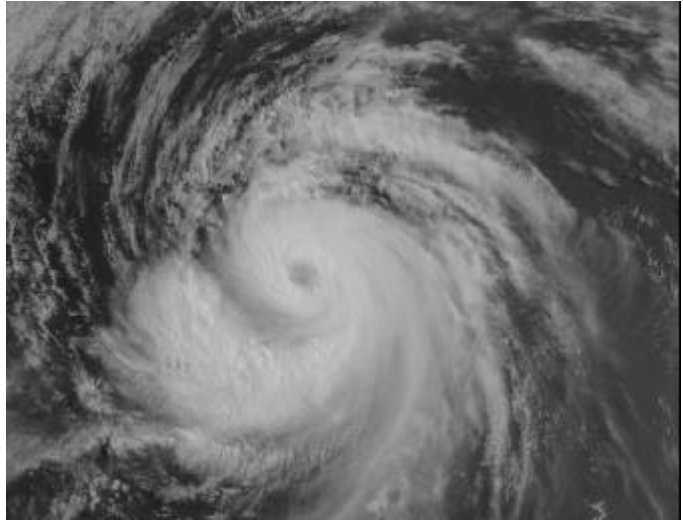
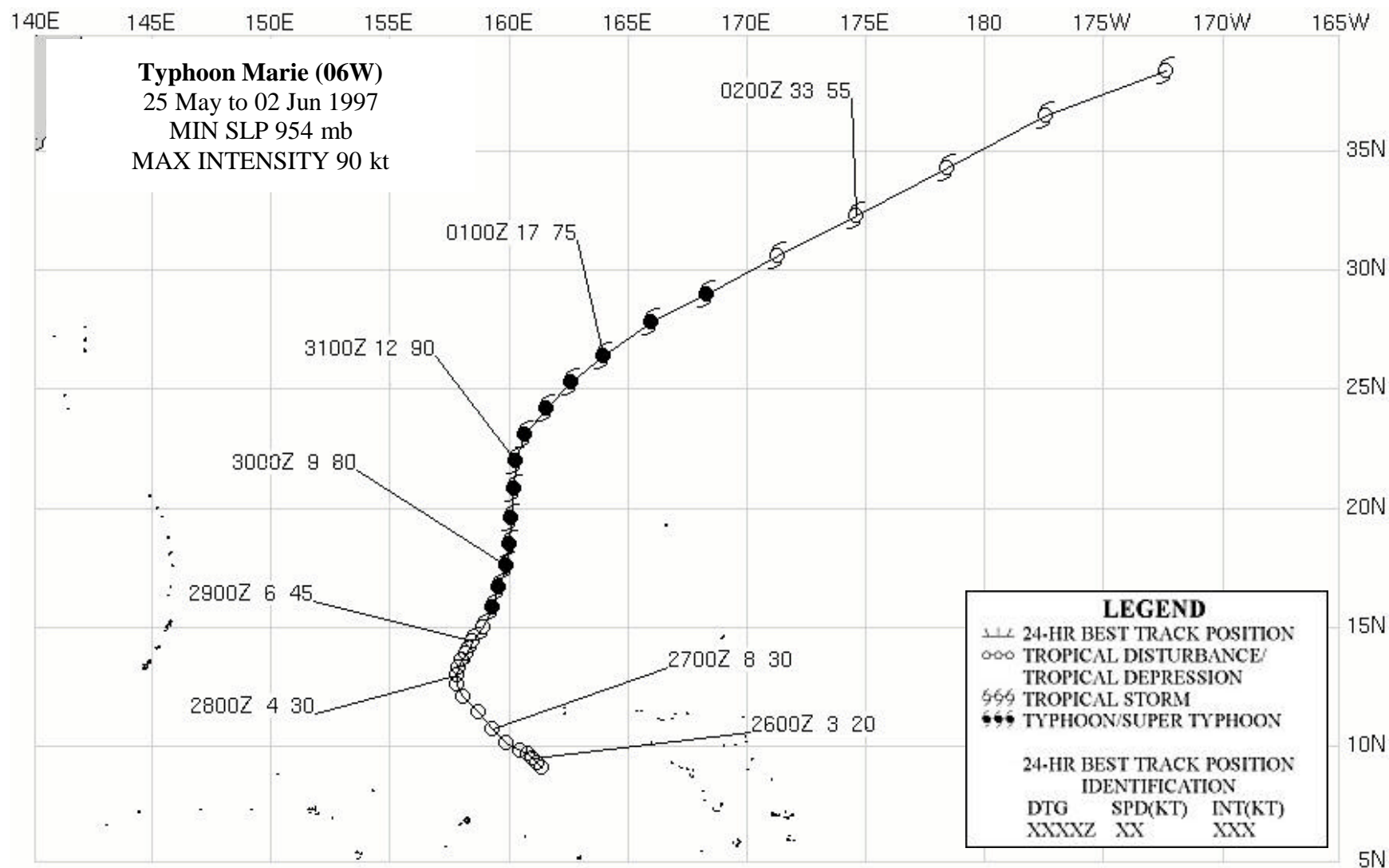


Figure 3-06-1. 302132Z May 97 GMS visible imagery of Typhoon Marie near its 90 kt (47 m/s) peak intensity. At this time, Marie was moving northward at 12 kt (22 km/hr).

slowly as it moved northward through the subtropical ridge, which had been bisected by the passage of a short wave trough. The system reached tropical storm strength at 1800Z on the 28th and then intensified for the next 24 hours, while moving to the north-northeast at 5-9 kt (9-17 km/hr). At 1200Z on 29 May, Marie achieved typhoon intensity. While moving on a nearly northward track, Typhoon Marie continued to intensify, reaching its maximum intensity of 90 kt (46 m/s) at 0000Z on 31 May. Afterwards, the typhoon moved towards the northeast and began to slowly weaken. By 1800Z on 1 June, Marie's intensity had fallen below typhoon intensity, and the system was undergoing extratropical transition. The final warning was issued at 0600Z on the 2nd as the system accelerated to over 40 kt (74 km/hr), and its transition was nearly complete. Marie spent its entire life over water, and there were no reports of significant impact received by JTWC.



SUPER TYPHOON NESTOR (07W)

I. HIGHLIGHTS

Super Typhoon Nestor (07W) was the strongest of three typhoons to develop in June, and was the second of 11 super typhoons to occur in 1997. It was a spin-off of strong equatorial westerly winds associated with the developing 1997 El Niño. Nestor's development in the southern Marshall Islands is the farthest east a June typhoon has developed since records have been kept.

II. TRACK AND INTENSITY

In early June, strong equatorial low level westerly winds extended to the International Date Line (IDL) in association with the development of the 1997 El Niño. As Typhoon Marie (06W) was nearing the end of its tropical life, the disturbance that would become Super Typhoon Nestor (07W) was beginning its 2-week tropical existence. It was first identified on the

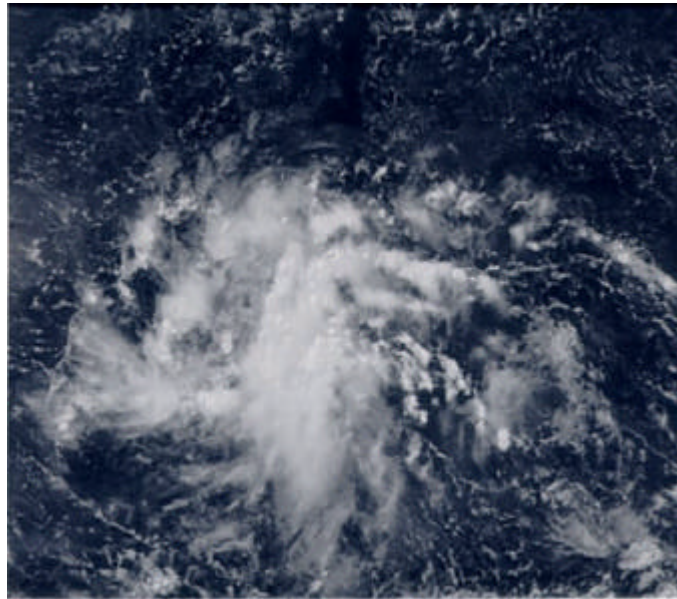


Figure 3-07-1 040232Z June 1997 GMS visual imagery of the tropical disturbance that would eventually become Super Typhoon Nestor (07W).

Significant Tropical Weather Advisory (ABPW) at 0600Z on 1 June as a persistent area of convection about 70 nm (130 km) south-southwest of Majuro. For the next two days, the disturbance moved to the west-southwest at 5-7 kt (9-13 km/hr), with no noticeable intensification. On the evening of 03 June, near 165E, the system turned to the northwest, but it continued to have difficulty organizing (Fig. 3-07-1). A Tropical Cyclone Formation Alert (TCFA) was issued at 0830Z on the 4th. A second TCFA was issued 24 hours later. Beginning at 1800Z on the 5th, the system quickly pulled itself together and reached tropical storm intensity by the time the first warning was issued at 0000Z on the 6th. Nestor assumed a heading toward the Mariana Islands. Statistical and statistical-dynamic prediction models indicated west-northwestward movement for several days, initially taking the storm south of Guam. However, these models soon started walking the track up over Saipan. On the morning of 08 June, Tropical Storm Nestor (07W) veered away from the Mariana Islands to a north-northwestward track and continued intensifying for four days, reaching peak intensity of 140 kt (72 m/s) at 1200Z on the 10th, approximately 200 nm (370 km) northeast of Saipan. Figure 3-7-2 compares the Dvorak enhancement image (a) with the microwave image (b) just before Nestor attained its maximum intensity. The system temporarily heeled over to the northwest before turning to the north and recurving about 20 nm (37 km) east of Iwo Jima (WMO 47981). Iwo Jima recorded wind gusts to 102 kt (51 m/s) at 1500Z on the 12th when the typhoon passed about 20 nm (37 km) to the

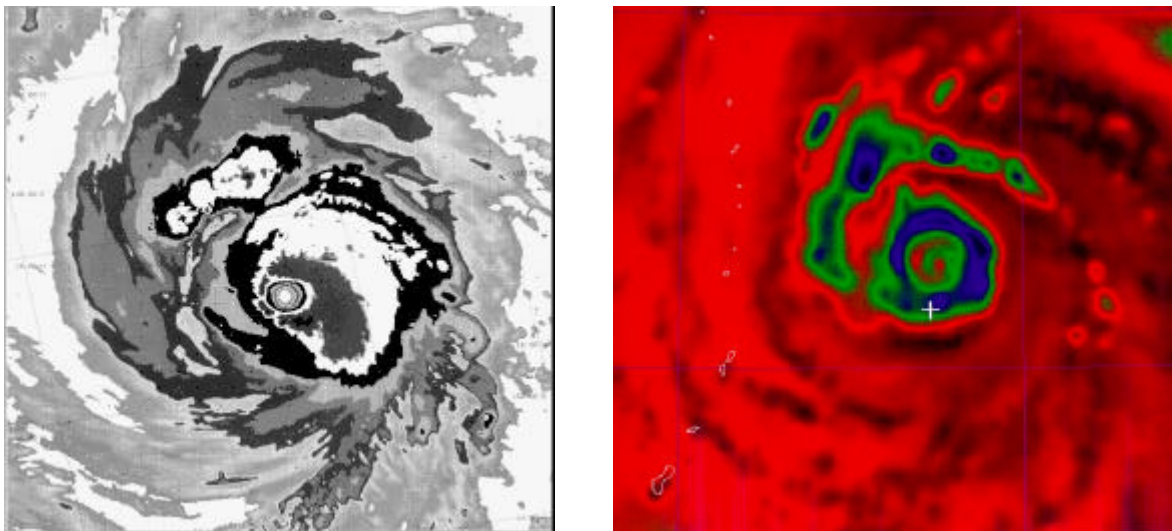


Figure 3-07-2 (a) 091547Z June 1997 enhanced infrared imagery using the BD enhancement curve and (b) 092013Z June 1997 DMSP microwave imagery (SSM/I) of Super Typhoon Nestor (07W) at an estimated intensity of 125-130 kt (65-68 m/s). The system is approximately 190 nm (352 km) east-northeast of Saipan.



Figure 3-07-3 120332Z June 1997 GMS visual imagery of the eye of Nestor just prior to recurvature. The intensity at this time was estimated to be 115 kt (60 m/s).

east. At 0200Z on the 13th, the typhoon passed about 30 nm (56 km) west of Chichijima (WMO 47971), which reported wind gusts to 96 kt (50 m/s). Nestor took a parabolic track to the northeast and east, eventually doubling its forward speed to over 30 kt (56 km/hr). The final warning by JTWC was issued at 0000Z on the 15th. Twelve hours later, the system had become a 50-kt (26-m/s) extratropical cyclone.

III. DISCUSSION

Statistical and statistical-dynamic models from 04 June to 08 June predicted west-northward motion for Nestor's circulation. These models consistently targeted an area 100 nm (185 km) to either side of Guam. When the first dynamic models became available, they predicted a northward turn as early as 06 June. This was first indicated by an abrupt turn to the north by NOGAPS, followed by northwestward motion. The Geophysical Fluid Dynamics Navy model (GFDN) and the British Meteorological Office model (EGRM) mimicked the motion of NOGAPS, but were slower to accelerate the system to the northwest. The short term predictions turned too abruptly (nearly perpendicular to the actual track), but the longer term predictions of NOGAPS were relatively accurate. This occurrence of premature and abrupt track changes has been discussed by Carr and Elsberry (1997), who attribute it to a tendency towards early pattern/region transition from the Standard/Dominant Ridge to Poleward/Poleward Oriented, especially for early (12 to 24 hrs) forecast points. They point out the characteristic good accuracy of the 72-hour forecasts and recommend using the 72-hour dynamic model prediction guidance and merging it into the shorter term statistical predictions to derive an overall forecast. The daily changes in the NOGAPS predictions are superimposed upon Nestor's best track to illustrate the premature turning of the short term predictions.

IV. IMPACTS

Aside from passing through the Volcano Islands and the Bonin Islands of Japan, Nestor remained over water. Nestor did produce some high waves on Saipan. No reports of significant damage were received at JTWC.

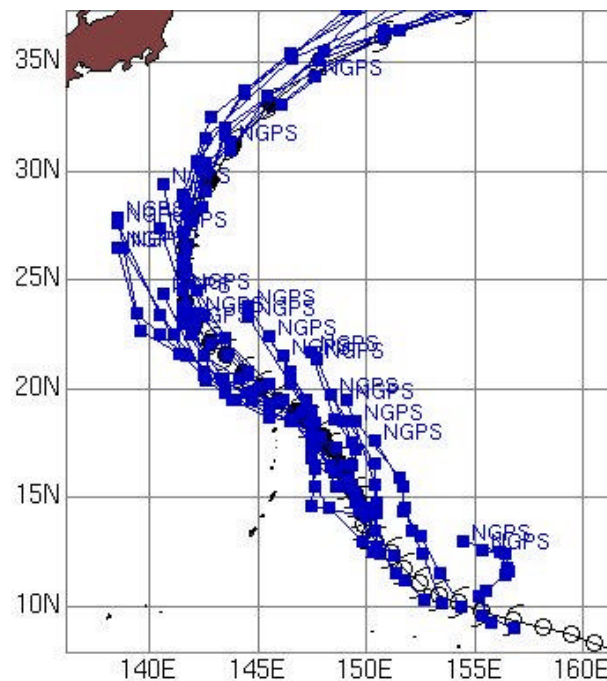
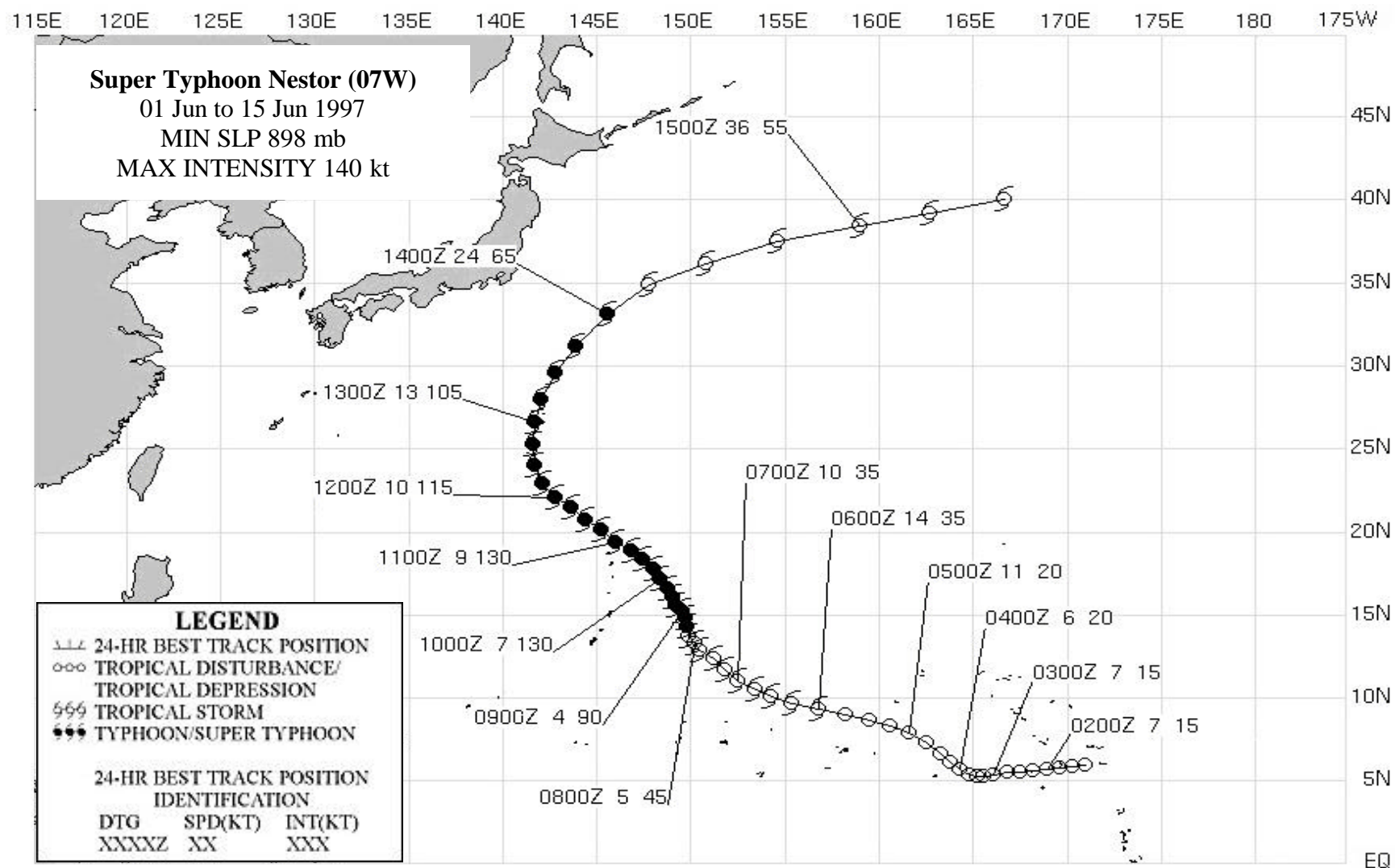


Figure 3-07-4 A history of NOGAPS track forecasts illustrating the models tendency toward premature short term turning.



TYPHOON OPAL (08W)

The disturbance that was to become Typhoon Opal (08W) was first mentioned on the Significant Tropical Weather Advisory (ABPW) on 12 June as an area of persistent convection about 150 nm (278 km) southwest of Guam. The disturbance was slow to develop as it moved to the west-northwest at 6-8 kt (11-15 km/hr). However, by 14 June at 2030Z, the system had organized sufficiently to warrant the issuance of a Tropical Cyclone Formation Alert (TCFA). The first warning on Tropical Depression 08W was valid at 0000Z on the 15th. One day later, the depression attained tropical storm strength (35 kt or 18 m/sec), and began to track toward the north. By 0000Z on 17 June, it had reached an intensity of 65 kt (34

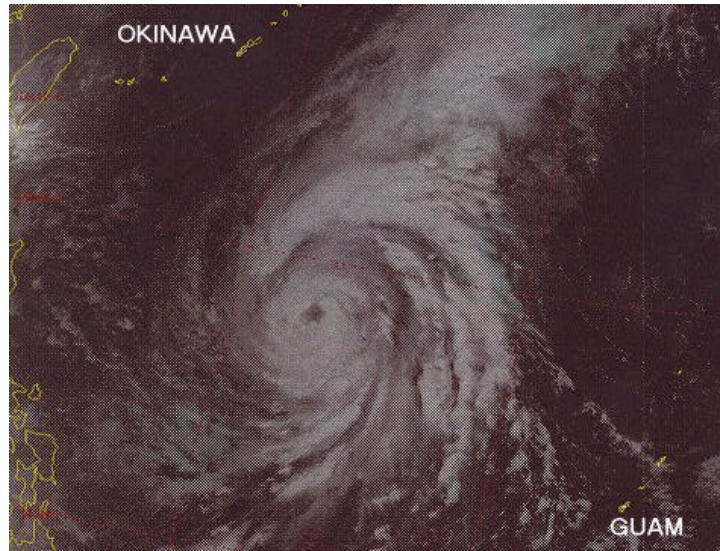
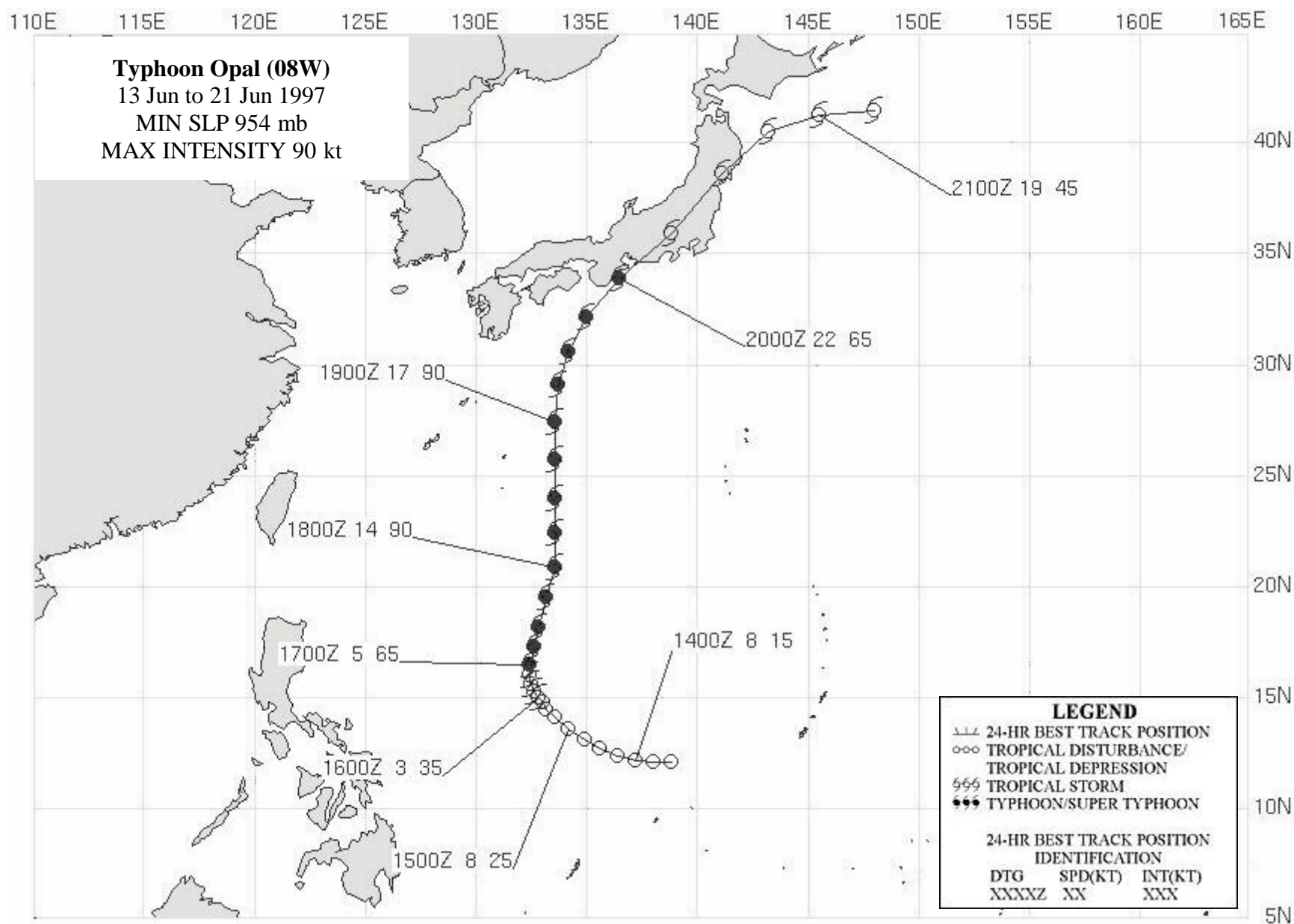


Figure 3-08-1. Opal reaches its peak of 90 kt (47 m/s) while moving on a north-oriented track (171059Z June low-light visible DMSP imagery).

m/sec). Twelve hours later, Typhoon Opal was at its maximum intensity of 90 kt (47 m/sec), which it maintained for 36 hours (Figure 3-08-1). As Opal approached 20N latitude, it accelerated to speeds ranging from 14-17 kt (26-31 km/hr). By 0000Z on 18 June, westerlies from a trough to the northwest began to impinge upon Opal's outflow. This can be seen in Figure 3-08-1. As Opal neared 30N latitude, it began to turn to the northeast, subsequently accelerating and weakening. Opal made landfall near Shionomisaki, Japan (WMO 47778) at 2200Z on 19 June with an intensity near 65 kt (33 m/sec). A minimum pressure of 980.3 mb was observed during the passage. Six hours after making landfall, Tropical Storm Opal (08W) passed about 50 nm (93 km) northwest of Tokyo, and at 1500Z on 20 June, Opal exited Honshu on an east-northeast track with 55 kt (29 m/sec) winds. The final warning was issued at 0600Z on the 21st as the system became extratropical near 42N 167E while maintaining 40 kt (21 m/sec) winds.

Opal was one of three typhoons to develop in June. This level of activity has not been seen in the western North Pacific in June since 1965. It was the first tropical cyclone of 1997 to strike Japan.

As Opal approached south central Japan, a fisherman drowned while tying his boat to a pier. Opal caused only minor damage in Yokohama and Tokyo. Transportation was disrupted throughout eastern Japan, and 70 domestic flights were canceled.



TYPHOON PETER (09W)

I. HIGHLIGHTS

One of three typhoons to develop in June, Typhoon Peter (09W) achieved only minimal typhoon intensity. The cyclone moved on a northward track nearly 900 nm (1665 km) before recurving. It made landfall near Sasebo, Japan, paralleled the mountainous spine of Honshu, and eventually became one of the most intense extratropical cyclones of the year.

II. MOVEMENT AND INTENSITY

Typhoon Peter (09W) developed from a disturbance that was first detected early on the morning of 19 June as an area of persistent convection at the eastern edge of the monsoon trough, about 300 nm (560 km) southeast of Guam. This area, mentioned on the Significant Tropical Weather Advisory (ABPW) on 20 June, had characteristics of a monsoon depression with most convection on the south and east peripheries. After two days of slow development, deep convection began to consolidate near the center. As a result, the first Tropical Cyclone Formation Alert (TCFA) was issued at 0400Z on 22 June and a second TCFA was issued 24 hours later. However, when ERS-2 and NSCAT scatterometer-derived winds became available a short time later, the first warning was issued on Tropical Depression 09W at 0600Z on the 23rd. Scatterometer data played a critical role in ascertaining the cyclone's location and intensity throughout its life (see the discussion section). The developing cyclone spent its first four days on a west-northwest track, except for a temporary stair-step to the northwest on 20 June. Scatterometer wind data was again valuable as it indicated that the depression reached tropical storm intensity at 1200Z on the 23rd. By 24 June, a mid-tropospheric ridge had built to the southeast of Peter. This ridge imposed southerly steering, causing the tropical cyclone (TC) to take a sharp northward turn. Peter maintained this track for three days, covering about 900 nm (1665 km). On 25 June, conventional satellite imagery indicated that Peter was moving to the northeast, but microwave imagery data (SSM/I) revealed that the low level circulation center (LLCC) was maintaining a northward motion (Fig. 3-09-1). On 260600Z, Peter was upgraded to typhoon. It maintained a 65 knot (33 m/s) intensity for 36 hours, but developed no further. While tracking northward, Peter accelerated from an average speed of 10 kt (19 m/s) to 20 kt (38 m/s). Late on 27 June, Typhoon Peter began to weaken and turn northeastward. At 1800Z, on the 27th, Peter passed over

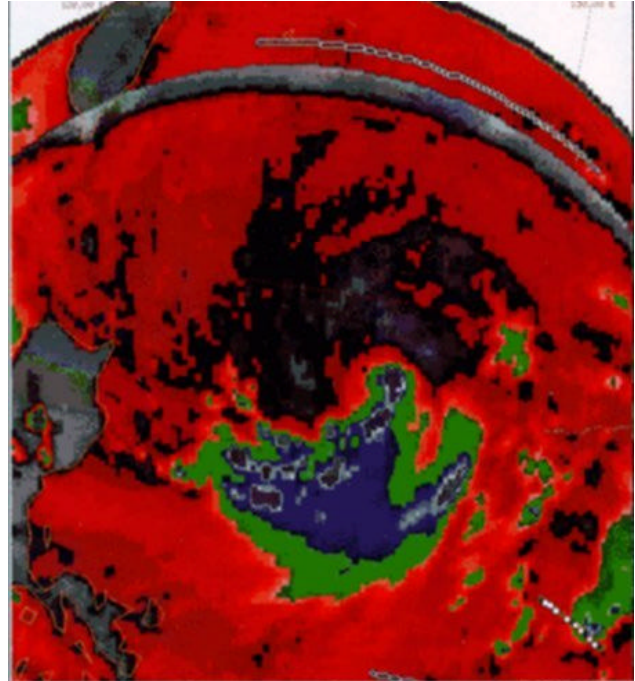


Figure 3-09-1. 251023Z June 1997 microwave image of Tropical Storm Peter (09W).

Nagasaki, Japan (WMO 47817) with 55-kt (29-m/s) 1-minute average sustained winds. Peter traveled to the northeast along the mountainous spine of Honshu and, less than one day after landfall, had nearly traversed the entire country from the southwest to the northeast. At 1900Z on the 28th, the weakened tropical storm entered the Pacific Ocean near Sendai (WMO 47590). On 29 June, Peter merged with a frontal system and completed its extratropical transition. As an extratropical system, the remnants of Peter became more intense than the system had been as a tropical system, reaching an intensity of 70 kt (36 m/s) on 30 June. It eventually weakened, and could no longer be found by 04 July.

III. DISCUSSION

Microwave and scatterometer data was used extensively to track and to ascertain the intensity and wind distribution of Peter. Figure 3-09-2 shows the scatterometer derived winds used to justify the issuance of the first warning on Tropical Depression 09W and then, later, to upgrade it. Scatterometer data was gathered from both the European Research Satellite (ERS-2) and the joint US-Japan Adobe satellite (N-Scat). The ERS provided a single swath of data, while the N-Scat provided dual swaths. Unfortunately, the N-Scat instrument ceased operation late in 1997. Figure 3-09-1 illustrates the value of microwave imager data in locating the center of a TC where the center is obscured by clouds. Both visual and infrared imagery from 1800Z on the 24th through 1800Z on the 25th suggested that Peter was moving to the northeast. However, microwave data allowed the analysts to confidently position the LLCC well to the west of the location indicated by conventional satellite imagery. Another data source became available when Peter moved within view of the Japanese weather radar network in the Ryukyu Islands, Kyushu, Shikoku, and Honshu.

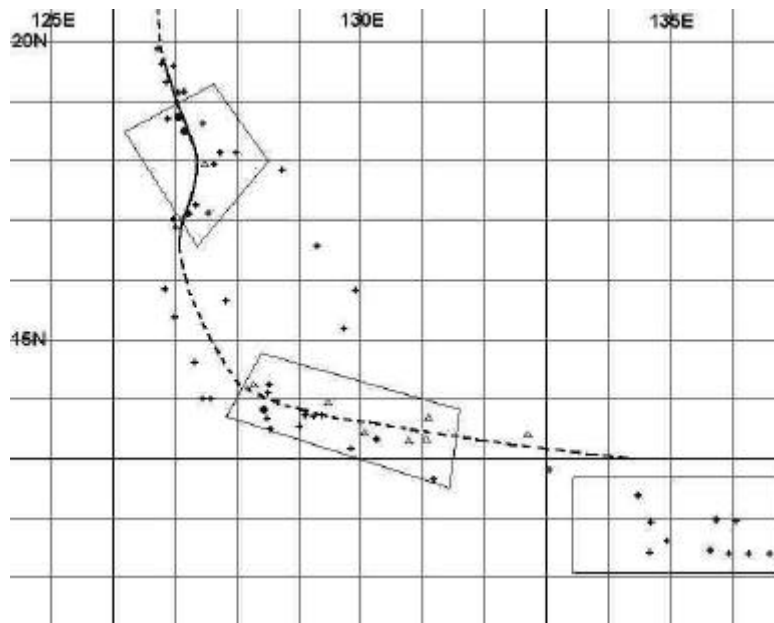
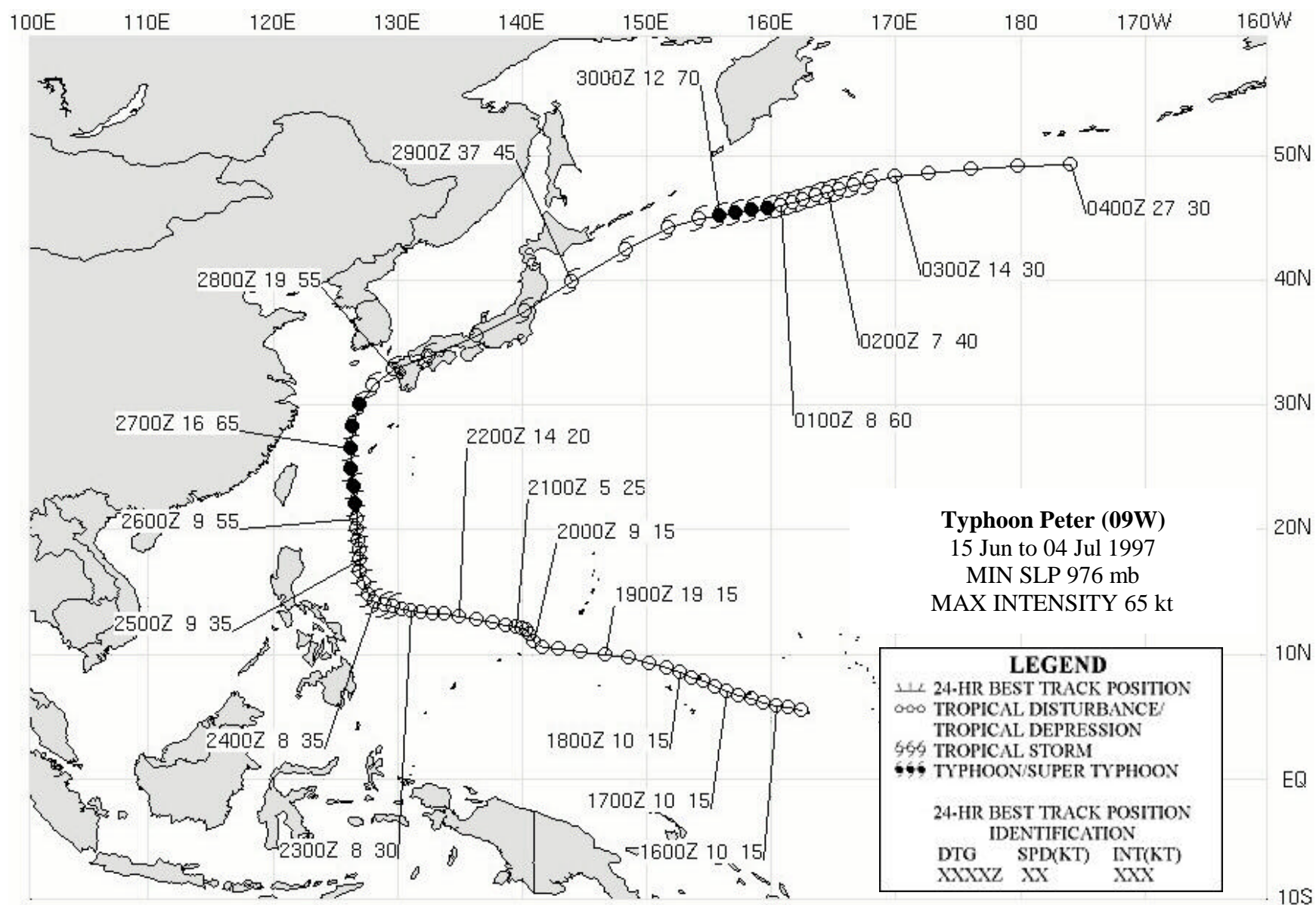


Figure 3-09-2. Conventional satellite fixes (+), scatterometer fixes (Δ), and microwave imager fixes (●) superimposed along the best track of Peter. The significance of the three boxes is explained in the text in the Discussion Section.

IV. IMPACT

Two American servicemen from Iwakuni Marine Corps Air Station were washed away in the high surf produced by Peter. At the Sasebo Naval Facility, damage was reported to be light. In port at Sasebo, the USS BELLEAU WOOD reported gusts to 54 kt (28 m/s), and the USS DUBUQUE measured gusts to 45 kt (23 m/s).



SUPER TYPHOON ROSIE (10W)

Super Typhoon (STY) Rosie (10W) originated as a tropical disturbance in the western Caroline Islands along the monsoon trough. The disturbance was first noted on the 15 July Significant Tropical Weather Advisory (ABPW) as an area of persistent convection. The pre-Rosie disturbance slowly tracked west-northwestward over the next few days; and on 18 July at 1400Z, a Tropical Cyclone Formation Alert (TCFA) was issued by JTWC. The first warning on Tropical Depression (TD) 10W was issued only four hours later. The now northwestward moving TC intensified to a typhoon by 0000Z on 21 July and reached its peak intensity of 140 kt (72 m/s) on the 22nd at 1200Z. Twelve hours later, Rosie began to weaken and slowly accelerate toward the north-northeast. The system made landfall near Okayama on the Japanese island of Shikoku around 0800Z on 26 July as a minimal typhoon with 65 kt (33 m/s) winds. Crossing over land, Rosie rapidly weakened as the main convection sheared away from the low-level circulation. It continued to weaken in the Sea of Japan as the exposed low-level and its remnants were tracked back over Japan and into the Philippine Sea where it dissipated. Rosie left two dead in Japan; and its passage resulted in power failures, landslides and widespread damage to buildings in the southern and central parts of the country.

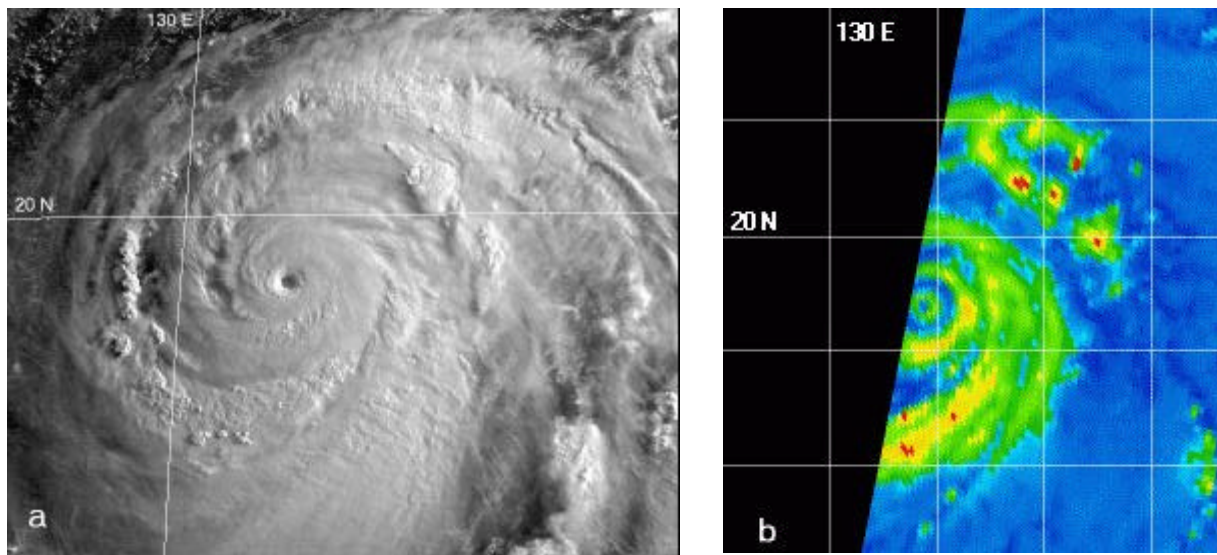
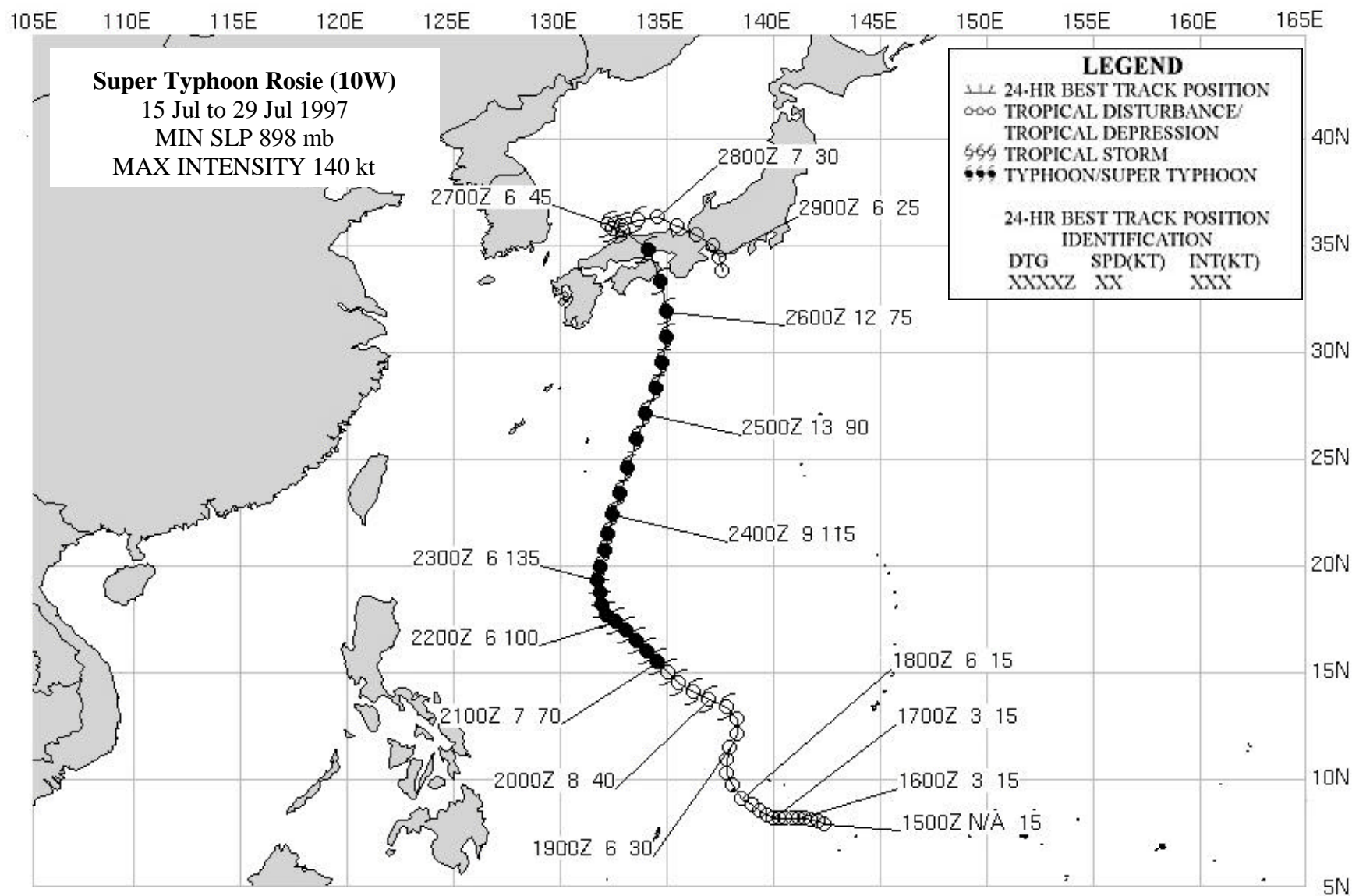


Figure 3-10-1 Rosie near peak intensity. (a) 222131Z July visible GSM imagery and (b) 222147Z July 85 GHz horizontally polarized DMSP imagery.



TROPICAL STORM SCOTT (11W)

Tropical Storm Scott formed in mid-July near 24N 150E from a Tropical Upper Tropospheric Trough (TUTT)-induced mid level disturbance. It was first noted on the 20 July Significant Tropical Weather Advisory (ABPW) as a closed low-level circulation with associated scattered convection. Initial development of the pre-Scott disturbance was inhibited by outflow from Super Typhoon (STY) Rosie (10W). However by 0000Z on 24 July system organization improved significantly, leading to issuance of a Tropical Cyclone Formation Alert (TCFA). The first warning on Tropical Depression (TD) 11W was issued just 6 hours later, at which time Rosie was located approximately 20 degrees west of TD 11W and moving

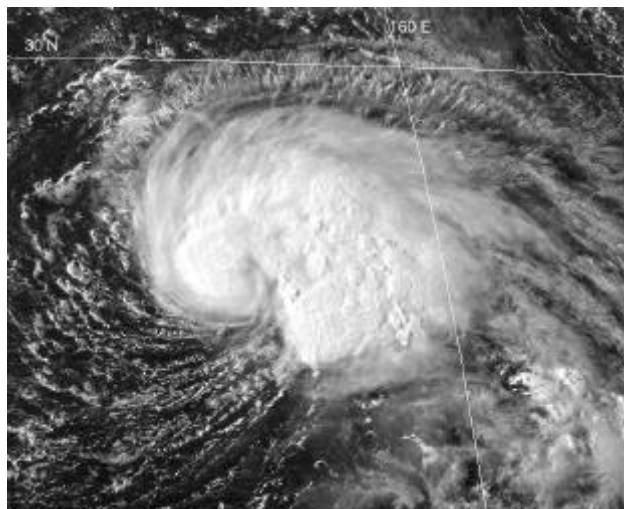
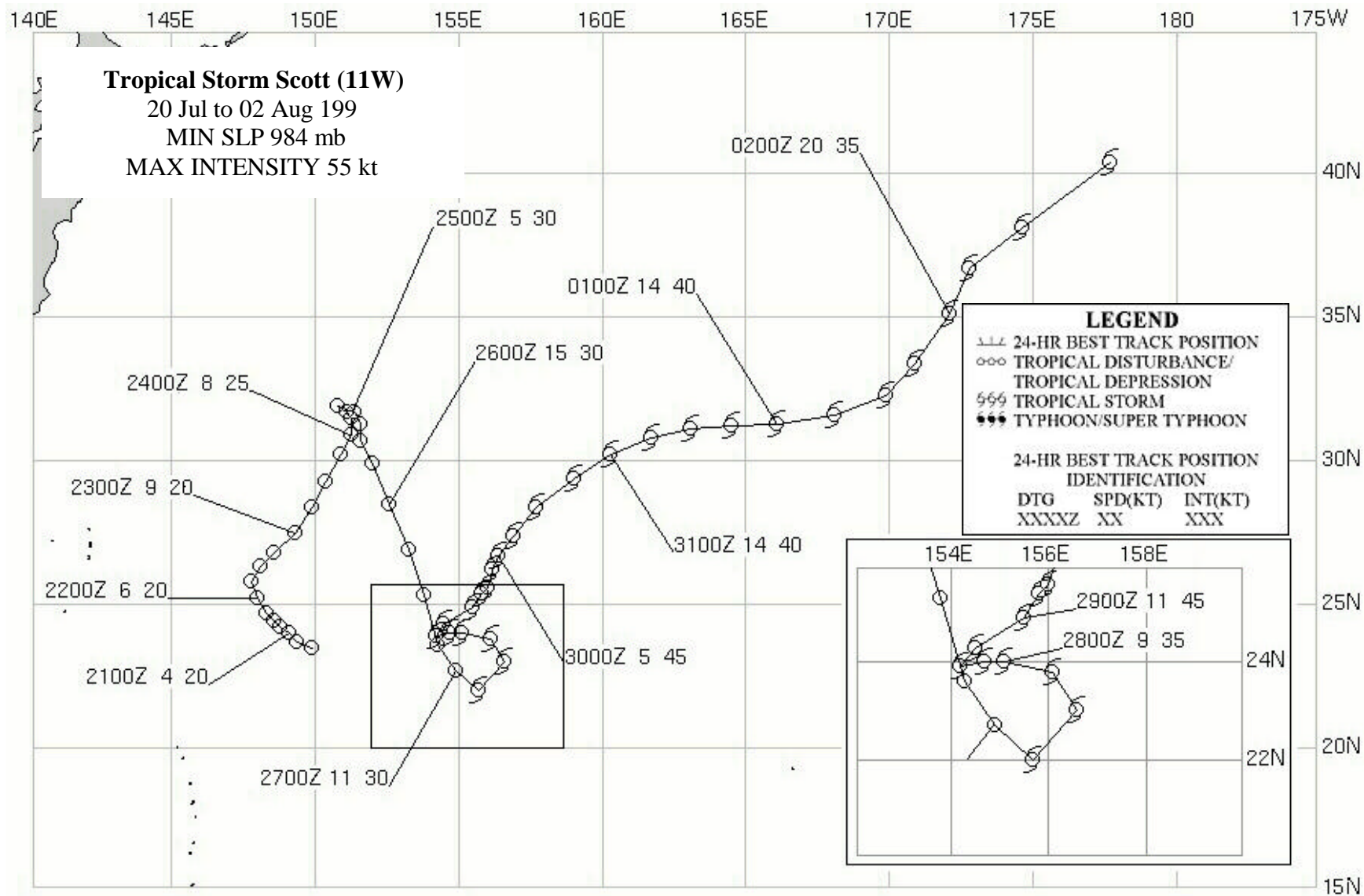


Figure 3-11-1 Tropical Storm Scott at peak intensity of 55 kt (28 m/s) on 29 July at 0633Z

north-northeastward with a large trailing anti-cyclone. The influence of this anti-cyclone caused TD 11W's northward track to shift to the southeast. TD 11W took a southeastward track instead of the more usual southwestward track attributed to the Indirect Tropical Cyclone Interaction (ITI) pattern because of the northwest-southeast orientation of the trailing anticyclone. After Rosie (10W) made landfall in Japan, this anticyclone became less significant as a steering influence on TD 11W. By 26 July, TD 11W appeared to be dissipating and JTWC issued what was thought to be the final warning. Soon afterward, development recommenced, resulting in a second TCFA issued at 1730Z on the 26th. Scott reached tropical storm intensity at 0600Z on the 27th and began its second major track change as it turned first toward the northwest for 24 hours and then finally to the northeast. The system reached its peak intensity of 55 kt (28 m/s), at 0600Z on the 29th and held it through 1800Z the same day. Scott began to slowly weaken, continuing northeastward, until it merged with a frontal system on 2 August. JTWC issued a final warning at 1200Z on this day. Tropical Storm Scott remained over water for its entire existence and JTWC received no reports of damage.



TYPHOON TINA (12W)

The tropical disturbance that became Typhoon Tina (12W) initially formed as an area of convection in the eastern Caroline Islands and was first noted on the Significant Tropical Weather Advisory (ABPW) at 0600Z on 21 July. The first Tropical Cyclone Formation Alert (TCFA) was issued at 1000Z on 23 July. However, upper level wind shear caused the system to lose much of its deep convection and the TCFA was cancelled. As the disturbance continued to track northwestward, vertical wind shear gradually relaxed and the system began to reorganize. A second TCFA was issued at 0830Z on the 29th. The system's organization continued to improve and the first warning on Tropical Depression (TD) 12W was issued at 1800Z the same day. TD 12W continued to track northwestward under the steering influence of the subtropical ridge, and was upgraded to Tropical Storm Tina (12W) with the 30 July 1800Z warning. The system reached typhoon strength by 1200Z on 3 August, with continued movement to the northwest. Interaction between the cyclone and the subtropical ridge resulted in a Poleward/Poleward Oriented pattern/region (see chapter 1), causing a gradual track change from northwestward to northward. Typhoon Tina (12W) reached its peak intensity of 90 kt (46 m/s), on 5 August at 0600Z. Naha airport in Okinawa reported 50 kt (26 m/s), sustained winds on the evening of 6 August as Tina passed west of the island. The system began to weaken as it moved toward the Korean Peninsula and encountered vertical wind shear. Tina made landfall along the South Korean coast at approximately 2200Z on 8 August. JTWC issued the final warning on the system at 1200Z, 9 August. Tina passed close to Pohang, Korea, early on the 9th, which recorded wind of 25 kt (13 m/s) sustained with gusts to 48 kt (25 m/s), and a minimum pressure of 995.3 mb. The system continued to track northeastward and dissipated over the Sea of Japan.

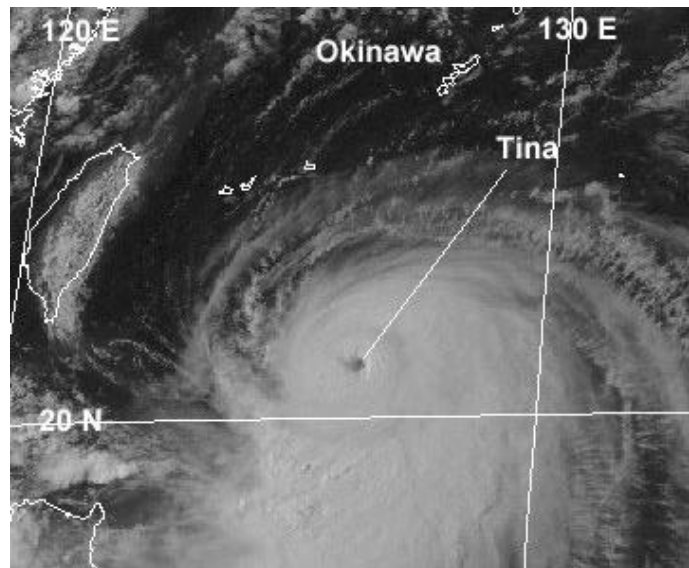
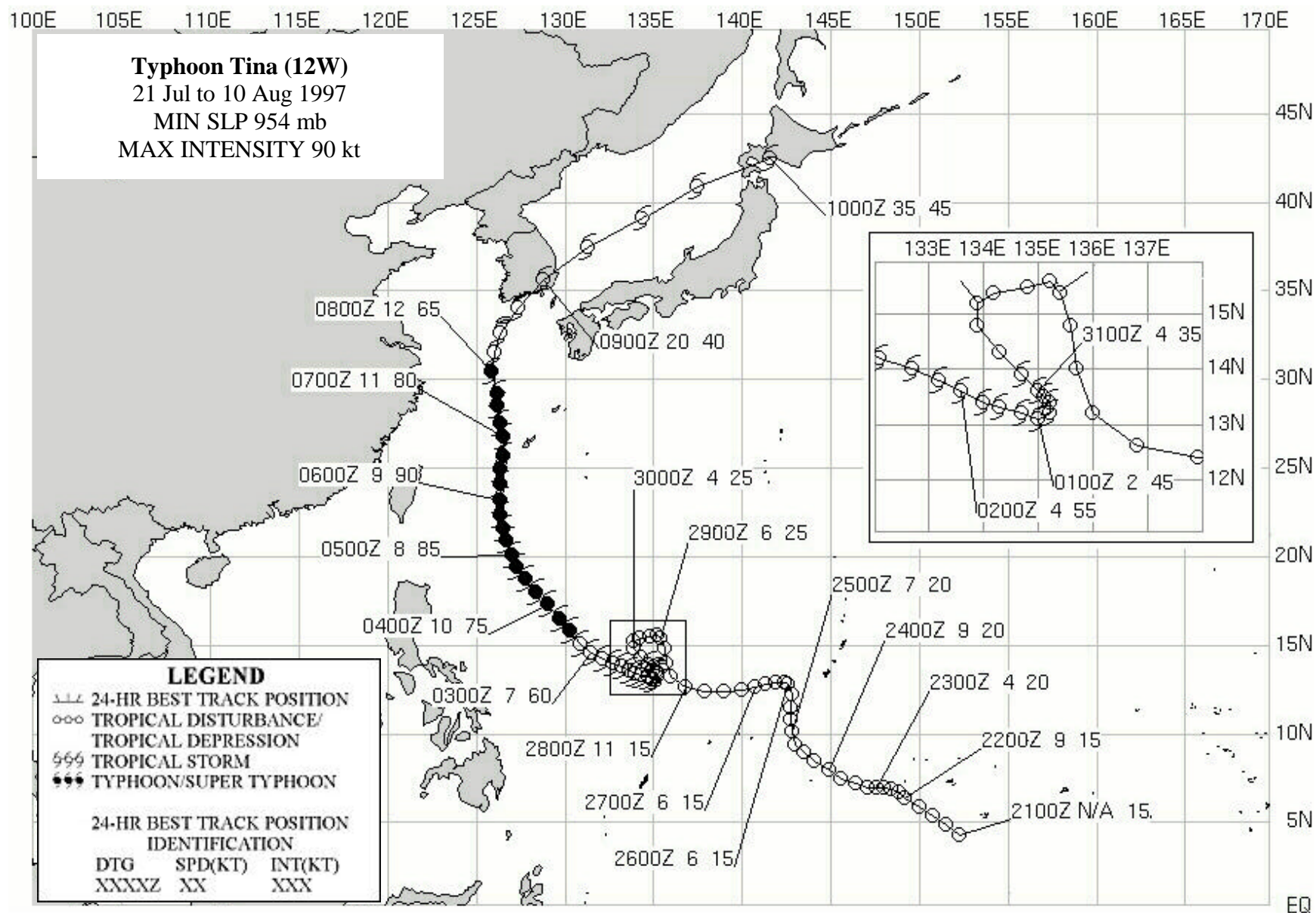


Figure 3-12-1 Typhoon Tina (12W) at 0730 on 5 Aug, near peak intensity of 90 kt (GMS 5 visible imagery).



TYPHOON VICTOR (13W)

The topical disturbance that became Typhoon Victor (13W) initially formed around 28 July, developing from an area of convection moving west-northwestward within the monsoon trough, just west of Luzon. Initially, moderate upper-level wind shear kept the deep convection to the south of the low-level circulation center. The disturbance was first noted on the Significant Tropical Weather Advisory (ABPW) at 0600Z on 30 July. The first warning on Tropical Depression 13W was issued at 1800Z the same day (A TCFA was not issued). TD 13W was initially steered by a mid-level ridge located to its southeast, resulting in a northward track. At 1200Z on 31 July, the system was upgraded to a tropical storm. Victor continued tracking northward, intensifying slowly under moderate vertical wind shear. By 0600Z on 2 August the deep convection consolidated over the low-level circulation center and intensification became more rapid. Victor reached its peak intensity of 65 knots just prior to making landfall at 1200Z on 2 August near Hong Kong (Figure 3-13-1). The cyclone weakened over land as it accelerated and tracked northward over southern China. By 4 August, the remnants of Victor merged with a frontal boundary west of Shanghai.

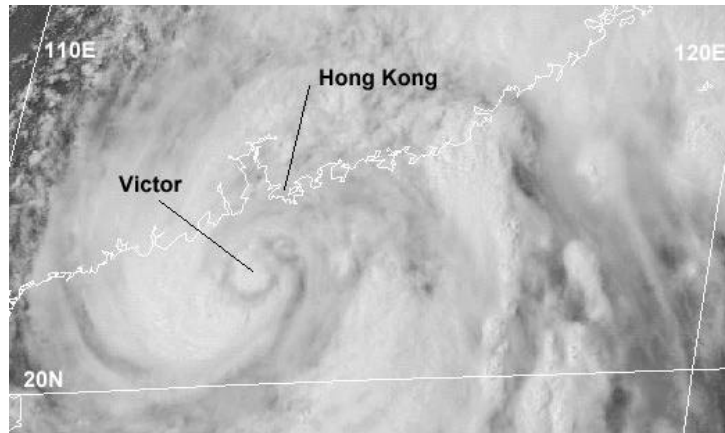
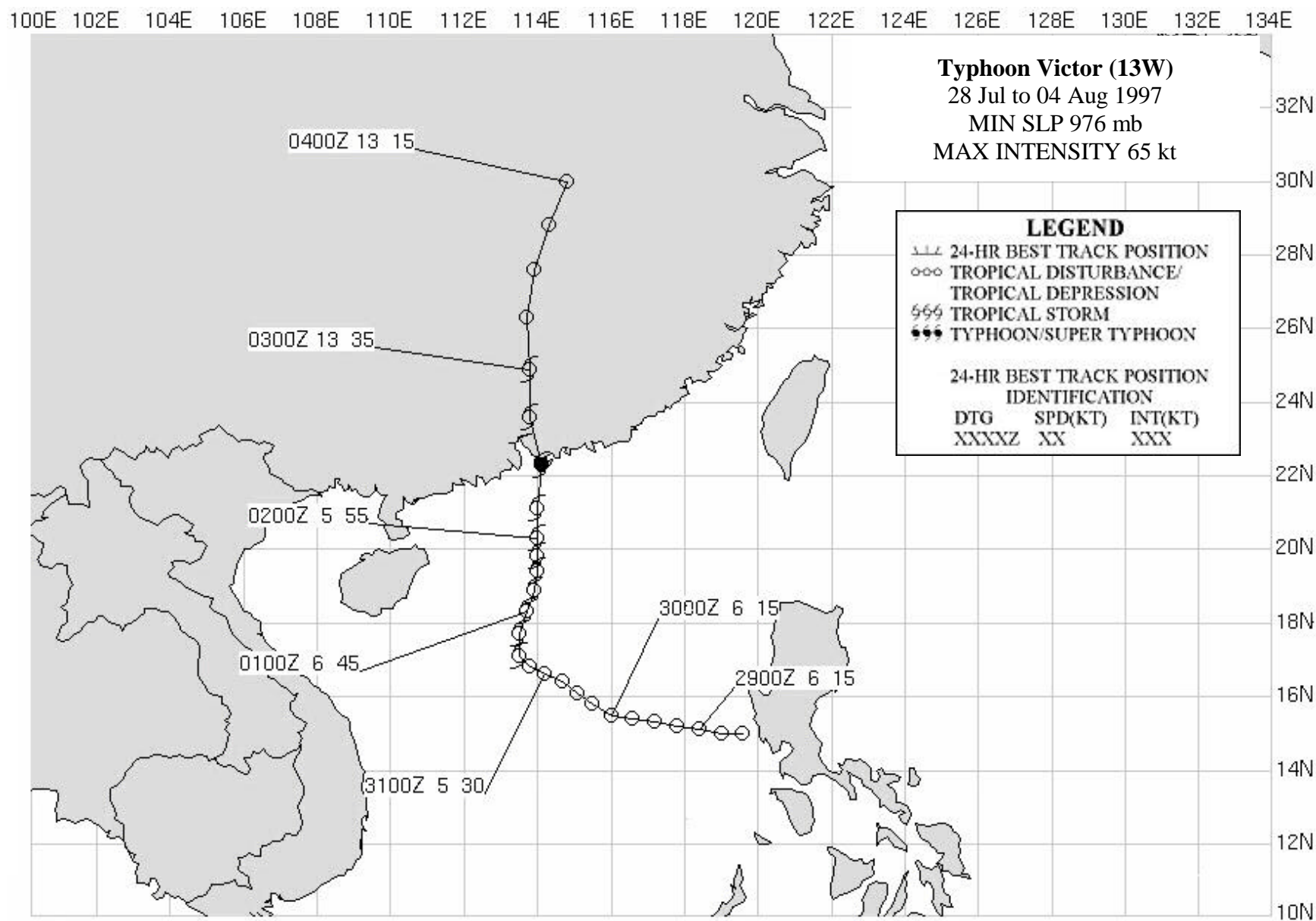


Figure 3-13-1 Typhoon Victor (13W) at 020634Z August, just prior to landfall (GMS 5 visible imagery).

Although originally classified as a tropical storm, Victor was upgraded to a minimal strength typhoon in post analysis, based on synoptic data recorded as it made landfall. Published press reports attributed one death and over 30 injuries in Hong Kong to Victor. In Guangzhou Province, China, heavy flooding left 49 dead and 12,000 homes destroyed.



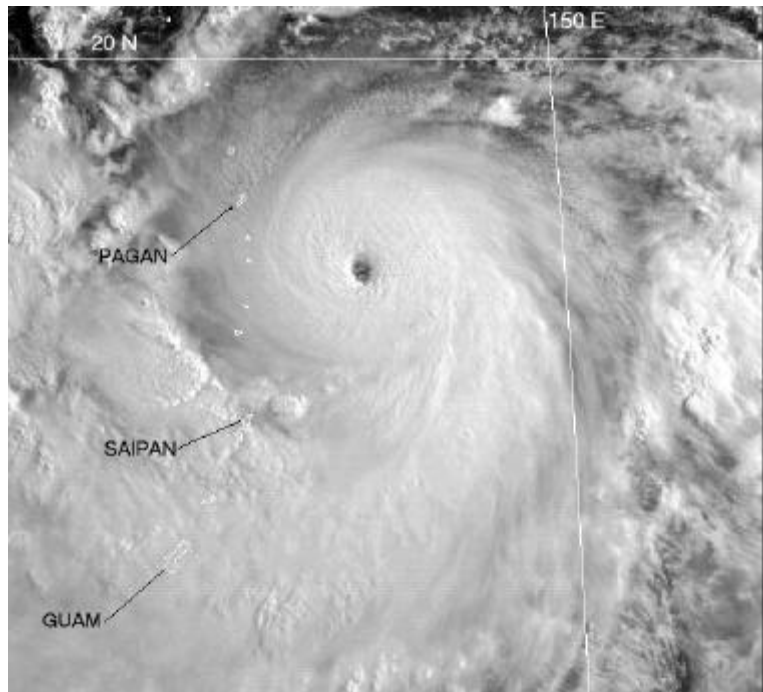
SUPER TYPHOON WINNIE (14W)

I. HIGHLIGHTS

Winnie formed at low latitudes in the Marshall Islands and was the fourth of eleven tropical cyclones (TCs) to attain super typhoon intensity in the western North Pacific during 1997. It was one of ten TCs that formed east of 160E and south of 20N; the "El Niño" box in Figure 3-3a. Winnie was a straight running TC that passed over Okinawa, and later made landfall on the eastern coast of China, where it was responsible for loss of life and considerable damage. When it was near Okinawa, the typhoon formed concentric eyewall clouds. The 200 nm (370 km) diameter of the outer eyewall cloud, observed by satellite and radar, was one of the largest ever recorded.

II. TRACK AND INTENSITY

During the first week of August, two TCs, Tina (12W), and Victor (13W), moved northward in the western portion of the West North Pacific (WNP) basin. Concurrent with the evolution of these TCs, an area of deep convection associated with the El Niño related low latitude westerly wind flow east of 160E persisted near the Marshall Islands. The disturbance was added to the 5 August Significant Tropical Weather Advisory (ABPW) after satellite imagery and synoptic data indicated a low-level cyclonic circulation with sea-level pressure in the region approximately 2 mb below normal.



The monsoon depression gradually became better organized as it moved steadily toward the west-northwest. The deep convection became more consolidated and cirrus outflow

became organized in a well-defined anticyclonic pattern, while the sea-level pressure slowly fell. Based on increased organization of the deep convection, sea-level pressures estimated at 1006 mb, and divergent outflow aloft (as indicated by animated water-vapor imagery) a Tropical Cyclone Formation Alert (TCFA) was issued at 0230Z on the 8th. The first warning on Tropical Depression (TD) 14W soon followed, valid at 0600Z the same day, based on a satellite intensity estimate of 30 kt (15 m/sec). This large TC intensified and was upgraded to Tropical Storm

Figure 3-14-1 Winnie nears its peak intensity of 140 kt (72 m/sec) as it approaches the Northern Mariana Islands (112133Z August visible GMS imagery).

Winnie (14W) with the 0600Z warning on 9 August. Winnie intensified quickly and became a typhoon by 0000Z on the 10th, and peaked at an intensity of 140 kt (72 m/sec) at 0000Z on the 12th (Figure 3-14-1). While still east of the Mariana Island chain. At 0600Z on the 12th, the system passed between the islands of Alamagan and Pagan. Winnie continued on its west-northwestward course and maintained an intensity of 140 kt (72 m/sec) for 24 hours, then began to slowly weaken as it approached the Ryukyu Islands. By 14 August, Winnie showed signs of developing concentric wall clouds which became more distinct on 15 and 16 August. As the typhoon passed through the Ryukyu Islands on 17 August, the inner wall cloud began to dissipate as the large-diameter outer wall cloud became well defined (see discussion below). Winnie moved across the East China Sea and made landfall on the eastern coast of China approximately 140 nm (260 km) south of Shanghai shortly before 1200Z on 18 August. The system passed across Manchuria and quickly dissipated as it moved into the mountainous terrain north of Vladivostok. The final warning was issued valid at 0000Z on the 19th. The remnants of Winnie were eventually observed to have recurved to the northeast.

III. DISCUSSION

a. Winnie's large-diameter outer eye wall cloud.

The well-defined eye of a mature TC is probably one of nature's most remarkable and awe-inspiring phenomena. In the Dvorak (1975, 1984) classification scheme, the intensity of a TC is estimated from several characteristics of satellite imagery. These include the distance of the low-level circulation center to the deep convection; the size of the central dense overcast; the cloud-top temperatures, the horizontal width of the eye wall cloud; and the width and extent of peripheral banding features. The basic TC pattern types identified by Dvorak are: (1) the "shear" pattern; (2) the "curved band" pattern; (3) the "central dense overcast" pattern; and, (4) the "eye" pattern. Of these pattern types, the "eye" pattern is probably the best known to the laymen.

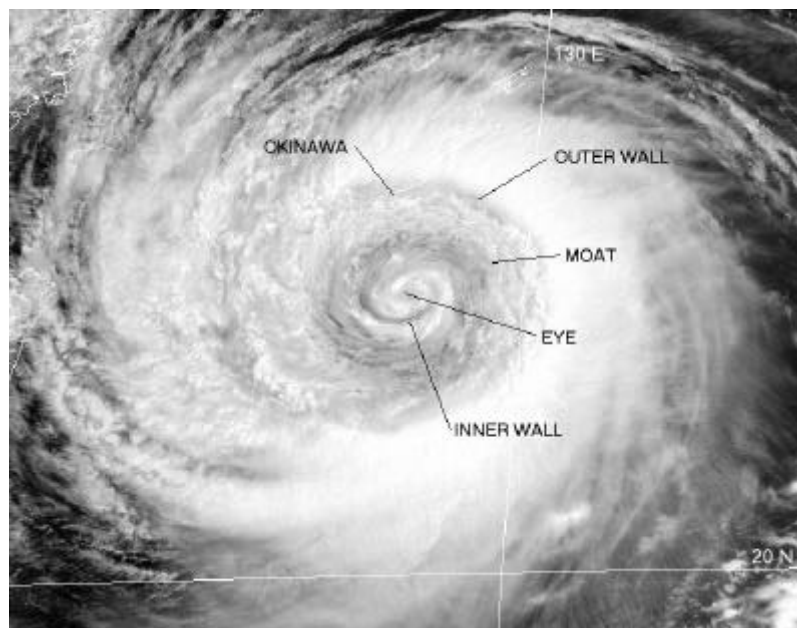


Figure 3-14-2 Winnie's outer wall cloud passes over Okinawa bringing typhoon-force winds as the small eye and inner wall cloud (within a relatively cloud-free moat) pass to the south. (170133Z August visible GMS imagery.) The black dot indicates the Kadena NEXRAD location.

The TC eye can be ragged or well-defined. In general, the more sharply defined the eye becomes on satellite imagery, the more intense the TC is likely to be. The average satellite-observed TC

eye diameter is between 30 and 45 nm (55 - 85 km) (Weatherford 1984). Eyes with diameters less than 30 nm (55 km) are considered to be small, while those with diameters greater than 45 nm (85 km) are considered to be large. In the Dvorak scheme, the intensity of a TC with a large well-defined eye is capped at 115 kt (59 m/sec), and the intensity of a TC with a large ragged eye is capped at 90 kt (46 m/sec), regardless of other characteristics observed on the satellite imagery. Some extremes of eye sizes include the small, 8-nm (15-km) diameter eye of Super Typhoon Tip (JTWC 1979 - observed by aircraft), and the radar-observed, large, 200-nm (370-km) diameter eye of Typhoon Carmen (JTWC 1960).

Some TCs, especially the intense ones, develop concentric wall clouds separated by a relatively cloud-free moat. In such cases, the outer wall cloud may contract while the inner one collapses in a process known as eyewall replacement. This has been discussed at length by Willoughby et al. (1982) and Willoughby (1990). These authors also note that TC eyes almost invariably contract during intensification so that smaller eyes and extreme intensity tend to be correlated. The Dvorak scheme has no special rules for concentric eyewall clouds. This is most likely because a cirrus overcast normally obscures the outer wall cloud in satellite imagery.

As Winnie moved toward Okinawa on August 16, a large outer rain band began to encircle the wall cloud that defined the eye. By the time the typhoon passed over Okinawa, the rainband had become a complete, 200 nm (370 km) diameter, concentric outer wall cloud (Figures 3-14-2 and 3-14-3).

The largest eye diameter ever reported by JTWC was that of Typhoon Carmen (JTWC 1960) as it passed over Okinawa. By coincidence, Winnie also passed over Okinawa. Carmen's eye diameter, as measured by the weather radar at Kadena Air Force Base was 200 nm (370 km), approximately the same diameter as Winnie's outer eyewall cloud. The 1960 Annual Typhoon Report commented: "Another feature quite unusual about this typhoon was the diameter of its eye. Reconnaissance aircraft frequently reported eye diameters of 100 [nm] [185 km], using as the basis of measurement, surface winds and pressure gradient. However, with respect to wall clouds surrounding the eye, radar photographs taken from the CPS-9 at Kadena AB show quite clearly that on 20 August, the eye had a diameter of approximately

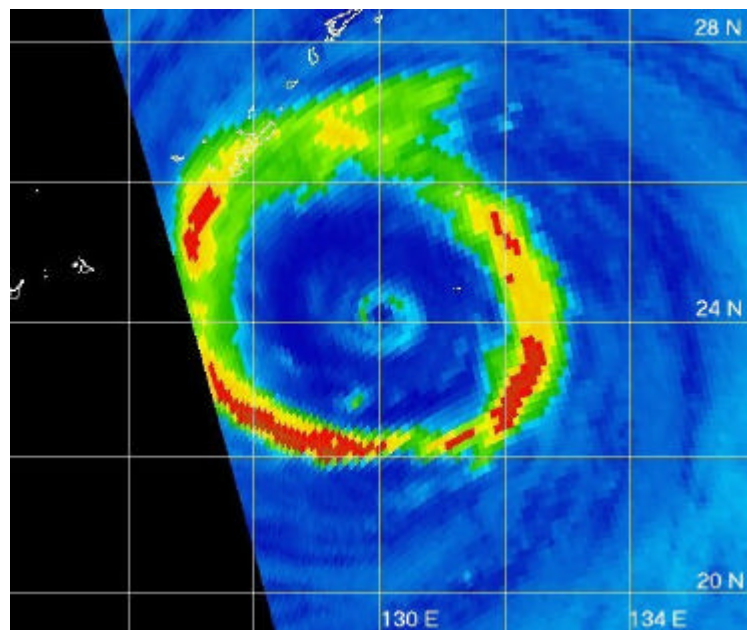


Figure 3-14-3 Winnie's outer wall cloud is nicely highlighted by microwave imagery. This is sensitive to regions containing precipitation-sized hydrometeors (especially large ice-phase particles). The eye and inner wall cloud are present but less distinct. (161311Z August horizontally polarized 85 GHz microwave DMSP imagery.)

200 [nm] [370 km]. The eye diameter of Carmen was probably one of the largest ever reported . . ." Winnie, like Carmen, was also viewed by radar at Kadena AB, a NEXRAD WSR 88D (Figure 3-14-4a,b).

As the outer wall cloud passed over Okinawa on 16 August, wind gusts of 82 kt (42 m/sec) were recorded (Figure 3-14-5) and the sea level pressure (SLP) fell to 964 mb (Figure 3-14-6). The center of the eye passed approximately 80 nm (150 km) south of the island. Doppler radar indicated 100-kt (51-m/sec) winds in the large outer eye wall in a layer from 3,000 ft (914 m) to 6,000 ft (1829 m). The NEXRAD base velocity product (Figure 3-14-4b) shows inbound wind speeds between 50 kt and 80 kt (26 m/sec and 41 m/sec) at an altitude of 8,000 ft (2438 m) above sea level on the eastern side of the inner wall cloud.

Although concentric wall clouds are not rare, especially for intense TCs, the extreme diameter of Winnie's outer eyewall cloud is an infrequent occurrence. Such large diameters are restricted primarily to the western North Pacific basin. In the Atlantic, TCs with large-diameter outer eye wall clouds have been observed, but not as large as these WNP examples. Such Atlantic storms include Allen (1980), Diana (1984), Gilbert (1988), and Luis (1995). These had outer eyewall clouds with diameters greater than 135 nm (250 km) and very small inner eyewall clouds with diameters less than 15 nm (28 km).

Sometimes typhoons which form in the monsoon trough of the western North Pacific generate very large circulations and eyes. The 370 km diameter of Winnie's outer eye wall cloud during passage over Okinawa is one of the largest ever observed in a TC. These cases are important because they define the most extreme possibilities of TC dynamics.

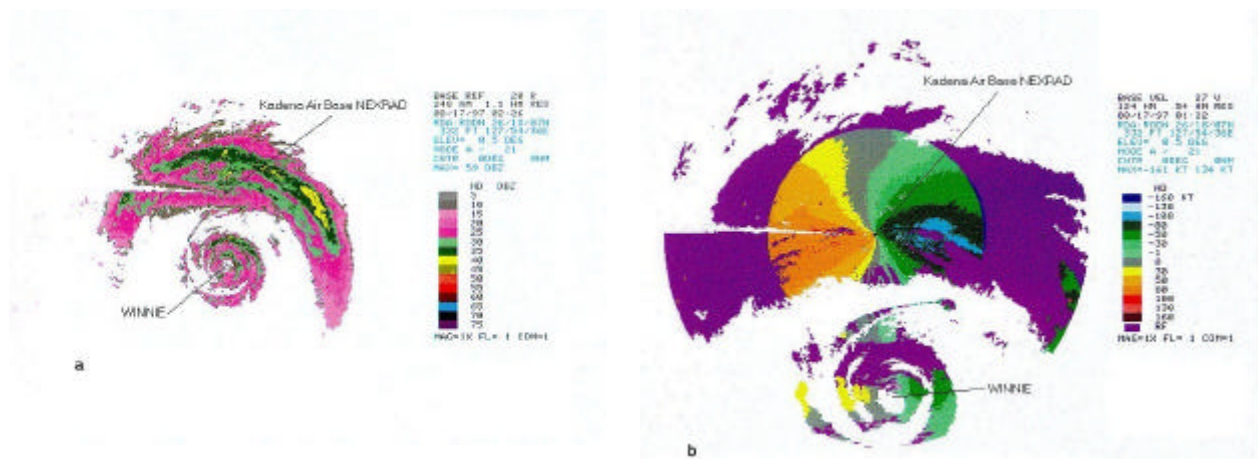


Figure 3-14-4 Winnie's outer wall cloud, and smaller inner wall cloud and eye, as depicted by the NEXRAD WSR 88D located near Kadena AB on Okinawa. (a) The base reflectivity at 170226Z August, and (b) the 170122Z August base velocity product. The NEXRAD is able to compute Doppler velocities within 125 nm (230 km) of the radar. The black dot (with arrow) shows the location of the NEXRAD in both panels.

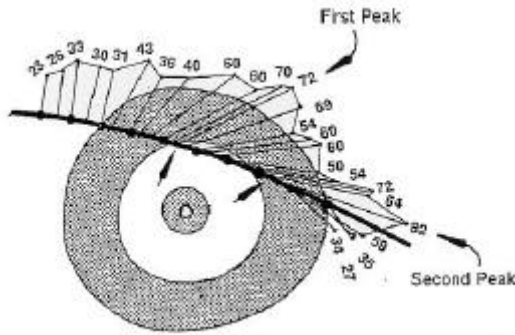


Figure 3-14-5 Wind reports from Kadena AB received at JTWC are plotted with respect to Winnie's cloud system (shaded regions). Winds are peak gusts in kt. Note that the peak gusts (indicated by arrows) at Kadena occur on the inward edge of the outer wall cloud in agreement with Jorgensen's (1984) synthesis of aircraft observations of the wind distribution in the large outer wall cloud of Hurricane Allen (1980). The small black dots along the indicated track are at 5-hour intervals from 160100Z to 172200Z August.

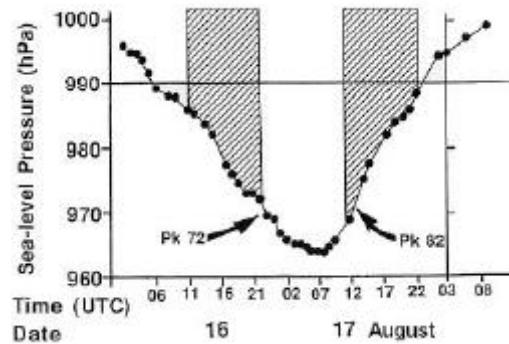


Figure 3-14-6 A time series of the sea-level pressure (SLP) recorded at Kadena AB as Winnie's outer wall cloud (hatched region) passed. Again, note the peak gusts occurring near the inner edge of the satellite observed outer wall cloud.

b. Winnie's Digital Dvorak (DD) time series

The magnitude of Winnie's Digital Dvorak (DD) numbers increased more rapidly than the warning intensity as the TC intensified on 11 and 12 August (a frequent occurrence). Winnie's series did not exhibit any obvious diurnal variations. Some typhoons exhibit a strong diurnal variation, while others (like Winnie) show little or none. Although not shown below, DD numbers were calculated for Winnie on 16 and 17 August when it possessed a very large diameter outer eye wall cloud by adapting the DD algorithm to use cloud-top temperature of the outer eye wall cloud to arrive at an intensity estimate. These DD numbers were observed to fluctuate between about 4.5 and 5.0. The corresponding intensity range of 77-90 kt

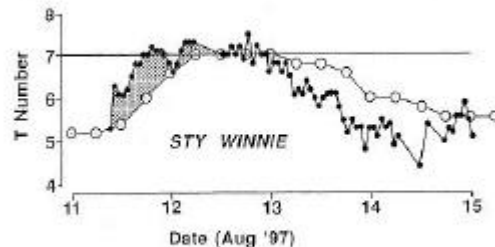
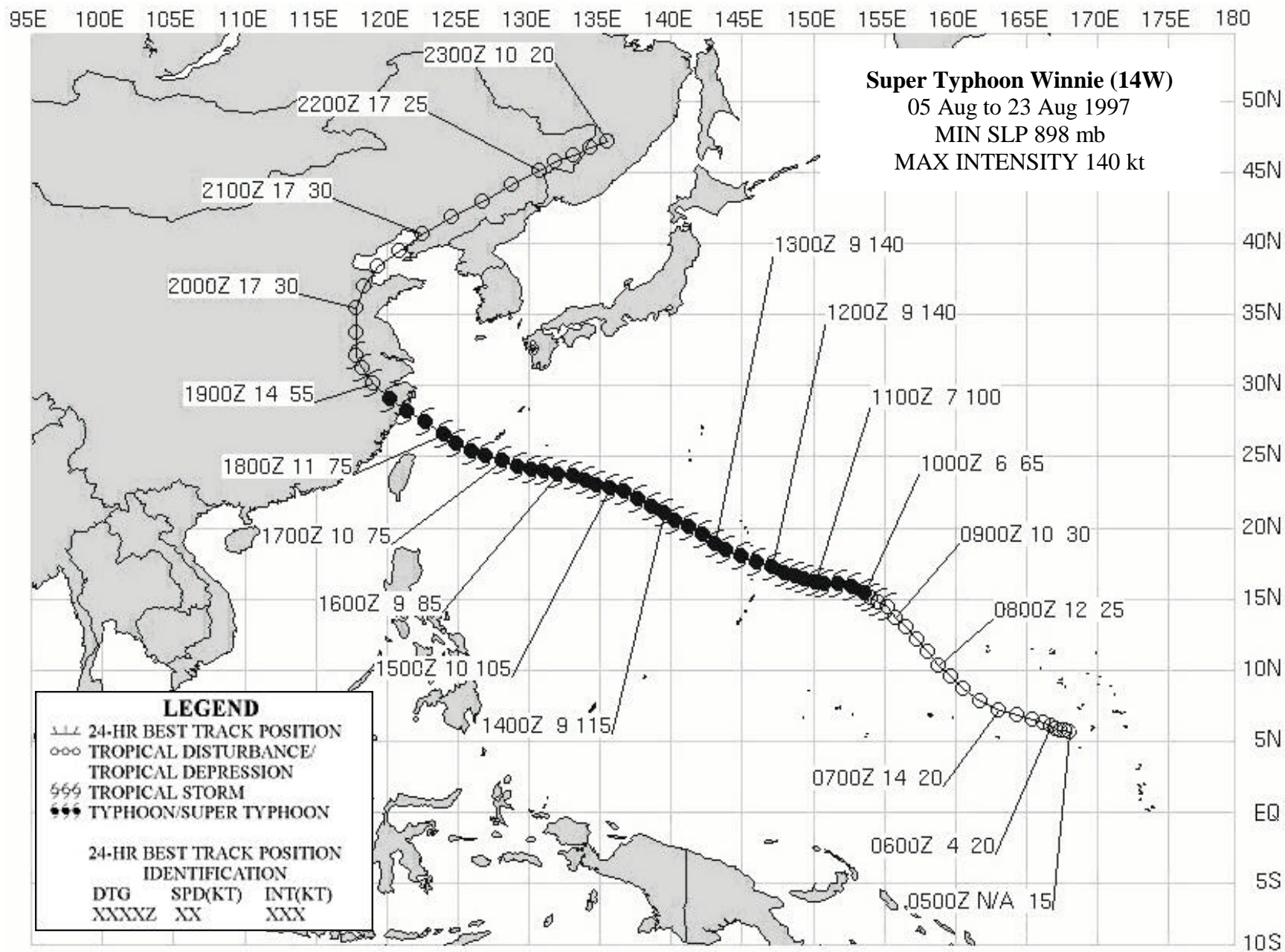


Figure 3-14-7 A time series of Winnie's hourly DD numbers (small black dots) compared with the warning intensity (open circles). As the TC was intensifying on 11 and 12 August, the DD numbers increase faster than the warning intensity (shaded region) -- a common behavior of the DD numbers. Note that the warning intensity is higher than the DD numbers as the TC begins to weaken, which is consistent with Dvorak's rule to delay the current intensity behind the decreasing data T-numbers.

(40-46 m/sec) fits well with synoptic reports from Okinawa (e.g., the 82 kt (42 m/sec) peak gust at Kadena, and the NEXRAD indications of 100 kt (51 m/sec) winds within the outer eyewall layer between 3,000 ft (914 m) and 6000 ft (1829 m)).

IV. IMPACT

As Winnie passed through the northern Mariana Islands, the populated islands of Guam, Rota, Tinian, and Saipan (well to the south of Winnie's track, but within its gale area) reported damage to crops and vegetation from winds and sea-salt spray. In Taiwan, 27 people were reported killed when an apartment building collapsed. Another 12 people were reported killed from mudslides, flooding and high wind. In mainland China, torrential rains and winds caused at least 25 deaths. Damage from wind and flooding was extensive.



TYPHOON YULE (15W) AND TROPICAL DEPRESSION 16W

I. HIGHLIGHTS

Yule and Tropical Depression (TD) 16W were two of ten tropical cyclones (TCs) during 1997 which formed east of 160E and south of 20N — within the "El Niño box" in Figure 3-5b. These two TCs existed simultaneously, and underwent a binary interaction resulting in their merger. After merger, the single resultant TC (retaining the name Yule) moved on a north-oriented track and passed close to Wake Island. When it reached the mid-latitudes, the system became a vigorous hybrid system possessing typhoon-force winds.

II. TRACK AND INTENSITY

During the middle of August, as the large-sized Winnie (14W) approached Okinawa and the east coast of China, low-level westerly winds persisted at low latitude from the Philippines eastward across Micronesia as

far as the international date line (IDL). A monsoon cloud band (with some well-defined tropical upper tropospheric trough (TUTT) cells to its north) stretched from Winnie to the eastern end of the monsoon trough. Yule and TD 16W originated from tropical disturbances located at low latitude: Yule from a tropical disturbance west of the IDL in the Marshall Islands, and TD 16W from a tropical disturbance east of the IDL at low latitudes to the southwest of Hawaii.

a. Yule (15W)

Yule (the westernmost of the Yule-TD 16W pair) originated from a very poorly organized tropical disturbance in the monsoon trough which stretched at low latitude across the eastern Caroline and Marshall Island groups. It was first mentioned on the 090600Z August Significant Tropical Weather Advisory (ABPW) when satellite imagery indicated that a possible low-level circulation center was associated with an area of deep convection at very low latitude (3N) and

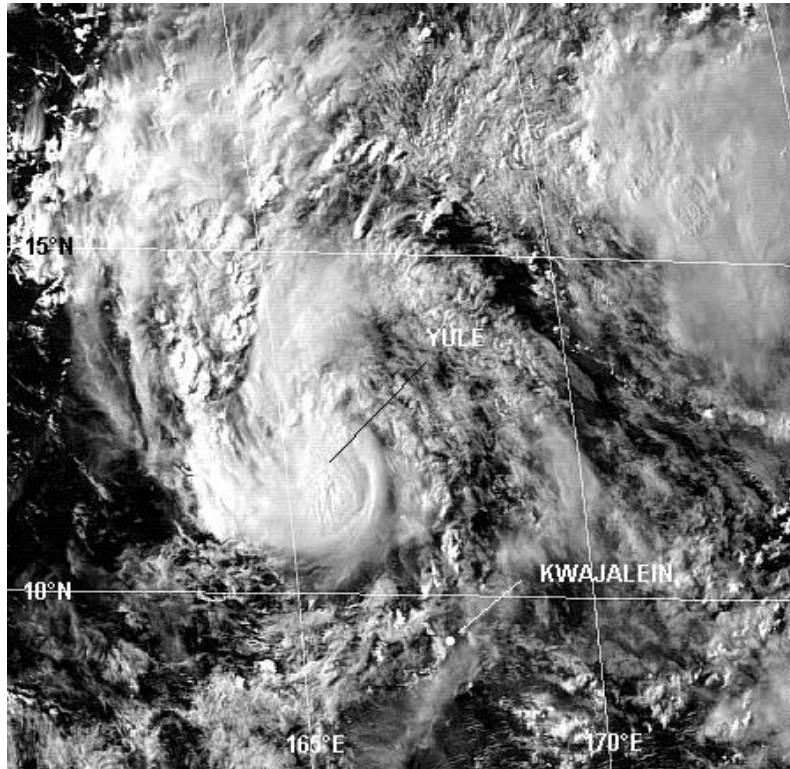


Figure 3-15/16-1 Yule becomes a tropical storm when located about 180 nm (330 km) northwest of Kwajalein (170533Z August visible GMS imagery). Properties of the centroid-relative motion help to reveal the nature of the interaction (which is not always apparent in the actual earth-relative tracks).

just to the west of the IDL. For nearly a week, this tropical disturbance remained poorly organized and difficult to follow. Then, on 15 August, satellite imagery indicated deep convection had increased and the organization of this deep convection (and other cloud lines) had improved. The first Tropical Cyclone Formation Alert (TCFA) — of two — was issued at 150730Z August. Because of unusual north-northeastward motion of the low-level circulation center, a second TCFA was issued at 160030Z to reposition the alert box. The influence of monsoonal westerlies to its south, and the onset of a binary interaction with the pre-TD 16W tropical disturbance may have been responsible for this north-northeastward motion.

When satellite intensity estimates reached 30 kt (15 m/sec), the first warning, valid at 161800Z, was issued on TD 15W. The warning indicated TD 15W would move northwest and intensify. Although the TD did intensify, it continued tracking to the north-northeast. On the second warning, valid at 170000Z, the warning acknowledged the north-northeast motion and forecast it to become northwest during the forecast period. Based on satellite intensity estimates of 35 kt (18 m/sec), TD 15W was upgraded to Tropical Storm Yule at 170600Z (Figure 3-15/16-1). Once again, the system, though moving north-

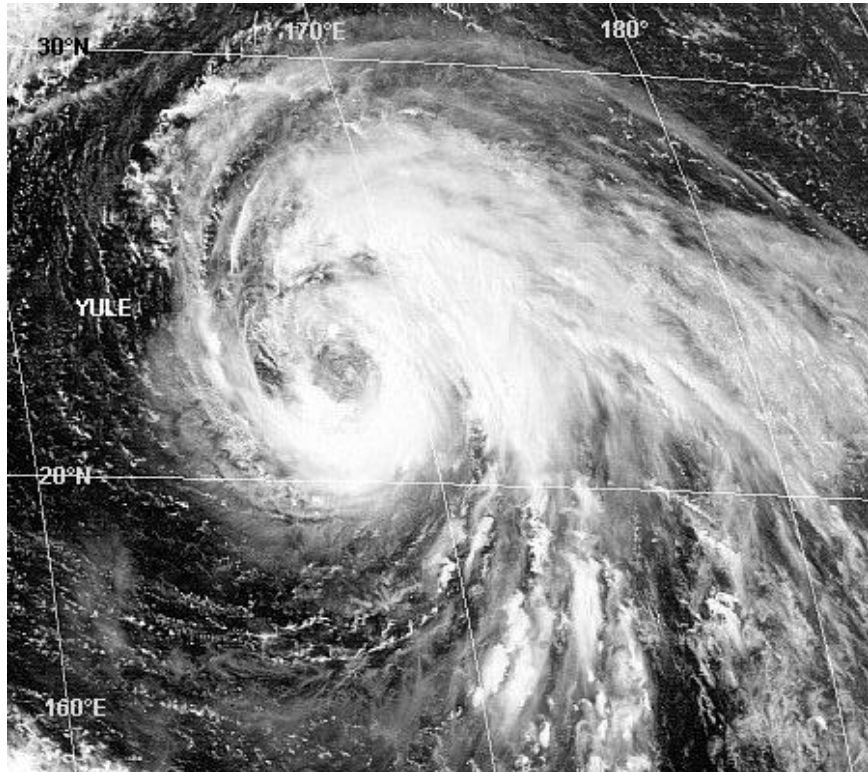


Figure 3-15/16-2 Possessing a large ragged eye, Yule briefly attains typhoon intensity (210333Z August visible GMS imagery).

northeast, was expected to turn to the northwest after 24 hours. By 180000Z, it was recognized that Yule was interacting with the newly formed TD 16W. The official forecast given on the warning valid at 180000Z was for Yule to move northeast for 24 hours and then turn toward the west and follow TD 16W. The alternate scenario of merger with TD 16W was mentioned on the Prognostic Reasoning message accompanying this warning.

At 190000Z, Yule and TD 16W merged (for more details on this merger, see the Discussion Section). The merger was asymmetric in that the low-level circulation center of TD 16W was horizontally sheared and swept into the intact circulation of Yule. Based on this analysis, JTWC decided the merged system would retain the name Yule. The system continued to move north-northeast on a long north-oriented track following the merger. The system also intensified, and briefly became a typhoon with a large ragged eye at 210600Z (Figure 3-15/16-2).

On 22 August, Yule approached a cloud band which was located to the east of an upper-level midlatitude trough and to the west of a blocking high. Entering this baroclinic cloud zone on 23 August, Yule was steered back toward the northwest. Acquiring extratropical characteristics, the final warning on Yule was issued valid at 230600Z. Instead of weakening, Yule intensified after it transitioned to an extratropical low. This was anticipated and was mentioned on the final warning. As a vigorous extratropical low (with some tropical characteristics) (see the Discussion Section) the system possessed typhoon-force winds of 65 kt (33 m/sec) during the period 231200Z to 251800Z. At nearly 50°N, the system finally entered weak westerly steering. It turned to the east after 241800Z. The system dropped below typhoon intensity after 251800Z as it drifted slowly eastward and weakened.

b. Tropical Depression 16W

Tropical Depression 16W (the easternmost of the Yule-TD 16W pair) originated from a poorly organized tropical disturbance which was first detected when it was east of the IDL. This tropical disturbance was first mentioned on the 130600Z August Significant Tropical Weather Advisory when synoptic data indicated a low-level cyclonic circulation was associated with a persistent but disorganized area of deep convection, and water vapor imagery indicated good upper-level outflow. The system was still east of the IDL at this time, but was heading westward. Moving slowly westward, the disturbance remained poorly organized for several days. It crossed the IDL and moved into JTWC's AOR on 15 August. On 17 August, the deep convection associated with this disturbance became better organized and a TCFA was issued at 172030Z. Located less than 450 nm (830 km) to the northeast of Tropical Storm Yule, the tropical disturbance which became TD 16W was already locked in a binary interaction with Yule (Figure 3-15/16-3). The first warning on TD 16W was issued valid at 180000Z based upon satellite intensity estimates of 25 kt (13 m/sec). Its binary interaction with Yule was entered as a comment on the warning message. Two scenarios of the outcome of the binary interaction of TD 16W with Yule were mentioned on the prognostic reasoning message for the first warning: the primary scenario was for TD 16W to slow as it moved westward, lose latitude, and increase its separation distance from Yule; an alternate scenario called for TD 16W to merge with Yule. The latter scenario is what occurred. The final warning was issued on TD 16W, valid at 190000Z, when it was apparent that the two systems were merging (Figure 3-15/16-4), and the sheared remains of TD 16W were being swept into the dominant circulation of Yule.

III. DISCUSSION

a. Tropical cyclone merger

In order to study the interaction between two TCs, it is best to produce a diagram illustrating the motion of each TC with respect to their centroid.

In the case of Yule and TD 16W, the centroid-relative motion (Figure 3-15/16-5) indicates little interaction at first, then a period of rapid approach followed by merger at 190000Z. The common features of TC interaction noted by Lander and Holland (1993) of mutual approach followed by a period of cyclonic orbit ending in merger are present, albeit somewhat distorted from their ideal model: the centroid relative motion of Yule and TD 16W is dominated by a rapid, zonally-

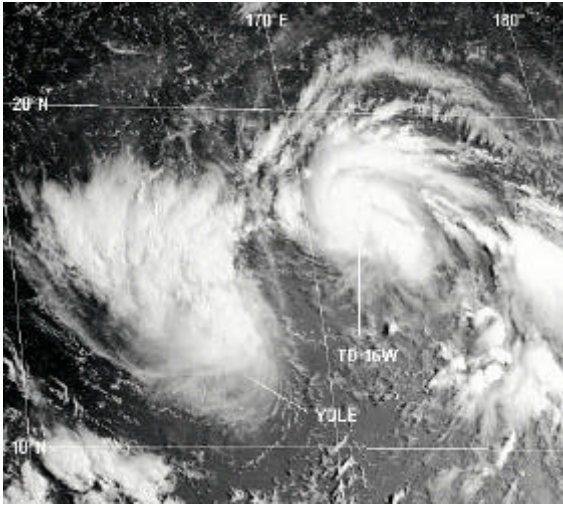


Figure 3-15/16-3 Yule and TD 16W are locked in a binary interaction that will end in merger (172133Z August visible GMS imagery).

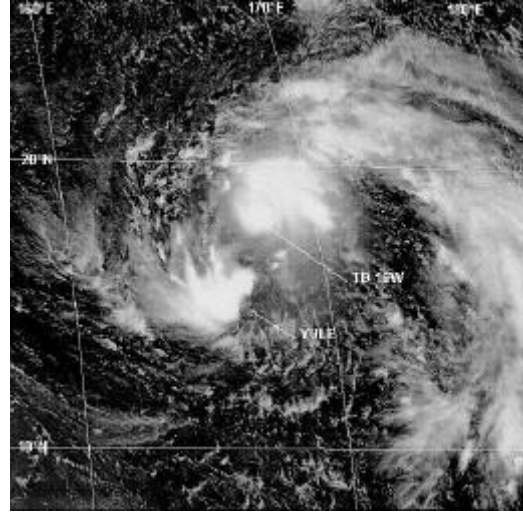


Figure 3-15/16-4 The merger of Yule and TD 16W is nearly complete (190133Z August visible GMS imagery).

oriented approach, with a curved cyclonic orbit noted only within 24 hours of merger. The location of these two TCs in a large-scale sheared flow (i.e., the monsoon trough with westerlies to its south and easterlies to its north) might lead one to expect such a departure from the idealized binary interaction of Lander and Holland. Such an effect is described by Dong and Neuman (1983).

In summary, Yule and TD 16W underwent a binary interaction ending in merger. Although satellite imagery was somewhat ambiguous, scatterometer data (Figure 3-15/16-6) clearly indicated that Yule was the dominant system during the merger and that TD 16W became horizontally sheared apart as the merger occurred.

b. The fate of a TC as it enters the midlatitudes

Establishing the defining characteristics of a TC is not a trivial exercise. For purposes of public warning, the nature of a TC has been simplified to a stratification based upon its intensity. Dvorak (1975, 1984) developed techniques for estimating the intensity of TCs from satellite imagery. The basic TC pattern types identified by Dvorak are: (1) the "shear" pattern; (2) the "curved band" pattern; the "central dense overcast" (CDO) pattern; and the "eye" pattern. These are the set of basic, or conventional, TC pattern types. At the highest taxonomic level, there are two categories of atmospheric storms of synoptic scale that possess a region of low pressure accompanied by a cyclonic wind circulation: the extratropical (ET) cyclone and the TC. Besides the basic differences of latitude of formation, the ET cyclone and the conventional TC differ in their primary source of energy and in their thermal structure. The ET cyclone derives the larger portion of its energy from potential energy present along the polar front of midlatitudes. The TC derives the bulk of its energy from the latent heat released by deep convection. The thermal structure of the ET cyclone is commonly said to be cold core, while that of the TC is said to be warm core. The term "cold core low", however, is actually an oxymoron, since lowered sea-level

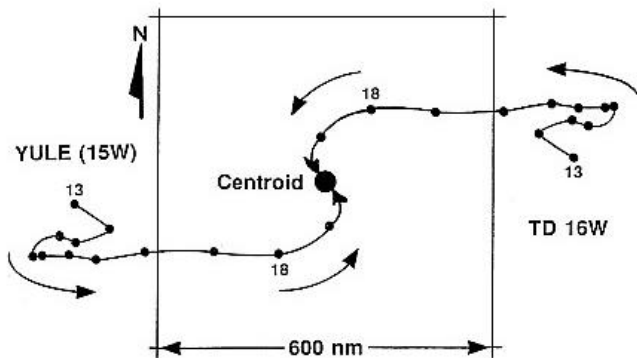


Figure 3-15/16-5 The centroid-relative motion of Yule and TD 16W. Black dots indicate positions at 12-hour intervals beginning on 130000Z August and ending at the merger location (large black dot) at 190000Z August. The square provides a length scale (as indicated) and the orientation of the cardinal directions.

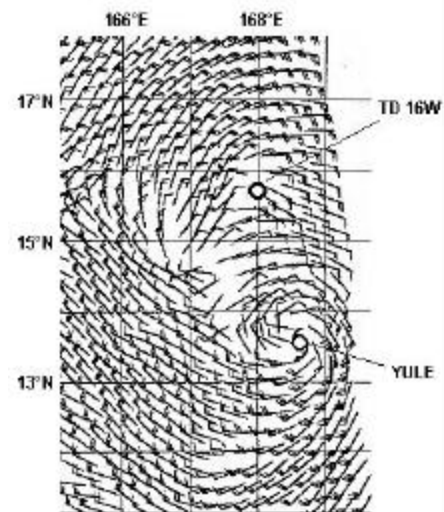


Figure 3-15/16-6 Scatterometer-derived marine surface wind speed and direction in a swath over both Yule and TD 16W (locations indicated). This scatterometer pass over these two TCs occurred approximately 12 hours prior to their merger. One can clearly see that the circulation of TD 16W is being sheared into the circulation of Yule (181131Z August ERS-2 scatterometer-derived marine surface wind vector).

pressure must, by hydrostatic considerations, be the result of an integrated density deficit in the atmospheric column above the area of lowered sea-level pressure. This density deficit is primarily the result of a warm anomaly somewhere in the atmospheric column. Therefore both the ET cyclone and the TC must possess warm cores; the true difference is in the location of the warm anomaly that results in the lowered sea-level pressure. In the mature ET cyclone, although much of the troposphere is generally colder than in the surrounding regions (hence its cold core designation), the tropopause is greatly lowered, and the stratosphere above the system is much warmer than in the surrounding regions. The lowered tropopause accompanied with the stratospheric warmth accounts for the lowered sea-level pressure in the mature ET cyclone. In the TC, the column density deficit due to higher core temperature occurs in the troposphere. In addition to tropospheric warmth above the TC low-pressure center, the TC differs from the typical ET cyclone in horizontal structure as well. The maximum winds in a mature TC are usually found very close to the center. The radius of maximum winds of even very intense TCs may be on the order of 10 km. The winds beyond the radius of maximum wind may fall off quickly. The maximum winds in an ET cyclone are usually displaced farther from the center than they are in the TC, and the highest winds are spread out across a larger area.

So far, it seems as if the differences between the ET cyclone and the conventional TC are so

great that their differential diagnosis should be simple. This, however, is not the case. There exists, in nature, types of cyclones that possess characteristics of both ET cyclones and conventional TCs. For example, the subtropical cyclone (Hebert and Poteat 1975), the arctic hurricane (Businger and Baik 1991), the monsoon depression (Ramage 1971, and JTWC 1993), and the monsoon gyre (Lander 1994, Carr and Elsberry 1994). These types of cyclones have caused confusion and forecast problems for decades. Further complicating things is the fact that transitions among the types are possible. For example, at what point does a TC entering the midlatitudes become extratropical?

In the case of Yule, it transformed into a vigorous extratropical low (Figure 3-

15/16-7) after it moved into the cloud band associated with the baroclinic zone located between a midlatitude upper-level trough and a blocking high. Yule, as a transforming — or transformed — low, intensified. Maximum wind speeds increased to typhoon intensity as the system moved northwest from 45°N to 50°N. Few TCs intensify as they become extratropical, nor is the extratropical low into which they transform generally more intense than the transforming system. Some TCs dissipate when they enter the midlatitudes. According to Harr (personal communication 1997) the fate of a TC which enters the midlatitudes may be governed primarily by what type of mid-latitude flow pattern is in place when the TC arrives there. Certainly the extratropical transition of TCs is a topic requiring much study.

IV IMPACT

Prior to becoming a typhoon, and as it moved to the north-northeast, Yule passed to the east of Wake Island. Peak winds on Wake (WMO 91245) reached 45 kt (23m/sec) sustained with a gust to 58 kt (30 m/sec) from the north at 201000Z August. Damage on Wake was light with one power pole down. A few palm and ironwood trees were also downed. No buildings were damaged. High surf pushed rocks onto the road going around the east end of the main runway, forcing the road's closure.

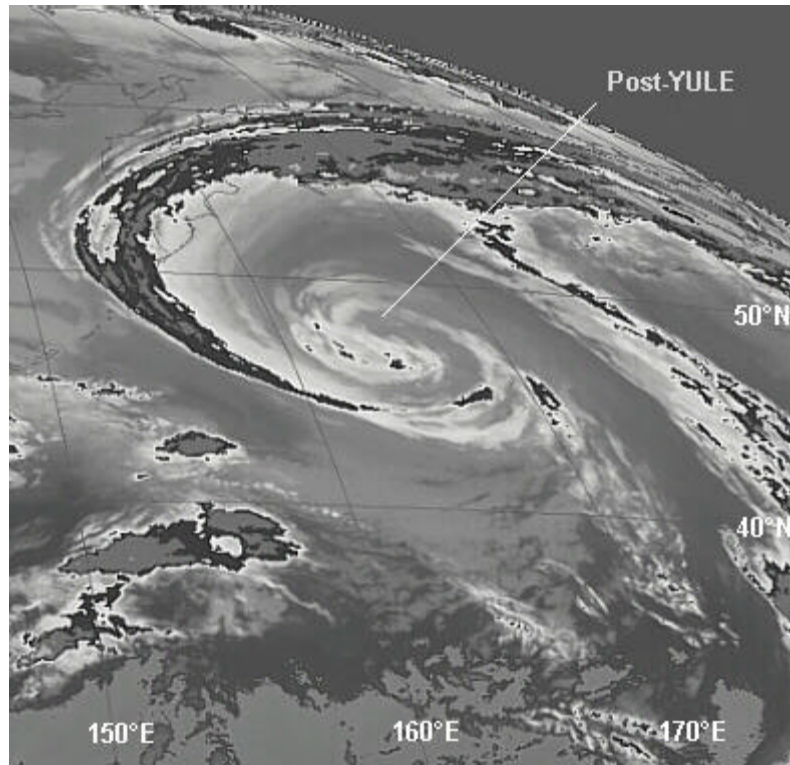
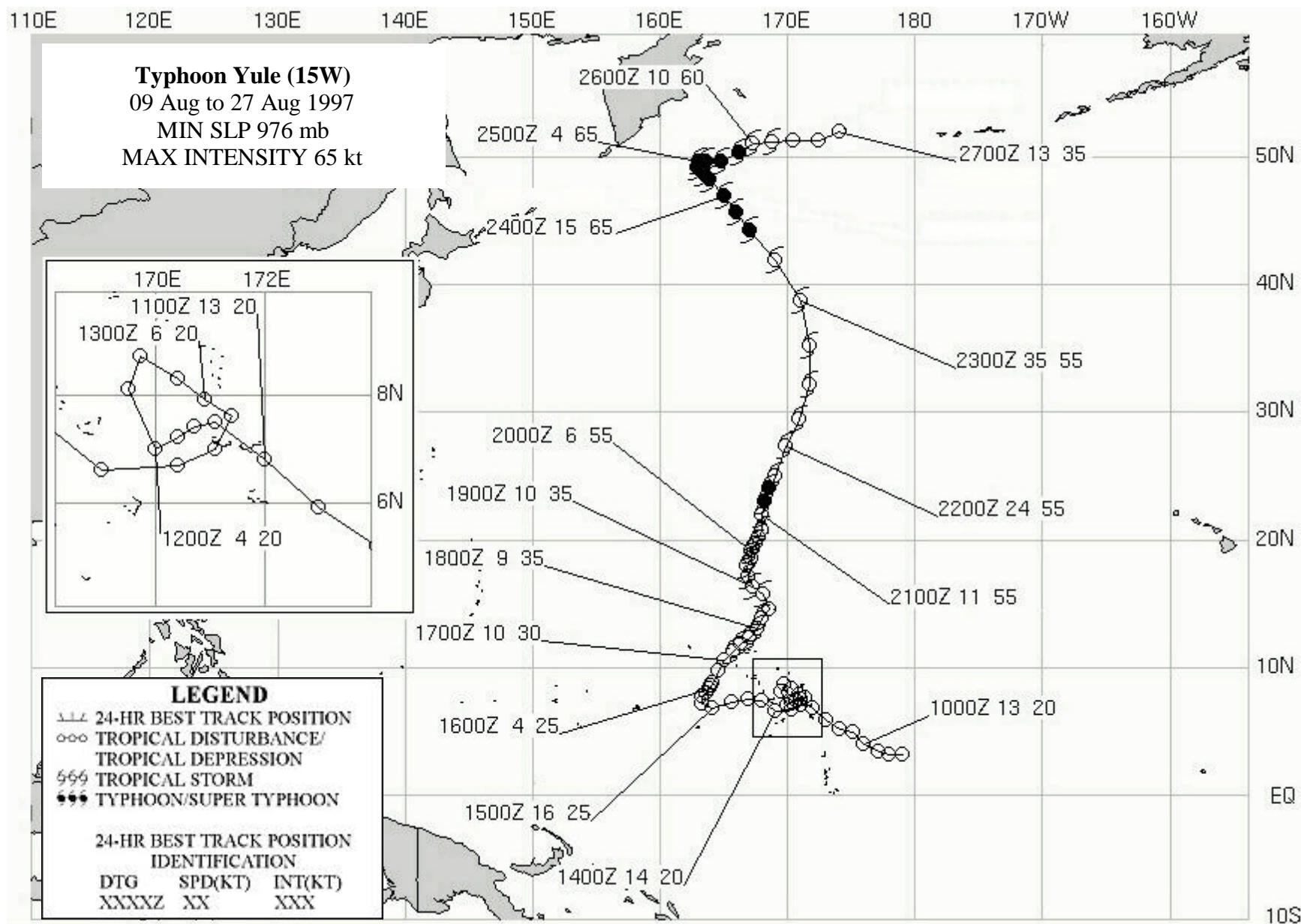
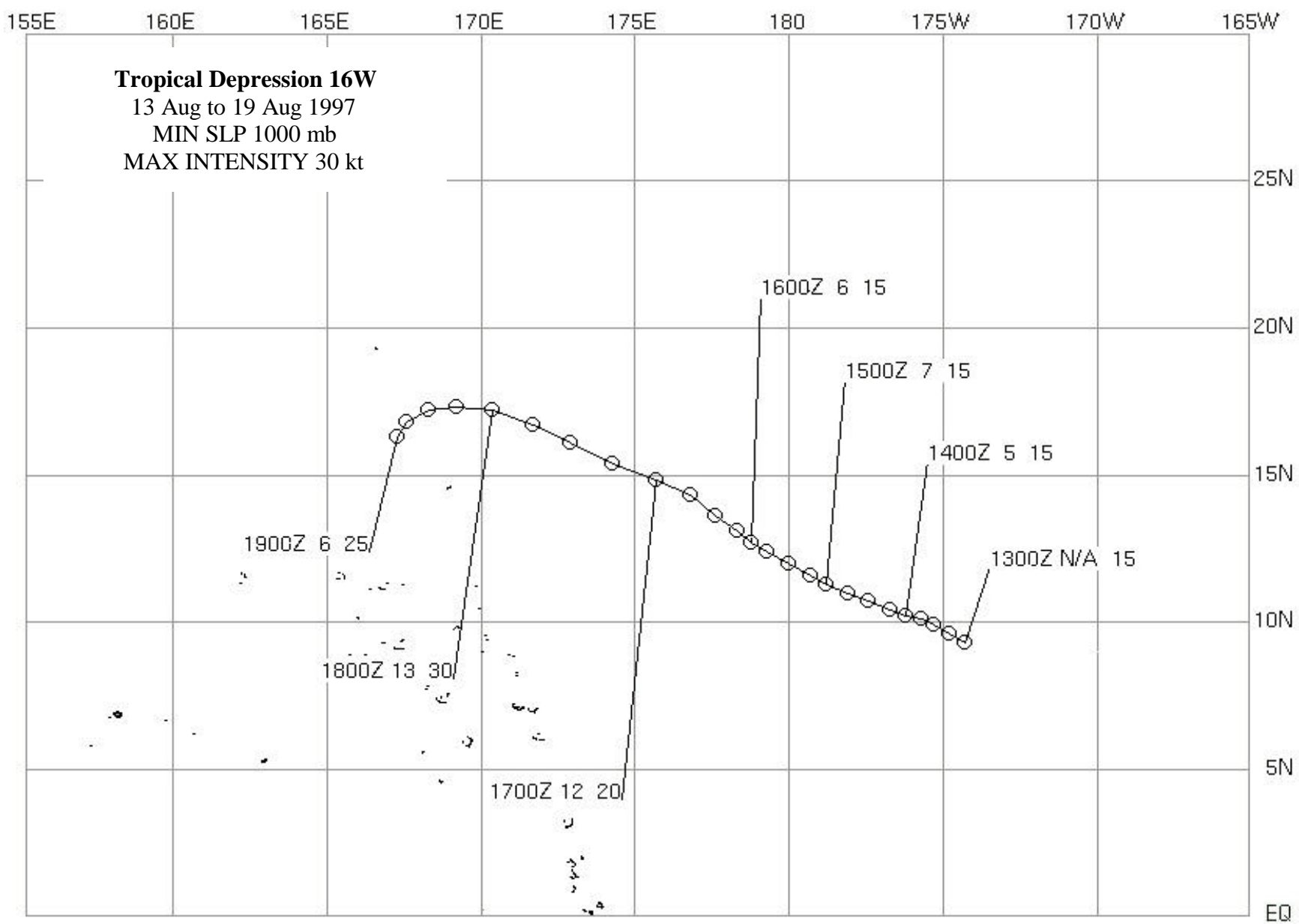


Figure 3-15/16-7 After Yule entered a baroclinic cloud band, it transformed into a vigorous extratropical low. In this enhanced infrared image, the transformed Yule is moving northwest toward the Kamchatka peninsula with maximum winds of typhoon intensity (282333Z August enhanced infrared GMS imagery). Enhancement curve is "BD" (Basic Dvorak).





TYPHOON ZITA (17W)

Typhoon Zita (TY) (17W) was the second of four tropical cyclones, TY Victor (13W), TY Zita (17W), TY Fritz (22W), and TY Linda (30W) to develop and reach typhoon intensity in the South China Sea during 1997. Although short-lived, the system reached a peak intensity of 75 kt (39 m/sec) as it entered the Gulf of Tonkin and maintained that intensity until landfall was made over Vietnam.

On 19 August, a tropical disturbance formed in the South China Sea approximately 300 nm (560 km) to the west of the Philippine island of Luzon. This disturbance was first mentioned on the 20 August Significant Tropical Weather Advisory (ABPW) after an area of deep convection had persisted for 12 hours in association with a weak low-level cyclonic circulation. As the system

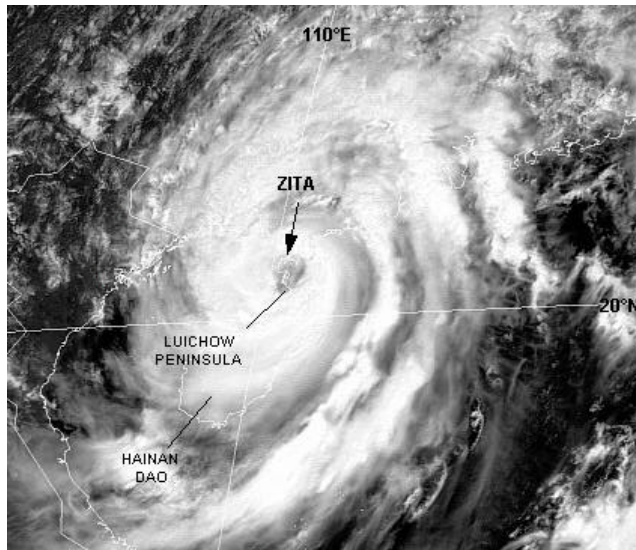
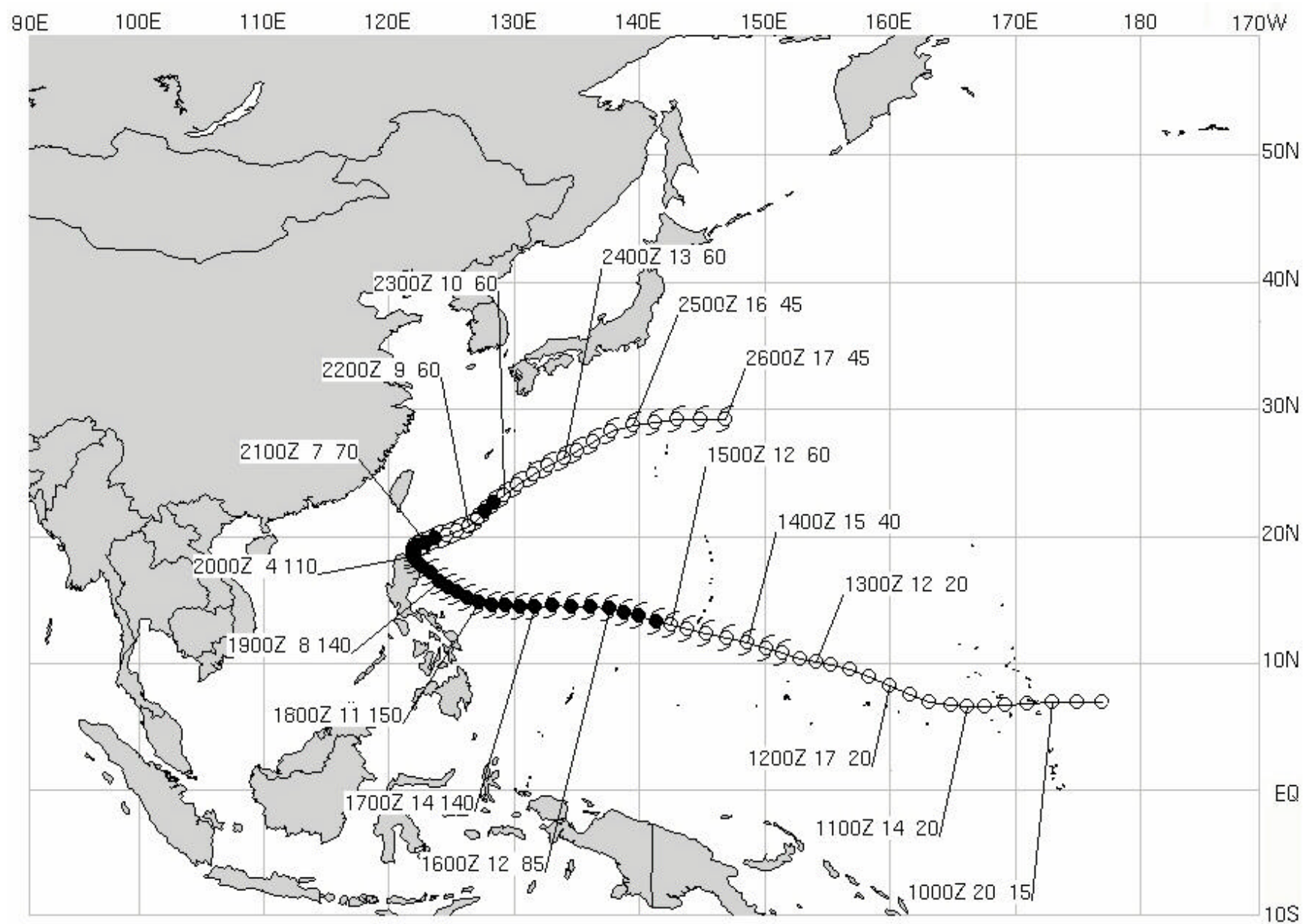


Figure 3-17-1 Zita develops a ragged eye over the Luichow Peninsula, just north of Hainan Dao. At peak intensity, (220427Z August visible GMS imagery).

moved into an area of easterly environmental steering flow, convective organization improved and became more centrally located. This prompted JTWC to issue a Tropical Cyclone Formation Alert (TCFA), valid at 2030Z on 20 August. Shortly thereafter, banding features developed and JTWC issued its first warning on Tropical Storm Zita (17W) valid at 0000Z on the 21st. Zita continued tracking towards the west under the influence of easterly steering flow, equatorward of the subtropical ridge. Outflow aloft was good in all quadrants with little to no vertical wind shear. Despite the proximity to China's southern coastline, the system reached typhoon intensity at 0000Z on the 22nd, approximately 180 nm (330 km) southwest of Hong Kong. Zita reached its peak intensity of 75 kt (39 m/sec) at 0600Z the same day over the Luichow Peninsula, just north of Hainan Dao (Figure 3-17-1). Zita maintained this intensity for 18 hours as it tracked westward through the Gulf of Tonkin. The cyclone made landfall over Vietnam on 2100Z on the 22nd and dissipated as it moved into the mountainous terrain. The final JTWC warning was issued at 0600Z on the 23rd. No reports of damage or injuries were received.



TYPHOON AMBER 18W

I. HIGHLIGHTS

Typhoon Amber (18W) was the second of four tropical cyclones which would develop within the monsoon trough during an eight day period. The system would later interact with Tropical Storm (TS) Cass (20W) then move across the island of Taiwan and the Formosa Strait and into China.

II. TRACK AND INTENSITY

By the 20th of August, the monsoon trough extended from southeastern Asia into the South China Sea, eastward through the Luzon strait, across the southern Mariana Islands and east-northeastward to Wake Island (where Typhoon Yule was approaching from the south-southwest). The monsoon trough was very active. Four different tropical cyclones would form during the next eight days: Typhoon Zita (17W) and TS Cass (20W), which formed in the South China Sea; Super Typhoon Bing (19W) which developed east of the Mariana Islands; and finally Typhoon Amber (18W) which began in the Philippine Sea. The pre-

Amber (18W) disturbance developed in a region of upper-level divergence overlying the surface trough. It was first mentioned on the Significant Tropical Weather Advisory (ABPW) on 20

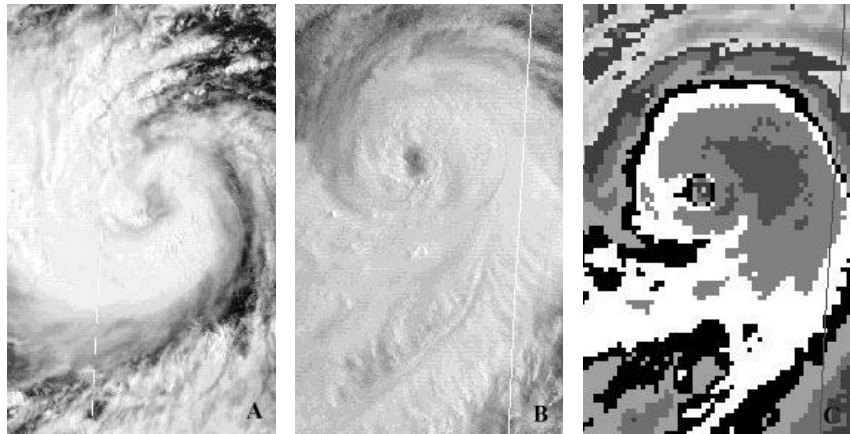


Figure 3-18-1 Typhoon Amber as seen by visible and infrared satellite imagery over a 36 hour period beginning 26 August at 0633Z. The valid times of the images are: far left 260633Z; middle and far right 242224Z. Note the banding type eye feature in the image at far left has developed into a more circular eye feature (better defined in the infrared imagery).

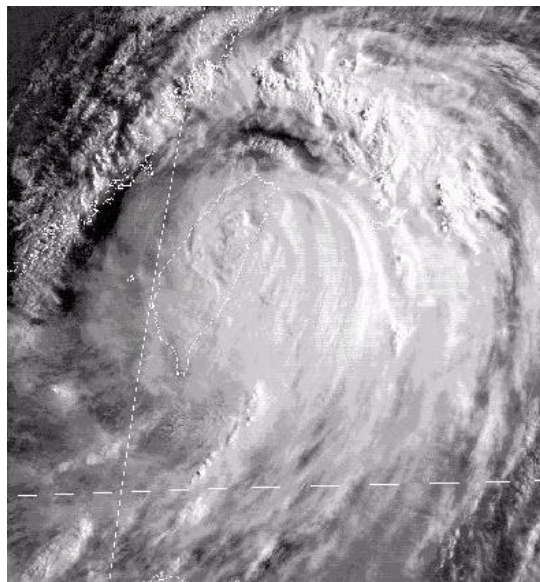


Figure 3-18-2 Visible imagery valid at 282227Z.

August. A scatterometer pass at 1340Z indicated at least 20 to 25 kt (10 to 13 m/s) of sustained wind. A Tropical Cyclone Formation Alert (TCFA) was issued at 0300Z on 21 August followed by a warning at 0600Z, prompted by a ship report of 40 kt (20 m/s).

Amber remained in deep monsoonal flow with the subtropical ridge to the north and ridging associated with Typhoon Zita (17W) to the west-southwest. This ridging allowed only a slow west-northwest motion ranging from 3 to 5 kt (6 to 9 km/hr), lower than what is normally associated with a tropical cyclone south of the sub-tropical ridge. This motion continued until 26 August when Tropical Storm Cass (20W) formed west-southwest of Typhoon Amber, close enough for direct interaction to occur. By 28 August, the effect of Tropical Storm Cass' circulation was to cause Amber's forward speed to increase to near 8 to 10 kt (15 - 19 km/hr) with a more northwestward motion. This motion continued as Amber moved across Taiwan and then China on 29 August.

Typhoon Amber (18W) intensified at a slightly faster than the climatological (one Dvorak 'T' number per day) rate. On 23 August at 0633Z, the intensity was estimated at 70 kt (35 m/s), based on visible satellite imagery which showed the development of a banding type eye. This eye became better defined in visible and infrared imagery on 24 August at 2246Z, when the intensity was 100 kt (50 m/s) (see figure 1). The system subsequently weakened to 85 kt (43 m/s) for a short time, but re-intensified to 110 kt (55 m/s) by the morning of 28 August as it began to approach Taiwan. Reports from the island indicated northeast winds of 75 kt (38 m/s) and a surface pressure of 992 mb at 0300Z 28 August; 6 hours later the pressure had dropped to 984 mb with north winds of 45 kt (23 m/s). By the morning of 29 August, Typhoon Amber began to move across Taiwan with an intensity of 95 kt (figure 3-18-2) maintaining typhoon intensity as it crossed the island's central mountains, some of which range from 8500 to 13000 feet (2600 to 4000 m). Land interaction weakened Typhoon Amber as it crossed into the Formosa Strait with an intensity of 80 kt (40 m/s). The system subsequently made landfall in China with an intensity of 65 kt (33 m/s).

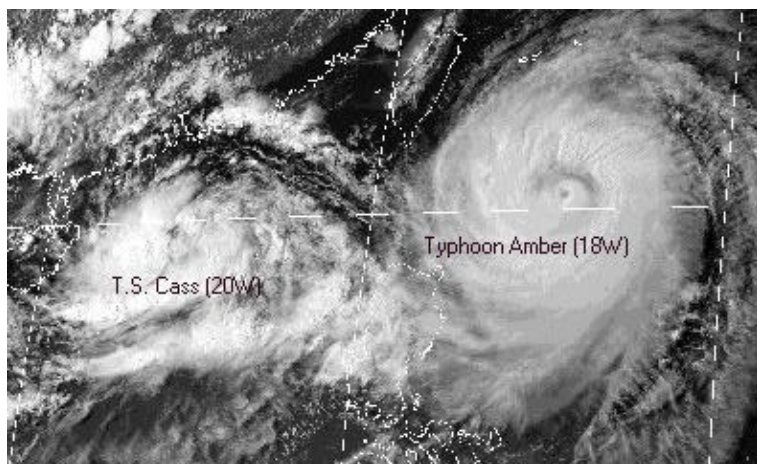


Figure 3-18-3 Visible satellite image (valid time, 27 August 0733Z) of Tropical Storm Cass and Typhoon Amber over the South China and Philippine Seas.

III. DISCUSSION

a) The formation of concentric eyes during intensification

Satellite imagery over a 48-hour period beginning from 25 through 27 August indicated that Typhoon Amber developed concentric eyes, a feature typically found only in intense tropical cyclones. The process starts when banding begins to wrap around the established central convective feature. An outer eye wall begins to form and dominates the inflow of moisture flowing towards the center, while

the inner eye wall begins to contract and may eventually dissipate. Refer to Figure 3-18-4. The image at top left shows a solid area of convection surrounding a cloud filled eye with a banding feature stretching from west to south of the center. The image at top right, which was taken about a day later, shows an area free of convection (known as the "moat" region) developing between the eyewall and the outer banding feature. The banding feature is closer to the eyewall and is wrapping around the center. The image at bottom left is 19 hours later and clearly shows a banding type structure. Microwave imagery 10 hours earlier indicated the presence of an eye; therefore cloud cover is probably obscuring it in this image. The image at bottom right shows fully developed concentric eyes with a moat in between. About 9 hours after the last image, Typhoon Amber reached a peak intensity of 110 kt (55 m/s). The concentric eye feature became less apparent in subsequent satellite imagery as Amber approached Taiwan.

***b) Interaction With TS Cass, and
Numerical Model Track
Performance***

While Typhoon Amber was transiting the Philippine Sea, TS Cass formed in the South China Sea approximately 700 nm (1300 km) to the west-southwest. The distance between these tropical cyclone, as shown in Figure 3-18-3, was close enough for direct interaction to occur (Carr and Elsberry, 1994). However, due to the smaller size and lesser organization of TS Cass, Typhoon Amber's track was only slightly more northwestward and faster than would otherwise be expected. The direct interaction was primarily one way as Typhoon Amber significantly altered the motion track of TS Cass. Although TS Cass had only a small effect on the actual motion of Typhoon Amber, it did complicate the forecasting process, because the models tended to exaggerate the extent of interaction Figures 3-18-5, 3-18-6 and 3-18-7 show the track reconstruction of Typhoon Amber along with the forecasted tracks from the NOGAPS, GFDN and FBAM models. Each model showed a poleward bias (as they normally do) early on, then switched to an equatorward bias as Typhoon Amber was just northeast of the island of Luzon.

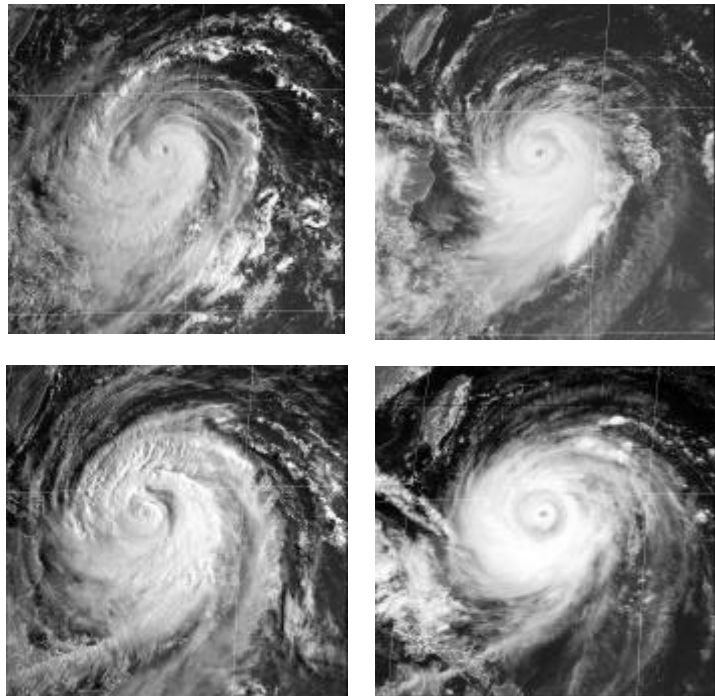


Figure 3-18-4 Development of concentric eye walls in Typhoon Amber during a 53 hour period beginning 242226Z August, as seen in visible satellite imagery. Valid times of satellite images are: top left, 242226Z; top right, 260334Z; bottom left, 262226Z; bottom right 270334Z. Peak intensity occurred shortly after concentric eye wall formation.

IV. IMPACT

No reports were received by the JTWC on damage, injuries or fatalities due to Typhoon Amber.

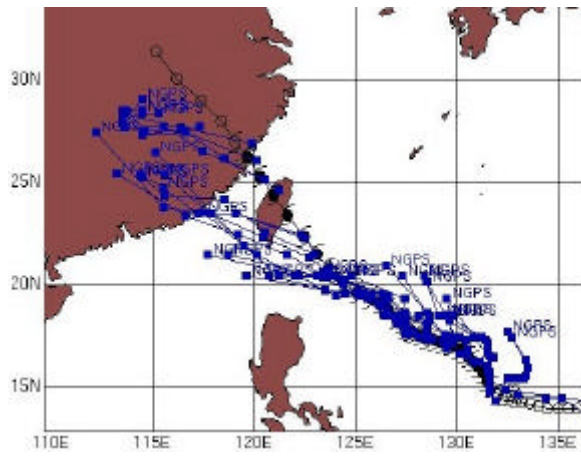


Figure 3-18-5 The best track and the NGPS forecast tracks for Amber (18W).

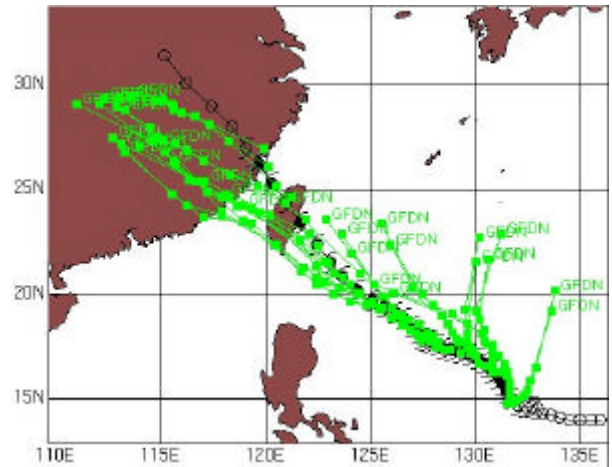


Figure 3-18-6 The best track and the GFDN forecast tracks for Amber (18W).

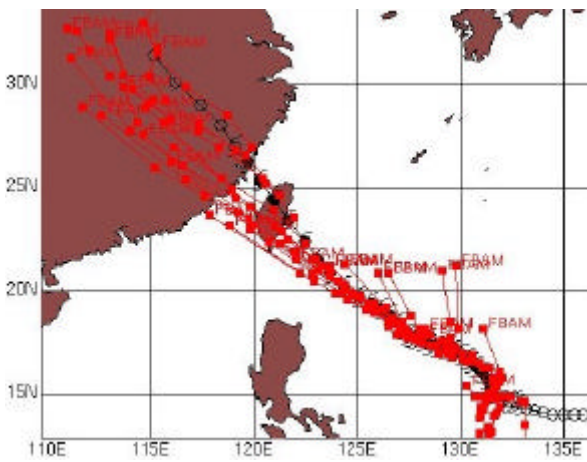


Figure 3-18-7 The best track and the FBAM forecast tracks for Amber (18W).

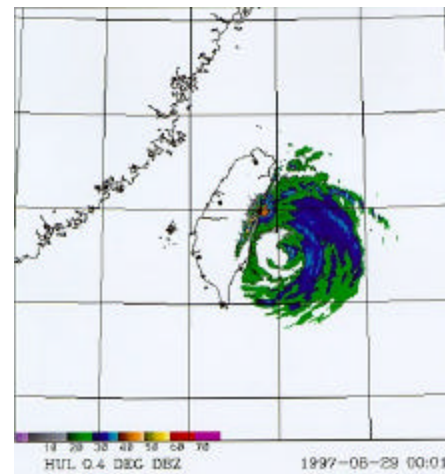
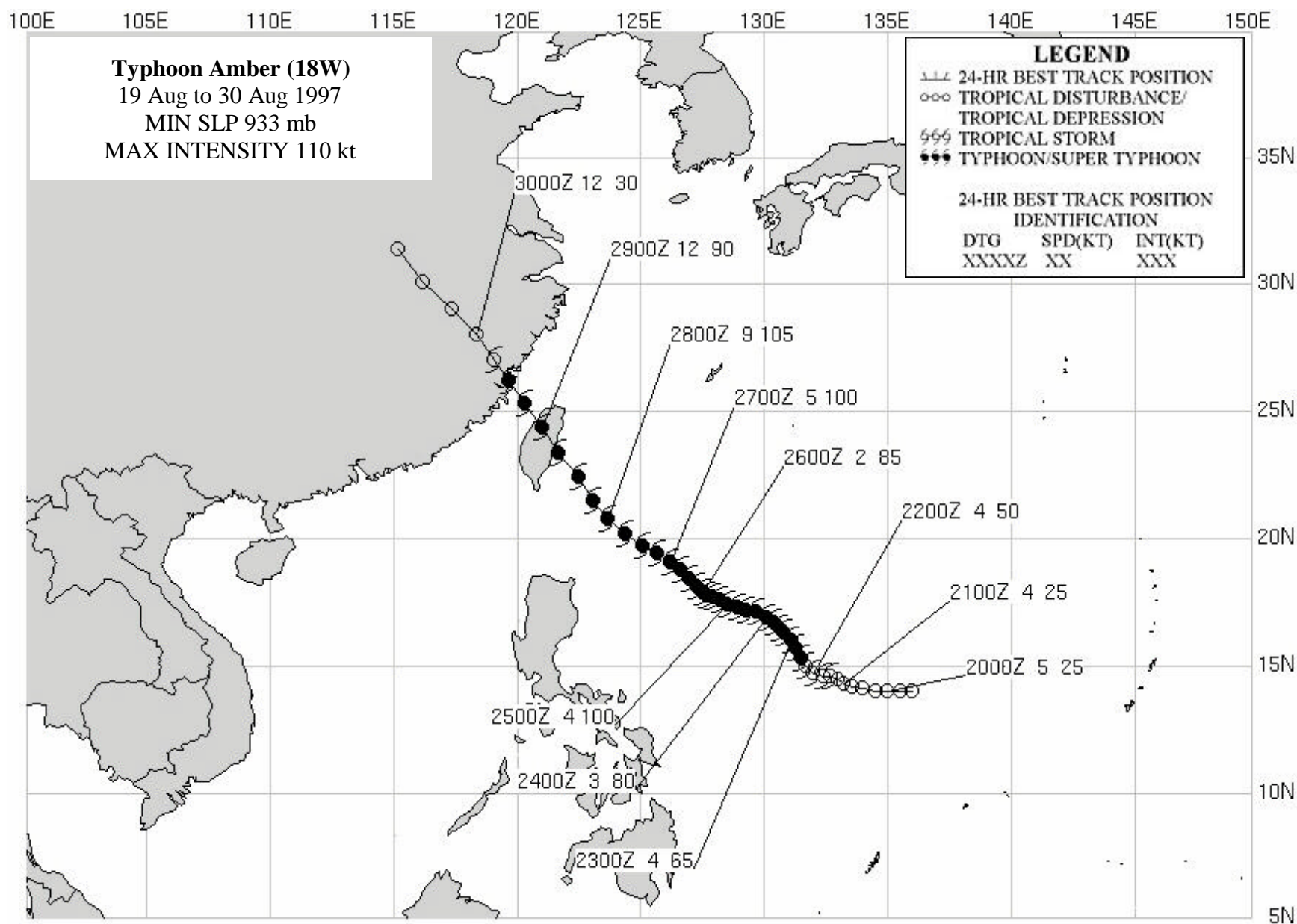


Figure 3-18-8 Radar image of Typhoon Amber as it is approaching Taiwan. Valid time is 290001Z



SUPER TYPHOON BING (19W)

I. HIGHLIGHTS

Super Typhoon Bing (STY) (19W) was the third of four tropical cyclones that would form within the monsoon trough during a period of eight days. It produced heavy rainfall while tracking near Guam as a tropical storm on 29 August. Rapid intensification began as Bing moved west of Guam, and two days later it became the fifth super typhoon of the 1997 season.

II. TRACK AND INTENSITY

By 26 August, the monsoon trough extended from the South China Sea to north of the Philippine Islands, through the central Mariana and Marshall Islands to the dateline. Low level westerly winds were observed all the way to 177E. During a normal year, the monsoon trough usually does not extend past 160E. The observed eastward extension was most likely an effect of El Niño.

The disturbance that became STY Bing (19W) started in the eastward extension of the monsoon trough near the Marshall Islands. The disturbance formed to the south-southeast of a large scale upper level anticyclone. Vigorous convection associated with the disturbance was enhanced by strongly divergent upper level wind flow. At 2330Z on 25 August, the Significant Tropical Weather Advisory (ABPW) was re-issued to add the disturbance as a suspect area. However, the convection (see Figure 3-19-1) quickly organized and a Tropical Cyclone Formation Alert (TCFA) was issued only eight hours later. At 0600Z on the 24th, the disturbance was upgraded to a Tropical Depression (TD).

The newly formed TD 19W tracked westward at speeds of 13 to 15 kt (24 to 28 km/hr). This was due to strong low to mid-level easterly steering flow south of the subtropical ridge. This westward track continued as it passed near Guam and Rota on 29 August. Fortunately for the islands, only slow intensification took place as it approached. At 1800Z on the 28th, Bing was upgraded to tropical storm intensity, but had an intensity of only 40 kt (21 m/sec) during its passage through the Marianas (Figure 3-19-2). Shortly after passing the Marianas, the system underwent a period of rapid intensification, beginning about 1200Z on 30 August and ending 54 hours later with a peak intensity of 135 kt (69 m/sec). Figure 3-19-3 shows visual satellite imagery which illustrates how quickly the central cloud structure changed in little more than a day. The satellite image at left shows Bing as a 80 kt (41 m/sec) typhoon with a developing eye, while the image at right, when Bing's intensity was near 130 kt (67 m/sec), shows a smooth eyewall with a very well defined eye. This represented a change of approximately two Dvorak "T" numbers. During the intensification process, mid-level ridging began to build to the east-southeast of the tropical cyclone causing the steering flow to gradually shift from an easterly to south-southeasterly. At approximately the same time, mid-latitude disturbances moving down the east side of a large mid-level ridge over eastern Asia were acting to weaken the mid level subtropical ridge structure north of the tropical cyclone. Both factors were significant in causing Bing's forward motion to slow as a turn to the north developed on 30 August. On 31 August, the

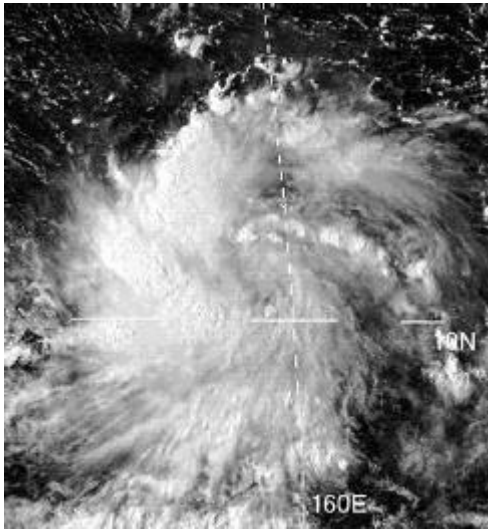


Figure 3-19-1 Visible satellite imagery of the tropical disturbance that became Bing. Valid time of imagery is 260533Z.

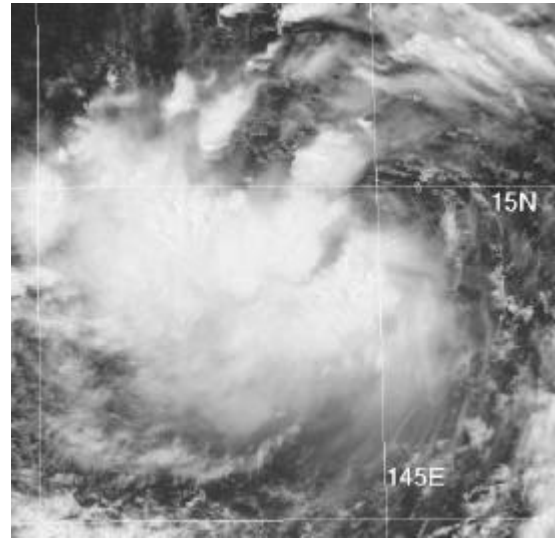


Figure 3-19-2 Visible satellite imagery of Tropical Storm Bing (19W) as it passed through the Rota Channel on 290333Z August.

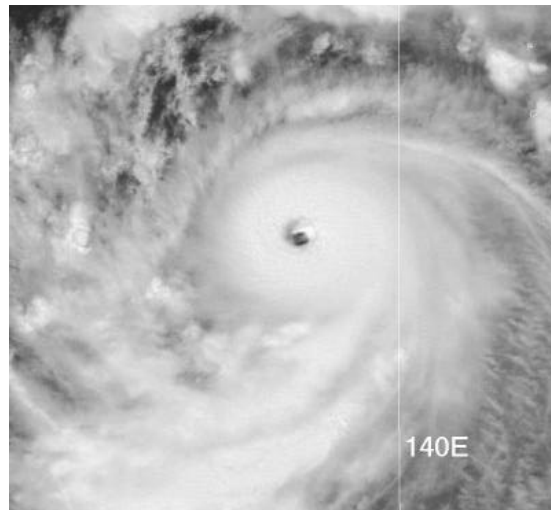
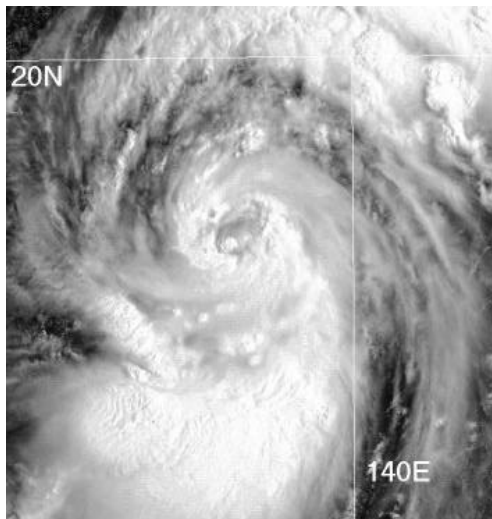


Figure 3-19-3 Visual Satellite imagery of Super Typhoon Bing (19W) during rapid intensification. The valid time of the left image is 302330Z August and the intensity was 80 kt (41 m/sec). The valid time of the right image is 010334Z September and the intensity was near 130 kt (67 m/sec).

cyclone began following a northward oriented track with speeds between 11 and 13 kt (20 to 24 km/hr), thus completing the transition from a Standard (S) to a Poleward Oriented (PO) synoptic pattern as described by the systematic and integrated approach of Carr and Elsberry (1994). As the cyclone continued north, it passed west of the islands of Iwo Jima and Chi Chi Jima on 01 and 02 September, respectively. During the closest point of approach, each island reported sustained winds of 30 kt (15 m/sec) with peak gusts ranging from 52 kt (26 m/sec), at Iwo Jima, to 40 kt (21 m/sec), at Chi Chi Jima. By 02 September, STY Bing was located south of the Japanese island of Honshu. Although the system was beginning to weaken, it remained a threat to Honshu. However, a shift in the sub-tropical ridge over Honshu enabled a band of relatively strong westerly winds to develop across the Japanese islands, causing the steering flow to become more westerly. Bing's track shifted to the northeast, and Honshu was spared.

By 03 September, Bing had moved far enough northward that it began to merge with a strong mid- and upper-level westerly wind flow. Accordingly, Bing turned towards the east-northeast and accelerated to speeds above 30 kt (15 m/sec) by 04 September. By 1000Z on the 4th, Special Sensor Microwave/Imager (SSM/I) indicated that upper-level westerly winds had sheared the system's convection and left the low-level circulation center exposed. Figure 3-19-4 shows Bing on 05 September. Although there was no longer central convection, it remained a potent extratropical cyclone with maximum sustained winds estimated to be 55 kt (28 m/sec).

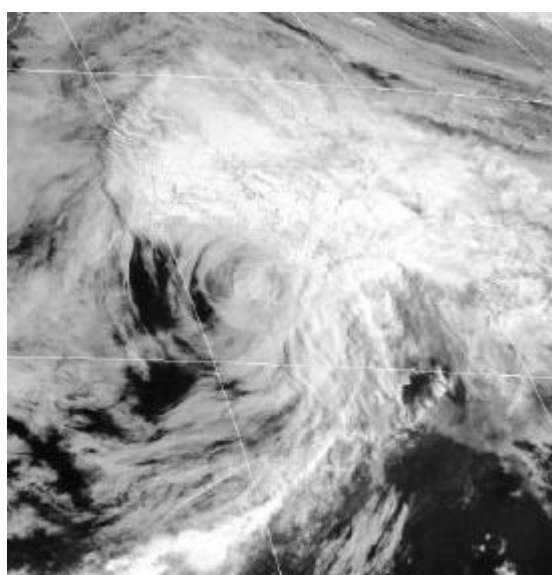


Figure 3-19-4 Visible satellite imagery of Super Typhoon Bing (19W) as a potent extratropical system with maximum sustained winds estimated to be 55 kt (28 m/sec). Valid time of image is 042227Z September.

III. DISCUSSION

a) Heavy Rainfall over Guam

Although STY Bing (19W) was a minimal tropical storm as it passed through the Rota channel, just north of Guam, it did bring a lot of rain. The National Weather Service Office at Tiyan reported 5.19 inches (13.2 cm) as Bing passed on 29 August. Andersen Air Force Base reported 6.17 inches (15.7 cm) of rain during a 36 hour period beginning at 0900Z on 28 August. The soil on the island was already saturated from repeated rainfall during the month, and the additional rain resulted in flooding of low-lying areas and around small streams. The excessive rainfall triggered a landslide in the village of Santa Rita on 30 August that caused extensive local damage. August 1997 turned out to be the wettest month in Guam's history as the final rainfall total reached 39.5 inches (100 cm). This was partially due to the monsoon trough being positioned over the southern and central Mariana Islands, allowing numerous tropical disturbances to track close to the island.

b) The Formation of Concentric Eye Walls

After Bing reached its peak intensity of 135 kt (69 m/sec), satellite and microwave imagery indicated the development of concentric eyewalls. Figure 3-19-5 shows the development over a 48 hour period. The image at the left shows Bing at peak intensity with a very small eye and intense convection in the eyewall. The middle image is about 24 hours later, when the cyclone had an intensity of 110 kt (56 m/sec). The central convection has diminished although a small eye feature is still discernable. However, convection in the outer bands has started to increase and wrap around the center. The image at right shows a newly formed, very large outer eye measuring approximately 90 nm (167 km) in diameter. The inner eye has almost disappeared with only a very small area of central convection remaining. At this point, the intensity has weakened to 85 kt (44 m/sec). This eyewall cycling process was very similar to that which occurred in STY Winnie (14W), TY Amber (18W) and STY Paka (05C) during the 1997 Western Pacific season.

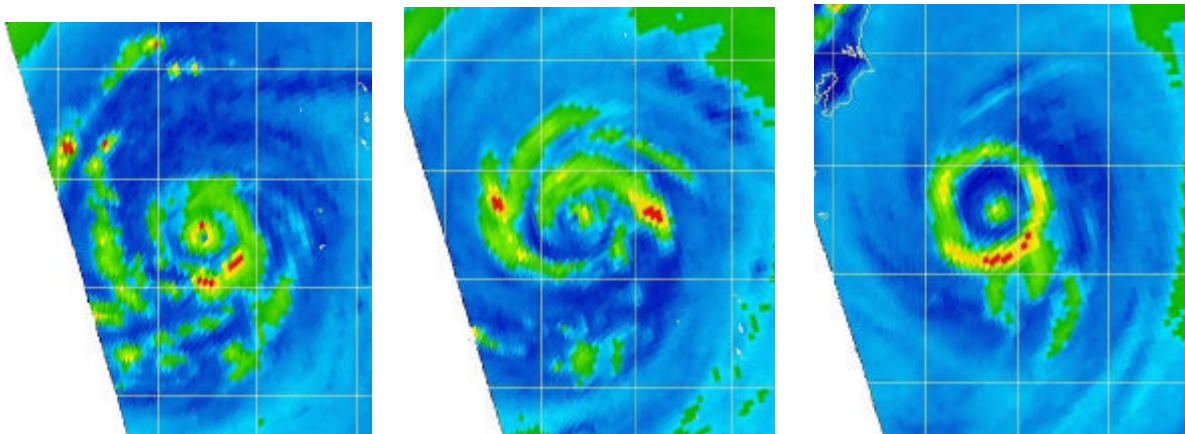


Figure 3-19-5 The development of concentric eye walls in Super Typhoon Bing (19W) as seen by SSM/I. From left to right, the valid times are 001011Z, 021205Z, and 030946Z September.

c) A comparison between two objective aids in forecasting Super Typhoon Bing's (19W) motion track

Many objective aids (forecast models) are used by the Typhoon Duty Officer (TDO) in determining the track forecast of a tropical cyclone. In order to produce the best forecast product possible, TDOs are thoroughly trained in the weaknesses and strengths of the various objective aids under certain synoptic conditions. Some examples of these strengths and weaknesses can be seen in an analysis of Bing's track. An example is the Colorado State University Model (CSUM), which is a statistical-dynamical model based on the work of Matsumoto (1984). The model is further discussed in Chapter 5, section 2.3.2. Because CSUM uses statistically developed regression equations, it has a problem predicting future changes in the synoptic environment which could alter the tropical cyclone's motion. This is illustrated in Figure 3-19-6. Although a distinct poleward bias can be seen, CSUM does a reasonable job of predicting the future track as long as the system remains south of the subtropical ridge. For example, during a 24-hour period beginning at 0000Z on the 28th, CSUM's 72-hour forecast errors averaged about

1.5 times lower than the Naval Oceanographic Global Atmospheric Prediction System (NOGAPS), a purely dynamical model. However, one to two days prior to the development of a poleward/poleward oriented pattern, CSUM continues to indicate westward motion. Westward forecasts continue until the model determines that the tropical cyclone is on the subtropical ridge axis, which is itself triggered by a northward (330 to 029 degrees) motion vector. Once the northward motion has been detected, CSUM begins to forecast northward motion. Bing's track was predominately northward by 1800Z on 30 August.

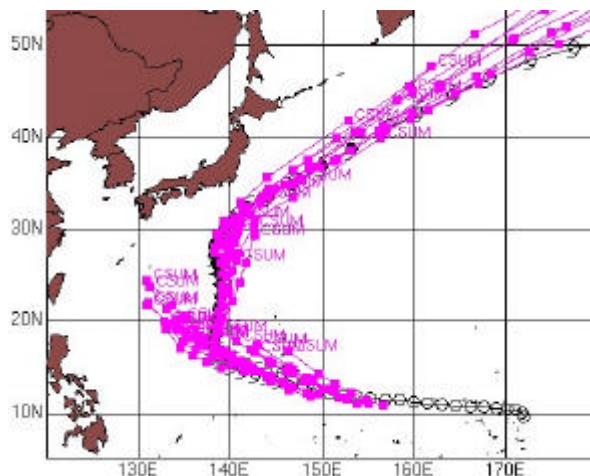


Figure 3-19-6 Forecast tracks given by CSUM for Super Typhoon Bing (19W).

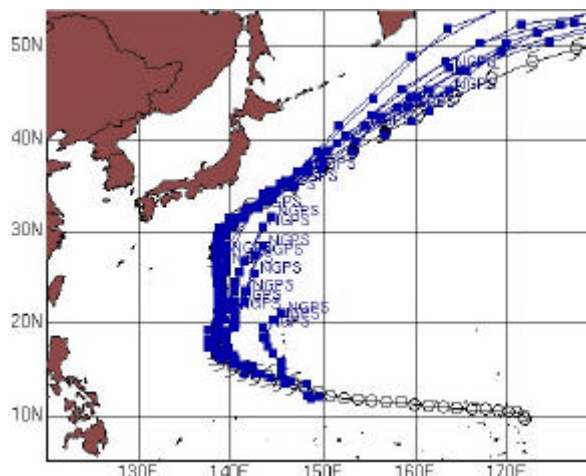
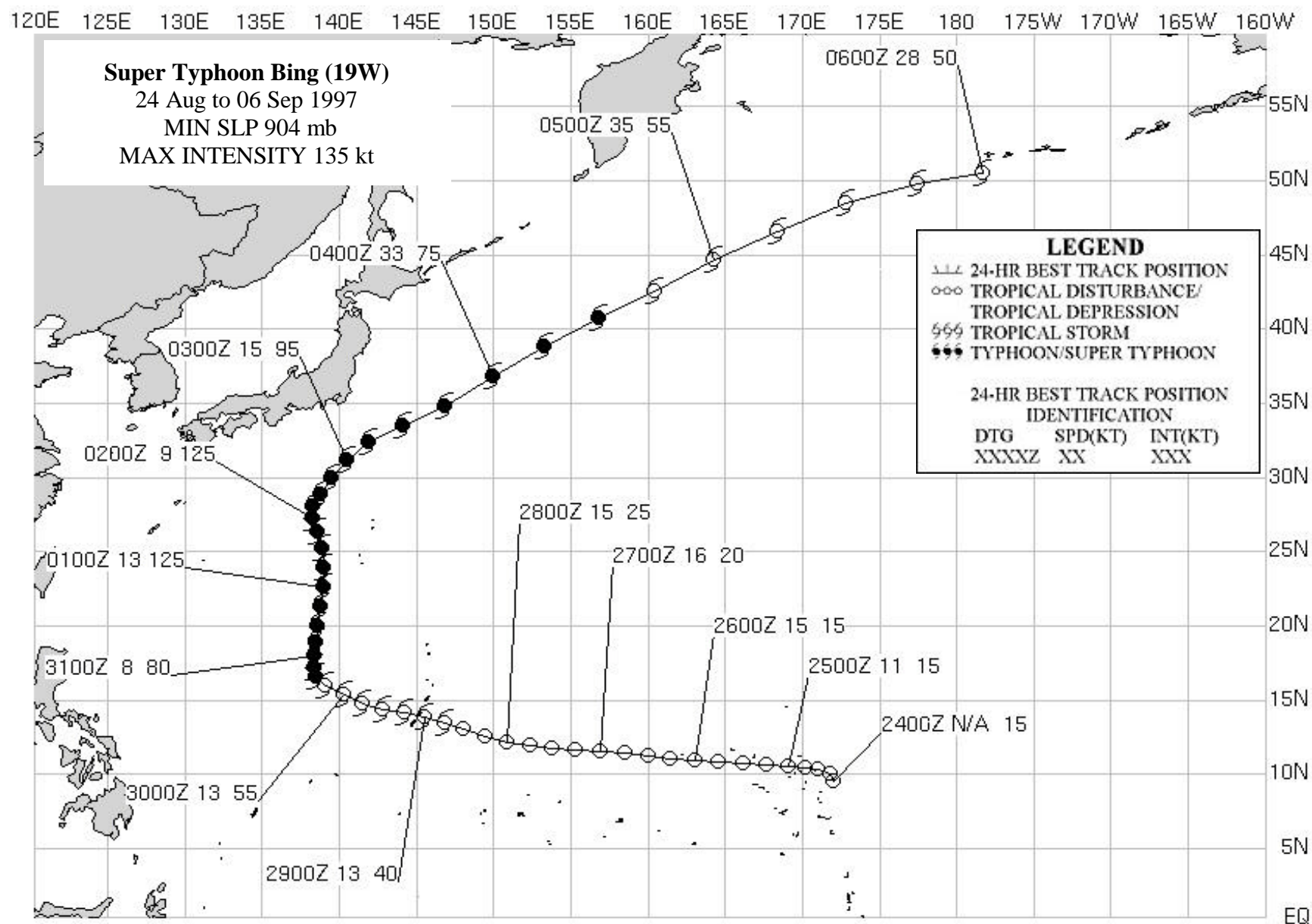


Figure 3-19-7: Forecast tracks given by NOGAPS for Super Typhoon Bing (19W).

On the other hand, NOGAPS is known to do fairly well when compared to other models in transitioning from a Standard/Dominant Ridge (S/DR) to a Poleward/Poleward Oriented (P/PO) environment. One documented bias of NOGAPS is to indicate northward motion for a TC a few days before it actually occurs. In the case of Super Typhoon Bing (19W), this is illustrated by Figure 3-19-7. Both NOGAPS and CSUM had a tendency to be right of the forecast track during the northward motion portion of the track. However, during the 54-hour period beginning at 0000Z on 31 August during which northward motion was prevalent, NOGAPS errors were about 2.3 times lower than CSUM. The tendency of NOGAPS to surpass CSUM in this synoptic regime has also been documented. These and other model tendencies are known by the TDOs, greatly enhancing their ability to choose among a plethora of aids during forecast development.

IV. IMPACT

The main impact on the island of Guam was heavy rainfall and associated flooding. The previously mentioned landslide in Santa Rita caused extensive damage to the Namo Falls Tourist Park, as well as some broken sewage pipes, which allowed open sewage to flow into the Namo River. However, there were no reports of injuries. There were no reports of injuries or damage from the islands of Iwo and Chi Chi Jima.



TROPICAL STORM CASS (20W)

On 26 August, an area of convection developed approximately 160 nm (297 km) to the south of Hong Kong, due east of Hainan Dao, in the South China Sea. Over a 24-hour period, this area became considerably more organized and at 1830Z on the 27th, a Tropical Cyclone Formation Alert (TCFA) was issued. An exposed low-level circulation was evident with convection developing near the center. However, development was inhibited by outflow from Typhoon Amber (18W), which was approximately 600 nm (1100 km) to the east. At 0000Z on the 28th, a warning was issued for Tropical Depression (TD) 20W with an intensity of 30 kt (16 m/sec). The system tracked very slowly towards the east as it continued to intensify, primarily due to a direct interaction with the steering flow from Amber. The cyclone became Tropical Storm

Cass (20W) at 0000Z on 29 August as inhibiting effects from Amber lessened. At this point, Cass turned toward the northeast and increased its forward speed slightly. On 29 August, Cass turned northward, as effects from Amber diminished and the steering flow became south-southwesterly. Outflow from Amber continued to inhibit full development of Cass, which peaked at 45 kt (23 m/sec) on 29 August at 1200Z. Cass maintained this intensity for 12 hours. On 30 August, Cass made landfall near Xinglin, China. The 0600Z synoptic reports from surrounding areas indicated winds of 35 kt (18 m/sec) in the immediate coastal area. At 1200Z the same day, the final tropical cyclone warning was issued by JTWC as the system tracked north-northwestward and dissipated in the mountains of southeastern China.

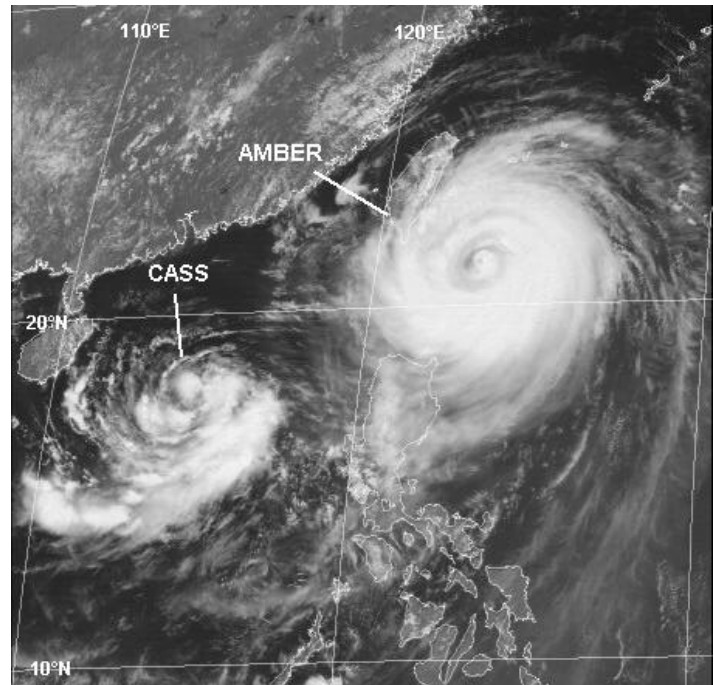
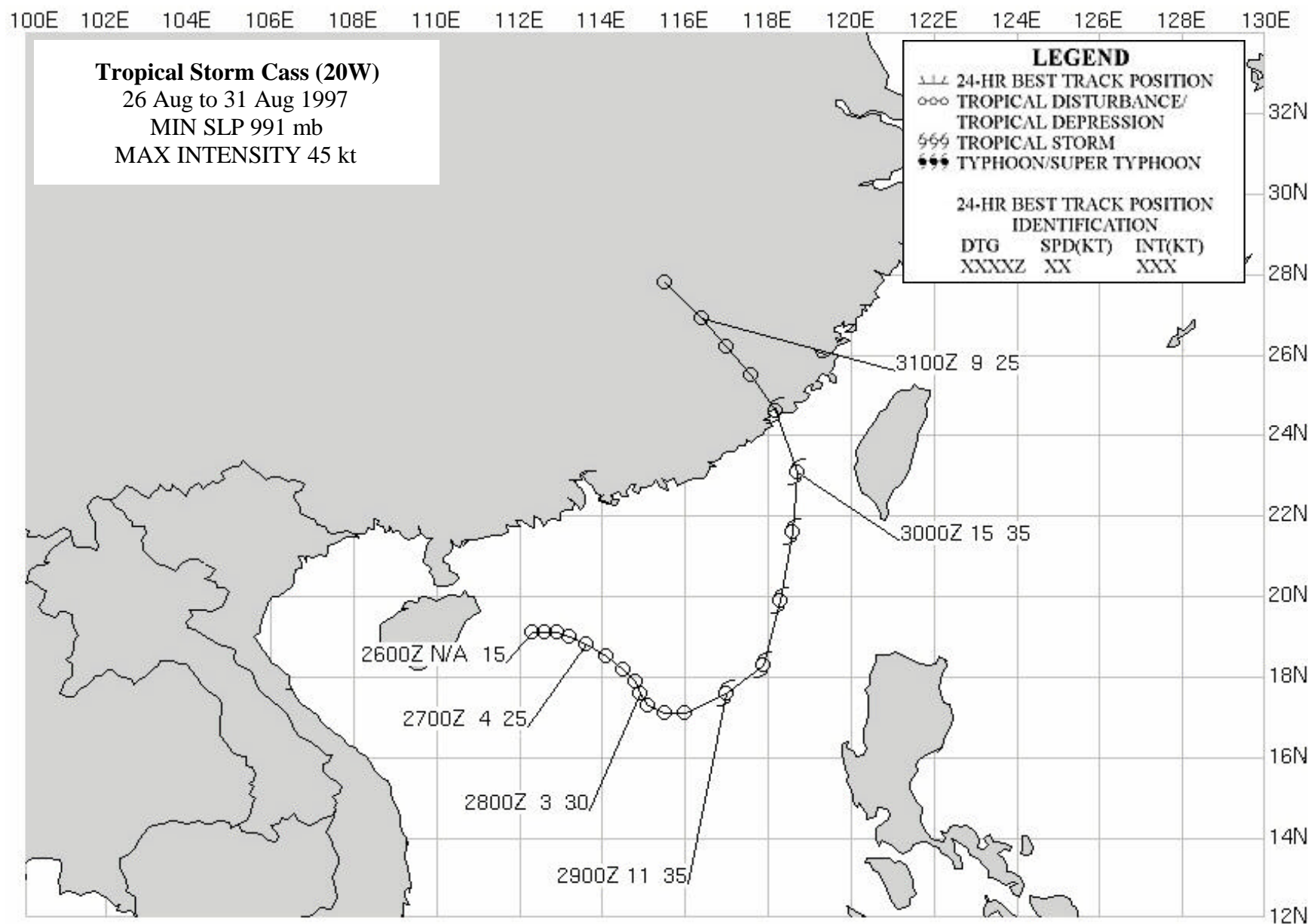


Figure 3-20-1 Tropical Storm Cass (20W) during its TD stage as it interacts with Typhoon Amber (18W) (280333Z August visible GMS imagery).



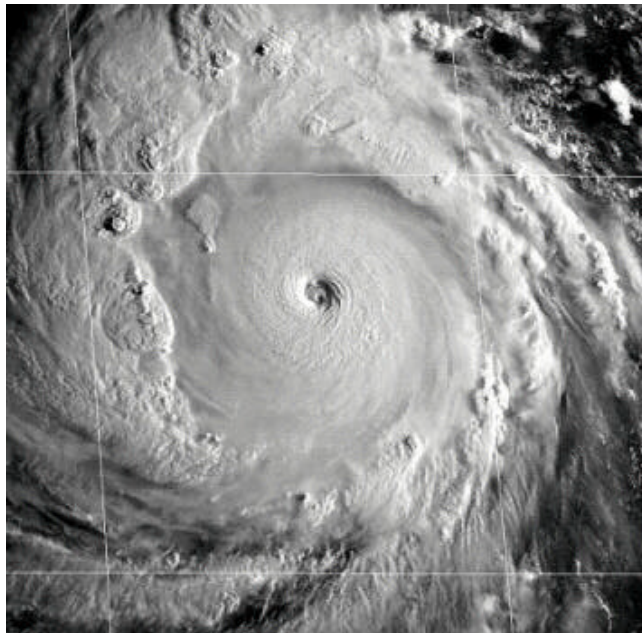
SUPER TYPHOON OLIWA (02C)

I. HIGHLIGHTS

The sixth of eleven tropical cyclones (TCs) to attain super typhoon intensity in the western North Pacific (WPN) during 1997, Oliwa formed east of the international dateline (IDL) and to the southwest of the Hawaiian Islands. After becoming a tropical storm in the Central Pacific Hurricane Center (CPHC) area of responsibility (AOR), this TC was named Oliwa. Oliwa moved on a long straight running track which brought it across the IDL into the WPN, and eventually to landfall in southwestern Japan. As it moved westward from its region of formation in an eastward displaced monsoon trough and into the WNP basin (which was unusually cloud free for the time of year), the intensity forecasts for Oliwa were nearly all too low. Early in its life, Oliwa was accompanied by a weak, unnamed Southern Hemisphere twin. While near its peak intensity, a possible eye-wall meso vortex was revealed by visible satellite imagery. After its peak, well-defined concentric eye wall clouds were observed, which were especially distinct in microwave imagery.

II. TRACK AND INTENSITY

During late August, low-level monsoon westerlies extended across the IDL and stretched eastward at low latitudes to the southwest of Hawaii. At the end of August, a tropical disturbance formed southwest of Hawaii at the eastern end of the monsoon trough associated with these eastward-displaced low-latitude westerlies. This disturbance moved slowly westward and intensified. On 02 September, while it was still east of the IDL, the CPHC (located in Honolulu, Hawaii) upgraded it to Tropical Depression (TD) 02C. After becoming a tropical storm in CPHC's AOR at 030000Z September, TD 02C was named Oliwa (Hawaiian for "Oliver", the letter "w" in Oliwa is pronounced as a "v" in this case). On 04 September, Oliwa crossed the IDL and entered the JTWC AOR. The first warning issued by JTWC was valid at 040600Z September.



3-02C-1 The low-angle morning sun nicely highlights the features of the cloud tops of Oliwa's eye wall cloud and peripheral rainbands as the typhoon reached its peak of 140 kt (72 m/sec) (092034Z September visible GMS imagery).

After crossing the IDL into the WNP basin, Oliwa moved on a steady west-northwestward track and intensified. At first, the rate of intensification was slow; during the 72-hr period from 0600Z on 04 September to 0600Z on 07 September, Oliwa's intensity increased from 35 kt (18 m/sec) to only 50 kt (26 m/sec). After another 30 hours (by 1200Z on the 8th), its intensity had slowly climbed to that of a minimum typhoon (65 kt or 33 m/sec). Between 1800Z on the 08th and 1800Z on the 09th, Oliwa explosively deepened as its intensity climbed from 75 kt (39 m/sec) to its peak of 140 kt (72 m/sec), as shown in Figure 3-02C-1. The 24-hour pressure drop associated with this wind-speed increase was 69 mb (see the discussion below for more details on Oliwa's explosive deepening).

For five days after reaching peak intensity, Oliwa continued its steady motion toward the west-northwest and slowly weakened. On 14 September, the typhoon passed to the northeast of Okinawa where it slowed, and on 15 September, it reached its point of recurvature and turned northeastward toward Kyushu. Early on the morning of 16 September, Oliwa made landfall on the coast of southern Kyushu, where despite having weakened considerably (down to 70 kt - 36 m/sec), it was responsible for loss of life and considerable damage (see the Impacts Section). After landfall, the typhoon moved across Japan and weakened. By the morning of 17 September, it had moved to the Sea of Japan where it dissipated. The final JTWC warning was issued at 170600Z.

III. DISCUSSION

a. Oliwa's Digital Dvorak (DD) time series: a case of explosive deepening

Oliwa was one of several typhoons during 1997 for which a time series of its hourly DD numbers (Figure 3-02C-2) was calculated. Oliwa's DD numbers are in overall agreement with the best-track intensity. The rate of intensification (a drop in the sea level pressure of 69 mb in 24 hours for an average of 2.9 mb/hr), as indicated by both the DD time series and the best-track intensities during the 24-hour period from 1800Z on 08 September to 1800Z on

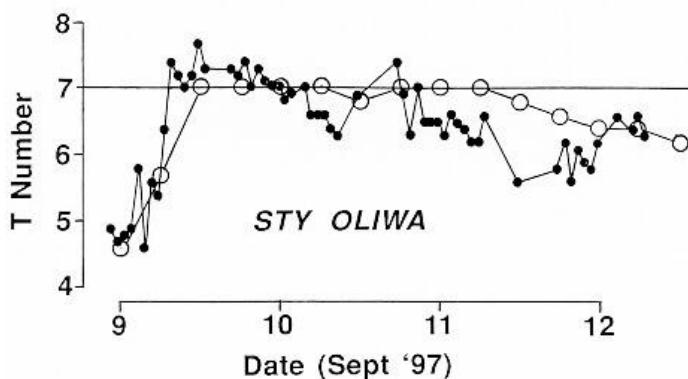


Figure 3-02C-2 A time series of Oliwa's hourly DD numbers (small black dots) compared with the warning intensity (open circles). On 09 September, the TC underwent a period of explosive deepening as indicated by both the DD numbers and the best-track intensities. After reaching its peak intensity, the typhoon's intensity changed very little for nearly two days.

09 September, qualifies as a case of explosive deepening (a drop of minimum sea level pressure of 2.5 mb/hr for at least 12 hours (Dunnavan 1981)). Many typhoons which reach high peak intensities (i.e., more than 100 kt (51 m/sec)) undergo a period of rapid or explosive deepening which tends to commence when the TC reaches minimal typhoon intensity.

Oliwa's explosive deepening was unforeseen. Neither the official forecasts, nor numerical guidance indicated that this event would take place. The official forecasts prior to Oliwa's peak intensity were up to 40, 60, 65 and 90 kt too low for the 12-, 24-, 48- and 72-hour forecast periods respectively. While much progress has been made toward reducing the errors of track

forecasts, and real skill as measured against such benchmarks as CLIPER has been achieved, errors of intensity forecasts remain large, and there is much room for improvements.

b. A possible eye wall mesovortex

Eyewall mesocyclonic vortices (EMs) were first detected and documented in airborne Doppler radar data by Marks and Houze (1984) and also with aircraft inertial navigation equipment as noted by Black and Marks (1991). Stewart and Lyons (1996) identified EMs with the Guam NEXRAD in association with the passage of Ed (1993) over Guam. Until the implementation of the NEXRAD radar network in the United States during the early 1990s, only chance encounters with EMs have occurred during reconnaissance aircraft penetrations. However, now that Doppler velocity data are available, strong mesocyclones associated with TC outer convective bands and eyewall convection are frequently detected. Stewart et al. (1997) used NEXRAD data to show that mesocyclonic vortices in the wall clouds of TC eyes may be a mechanism for TC intensification and for extreme wind bursts in TCs, as noted with Hurricane Andrew damage (Wakimoto and Black 1993). In three cases, a TC underwent a period of rapid intensification during which time several vertically deep EMs formed prior to the occurrence of rapid intensification and persisted for several hours while rapid deepening was occurring.

In the case of Oliwa, a possible EM was observed in its eye on visible satellite imagery (Figure 3-02C-3) in the early daylight hours of 10 September. Possible EMs were evident on only two image frames: at 092030Z and 092130Z September. Unlike the cases investigated by Stewart et al. (1997), the EMs observed in Oliwa's eye wall cloud occurred after the TC had reached its peak intensity.

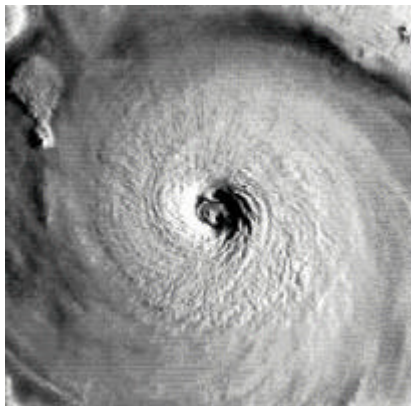


Figure 3-02C-3 A small comma shaped cloud along the inner edge of Oliwa's eye wall cloud is a possible manifestation of an eyewall mesovortex. This image is a zoom of the eye and eye wall cloud which appears in Figure 3-02C-1 (092034Z September visible GMS imagery).

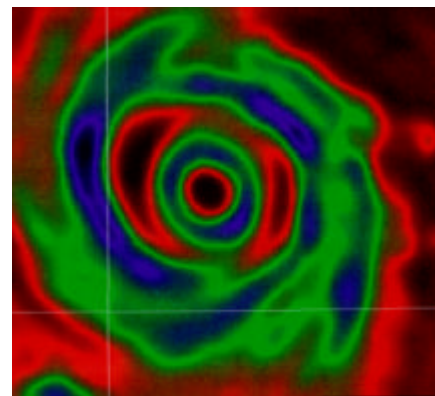


Figure 3-02C-4 Microwave imagery is especially suited to view concentric wall clouds in a TC. Oliwa developed well-defined concentric wall clouds as it began to weaken (120104Z September 85 GHz horizontally polarized microwave DMSP imagery).

c. Concentric wall clouds

Oliwa was yet another example of an intense WNP typhoon acquiring concentric eye wall clouds which were easily seen on conventional visible and infrared imagery, and especially well-defined on microwave imagery (Figure 3-02C-4). Microwave imagery is particularly well-suited to observe and document the evolution of concentric eye wall clouds (e.g., Paka's (05C) eye-wall replacement cycle was exceptionally well documented on microwave imagery) There is a tendency for high-end typhoons (i.e., those with peak intensity greater than 100 kt (51 m/sec)) to develop concentric eye wall clouds.

IV. IMPACT

Oliwa made landfall in southwestern Japan where it was responsible for widespread damage and for loss of life. On Japan's southern island of Kyushu, seven people were reported killed. One thousand homes were flooded and dozens of homes were destroyed. Along Korea's southern coast, twenty-eight ships sank or were wrecked in strong winds and high waves. A crabbing ship with 10 crewmen aboard was reported missing. Earlier in its life, Oliwa passed close to the island of Agrihan in the Marianas, which reported winds of about 85 mph (74 kt). No reports of damage or injuries were received at JTWC.

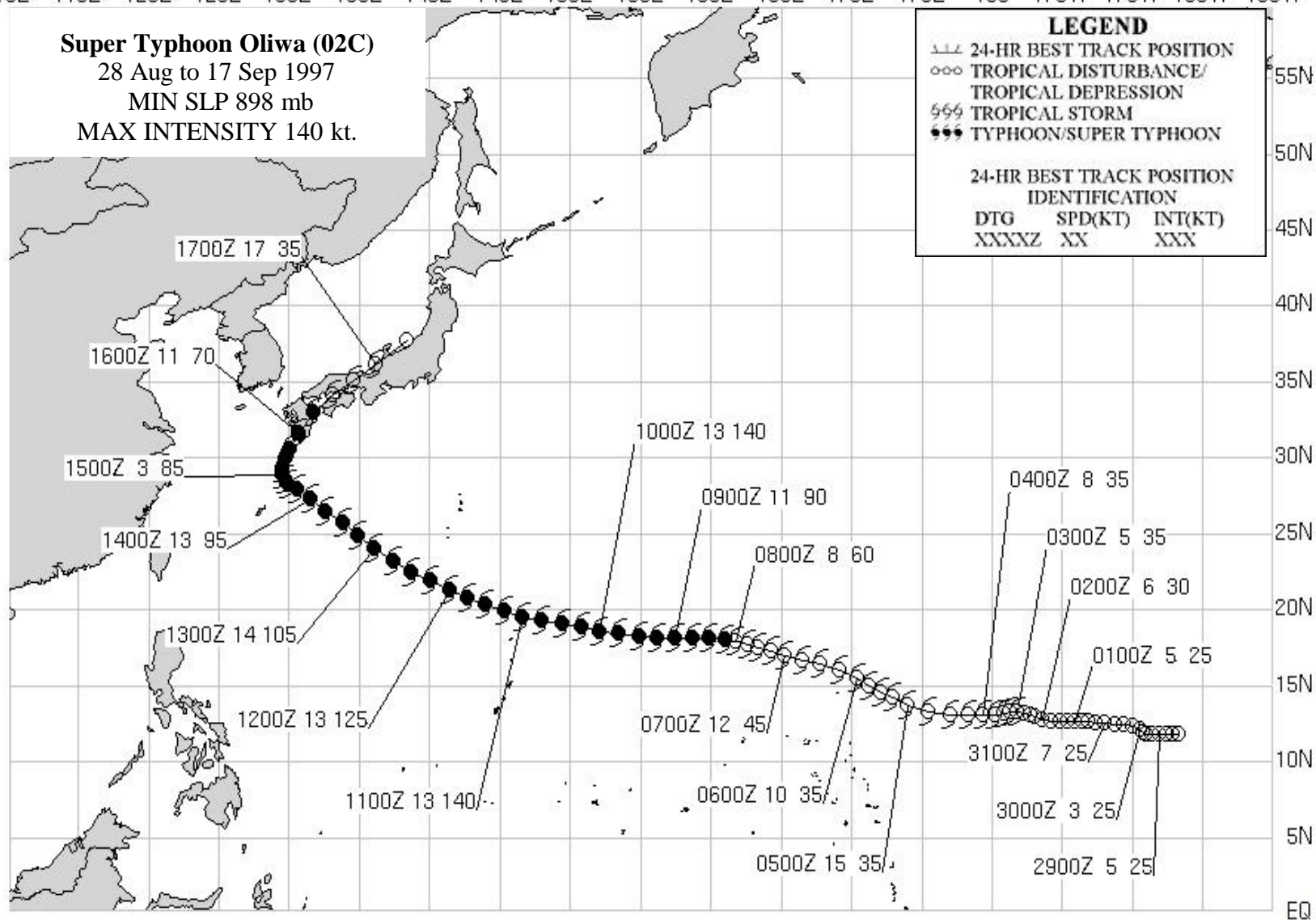
110E 115E 120E 125E 130E 135E 140E 145E 150E 155E 160E 165E 170E 175E 180 175W 170W 165W 160W

Super Typhoon Oliwa (02C)

28 Aug to 17 Sep 1997

MIN SLP 898 mb

MAX INTENSITY 140 kt.



TYPHOON DAVID (21W)

The disturbance which would become Typhoon David (21W) was first noted in the monsoon trough northeast of Kwajalein on 09 September. Visible satellite imagery on 10 September showed Super Typhoon Oliwa (02C), moving northwestward south of the subtropical ridge axis. Southeast of Oliwa, the monsoon trough extended from 155E to 175W along the 10N latitude line in conjunction with a weaker near-equatorial trough in the southern hemisphere that extended from 160E to 173E near 5S to 8S. The twin troughs were indicative of a large area of westerly winds straddling the equator between 10N and 8S. The system was initially mentioned on the Significant Tropical Weather Advisory (ABPW) at 0600 on 10 September; six hours later a Tropical Cyclone Formation Alert (TCFA) was issued. By 12 September at 0034Z, visible satellite imagery indicated that the developing depression had a very large associated low-level circulation, with westerly winds feeding into the vortex from as far west as 150E. On the eastern side, flow into the vortex extended well past the dateline. At 1800Z that day, JTWC issued the first warning on the system. Post-analysis would later indicate that the system had actually reached tropical depression intensity (25 kt(13 m/sec)) two days earlier on 10 September. The system continued to organize as it tracked northwestward at approximately 10 kt (19 km/hr).

David intensified at a climatological rate, becoming a typhoon by 1800Z on 13 September. The cyclone tracked steadily in a northwestward direction equatorward of the sub-tropical ridge (Standard Dominant Ridge pattern/region of the Systematic and Integrated Approach – see Chapter 1). David's large size contributed to the strong northwestward component of its motion due to the "Beta Effect". This is the mechanism by which large tropical cyclones tend to self-propagate northward due to their disturbance of the earth's vorticity field.

By 1800Z on 14 September, David had reached its peak of 95 kt (49 m/sec), remaining at this intensity for 36 hours. It continued traveling in a generally northwestward direction at speeds ranging from 12 - 15 kt (22 - 28 km/hr). By 16 September, strong mid-level ridging (related to the large Beta Effect) had developed east of the system. This was indicative of the formation of a Poleward/Poleward Oriented pattern/region (Systematic and Integrated Approach, see Chapter 1). Transition to the poleward pattern, along with a passing mid-latitude trough, caused David to recurve.

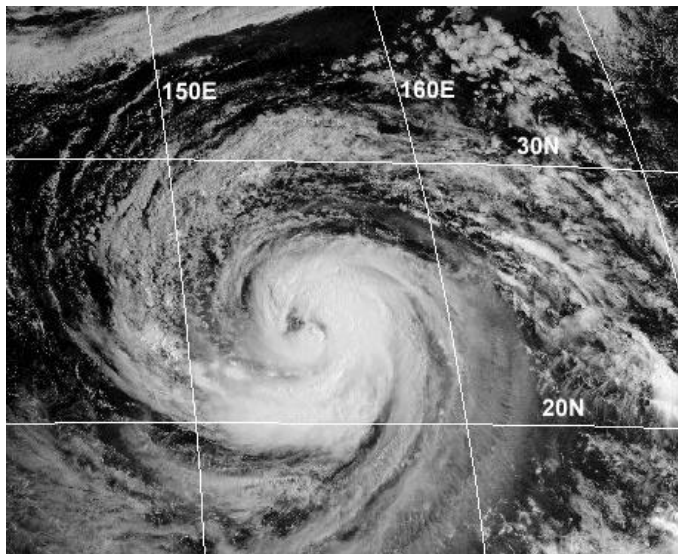
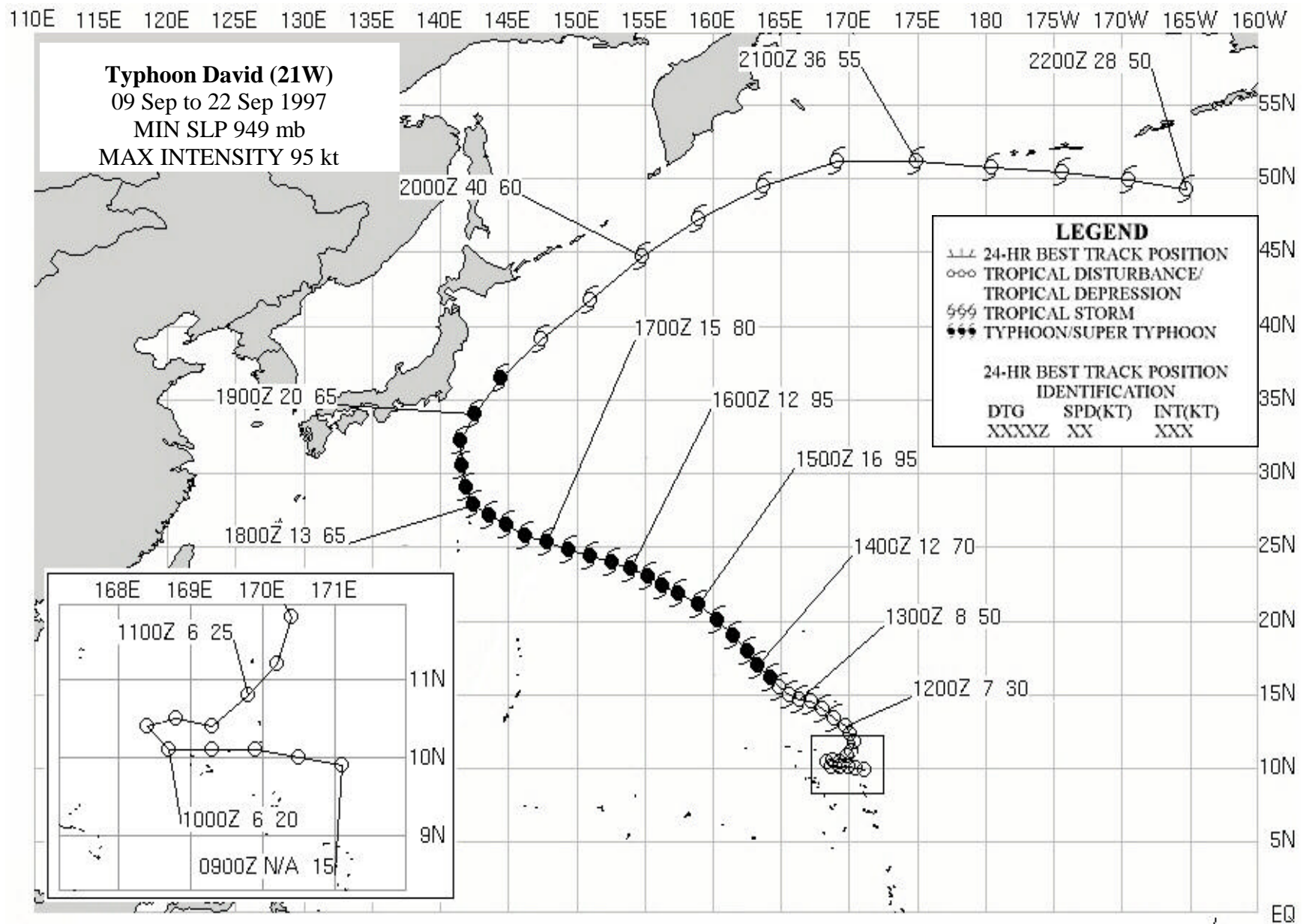


Figure 3-21-1 Typhoon David (21W) at 2230Z on 15 September 1997.

David passed near the island of Minami Tori Shima (WMO 479910) on the 16th, where sustained winds of 65 kt (33 m/sec) and a minimum sea level pressure of 968mb were recorded. Deep convection started to decrease near the system center as the cyclone began to weaken. However, the convection around the periphery began to increase and visible satellite imagery indicated a large cloud free area around the tropical cyclone's center.

At 0000Z on the 18th, David made its closest approach to the island of Chi Chi Jima (WMO 47971), where sustained wind speeds of 40 kt (21 m/sec) and a minimum sea level pressure of 967mb were reported. The intensity had dropped to 65 kt (33 m/sec), but the system remained a threat to the islands of Japan. Fortunately, David continued to turn toward the northeast, making its closest approach to Honshu on 19 September. Yokosuka reported 30 kt (15 m/sec) sustained winds at 0300Z.

JTWC issued its final warning at 0600Z on 20 September as the system transitioned to an extratropical low. The remnants of Typhoon David (21W) continued moving into the Gulf Of Alaska. There were no reports of damage or injuries as a result of David.



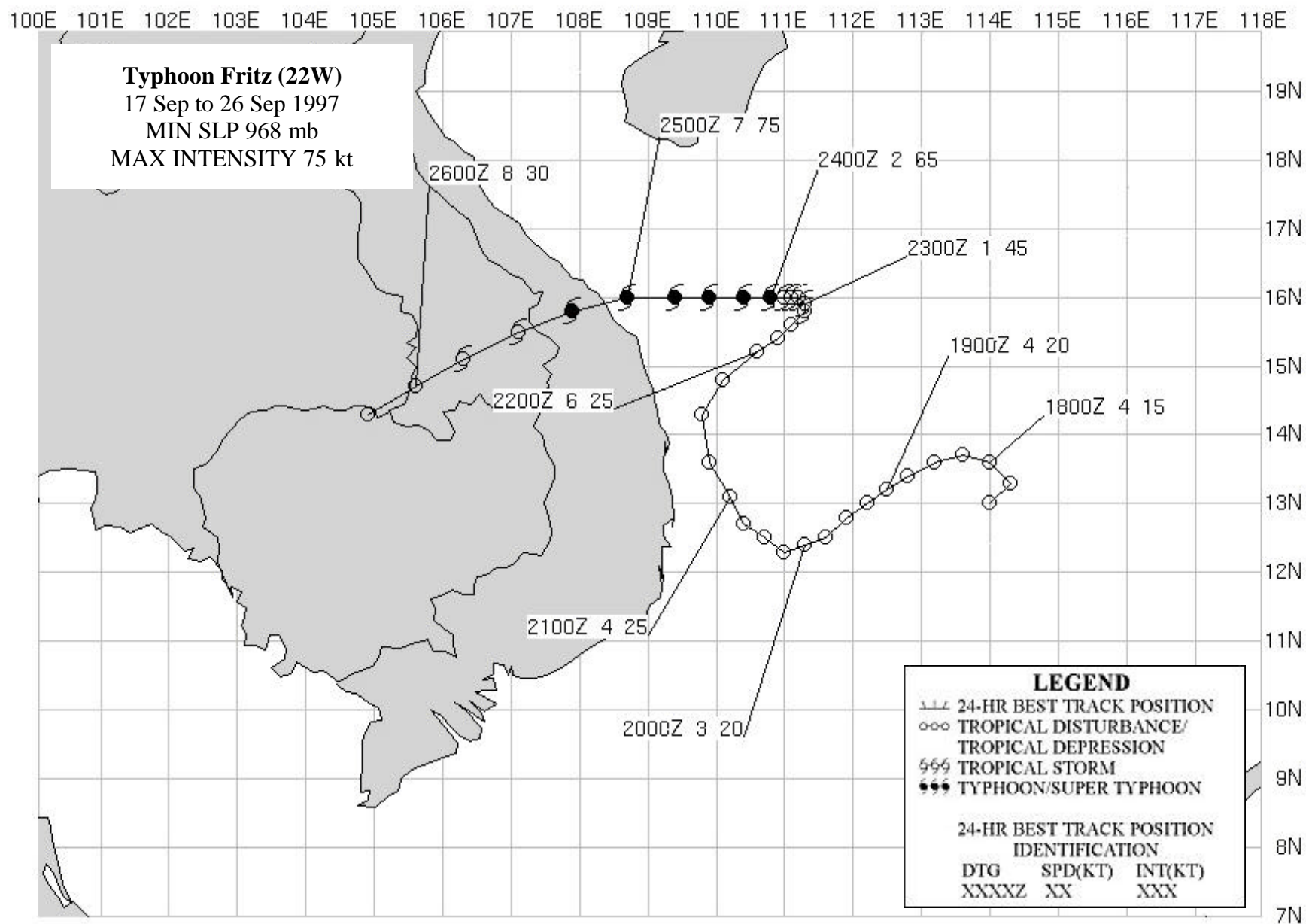
TYPHOON FRITZ (22W)

The tropical disturbance that became Typhoon Fritz (22W) originated in the South China Sea (near the Philippine archipelago) within a long east-west cloud band associated with the monsoon trough. When first mentioned on the 19 September Significant Tropical Weather Advisory (ABPW), the deep convection associated with this disturbance had formed a distinct cloud cluster embedded in an otherwise unbroken monsoonal cloud band that stretched eastward along 10N from Southeast Asia to 170E. On 20 September, JTWC went directly to the first warning on Tropical Depression (TD) 22W. At 1800Z that day, satellite data indicated that the winds in the system had increased to 25 kt (13 m/sec). The cyclone was expected to intensify after it moved into open water away from the coast of Vietnam. As expected, TD 22W turned sharply to the right and began a slow track



Figure 3-22-1 Tightly wrapped coils of deep convection surrounding a ragged eye indicate that Fritz has become a typhoon (240133Z September visible GMS imagery).

toward the north-northeast. The system failed to intensify until 22 September when it slowed southeast of Hainan Island, and organization of the deep convection began to improve. TD 22W was upgraded to Tropical Storm Fritz (22W) on the warning valid at 0000Z on the 23rd, based on satellite intensity estimates of 45 kt (23 m/sec). After becoming a tropical storm, Fritz turned toward the west and began to track toward the coast of Vietnam while continuing to intensify. Fritz reached typhoon intensity at 0000Z on the 24th (Figure 3-22-1). The intensity peaked at 75 kt (39 m/sec) at 0600Z on 24 September and held steady until the 25th when Fritz made landfall. Fritz steadily weakened after landfall, and the final warning was issued valid at 1800Z on 25 September, when it was expected that the system would dissipate over land within 24 hours. In Vietnam, at least 25 people were reported killed and dozens were missing. Most of the victims were gold prospectors buried in landslides triggered by flash flooding.



TROPICAL STORM ELLA (23W)

The disturbance that became Tropical Storm Ella (23W) began as a small circulation east of the dateline, with scattered convection emerging from a larger area of convection on 19 September. By 21 September, visible imagery indicated that the convection had become well developed over the system's center. Now a tropical storm, Ella moved rapidly to the west-northwest at 18 to 25 kt (33 to 46 km/hr) under the influence of easterly steering flow south of the subtropical ridge. However, by 22 September, the system began to slow as it approached a break in the ridge, and on 23 September Tropical Storm Ella (23W) moved through the break and recurved to the northeast.

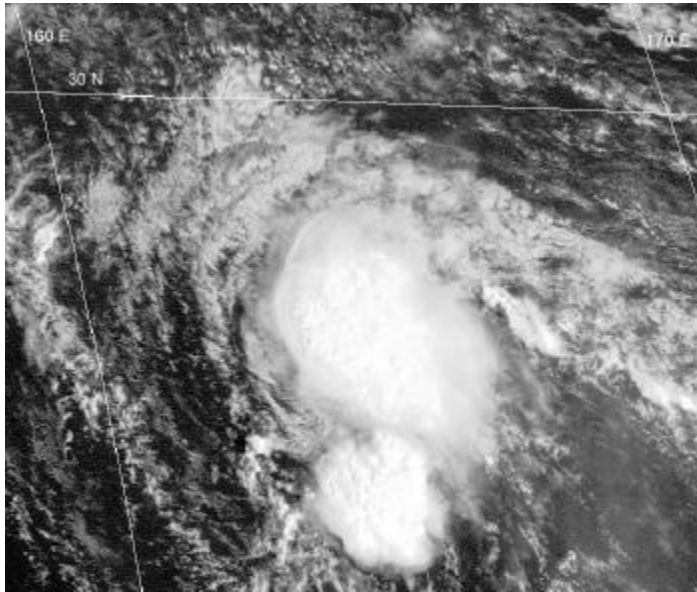
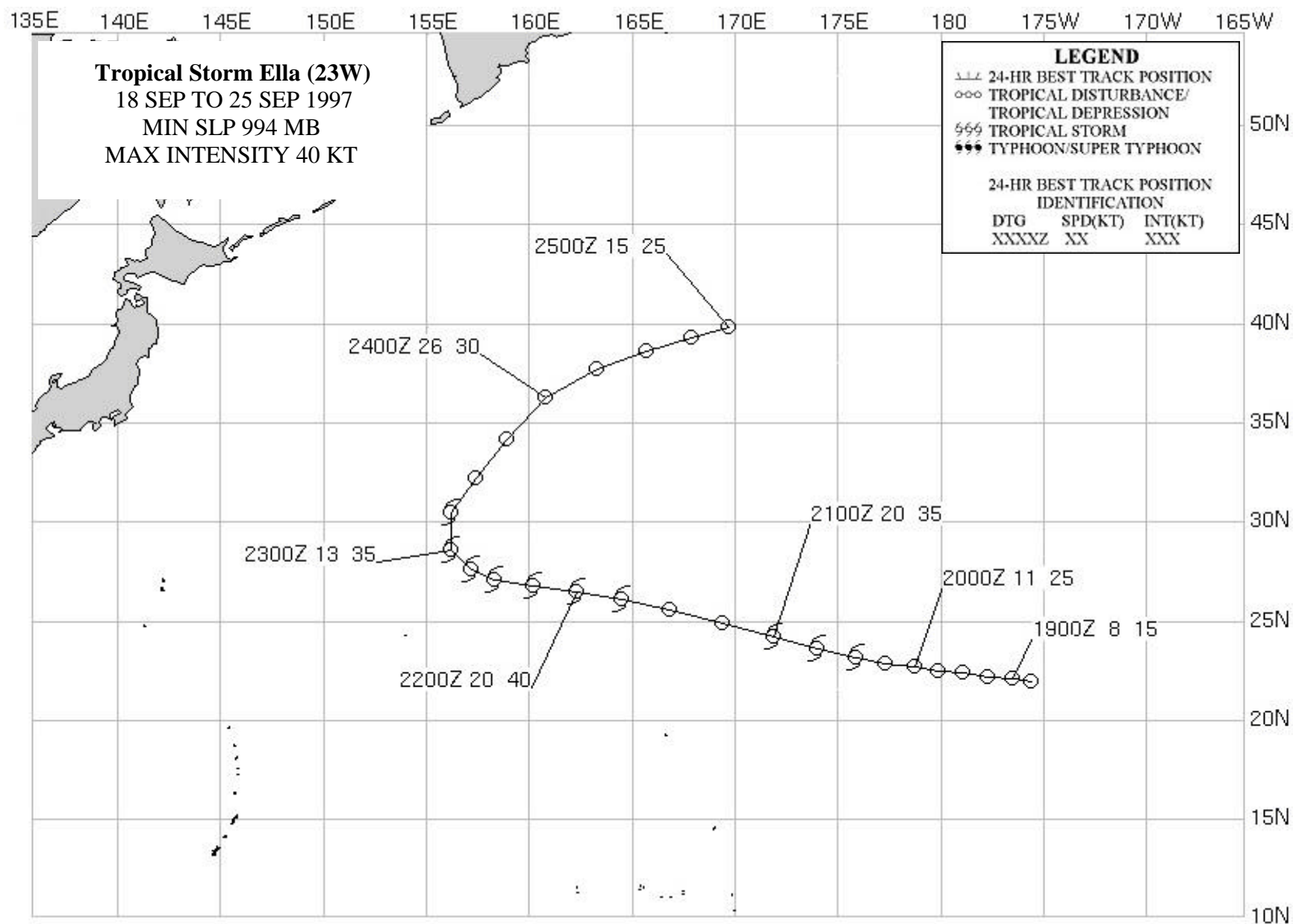


Figure 3-23-1 Tropical Storm Ella (23W) showing a partially exposed low-level circulation (212132Z September visible GMS imagery).

Tropical Storm Ella (23W) was an unusually small system. The central convection associated with the low-level circulation on 20 September was only about 30 nm (56 km) in diameter. The cyclone's small size in conjunction with moderate vertical wind shear kept Tropical Storm Ella (23W) from intensifying beyond a minimal tropical storm (peak intensity was 40 kt (20m/s) on 22 September). Tropical Storm Ella (23W) dissipated on 24 September near 40N 170E in the vicinity of a frontal zone.



SUPER TYPHOON GINGER (24W)

I. HIGHLIGHTS

The seventh of eleven Tropical Cyclones (TCs) to attain super typhoon intensity in the western North Pacific (WNP) during 1997, Ginger formed at low latitudes in the Marshall Islands. It was one of ten TCs that formed east of 160E and south of 20N; within the "El Niño" box in Figure 3-3a. Ginger moved on a north-oriented track through the eastern portion of the western North Pacific basin. As it neared its peak intensity, the typhoon possessed an extensive system of primary and peripheral rainbands. When it reached 30N, it accelerated within the mid-latitude westerlies where it transitioned into a vigorous extratropical low. Ginger was one of the many 1997 TCs that formed at the eastern end of the monsoon trough near the international dateline (IDL) and evolved into a large solitary TC's (i.e., much of the WNP basin, with the exception of the single typhoon, was unusually free of deep convection).

II. TRACK AND INTENSITY

During the first two weeks of September 1997, two TCs, STY Oliwa (02C) and TY David (21W), formed near the IDL, moved across the basin as large solitary typhoons, and recurved near Japan. On 21 September, as David was recurving east of Japan, the tropical disturbance that was to become Ginger had consolidated at low latitude near the IDL. On 22 September, this tropical disturbance became better organized, as evidenced by a low-level cyclonic circulation that was well-defined by synoptic data. Deep convection associated with the low-level circulation became organized into curved bands; and animated water vapor imagery indicated the presence of anticyclonic flow at upper levels over the low-level center. This disturbance was first mentioned on the Significant Tropical Weather Advisory (ABPW) valid at 0000Z on 22 September. A Tropical Cyclone Formation Alert (TCFA) was

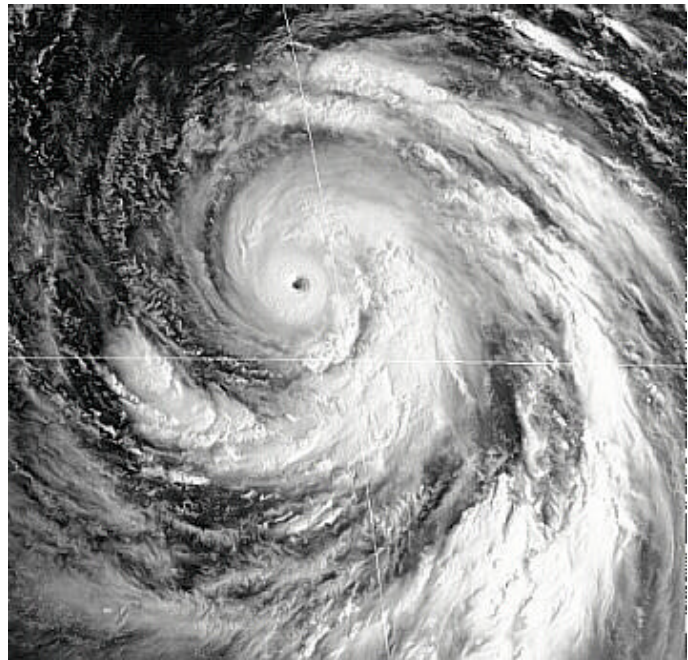


Figure 3-24-1 Ginger nears its peak intensity of 145 kt (75 m/sec). Extensive banding features accompanied this TC (262132Z September visible GMS imagery).

issued at 0530Z on the 22nd, when satellite data indicated continued improvement in the system's organization and the presence of factors deemed favorable for TC formation (e.g., the water vapor derived winds showed strong upper-level divergence over the system). Based on satellite derived intensity estimates of 25 kt (13 m/sec), the first warning on Tropical Depression

(TD) 24W was issued valid at 1800Z on 22 September. For 36 hours, TD 24W moved northwest and slowly intensified. Based on satellite intensity estimates, it was upgraded to Tropical Storm Ginger (24W) on the warning valid at 0600Z on 24 September. Ginger began to track in a more northerly direction. Intensifying at a normal climatological rate, it became a typhoon at 1200Z on the 25th. At this point Ginger began a period of explosive deepening (see Discussion Section) and in the 24-hour period from the 26th at 0000Z to the 27th at 0000Z, the intensity jumped from 75 kt (39 m/sec) to 145 kt (75 m/sec).

As it neared its peak intensity, Ginger's structure provided spectacular views via visible satellite imagery (e.g., Figure 3-24-1). It had a small well-defined eye embedded in a smooth symmetrical Central Dense Overcast (CDO), which in turn was surrounded by an extensive pattern of primary and peripheral cloud bands. The unusually cloud free structure of the large-scale environment served to highlight Ginger in the imagery (Figure 3-24-2).

After Ginger peaked on 27 September, it moved slowly north-northwestward and arrived at its point of recurvature 36 hours later at 1200Z on 28 September with an intensity of 110 kt (57 m/sec). Typically, weak typhoons peak at or near their point of recurvature, while more intense typhoons, like Ginger, experience a delay between reaching peak intensity and arriving at their point of recurvature (JTWC 1994).

After recurving, Ginger began a slow acceleration into the midlatitudes. Finally, the intensity fell below typhoon force at 1800Z on the 30th, and the system made a smooth transition into a vigorous extratropical low. The final warning was issued, valid at 0600Z on 30 September, when a complete extratropical transition was expected within six hours.

III. DISCUSSION

a. Ginger's Digital Dvorak (DD) time series

Ginger was one of several typhoons during 1997 for which a time series of hourly DD-numbers (Figure 3-24-3) was recorded. Ginger's DD-numbers are in overall agreement with the best-track intensity; although there are two notable exceptions. First, the drop of the DD-numbers below the values of the best track intensities as Ginger was weakening, is an intrinsic feature of Dvorak analysis for a TC weakening over water. The decrease of the Current Intensity (CI) is delayed, by about one day behind a falling computed Data T (DT) number. In general this results in the CI remaining one T-number higher than the DT for steadily weakening systems. The second discrepancy is harder to explain, and carries both operational and research implications with it. The best-track intensity values are all lower than their corresponding DD-numbers as Ginger intensified. The rate of intensification during the 24-hr period from 0000Z on 26 September to 0000Z on September, as shown by Digital Dvorak (50 mb for an average of 2.1 mb/hr), is quite different from that computed from the best track (74 mb for an average of 3.1 mb/hr). The former rate of intensification qualifies as a case of explosive deepening (defined as meeting or exceeding a drop of minimum sea-level pressure of at least 2.5 mb/hr for 12 hours (Dunnavan 1981)). The latter rate of deepening is not so extreme, but qualifies as a case of rapid deepening (defined as a drop of minimum sea-level pressure of at least 1.75 mb/hr, or 42 mb/24 hrs (Holliday and Thompson 1979)).

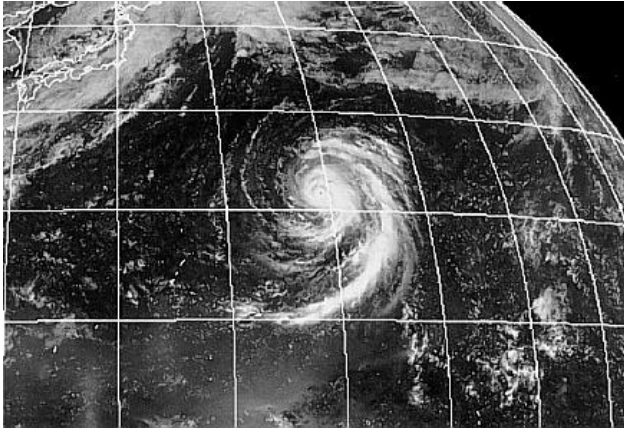


Figure 3-24-2 Ginger and its extensive pattern of primary and peripheral cloud bands are isolated in an otherwise relatively cloud free tropics (270033Z September visible GMS imagery).

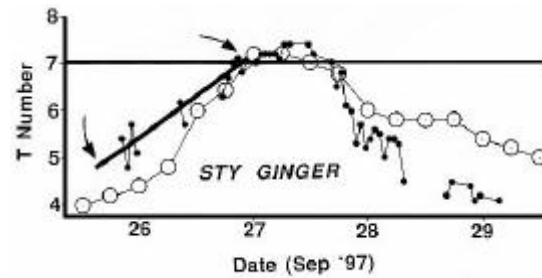


Figure 3-24-3 A time series of Ginger's hourly DD-numbers (small black dots) compared with the best-track intensity (open circles). Note that as Ginger was intensifying the best-track intensity rises faster than the value of the DD-numbers (indicated by the thick black line).

The discrepancy between the DD-numbers and best track intensities during intensification is not uncommon. However, in the case of Ginger, one can see that the resulting rate of deepening is quite different depending on whether the best-track or the DD-numbers are used to compute it. The results of research into TC intensification processes may be very different depending upon which method is used. DD-numbers are still experimental, and methods for incorporating them into operational practice are being explored. Reasons for the disagreement between the DD-numbers and the best-track intensities must be determined before any modifications are made to the current methods of estimating TC intensity utilizing satellite imagery.

b. Large and solitary

Ginger was one of many TCs of the 1997 season that formed at the eastern end of the monsoon trough near the IDL and became large solitary typhoons (Figure 3-24-2 and Figure 3-24-4). The persistent reduction of deep convection throughout much of Micronesia and within the low latitudes of the WNP basin became more pronounced during the latter half of 1997. The low-level monsoon westerlies and their associated deep convection moved eastward to the IDL (and beyond) in association with large-scale climatic anomalies related to El Niño. Other large and solitary typhoons during 1997 included TY David (21W), STY Oliwa (02C), STY Ivan (27W), STY Joan (28W), STY Keith (29W), and STY Paka (05C).

c. Concentric eye wall clouds

Ginger was yet another example of an intense WNP typhoon acquiring concentric eye wall clouds that are easily seen on conventional visible and infrared imagery, and are especially well-defined on microwave imagery (Figure 3-24-5). Microwave imagery is particularly well-suited to observe concentric eye wall clouds, and to document their evolution. (Paka's eye-wall replacement cycle was exceptionally well documented on microwave imagery; see the Paka

(05C) summary). The rapid fall of Ginger's DD-numbers (Figure 3-24-3) within 24 hours of its peak was a manifestation of its acquisition of concentric wall clouds. There is a tendency for the most intense typhoons (e.g., STY Dale (36W), in 1996, and STY Paka (05C)) to develop concentric eye wall clouds within 24 hours of their first or only peak.

IV. IMPACT

Ginger remained at sea for its entire life, and no reports of damage or injury were received at JTWC.

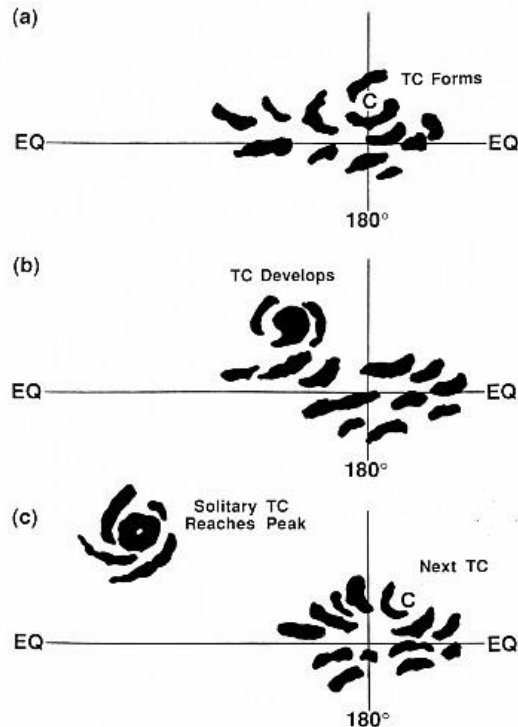


Figure 3-24-4 A graphic illustration of the process whereby a large solitary TC forms in an eastward displaced monsoon system, and then tracks northwestward, intensifies, and becomes isolated in a relatively cloud-free environment. This process was typical of most of the very intense TCs that occurred during the latter half of 1997

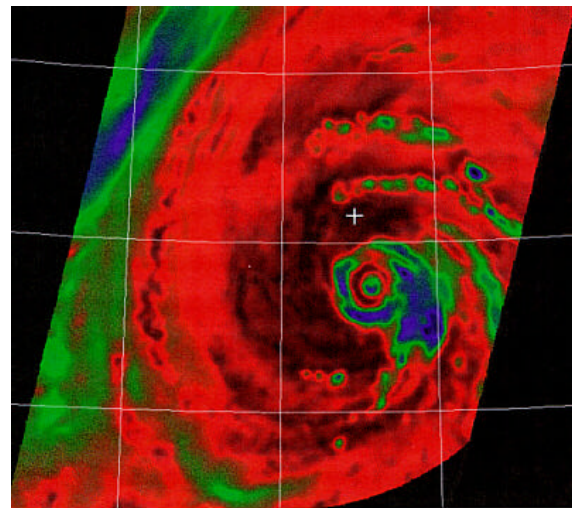
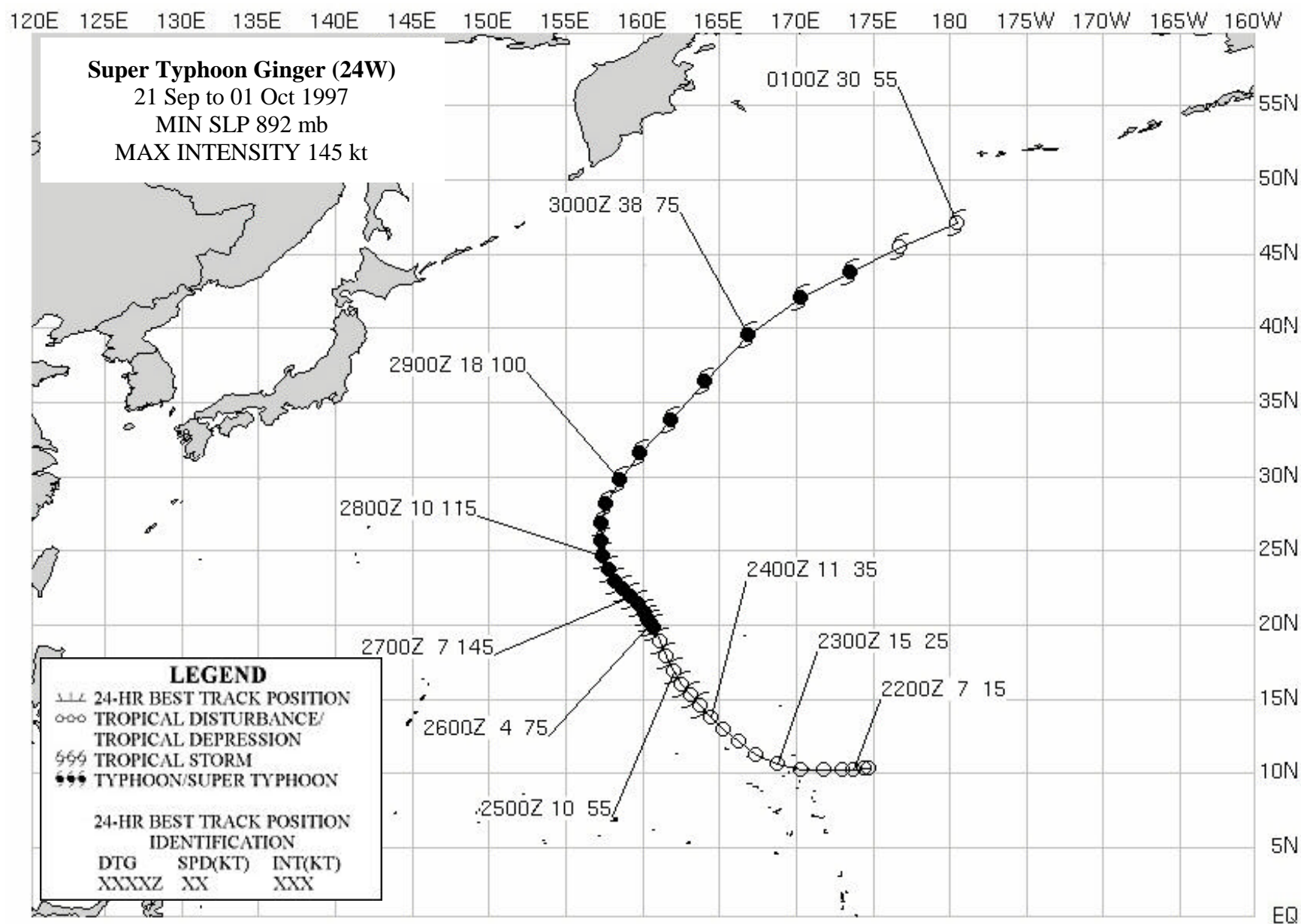
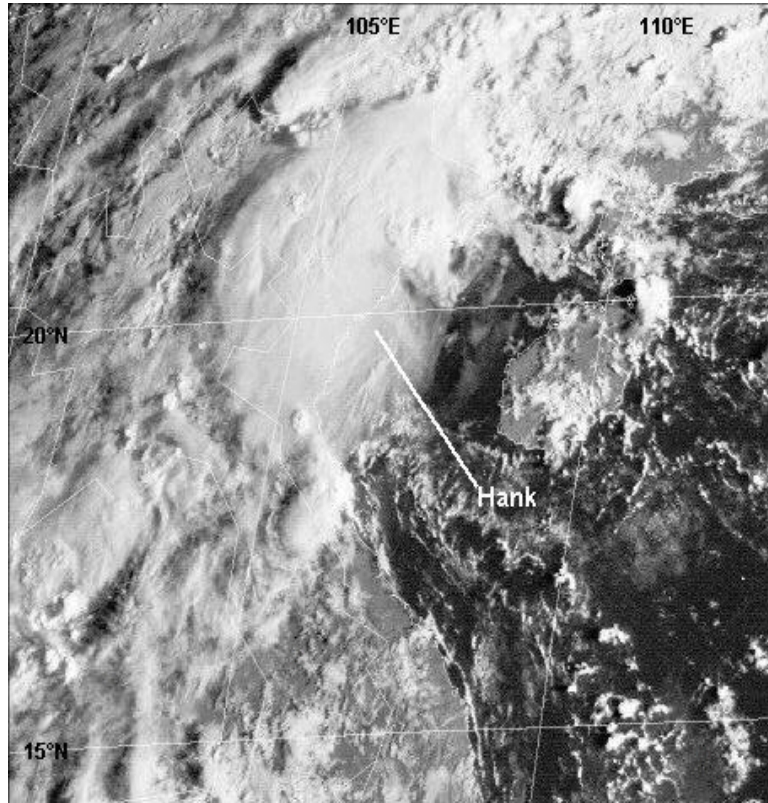


Figure 3-24-5 Microwave imagery clearly reveals the acquisition of concentric eye wall clouds by Ginger within 24 hours of reaching its peak intensity (272132Z September horizontally polarized 85 GHz microwave DMSP imagery).



TROPICAL STORM HANK (25W)

Tropical Storm (TS) Hank (25W) originated as a surface circulation in the South China Sea on the 27th of September. For several days, synoptic data suggested the presence of this circulation, but with light winds and minimal convection. It first appeared as a suspect area on the 30 September Significant Tropical Weather Advisory (ABPW). The system's convective signature experienced fluctuation over the next few days. No Tropical Cyclone Formation Alert (TCFA) was issued on this system; JTWC issued a warning at 0000Z on 3 October with a 35 kt (70 m/s) intensity based on synoptic data and cloud signature. Hank peaked at 40 kt (80 m/s) during the next 6 to 12 hours, before being subjected to strong vertical wind



shear. During its early existence, the disturbance drifted in the South China Sea, eventually

moving equatorward. At about the time JTWC began issuing warnings, it began tracking northward along the Vietnam coast. Although infrared imagery indicated very convincing convective cloud masses over land as early as 2032Z on October 3, the circulation center was actually further east and landfall was not made until about 0000Z on the 5th. Landfall occurred near 18°N (figure 3-25-1). No reports of damage were received by JTWC.

103E 104E 105E 106E 107E 108E 109E 110E 111E 112E 113E 114E 115E 116E 117E 118E

Tropical Storm Hank (25W)

27 Sep to 05 Oct 1997

MIN SLP 994 mb

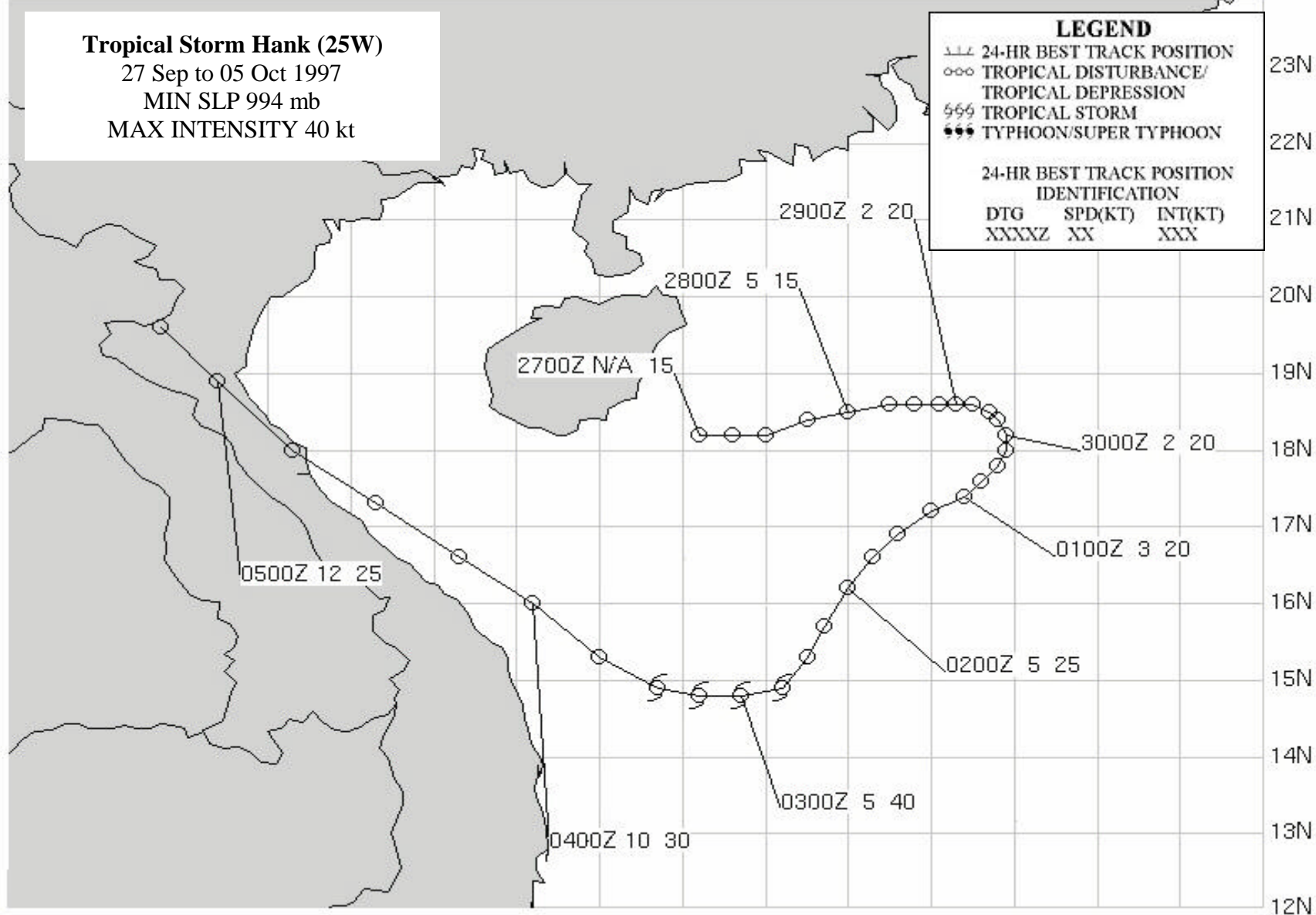
MAX INTENSITY 40 kt

LEGEND

- 24-HR BEST TRACK POSITION
- ○ ○ TROPICAL DISTURBANCE/
TROPICAL DEPRESSION
- 555 TROPICAL STORM
- 666 TYPHOON/SUPER TYPHOON

24-HR BEST TRACK POSITION IDENTIFICATION

DTG	SPD(KT)	INT(KT)
XXXXZ	XX	XXX



TROPICAL DEPRESSION 26W

Tropical Depression 26W initially formed as a disturbance southeast of the Marianas on 29 September. After an initial slow track to the north, the disturbance turned briskly westward at about 14 kts (26 km/hr) as the subtropical ridge built to its north. The disturbance tracked just north of Guam bringing the island showers and thunderstorms early on 02 October. The disturbance became Tropical Depression 26W northwest of Guam late on 02 October. On 03 October at 00Z, a 30 kt (60 m/s) sustained ship observation was reported within 1 degree of the system center. Satellite imagery at this time indicated a low-level circulation with only scattered convection near the center. The convection became more widespread during the next 24 hours as the

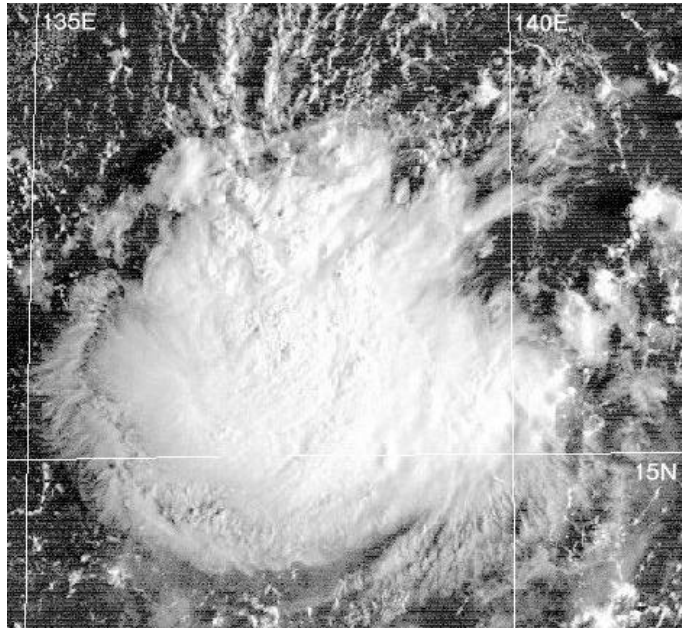


Figure 3-26-1 Tropical Depression 26W increasing in convection (032132Z October visible GMS imagery).

Tropical Depression 26W's forward motion slowed in the weak steering region associated with a break in the mid-level subtropical ridge. Tropical Depression 26W did not intensify further. Satellite imagery from 4 October and 5 October showed it to be affected by increasing vertical wind shear. By 5 October, Tropical Depression 26W had increased its westward speed as the subtropical ridge redeveloped to its north. Tropical Depression 26W continued to experience vertical wind shear, as evident by 00Z 6 October visible imagery indicating that the main area of convection was distinctly separated from its low-level circulation center. The system remained a tropical depression as indicated by 30 kt (60m/s) wind ship observations near its center. Tropical Depression 26W dissipated over the Philippine Sea on 7 October as it merged with a frontal boundary.

126E 128E 130E 132E 134E 136E 138E 140E 142E 144E 146E 148E 150E 152E 154E 156E 158E

Tropical Depression 26W

29 Sep to 07 Oct 1997

MIN SLP 1000 mb

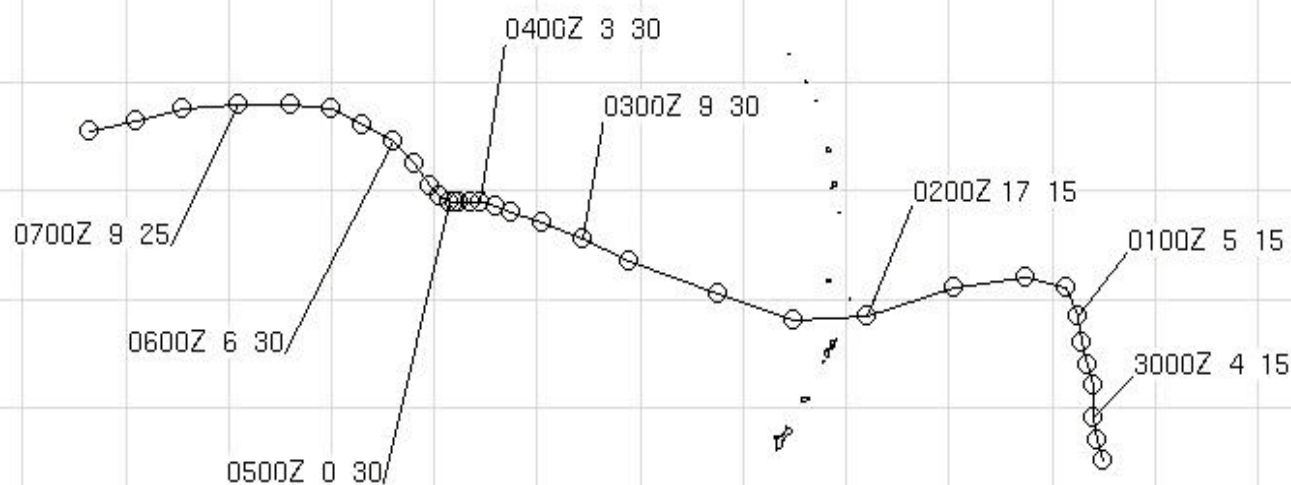
MAX INTENSITY 30 kt

LEGEND

--- 24-HR BEST TRACK POSITION
 ○○○ TROPICAL DISTURBANCE/
 TROPICAL DEPRESSION
~~---~~ TROPICAL STORM
~~---~~ TYPHOON/SUPER TYPHOON

24-HR BEST TRACK POSITION
 IDENTIFICATION
 DTG SPD(KT) INT(KT)
 XXXXZ XX XXX

26N
24N
22N
20N
18N
16N
14N
12N
10N
8N
6N



SUPER TYPHOONS IVAN (27W) AND JOAN (28W)

I. HIGHLIGHTS

Super Typhoon Ivan (27W) and Super Typhoon Joan (28W) were two of three tropical cyclones (TCs) in the western North Pacific (WNP) during 1997 to attain an extreme intensity of 160 kt (82 m/sec), and were the 8th and 9th super typhoons of 1997's unprecedented annual total of eleven. They reached their peak intensities at nearly the same time: Ivan at 171800Z October and Joan at 170600Z October. At 171200Z, Ivan was at 155 kt (80 m/sec) while Joan was still at 160 kt (82 m/sec); the first observation of two TCs of such extreme intensity existing simultaneously in the WNP. Both Ivan and Joan affected the Mariana Islands, and Ivan was the first and only TC during 1997 of at least tropical storm intensity to make landfall on Luzon. An equatorial westerly wind burst (bounded by twin near-equatorial troughs) preceded the formation of Ivan, Joan and a Southern Hemisphere twin, TC 02P (Lusi).

II. TRACK AND INTENSITY

During the first week of October, low-latitude, low-level, westerly winds blew along the equator from approximately 150E eastward, across the international dateline (IDL), to near 170W. Twin near-equatorial troughs (one in the Northern Hemisphere, the other in the Southern Hemisphere) bounded these westerly winds and a region of deep convection. As the deep convection along the equator diminished, three TCs emerged from this synoptic flow pattern. The first -- Lusi -- formed in the Southern Hemisphere on 08 October and moved southward between Fiji and Vanuatu. On 13 October, Ivan and Joan formed in the Northern Hemisphere in the eastern half of Micronesia and began to track toward the west-northwest. As they were initially poorly organized (Figure 3-27/28-1) and isolated in an environment relatively free of deep convection (Figure 3-27/28-2), neither numerical guidance nor human forecaster anticipated the extreme intensity which these two TCs would attain. Also lacking during the lifetimes of the two TCs was any significant monsoon flow to their south and west.

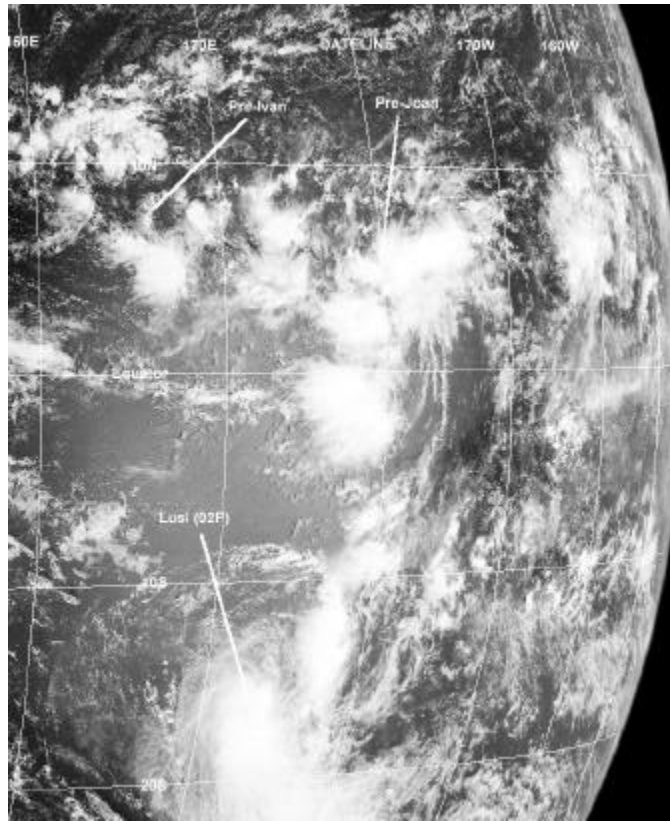


Figure 3-27/28-1 The pre-Ivan and pre-Joan tropical disturbances are poorly organized at low latitude in the eastern portion of the WNP basin. A Southern Hemisphere twin, Lusi, is passing southward between Fiji and the islands of Vanuatu (102132Z October visible GMS imagery).

a. STY Ivan (27W)

Ivan (the westernmost of the pair) originated from a very poorly organized tropical disturbance in the near-equatorial trough that stretched across the eastern Caroline and Marshall Island groups (see Figure 3-27/28-1). It was first mentioned on the 110600Z October Significant Tropical Weather Advisory (ABPW), when animated satellite imagery and synoptic data indicated the presence of a low-level circulation in association with an area of deep convection near 6N 165E. The pre-Joan tropical disturbance, located further to the east, was also first noted on this advisory.

With an increase in the organization and coverage of deep convection, a Tropical Cyclone Formation Alert (TCFA) was issued valid at 120800Z October as the pre-Ivan tropical disturbance (TD) moved rapidly (18 kt / 33 km/hr) west-northwest on a track which, if extrapolated, would pass just to the south of Guam. Based upon intensity estimates from satellite, the first warning on TD 27W was issued valid at 130600Z. There was still no expectation of any significant intensification, and remarks on the first warning indicated that the system was expected to intensify at a less than climatological rate. See the Discussion Section for further comments on Ivan (and Joan's) intensification. With increased banding of the deep convection, TD 27W was upgraded to Tropical Storm Ivan (27W) at 131800Z. Visible imagery on the morning of 14 October (Figure 3-27/28-3) gave clear indication of Ivan's location to the east-southeast of Guam. Passing 55 nm (102 km) to the south of Guam on the night of 14 October, Ivan's circulation center was well-defined on Guam's NEXRAD. A velocity cross section through Ivan's "eye" at 141120Z showed, at azimuth and range of 139 degrees and 75 nm (139 km) respectively, a maximum inbound velocity of 47 kt (24 m/sec) at 7,000 ft (210 m) (the lowest observable altitude); and, at azimuth 148 degrees and 79 nm (146 km) respectively, a

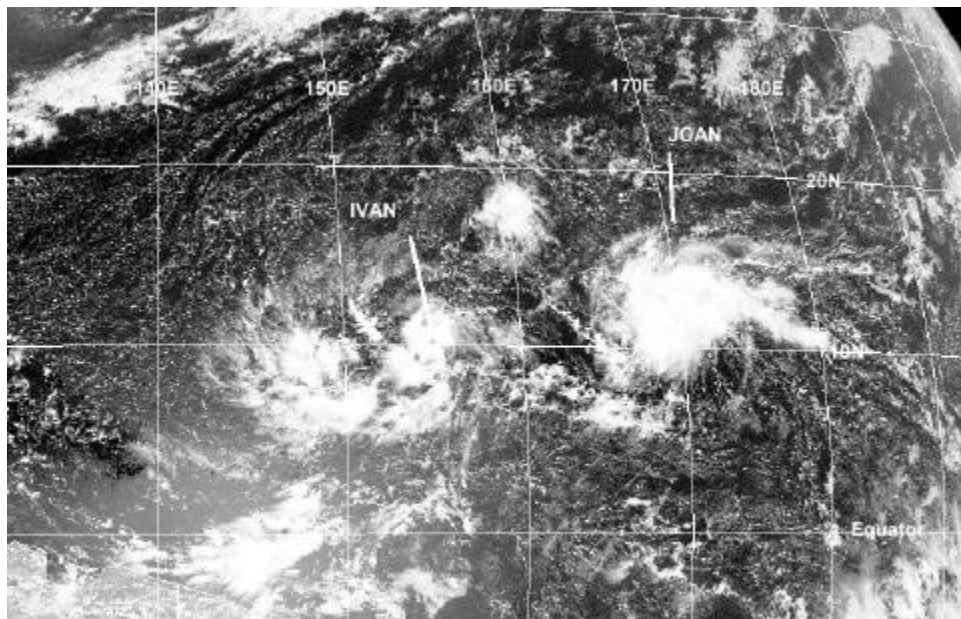


Figure 3-27/28-2. A high-contrast visible image shows the relative isolation of Ivan and Joan as they emerged from the near equatorial trough and moved west-northwestward across the relatively cloud-free basin (130132Z October visible GMS imagery).

maximum outbound velocity of 42 kt (22 m/sec), also at 7,000 ft (210 m). After passing Guam, Ivan became a typhoon at 150600Z, and then began to intensify at a fast rate (1.5 T numbers per day) (Figure 3-27/28-4). During the 48-hour period from 150600Z to 170600Z Ivan intensified from 65 kt (33 m/sec) to 145 kt (75 m/sec) approximately 3 T-numbers. The peak intensity of 160 kt (82 m/sec) was reached at 171800Z. On 16 October, Ivan slowed and began to track toward Luzon. Numerical guidance and the synoptic flow pattern suggested that the TC would recurve before reaching the Philippines. The anticipated northward turn did commence on 18 October, but it was too late to spare the Philippines. At approximately 191800Z October, the

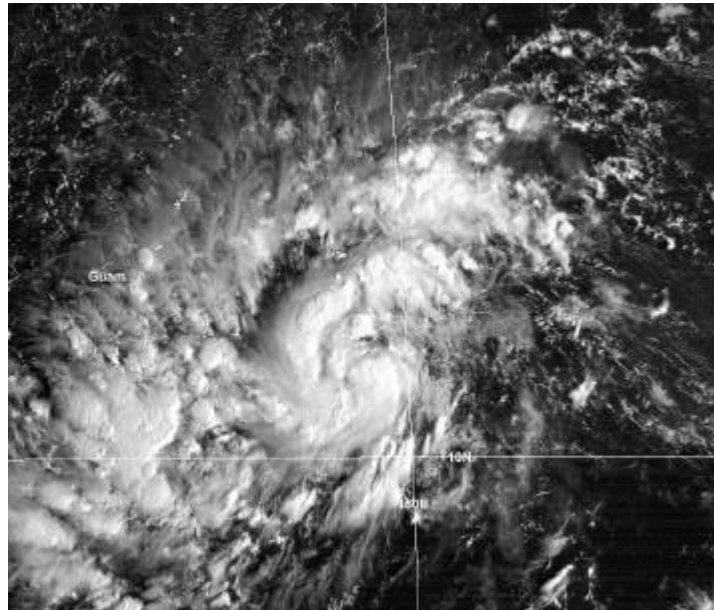


Figure 3-27/28-3 Ivan approaches Guam after becoming a tropical storm (132132Z October visible GMS imagery).

center of Ivan made landfall on the extreme northeastern tip of Luzon with an intensity of 120 kt (62 m/sec). On 20 October, the typhoon moved into the Luzon Strait and recurved. After recurving, it dropped below typhoon intensity on 21 October, then briefly reintensified to typhoon intensity on 22 October as it moved northeastward south of Okinawa. A steady weakening trend then set in, and the final warning was issued, valid at 241200Z, as the system became extratropical.

b. Joan (28W)

Joan (the easternmost of the Ivan-Joan pair) originated from a very poorly organized tropical disturbance in a near-equatorial trough that stretched across the eastern Caroline and Marshall Island groups (see Figure 3-27/28-1). The system was first mentioned on the 110600Z October ABPW. Animated satellite imagery and synoptic data indicated the possible presence of a low-level circulation in association with an area of deep convection at a low latitude near 4N 176E. Synoptic data indicated that equatorial westerlies were present to the south of this disturbance. The pre-Ivan tropical disturbance -- located further to the west -- was also first noted on this advisory. The pre-Joan tropical disturbance moved northwestward, and was north of 10N by 13

October. With an increase in the areal coverage and organization of deep convection, a TCFA was issued valid at 130400Z October.

The system now made a turn to the left and began to track to the west and slowly intensify. The first warning on TD 28W was issued, valid at 130600Z, based on satellite intensity estimates of 25 kt (13 m/sec). The system was expected to intensify at a climatological rate. Based upon satellite intensity estimates of 35 kt (18 m/sec), TD 28W was upgraded to Tropical Storm Joan (28W) on the warning valid at 140600Z. The system now tracked just north of due west, approached the Mariana Islands, and intensified. After becoming a typhoon, between 151200Z and 151800Z, Joan began to intensify very rapidly, increasing from 70 kt (36 m/sec) at 151800Z to its peak of 160 kt (82 m/sec) 36 hours later (Figure 3-27/28-5a,b). The equivalent pressure fall of 100 mb over this 36-hour period, for an average of 2.8 mb per hour, qualifies as a case of explosive deepening (Dunnavan 1981). As it approached the Mariana Islands, Joan made turned to the northwest. Weakening slightly, it passed between the Islands of Saipan and Anatahan on the morning of 18 October (see the Impact Section for details on the effects of Joan on the Marianas). Its well-defined eye was tracked by Guam's NEXRAD as it passed to the north. However, at a range of 155 nm (287 km) from the site, it was beyond Doppler radial velocity range. Joan remained at or above the super typhoon threshold (130 kt, 67 m/sec) for 4.5 days (170000Z to 211200Z) -- a record. Moving slowly, but making a sharp recurve during the 48-hour period 200000Z to 220000Z, Joan weakened steadily from 140 kt (72 m/sec) to 115 kt (59 m/sec). On 23 October, Joan moved eastward along 30N and continued to weaken. On 24 October, the system turned toward the northeast and accelerated. The final warning was issued, valid at 240000Z, when it appeared that Joan was transitioning into an intense extratropical low. In postanalysis, Joan remained at typhoon intensity until 241800Z, and its transition into an extratropical low was completed at 251800Z.

III. DISCUSSION

a. On the extreme intensities reached by Ivan and Joan

Ivan and Joan both emerged from a near equatorial trough in the Marshall Islands. As the two TCs moved west-northwestward in tandem, they both intensified to an extreme value of 160 kt (82 m/sec) -- two of three WNP TCs to do so during 1997 (the other was STY Paka (05C)). At 171200Z, Ivan was at 155 kt (80 m/sec) while Joan was still at 160 kt (82 m/sec); the first time noted that two TCs of such extreme intensity existed simultaneously in the WNP basin (Figure 3-27/28-6a,b). On the enhanced infrared image of Figure 3-27/28-5b, Joan's cold dark-gray eye

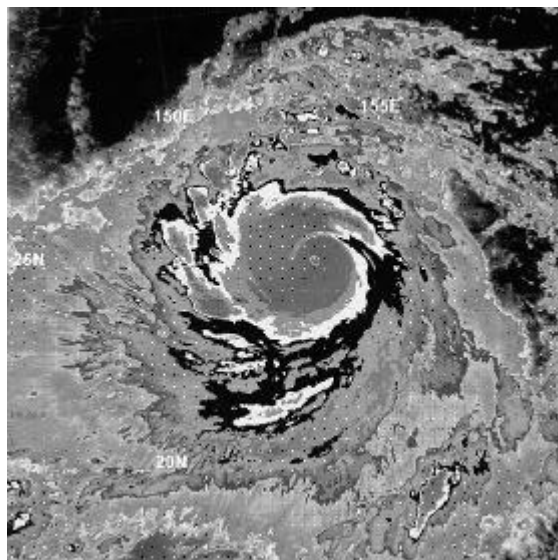


Figure 3-27/28-4 Ivan becomes the year's eighth super typhoon (161913Z October enhanced IR DMSP imagery). Enhancement curve is "BD".

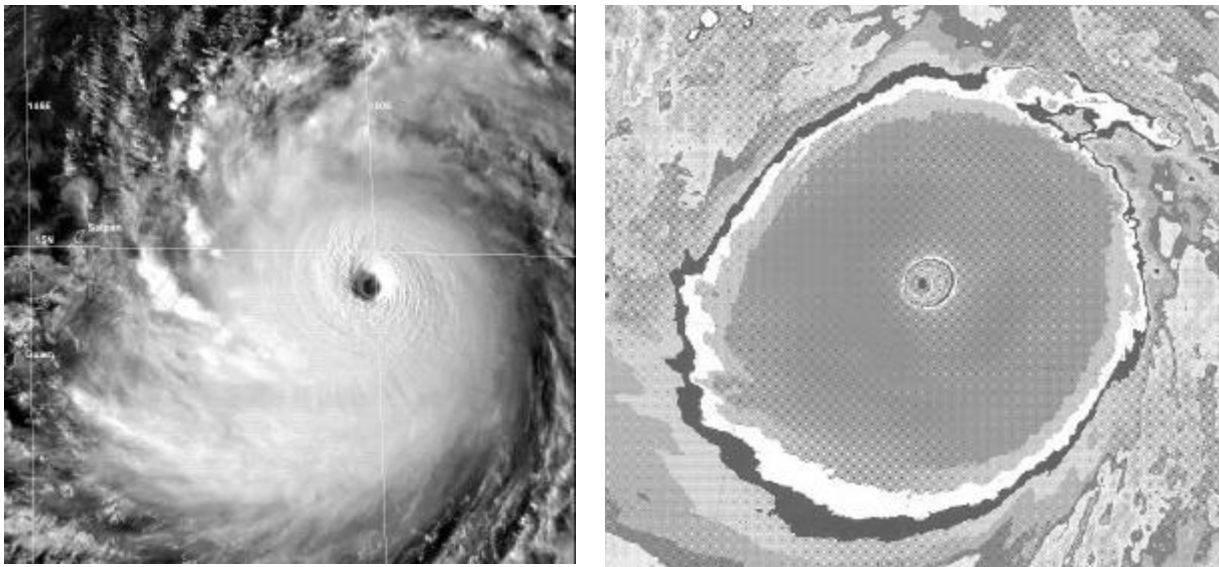


Figure 3-27/28-5 Joan reaches its peak intensity of 160 kt (82 m/sec). (a) The low sun-angle of late afternoon helps highlight features on the tops of Joan's eye wall cloud (170632Z October visible GMS imagery). (b) The cold dark gray ring surrounding Joan's eye-indicative of temperatures of -81C or colder-puts Joan off the scale of Dvorak's intensity estimation techniques using enhanced IR imagery (170803Z October enhanced IR DMSP imagery). Enhancement curve is "BD"

wall cloud (indicating cloud-top temperatures of -81 degrees C or colder), is off of Dvorak's scale for subjectively determining TC intensity from infrared imagery (Dvorak 1984). The Digital Dvorak (DD) algorithm, however, has no intrinsic upper bound (although there may be actual physical upper limits), and the DD numbers for both Ivan and Joan (Figure 3-27/28-7a,b) reached T8.0 (hypothetically equivalent to 170 kt (87 m/sec) intensity). Since 1995, the highest DD number computed for a typhoon by the DD algorithm on the satellite image processing equipment at JTWC was T8.3 for Super Typhoon Angela (29W) (1995), as it approached the Philippines. No other TC since then has reached a DD number of 8.0 or higher. Why these two TCs became so intense is unknown. Early in their lives, neither objective guidance nor human forecaster anticipated the extreme intensities that Ivan and Joan would reach. The initial disturbances from which they developed were very poorly organized and were isolated in an environment that was unusually free of deep convection. The monsoon trough across the WNP was relatively weak and sea-level pressures were near or above normal. For Ivan, nearly every intensity forecast leading up to its peak was low by as much as 40 kt (21 m/sec) for the 12-hour forecast, and 45, 50, 45, and 50 kt for the 24-, 36-, 48-, and 72-hour forecasts respectively. For Joan, the intensity forecasts were even lower: nearly all forecasts for the entire life of the TC were too low. Leading up to its peak, the intensity forecasts for Joan were low by as much as 30, 55, 65, 65, and 65 kt for the 12-, 24-, 36-, 48-, and 72-hour forecasts respectively. Despite the passage of these two TCs across much of the WNP basin, the monthly average wind for October (Figure 3-3) was more easterly than normal everywhere except in the low-latitudes east of 150E (an El Niño-related anomaly).

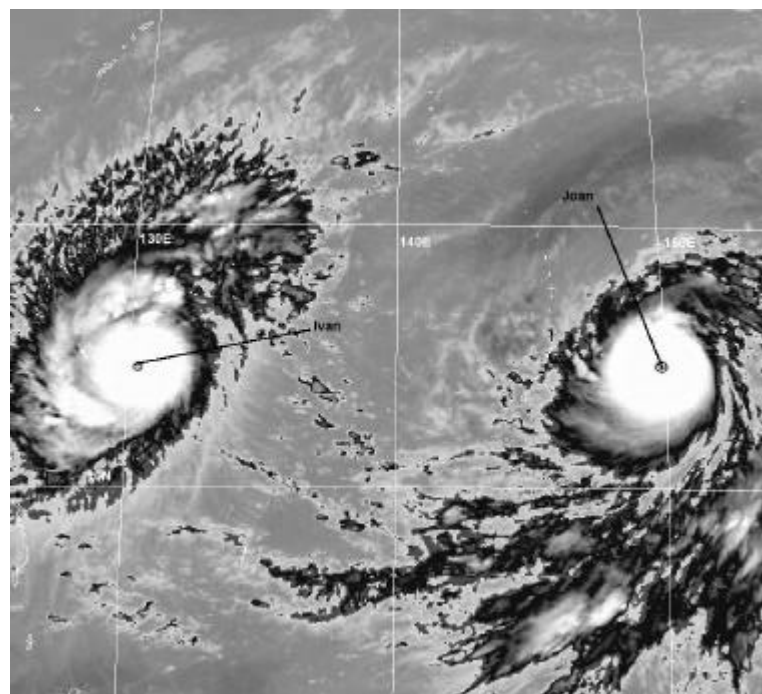
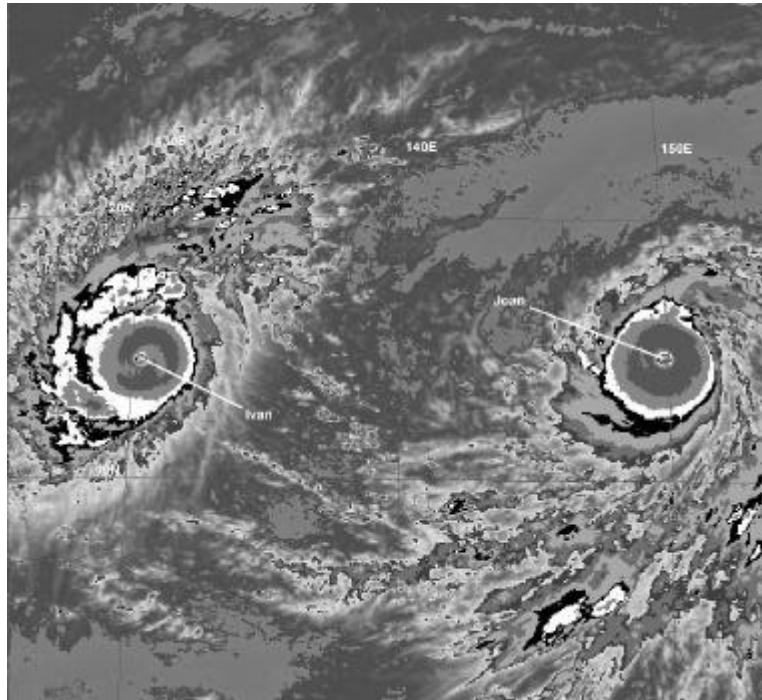


Figure 3-27/28-6 For the first time observed, two spatially proximate super typhoons coexisted in the WNP with near-record intensities. At the time of these images, Ivan is at 145 kt (75 m/sec) intensity and Joan is at 160 kt (82 m/sec) intensity. (170632Z October enhanced IR GMS imagery.) Enhancement curve in (a) is "BD", and enhancement curve in (b) is "MB".

b. TC-TC interactions?

In the Systematic and Integrated Approach to Tropical Cyclone Forecasting (Elsberry 1994) there are three basic modes of interactions between two spatially proximate TCs: 1) direct TC interaction (whereby each TC is advected by the flow of the other); 2) semi-direct TC interaction (whereby each TC is advected by the altered flow between the other TC and the high pressure system on the opposite side); and, 3) indirect TC interaction (whereby the TC to the west induces a ridge between the two TCs which, in turn, imposes an equatorward component to the steering flow on the eastern TC). In order to study the interaction between two TCs, it is best to produce a diagram illustrating the motion of each TC with respect to their centroid. Properties of the centroid-relative motion help to reveal the nature of the interaction (which is not always apparent in the actual earth-relative tracks). In the case of Ivan and Joan, the centroid-relative motion (Figure 3-27/28-8) does not seem to indicate that any form of TC interaction took place.

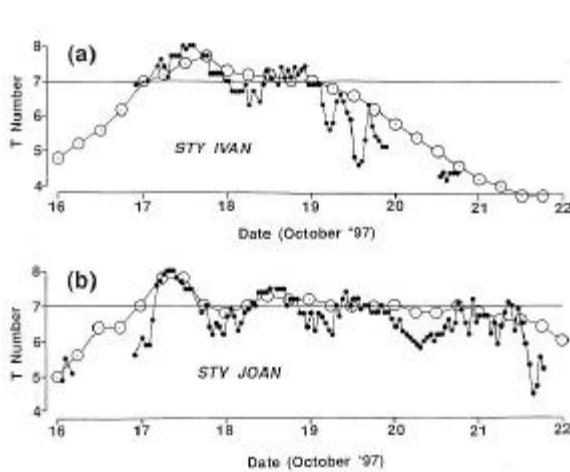


Figure 3-27/28-7 A time series of (a) Ivan's, and (b) Joan's hourly DD numbers (small black dots) compared with the best-track intensity (open circles). Both Joan and Ivan reached an extreme DD magnitude of 8.0 (equivalent to an intensity of 170 kt (87 m/sec)). There is a slight diurnal cycle apparent in these time series with a tendency for higher DD numbers just prior to sunrise (1800Z).

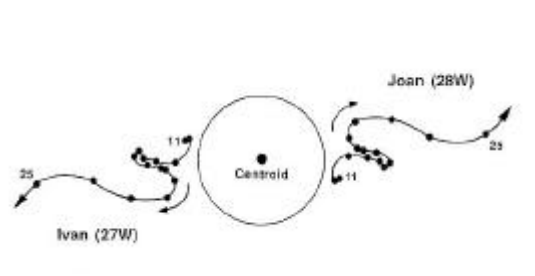


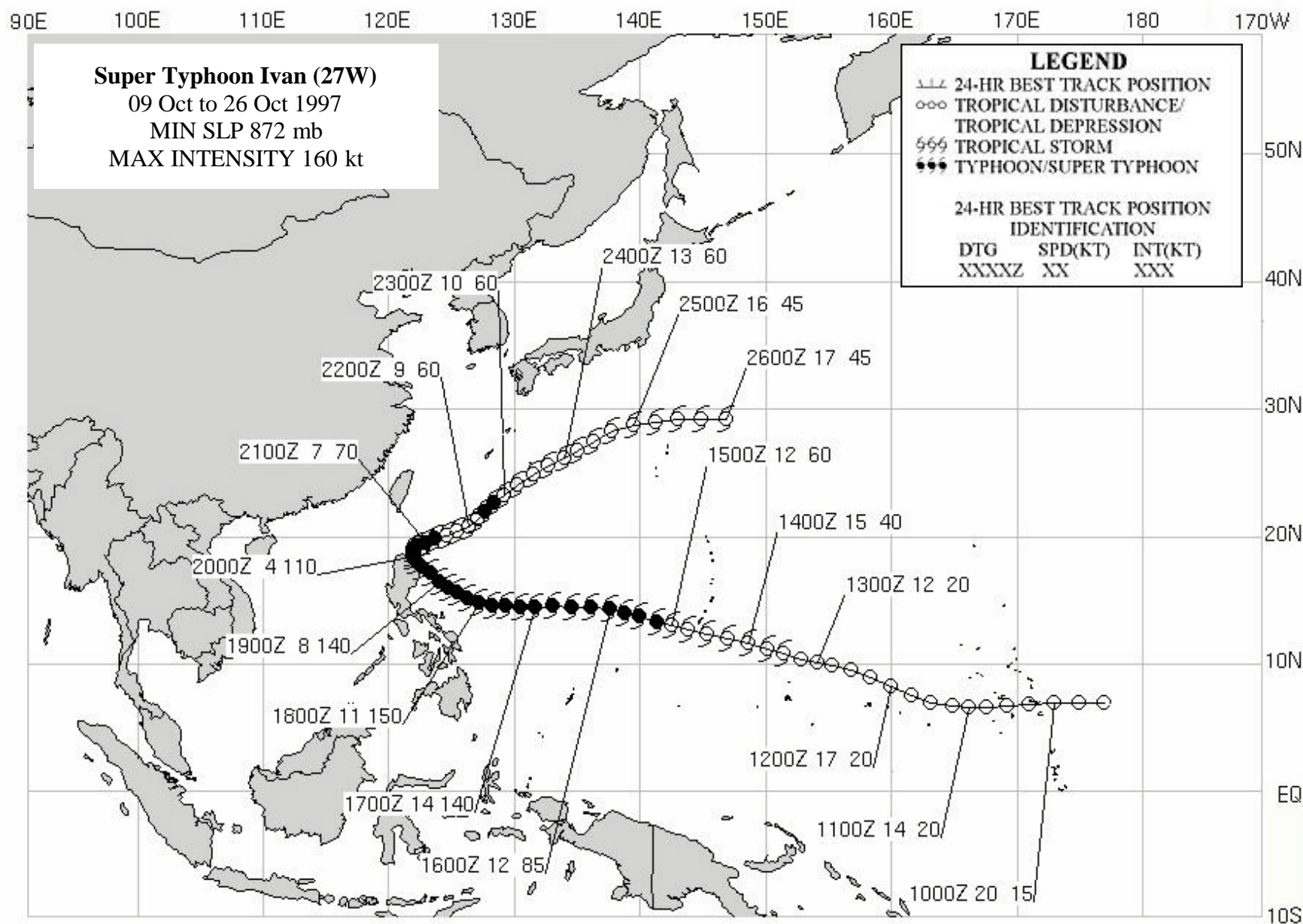
Figure 3-27/28-8 The centroid-relative motion of Ivan and Joan. Black dots indicate positions at 0000Z at 24-hour intervals beginning on 11 October and ending on 25 October. The inscribed circle has a diameter of 600 nm (1100 km).

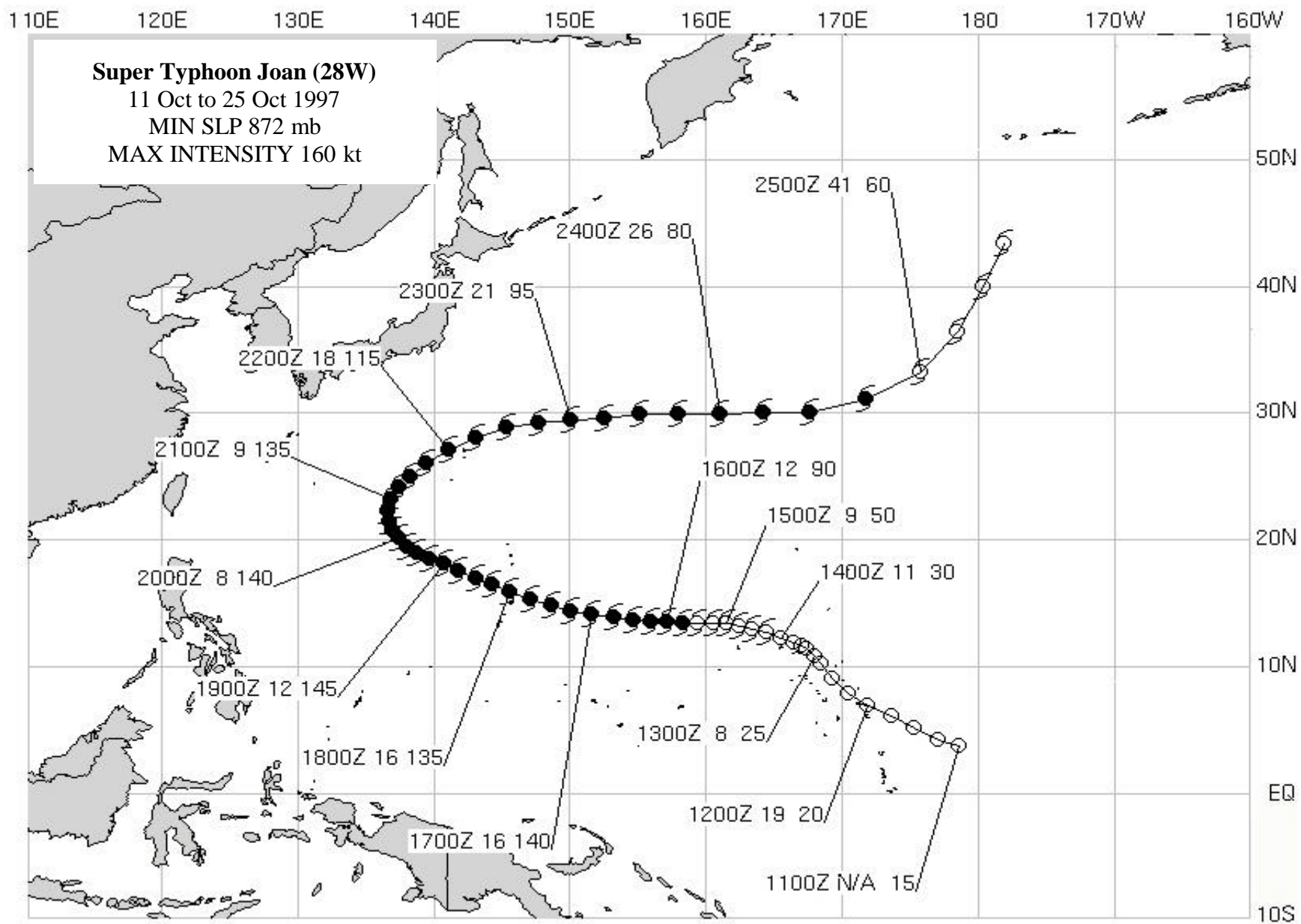
Although initially within the 780-nm (1446 km) threshold noted by Brand (1970) for mutual cyclonic rotation about the centroid to dominate, very little centroid-relative cyclonic orbit is noted for the period. The common features of TC interaction noted by Lander and Holland (1993) of mutual approach followed by a period of stable cyclonic orbit are also missing. Only the rapid increase of separation distance as the two TCs recurved is a typical feature of binary interaction noted by Lander and Holland. This so-called "escape" phase indicates that the binary interaction has ceased. In summary, Ivan and Joan appear to have undergone no form of TC interaction. They simply moved along similarly shaped adjacent recurving tracks and, recurving

at approximately the same time, the centroid relative motion became one of rapid increase in separation distance as Joan recurved east of Ivan and accelerated faster into the midlatitudes

IV. IMPACT

Both Ivan and Joan affected the Mariana Islands. On the night of 14 October, Ivan passed 55 nm (100 km) to the south of Guam where a peak wind gust of 41 kt (21 m/sec) was recorded at Andersen Air Force Base; the heaviest 24-hr rainfall of 5.85 inches was also recorded at Andersen. Ivan also affected the Philippines. At least one person was reported drowned and another missing on the northeastern tip of Luzon. Ivan damaged thousands of houses and destroyed large amounts of rice and corn in this region. More than \$US 500,000 worth of fish stocks in ponds and cages were also destroyed. Joan largely spared the Mariana Islands any significant damage when it passed between the Islands of Saipan and Anatahan on 18 October. Peak wind gusts of 85 kt (44 m/sec) were experienced on Saipan when Joan passed approximately 45 nm (80 km) to the north. A Red Cross initial assessment indicated that Joan destroyed four houses, caused major damage to 15 other tin and wood structures and caused minor damage to 17 homes on Saipan. On Guam, winds gusted to only 33 kt (17 m/sec) at the commercial port on the west side of the island.





SUPER TYPHOON KEITH (29W)

I. HIGHLIGHTS

The tenth of eleven tropical cyclones (TCs) to attain super typhoon intensity in the western North Pacific during 1997, Keith formed at low latitudes in the Marshall Islands. It was one of ten TCs which formed east of 160E and south of 20N — within the "El Niño" box in Figure 3-3a. Keith was a recurving TC which passed between the Islands of Rota and Tinian (only 50 nm (93 km) apart) on the west-bound leg of its recurving track. NEXRAD imagery from Guam indicated the eye wall cloud of Keith never touched land as it threaded the narrow channel between these two islands. As such, the Mariana Islands were spared the full force of Keith (see the Impacts Section). Keith's compact wind and cloud structure were revealed by Guam's NEXRAD (see the Discussion Section). Equatorial westerly winds bounded by twin near-equatorial troughs preceded the formation of Keith and a Southern Hemisphere twin, TC 03P 98.

II. TRACK AND INTENSITY

During most of October, low-latitude, low-level, westerly winds blew along the equator from approximately 150E and eastward across the international dateline to near 170W. Twin near-equatorial troughs (one in the Northern Hemisphere, another in the Southern Hemisphere) bounded these westerly winds and most of the region's deep convection. During the first week of October, deep convection increased between the twin troughs in association with an equatorial westerly wind burst; and then, during the second week of October, it decreased as three TCs emerged from the twin near-equatorial trough synoptic flow pattern: Ivan (27W) and Joan (28W) in the Northern Hemisphere, and a twin, Lusi (02P98), in the Southern Hemisphere.

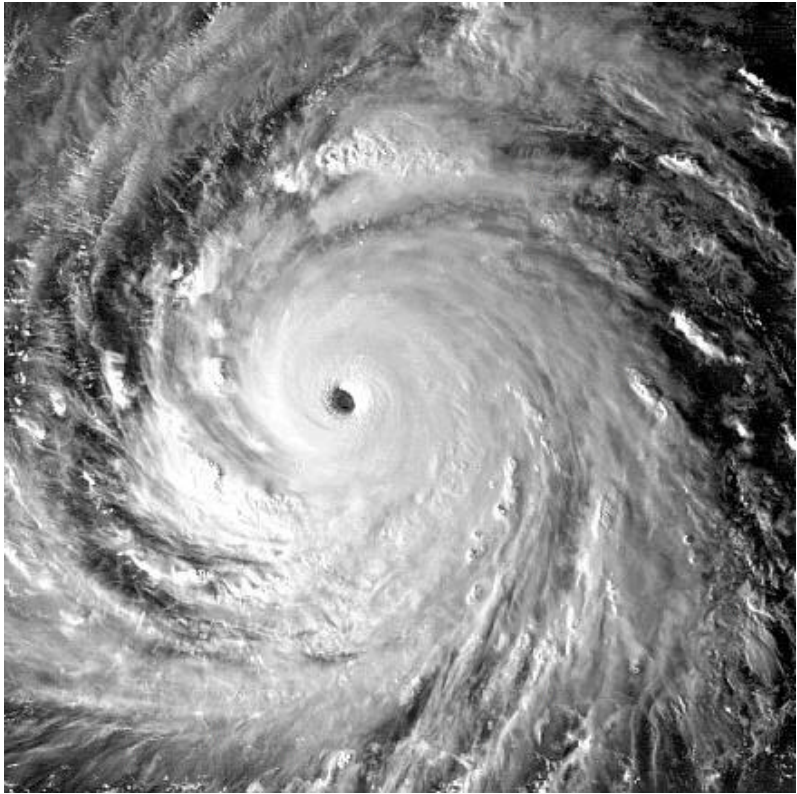


Figure 3-29-1 A low evening sun angle brings out the relief in Keith's clouds. From the satellite perspective, it is hard to imagine that the eye wall cloud, and the extreme winds remained over water between the relatively closely spaced islands of the Marianas (020632Z November visible GMS imagery).

When Ivan (27W) and Joan (28W) began to recurve, deep convection once again increased in the aforementioned region, and two more TCs emerged from the twin near-equatorial trough flow pattern: Keith developed in the Marshall Islands, and a Southern Hemisphere twin, TC 03P98, moved south between Fiji and the Islands of Vanuatu. An area of deep convection located in the Marshall Islands was, for several days (beginning at 181730Z October), mentioned on the Significant Tropical Weather Advisory (ABPW). Deep convection (in varying amounts) persisted in the Marshalls, and in postanalysis, the area of deep convection that could be unambiguously linked to the low-level circulation center which became Keith was mentioned on the 230600Z ABPW. This area of deep convection moved slowly westward and remained poorly organized for three days. On 26 October, the organization of the deep convection improved. Water-vapor derived winds showed anticyclonic outflow had become more symmetrical over the system, and synoptic data from Kwajalein and Majuro indicated falling sea-level pressure within a persistent low-level circulation. These factors prompted JTWC to issue a Tropical Cyclone Formation Alert (TCFA) at 260500Z October. During the valid period of this TCFA, the system failed to develop into a significant TC. Since conditions still appeared to be favorable for the formation of a significant TC, a second TCFA was issued at 270500Z. During the night of 27 October, the deep convection became better organized, and based on satellite intensity estimates of 25 kt (13 m/sec), the disturbance was upgraded to Tropical Depression (TD) 29W on the warning valid at 271800Z. On the morning of 28 October, satellite intensity estimates increased to 35 kt (18 m/sec) and TD 29W was upgraded to Tropical Storm Keith at 280000Z. At this time, Keith was anticipated to develop at a normal rate of one T-number per day, and move toward the west-northwest.

For two days, beginning on 280000Z, Keith intensified slowly, increasing by only one T-number (i.e., from 35 kt (18 m/sec) at 280000Z to 55 kt (28 m/sec) at 300000Z). Then, like Ivan (27W) and Joan (28W) before it, Keith underwent a period of rapid intensification which was unforeseen. By 310000Z, Keith had intensified to 105 kt (54 m/sec). The equivalent pressure drop of 43 mb in 24 hours (for an average of 1.79 mb/hr) qualifies as a case of rapid deepening (Holliday and Thompson 1979). Keith continued to intensify rapidly until 011200Z November when it reached its peak of 155 kt (80 m/sec).

When it reached its peak intensity, Keith was moving west-northwest and was just over a day away from passing through the Mariana Island chain. During the 6 hour period 020600Z-021200Z November, Keith passed between the Islands of Rota and Tinian. Though weakened slightly from its peak, it was still a powerful 140 kt (72 m/sec) super typhoon (Figure 3-29-1) as it made its closest approach to these islands. Fortunately, as Guam's NEXRAD showed, the eye wall cloud of Keith remained over water, and no island experienced the full force of Keith, although some damage was reported (see the Discussion and the Impact Sections).

Keith remained at or above super typhoon intensity for three-and-one-half days (311800Z October to 030600Z November), dropped to 125 kt (64 m/sec) for two warning times at 031200Z and 031800Z, and became a super typhoon briefly again for two warning times at 040000Z and 040600Z. Then, late on 04 November, Keith slowed, weakened, and began to recurve. For two days (05-06 November), Keith moved slowly northeastward and continued to weaken. On 07

November, Keith turned more eastward, weakened further, and began its acceleration in the westerly flow to the north of the subtropical ridge. The final warning was issued, valid at 0812200Z, as Keith raced east-northeastward with a translation speed of 45 kt (23 m/sec) and became extratropical.

III. DISCUSSION

a. Keith's structure as revealed by Guam's NEXRAD

As Keith moved between the islands of Rota and Tinian on 02 November, it passed well within the range of Guam's NEXRAD. The most striking aspect of the NEXRAD data was the compact structure of the TC core. A 5-nm-wide (9-km-wide) eye wall cloud surrounded a 20-nm-wide (37-km-wide) eye at beam altitude of approximately 7,000 ft (2134 m) (Figure 3-29-2a). The base velocity product (Figure 3-29-2b) showed that winds in excess of 100 kt were occurring in the eye wall cloud. Peak NEXRAD-observed winds of 135-140 kt (69-72 m/sec) were found in the eye wall cloud; and, as a velocity cross section (Figure 3-29-2c) revealed, these highest wind speeds were found at the lowest altitudes of the cross section.

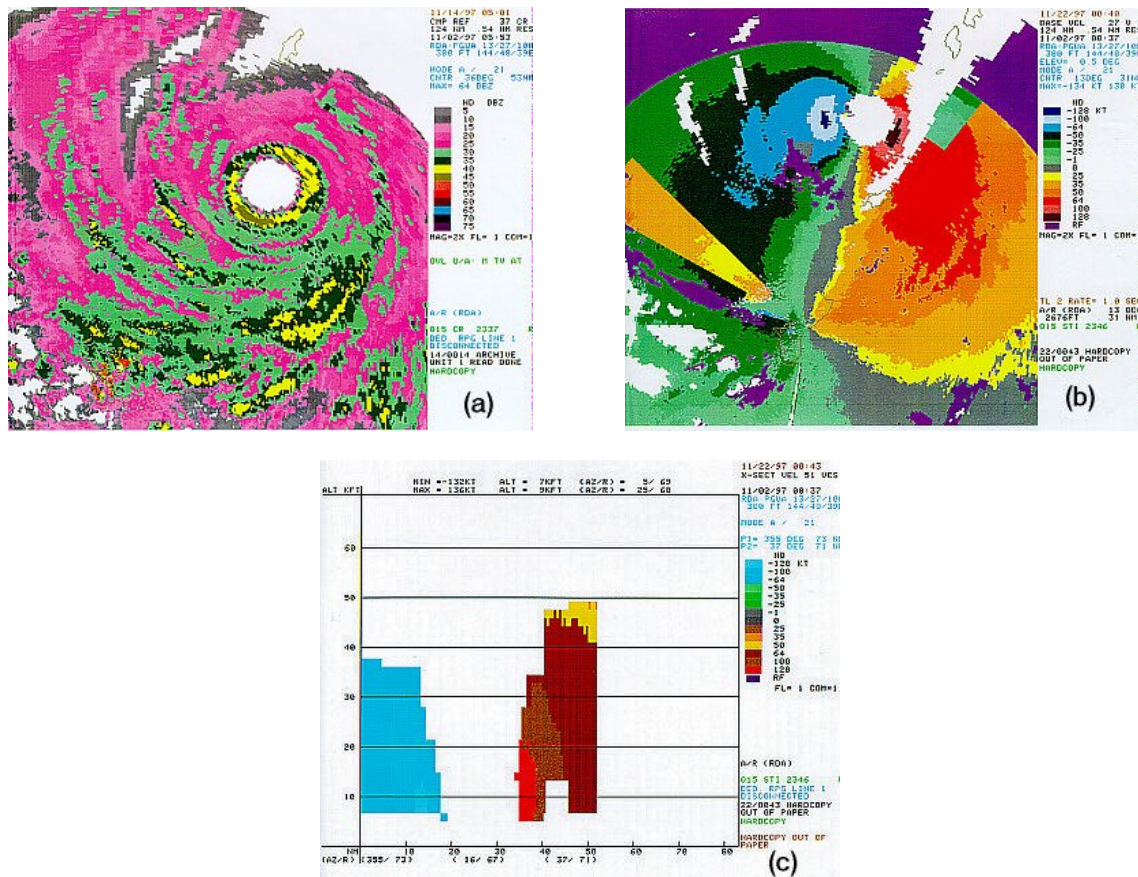


Figure 3-29-2 (a) Keith's eye and eye wall cloud pass between the islands of Rota and Tinian (020553Z November NEXRAD Composite Reflectivity product). (b) A dramatic couplet of high inbound wind and high outbound winds within Keith's eye wall cloud is revealed by the NEXRAD (020837Z November NEXRAD Base Velocity product). Note the narrow width of the region of inbound and outbound winds of 128 kt (66 m/sec) or

greater. (c) Typical of the structure of warm-core vortices, the peak azimuthal flow is at the lowest levels of the vortex and decreases with height (020837Z November NEXRAD velocity cross section in an east-west slice through Keith's eye).

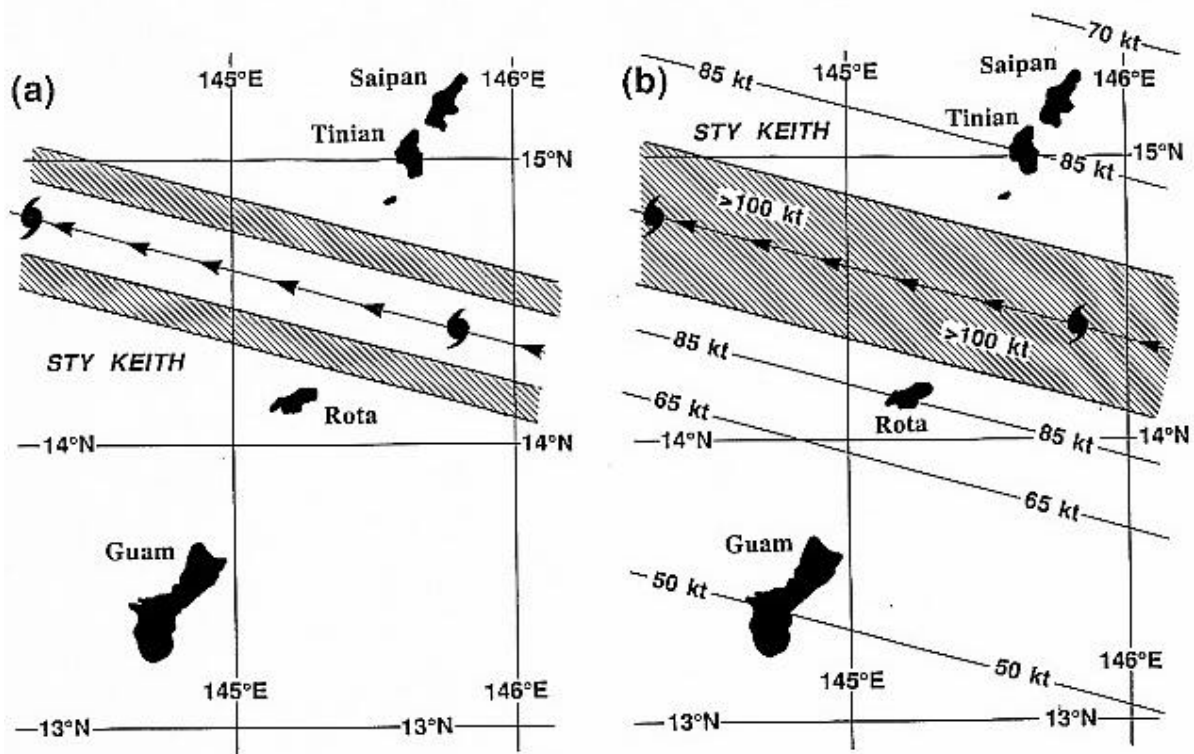


Figure 3-29-3 (a) The path of Keith's eye through the Marianas as depicted by Guam's NEXRAD. The typhoon symbols indicate the position of Keith at 020600Z and 021200Z November. The path of the 5-nm-wide (9-km-wide) eye wall cloud is indicated by the hatched swaths. (b) The wind distribution of Keith as it passed through the Marianas based upon the NEXRAD Base Velocity product, and from synoptic data from Guam and Saipan. Winds of 100 kt (51 m/sec) or greater occurred in Keith's eye wall cloud. An asymmetry in the wind field has been introduced by considering Keith's 15-kt (28-km/hr) speed of translation.

The NEXRAD data showed that the eye-wall cloud of Keith did not touch any land as it passed between islands only 50 nm (93 km) apart (Figure 3-29-3a). Also, the base velocity measurements (coupled with synoptic reports from the islands) indicated that sustained winds in excess of 100 kt (51 m/sec) most likely did not occur on any of the islands (Figure 3-29-3b), but passed between them in the same 30-nm-wide (56-km-wide) swath as traversed by the eye wall cloud. The super typhoon pictured in Figure 3-29-1 passed through the Marianas and left the islands relatively untouched. On a clear day, free of salt haze, each of the Mariana Islands can be viewed from the shores of its immediate neighbors. It is hard to imagine, viewing the neighbor islands from the shore, that the eye, eye wall cloud, and the destructive winds of a super typhoon can all fit over the waters of the channel and largely spare the islands. In Paka's (05C) summary, this is borne out even more dramatically. As Paka passed over the northern half of the island of Guam, wind gusts of approximately 150 kt (77 m/sec) and major damage to vegetation and structures were experienced on the parts of the island where the eye wall cloud passed, while

only 10 nm (20 km) to the south, outside of the eye wall cloud, gusts reached only to minimal typhoon intensity and little damage to structures or vegetation was noted.

b. Keith's Digital Dvorak (DD) time series

Keith was one of several typhoons during 1997 for which a time series of its hourly DD-numbers (Figure 3-29-4) was calculated. Keith's DD-numbers are unusually well-behaved. During the two-day period 010000Z-030000Z November, the DD-numbers fluctuated only a few tenths above and below T 7.0. The eye was obscured by cirrus on 03 November (possibly as a manifestation of an eyewall replacement cycle), but then reappeared and became well-defined on 04 November as Keith neared its point of recurvature. Keith's DD time series shows little or no diurnal variation, which for some typhoons is quite prominent. Why some typhoons show a strong diurnal signal in the DD-numbers and why others do not is an unsolved mystery.

c. Asymmetries in pressure fluctuations on microbarographic recordings

In the microbarograph trace of the pressure recorded at JTWC as Keith passed to the north of the station (Figure 3-29-5), an asymmetry is observed in the small fluctuations of pressure which are superimposed on the general longer period trends: the fall of pressure as the typhoon approaches is smoother than the rise of pressure after the TC is moving away from the station. This feature is presented here, because it also occurs in pressure traces from two different locations recorded as Super Typhoon Paka (05C) passed over Guam. While only a curiosity with perhaps a simple explanation, its repeated occurrence in two different typhoons, and at two separate locations during the same typhoon, raises the level of interest.

IV. IMPACT

Despite its track between the islands, Keith caused damage on Rota, Tinian, and Saipan in the Marianas. Red Cross officials reported that at least 790 houses were destroyed or damaged on these islands. About 15 power poles were reported downed on Saipan, and 20 on Tinian. Wind gusts of 95 kt (49 m/sec) were reported at Saipan's International Airport. Sea-level pressures fell to 964 mb on Rota and to 977 mb on Saipan. On Guam, little damage occurred, but power was knocked out to the entire island for nearly a day. Wind gusts reached 67 kt (35 m/sec) and nearly 6 inches of rain fell on parts of the island. Very large surf from the east deposited rubble on the coastal road on the southeast side of the island, forcing officials to close the road.

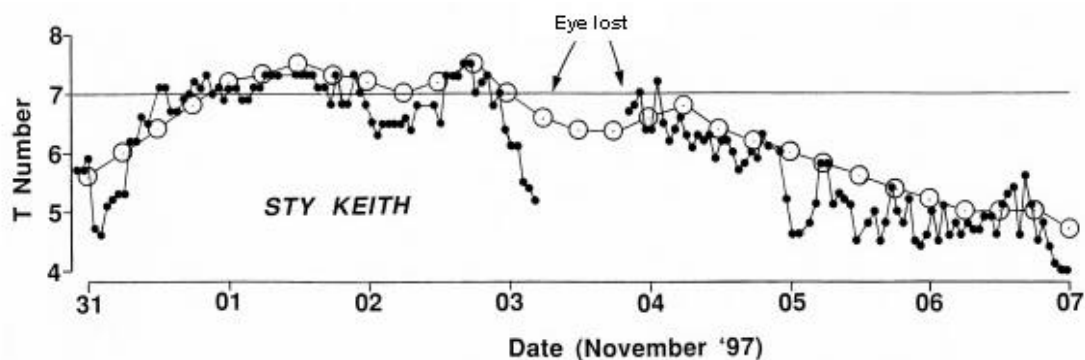


Figure 3-29-4 A time series of Keith's hourly DD numbers (small black dots) compared with the best-track intensity (open circles).

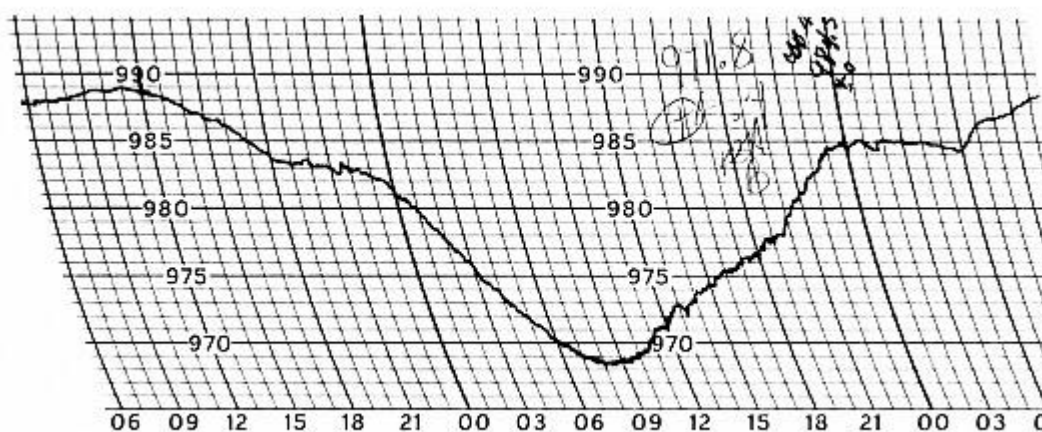


Figure 3-29-5 Microbarograph trace of the station pressure (in millibars) at the JTWC as Keith passed to the north of the island. At the 600-ft (183-m) elevation of the station approximately 18.5 mb must be added to obtain an estimate of the SLP. Note the smooth fall of pressure followed by and increase in small fluctuations as the pressure begins to rise.

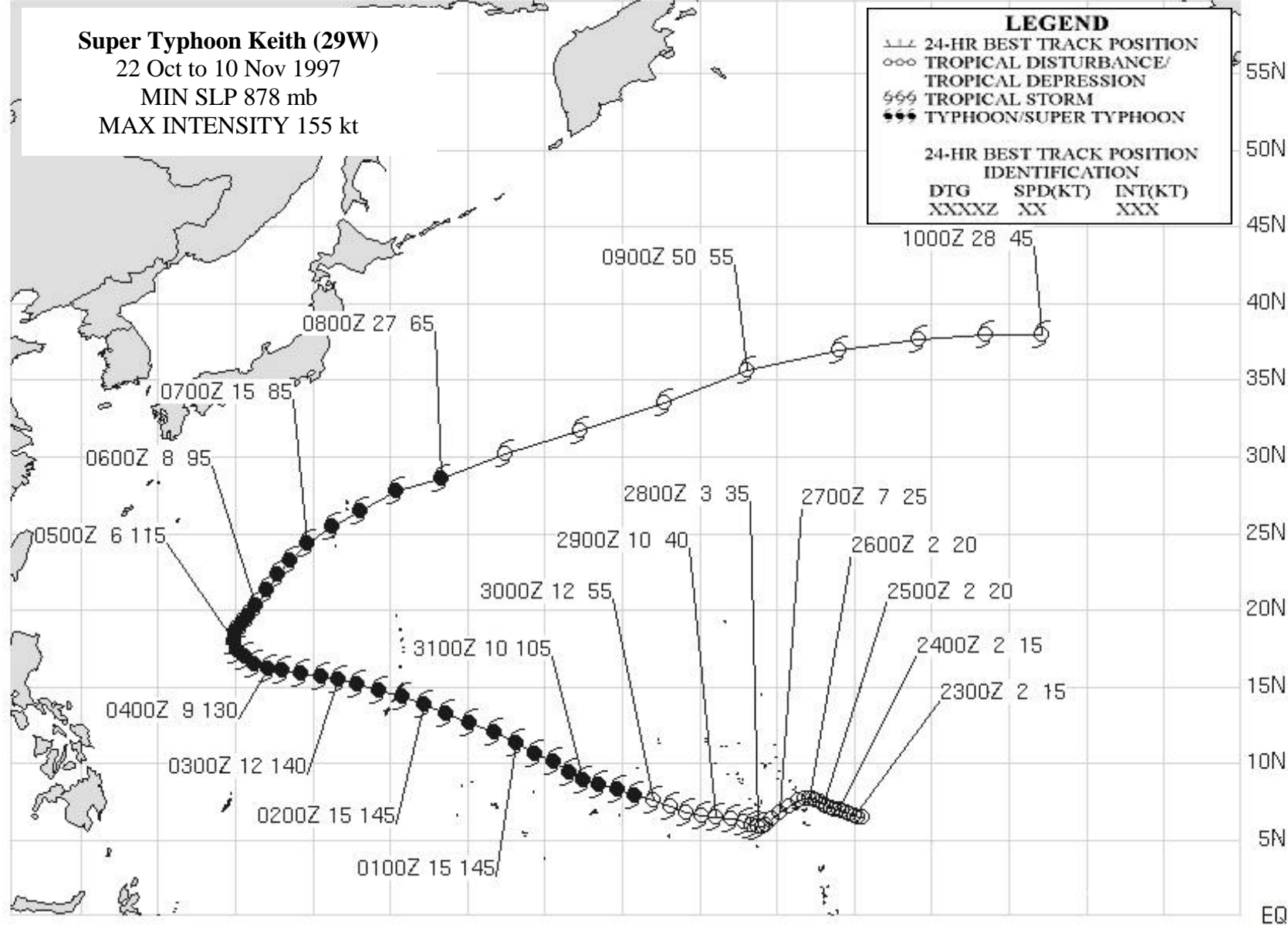
120E 125E 130E 135E 140E 145E 150E 155E 160E 165E 170E 175E 180 175W 170W 165W 160W

Super Typhoon Keith (29W)
 22 Oct to 10 Nov 1997
 MIN SLP 878 mb
 MAX INTENSITY 155 kt

LEGEND

--- 24-HR BEST TRACK POSITION
 ○○○ TROPICAL DISTURBANCE/
 TROPICAL DEPRESSION
 555 TROPICAL STORM
 *** TYPHOON/SUPER TYPHOON

24-HR BEST TRACK POSITION
 IDENTIFICATION
 DTG SPD(KT) INT(KT)
 XXXXZ XX XXX



TYPHOON LINDA (30W)

The tropical disturbance that would become Typhoon Linda (30W) formed within an area of convection east of the Philippine Islands near 10N 130E on 26 October. The disturbance was mentioned in the Significant Tropical Weather Advisory (ABPW) as it tracked westward over the next several days under the subtropical ridge to the north. Convection began to increase over the disturbance as it entered the Sulu Sea on 30 October. At 0730Z on the 31st, a Tropical Cyclone Formation Alert (TCFA) was issued as deep convection continued to organize about the disturbance's center. The first warning on Tropical Depression (TD) 30W was issued approximately 12 hours later.

The newly formed tropical cyclone reached tropical storm intensity within 24 hours as it tracked over the South China Sea. At this point, Tropical Storm Linda (30W) accelerated westward toward the southern tip of Vietnam. It tracked over the Vietnamese province of Ca Mau at 0900Z on 02 November with an intensity of 55 kt (28 m/sec).

Linda reached typhoon intensity shortly after entering the Gulf of Thailand. The cyclone turned northwestward following steering from the subtropical ridge. The system weakened slightly to 55 kt (28 m/sec) prior to striking the Malay Peninsula at 1600Z on 03 November. Crossing the Malay Peninsula, Linda further weakened as it encountered the region's 3000 ft (914 m) to 5000 ft (1524 m)

mountains. However, once over the warm waters of the Andaman Sea, the system began to reconsolidate. This was the first tropical cyclone since Typhoon Forrest (30W) in 1992 to cross from the Western North Pacific to the North Indian Ocean.

Soon after moving into the Andaman Sea, a weakness in the subtropical ridge began to develop to the north, causing Linda's forward speed to slow. Over open water once again, Linda reintensified and became a typhoon once again at 0000Z on the 6th. This was short-lived, however, as interaction with a mid-latitude trough began to introduce vertical wind shear. Linda stalled in the Bay of Bengal within an area of weak steering located between the subtropical

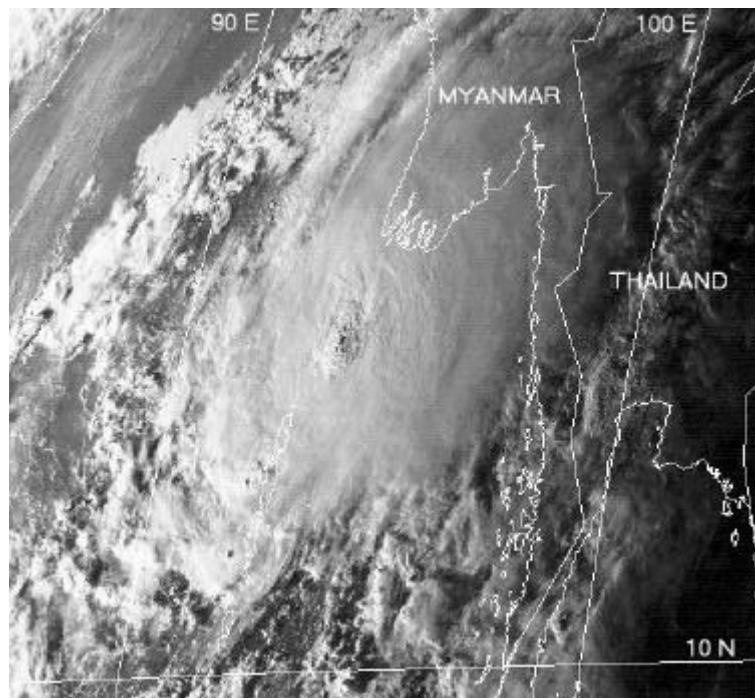
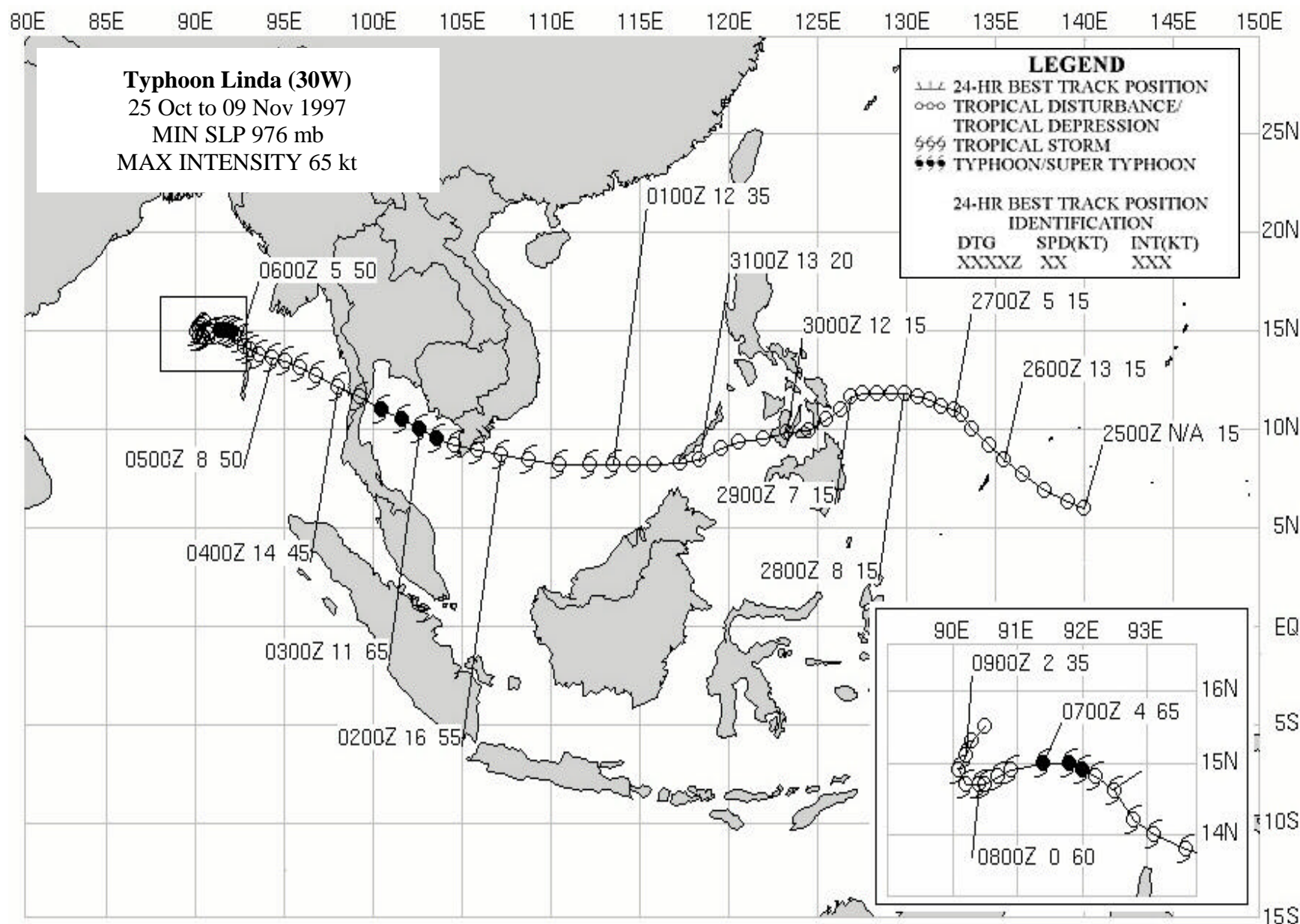


Figure 3-30-1 Typhoon Linda (30W) re-intensifying over the Andaman Sea after crossing the Malay Peninsula (051025Z November visible GMS imagery).

ridge axis at 500 mb and sub-tropical ridge axis at 200 mb. Upper level vertical wind shear continued across the system center, allowing slow weakening of the system for several days. By 10 November, Linda had dissipated.

Linda produced considerable damage and loss of life in Vietnam and Thailand. Vietnam's Ca Mau province, located to the northern side of Linda's passage, reported significant damage. Newspaper reports as late as 08 November indicated that at least 330 people were killed in Vietnam and Thailand with approximately 2250 people still missing. Many of the missing were Vietnamese fisherman or sailors caught at sea in the path of the tropical cyclone.



TYPHOON MORT (31W)

I. HIGHLIGHTS

Typhoon Mort (31W) was the last tropical cyclone to form west of the international dateline (IDL) for the western North Pacific season. It tracked over the open waters of the Philippine Sea but vertical shear weakened it to a tropical depression by the time it made landfall over the island of Luzon.

II. TRACK AND INTENSITY

The disturbance that would become Typhoon Mort (31W) was first noted on the Significant Tropical Weather Advisory (ABPW) as an area of convection south of Guam on 08 November at 0600Z. The convection was located within a weak monsoon trough that stretched from the southern Philippine Sea to just south of Guam. An area of divergence overlaid the disturbance, which was located equatorward

of mid-level ridging. By 09 November, the disturbance had become better organized with satellite imagery indicating a developing banding feature. Animation of satellite imagery also indicated some cyclonic motion within the convection. As development continued to progress, a Tropical Cyclone Formation Alert (TCFA) was issued at 1900Z on 09 November. The disturbance was upgraded to tropical depression (TD) status with a 101800Z warning. Figure 3-31-1 shows the TD just four and a half hours after this warning, and is an example of how a typical 25 - 30 kt (13 - 15 m/sec) system appears in visible satellite imagery.

The system tracked in a westerly direction at speeds of 7 to 9 kt (13 to 17-km/hr) due to easterly steering flow in the lower to mid-levels south of the subtropical ridge. This motion would continue for the remainder of the tropical cyclone's lifecycle. Figure 3-31-2 indicates the progression in development as seen by visible satellite imagery during a 66- hour period beginning at 0425Z on 11 November. The image at top left is Mort near the time it was upgraded to a tropical storm. Eighteen hours later (top right image), Mort is a strong tropical storm with winds estimated to be 55 kt (28m/sec). The system has a cold dense overcast over the center, with a good banding feature. Twenty-four hours later (bottom left image), the overall convective cloud structure is becoming disorganized, probably due to increased vertical wind shear relative to the moving system. At this time, Mort was at its peak intensity of 65 kt (33 m/sec), and would develop no further. Between 0600Z and 2100Z on the 13th, vertical wind shear caused the low-

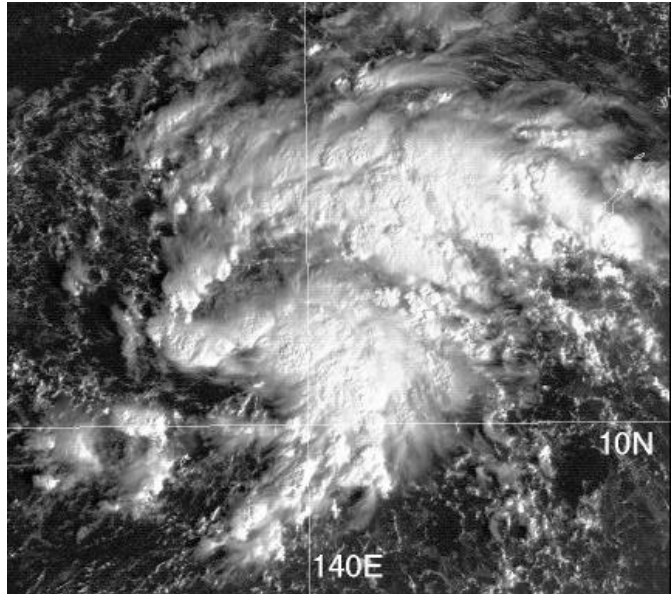


Figure 3-31-1 Visible satellite imagery of TD 31W; valid time is 102225Z November

level circulation to separate from the deep convection. The convection was sheared off to the east-southeast of the low-level circulation, which continued to track westward toward the Philippine Islands. The low-level circulation, and the associated convection can be seen in the image at bottom right. Due to the presence of an exposed low level circulation, the system was downgraded to tropical storm intensity (35 kt/ 18 m/sec) on the 14th at 0000Z. However, vertical wind shear lessened over the next day and a convective banding feature soon re-developed. This was only short-lived as vertical wind shear once again increased late on the 15th, eventually causing convection to shear to the south of the center. Mort proceeded to weaken to TD strength by 0600Z on the 16th and shortly thereafter made landfall on the island of Luzon. The system subsequently dissipated over the mountains within the island's interior.

III. DISCUSSION

Unexpected Vertical Wind Shear

The shearing of Mort's convection on the 14th was unexpected and surprised JTWC forecasters. Strong vertical wind shear was not indicated by NOGAPS prognostic charts. Although animated satellite imagery indicated the system's development had arrested on the 13th, it didn't appear to indicate the presence of strong vertical wind shear. Some calculations were made using upper-level water vapor wind derived data (supplied by the University of Wisconsin) and the storm's motion. The upper-level wind data was used to find an average wind vector across the system center, and the storm's motion vector was used as a proxy for the lower-level wind vector. The difference between the two vectors gave the shear across the system center. Values were calculated for the 13th and 14th at 0000Z. The shear vector value more than doubled over the 24-hour period, changing from a west-southwest direction at 12 kt (22 km/hr), to west-southwest at 26 kt (48 km/hr). In a statistical study, Zehr (1992) found a shear value of 20 kt generally inhibits tropical cyclone development. This illustrates one of the ways in which water vapor wind derived wind data can help forecasters in evaluating tropical cyclones.

IV. IMPACT:

No reports of damage or injuries associated with Typhoon Mort (31W) were received by JTWC.

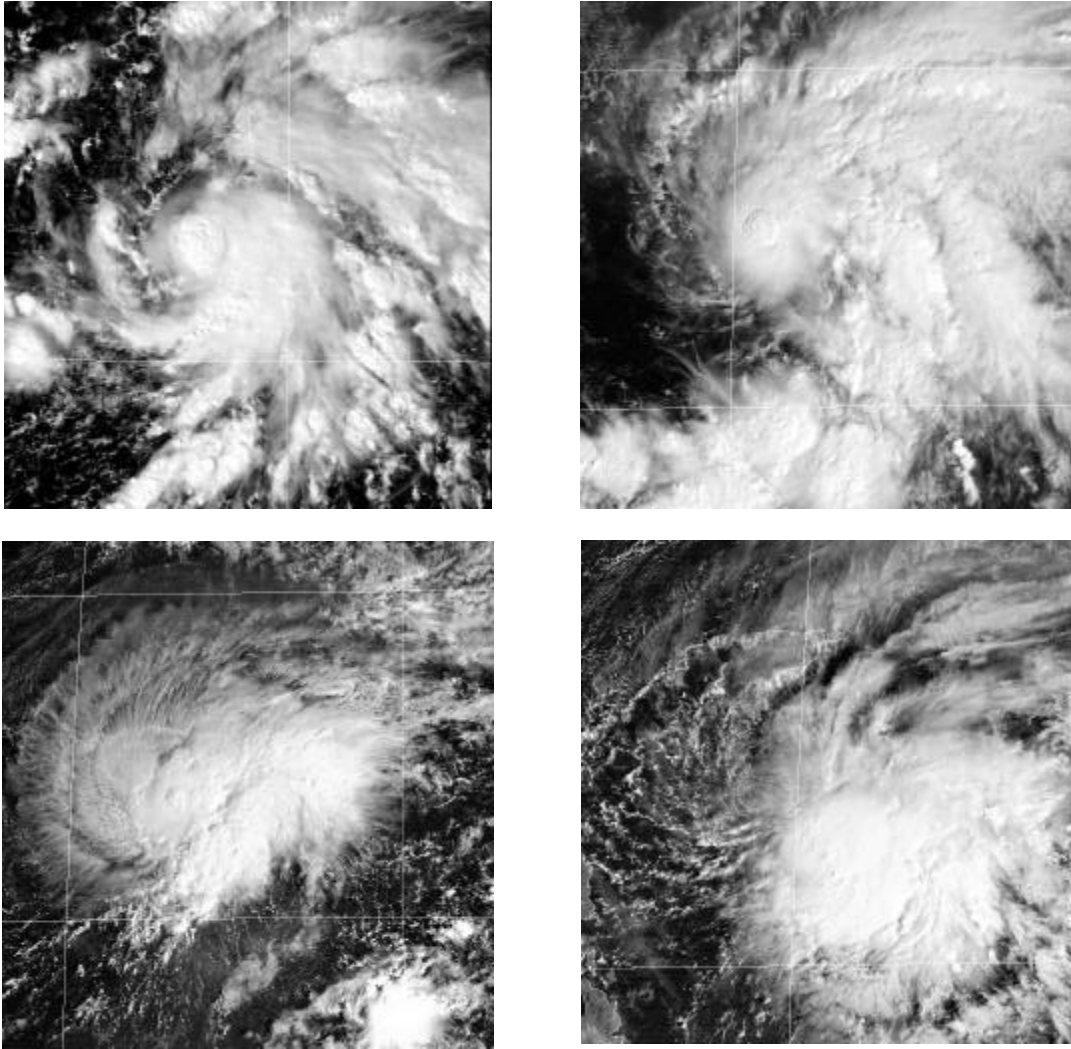
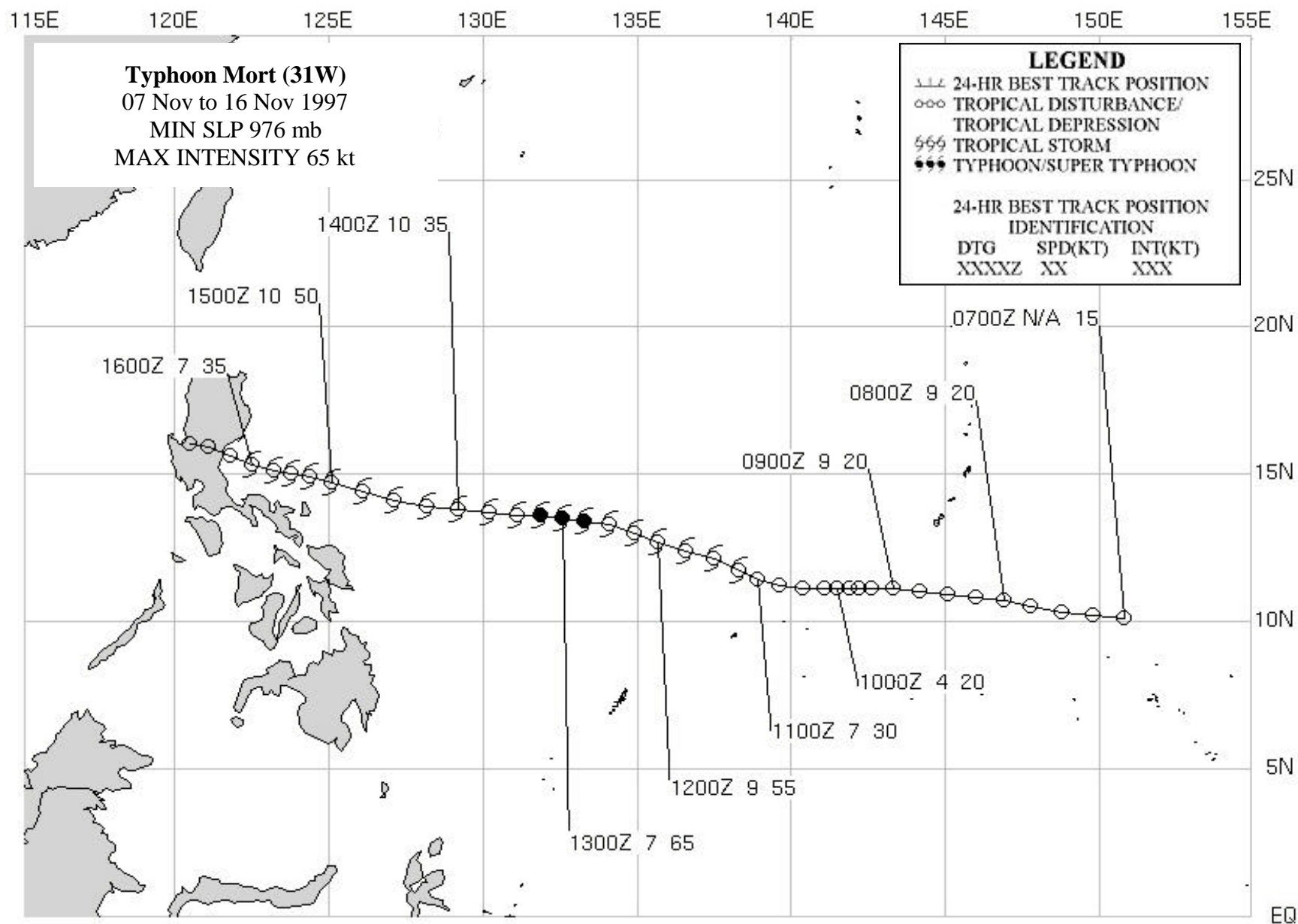


Figure 3-31-2 The different developmental stages of Typhoon Mort as seen by visible satellite imagery over a 66-hour period. Tropical cyclone best track intensities and valid times of imagery are: top left, 35 kt (18 m/sec) at 110425Z; top right, 55 kt (28 m/sec) at 112225Z; bottom left, 65 kt (33 m/sec) at 122225Z; bottom right, 35 kt (18 m/sec) at 132225Z. Note the exposed low level circulation center northwest of the convection at 132225Z.



SUPER TYPHOON PAKA (05C)

I. HIGHLIGHTS

Paka formed in the Central Pacific southwest of Hawaii on 28 November 1997. Paka tracked steadily westward for two and one half weeks before slamming into the islands of Guam and Rota. As Paka's eye passed over northern Guam, destructive winds caused extensive damage to private and commercial buildings, infrastructure, crops, and vegetation. More intense than Typhoons Pamela (May 1976) and Omar (August 1992), Paka, with estimated maximum sustained surface winds of 130 kt (67 m/sec) gusting to 160 kt (82 m/sec) approached, but did not exceed, the intensity of Karen (estimated 135 kt (69 m/sec) gusting to 165 kt (85 m/sec)) in November 1962. No life was lost as a direct result of Paka's passage. Preliminary estimates of total losses run in the hundreds of millions of dollars.

II. TRACK AND INTENSITY

During the last week of November convection associated with an equatorial westerly wind burst flared up 1080 nm (2000 km) southwest of Hawaii. This led to the formation of twin tropical cyclones - Paka (05C), in the Northern Hemisphere, and Pam (07P) in the Southern. Pam (07P), in the summer hemisphere, became a hurricane and began recurving southeastward (Figure 3-05C-1). After issuing the first 17 advisories on Paka, the Central Pacific Hurricane Center transferred warning responsibility to the Joint Typhoon Warning Center as the system approached the international dateline (IDL). The first JTWC warning was number 18, valid at 1800Z on 06 December. After reaching 60 kt (31 m/sec) on 08 December, Paka began to weaken again. JTWC forecasters believed this

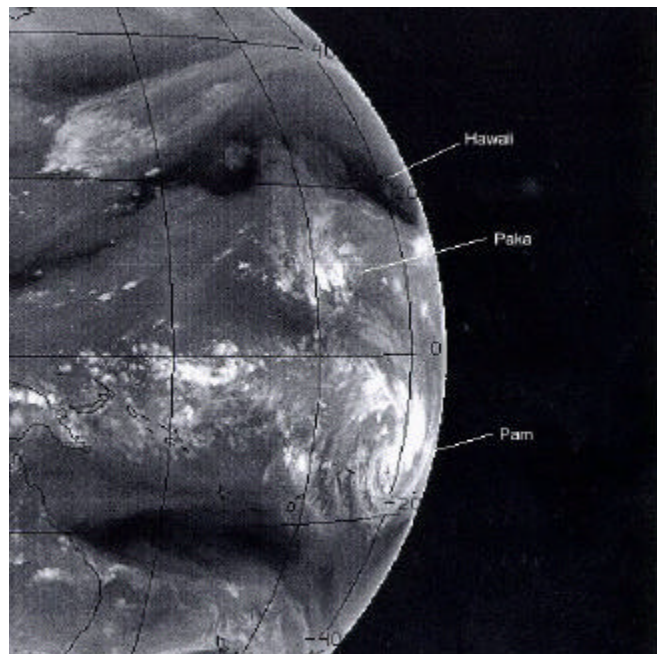


Figure 3-05C-1 Paka (05C) and Southern Hemisphere twin Pam (07P) early on 6 December, 1997

weakening trend would continue, because upper level analysis and prognostic charts indicated that the cyclone would remain in a region of significant vertical shear. At 1800Z on 09 December, JTWC analyzed the cyclone as a 45 kt (23 m/sec) system and forecast this to remain constant for 36 hours, followed by a weakening trend. However, by 0600Z on 10 December, this thinking had begun to change, as upper level analysis showed that vertical shear was lessening. JTWC now depicted a 55 kt (28 m/sec) system which would peak as a minimal strength typhoon within 24 hours. Eighteen hours later, it became apparent that Paka was continuing to develop, and the 00Z warning on 11 December predicted it would peak at over 100 kt (50 m/sec). Majuro

and Kwajalein atolls both received peak wind gusts of over 40 kt (20 m/sec) as Paka passed near on the 10th and the 11th, respectively.

After reaching an intensity of 115 kt (59 m/sec) on 12 December, Paka briefly weakened as along-track acceleration commenced. Despite forward speeds of 16 and 17 kt (30 and 31 km/hr), the typhoon started to intensify once again, peaking at 140 kt (72 m/sec) (160 mph) on 15 December. Paka was now a very serious threat to the southern Marianas. For Guam and Rota, the question rapidly changed from "if it arrives" to "when will it arrive?"

A day away from Guam, Paka began slowing, as anticipated, and there were signs of weakening. Now within NEXRAD Doppler radar range, the inner structure of Paka was revealed. There were concentric wall clouds - a primary approximately 40 nm (74 km) in diameter and a secondary fragmented inner wall cloud 10 nm (19 km) in diameter (Figure 3-05C-2). At 0600Z on 16 December, the center of Paka's eye was located 25 nm (46 km) south of the eastern point of Rota. The along-track speed was down to nine kt (17 km/hr), and the estimated intensity at 125 kt (64 m/sec) gusting to 150 kt (77 m/sec). At 161200Z, Paka had slowed to 6 kt (11 km/hr), and was at its closest point of approach (CPA) 15 nm (28 km) north of Agana, Guam. However, intensification was, once again, underway reaching an estimated maximum of 130 kt (67 m/sec) gusting to 160 (82 m/sec).

After seriously damaging the islands of Guam and Rota, Paka continued to intensify and reached a peak of 160 kt (82 m/sec) briefly on 18 December. Then, rapid weakening began and persisted until the cloud system completely dissipated four days later on 22 December. See Chapter 6 for a listing of the 6-hourly best track position, intensity, track direction and speed.

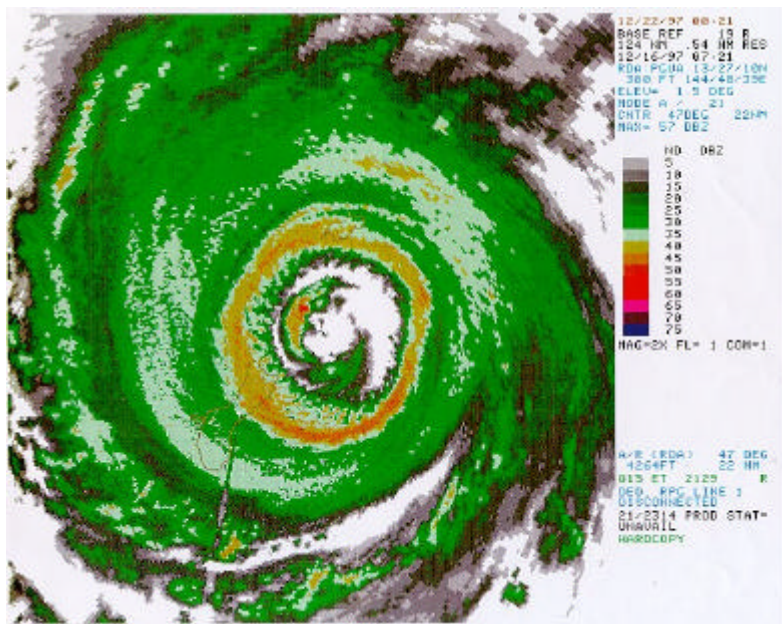


Figure 3-05C-2 NEXRAD imagery of Paka early on 16 December, 1997.

III DISCUSSION

a. Data Collection Difficulties

Considering the strength and duration of Paka's surface winds, it is not surprising that the wind records for areas that experienced passage of the primary wall cloud were fragmentary. The approach taken with these incomplete and noisy raw data records was to work sustained wind observations against the peak wind gusts, using a standard gust factor of 1.20 to 1.25 over water (Atkinson, 1974) and 1.60 overland. For example, gusts to 120 kt (62 m/sec) over water would be associated with a sustained surface wind of 100 kt (51 m/sec); overland gusts to 120 kt

(62 m/sec) would relate to 75 kt (39 m/sec) sustained wind. This technique identifies the representative data, for example: Commercial Port NWS HANDAR at Apra Harbor reported sustained/peak gust of 100/149 kt (51/77 m/sec) which is plausible; the Andersen AFB anemometer recorded 96/205 kt (49/105 m/sec) which is not considered representative. The Commercial Port sensor failed after recording four hours of 135 to 149 kt (69 to 77 m/sec) gusts in the wall cloud, Andersen AFB sensor lost power during passage of the western wall cloud. Additionally, the NWS sensor at Tiyan lost power during the onset of the primary wall cloud, the NPMOCW/JTWC anemometer at Nimitz Hill failed at 103 kt (53 m/sec) before the wall cloud arrived, the wind bird at the Apra Harbor tide gauge failed in the wall cloud, and the NWS HANDAR at the University of Guam, Mangilao weathered the storm to report a peak gust to 123 kt (63 m/sec). In the final analysis the HANDAR instrument at Apra Harbor becomes the benchmark. It faithfully recorded peak gusts up to 149 kt (77 m/sec) until the winds began backing to the southwest, at which point it failed. This implies that the later southwesterly flow or second wind was stronger than the initial northwest to west wind (or first wind). This is borne out by the reports from other records at the Rota HANDAR and airport, DanDan and Merizo (Figure 3-05C-3). The only complete wind trace that records the peak winds in the wall cloud and the relative calm within the eye was from the Kuentos Communications, Inc. in Maite (Figure 3-05C-4). Relative to the lowest pressure which occurred at the CPA of Paka, the strength and duration of the highest winds on either side were compared. The wind from the southwest after the eye passage was more intense and of a longer duration. If this increase of 10 kt (5 m/sec) at Maite is applied to the Apra Harbor benchmark, a peak gust of 160 kt (82 m/sec) can be inferred.

b. Pressure Assessment

Microbarographs fortunately are less exposed than wind sensors which accounts for their survival, hence the pressure records were complete for Guam. The minimum sea-level pressure (MSLP) values (see Figure 3-05C-3) dropped from a high at DanDan (983 mb) and Merizo (980 mb) to Mangilao (953 mb), Apra Harbor (953 mb) and Tiyan (951 mb) to the lowest at Andersen AFB of 948 mb (Figure 3-05C-5). Using the MSLPs, which occurred at CPA, the passage of the center of Paka to the north of Guam can be followed across the checkerboard (Figure 3-05C-3). In addition, there is an empirical relationship (Dvorak, 1984) that can be used to relate the intensity (maximum sustained 1-minute mean surface winds over water) with the MSLP. The relationship has two scales: one for the Pacific and one for the Atlantic (Figure 3-05C-6). The reason for this is that the ambient pressure for the Pacific is in the mean lower than the Atlantic Ocean. Applying Dvorak's scale to Paka's 130 kt (67 m/sec) estimated intensity yields a 914 mb MSLP on the Pacific scale, which is much too low in relation to the values observed on Guam. However, a value for the Atlantic is 935 mb which is closer to what was observed. In summary, the basic reason for the difference between Pacific and Atlantic scales is that most tropical cyclones in the western North Pacific occur during the summer monsoon season when the ambient pressures are lower because of the presence of the monsoon trough. The Pacific scale doesn't address seasonal differences, therefore a bias exists. If a tropical cyclone, such as Paka, occurs in the winter, it follows that the scale will yield too low a MSLP. Therefore, a MSLP of 935 mb for Paka's 130-kt intensity appears reasonable.

SUPER TYPHOON PAKA OBSERVATIONS 16 DECEMBER 1997






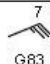

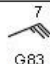















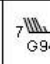
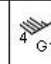


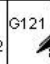

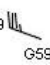
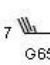



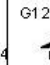

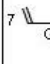
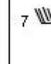



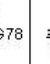
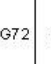
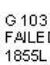

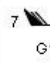


ZULU TIME	0400	0500	0600	0700	0800	0900	1000	1100	1200	1300	1400	1500
LOCAL TIME	1400	1500	1600	1700	1800	1900	2000	2100	2200	2300	0000	0100
			 G80	 G95	 G100	 G100						
ROTA ARPT			LOWEST PRESSURE									
	 G60	 G72	 G76	 G83	 G86	 G70	 G60	 G66				
ROTA HANDAR				981 mb								
		 G153	 G161	 G140	 G140	 G125	 G110	 G110				
AAFB												
			 G65	 G79	 G 97 FAILED 1845L							
TIYAN						2020I 951 mb						
				 G72	 G94	 G123	 G114	 G122	 G121		53 KT G 104	39 KT G 82
MANGILAO U OF G HANDAR							LOWEST PRESSURE					
		 G53	 G59	 G65	 G83	 G92	 G114	 G122	 G82			
DAN DAN INARAJAN HANDAR							983 mb					
					 G52	 G66	 G80	 G85	 G78	 G72	 G62	
MERIZO HANDAR							980 mb					
						 G 103 FAILED 1855L			LOWEST PRES 1215Z			
NIMITZ HILL												
						 G135	 G149	 G140	 G137	FAILED		
COMMPORT HANDAR APRA HARBOR								953 mb				
TIDE STN APRA HARBOR								957 mb				

Figure 3-05C-3 Wind and pressure reports during the passage of Paka (05C) near Guam.

c. Radar Assessment

- 1) The NEXRAD Doppler radar, which is located at Mangilao and is maintained by Andersen AFB proved to be an invaluable tool for locating the center of Paka's eye and observing its convective structure. The last reflectivity product (Figure 3-05C-2) shows Pati Point, at the extreme northeastern end of Guam, just entering the relatively convection-free portion of the eye. The fragmented inner wall cloud is located over the Rota Channel to the

northeast. The comparison radial velocity product (Figure 3-05C-7) indicates 144 kt (75 m/sec) inbound at the radar at 2000 feet (610 m) and 124 kt (64 m/sec) outbound. The 1-hour precipitation product (Figure 3-05C-8) indicates 1.50 to 2.00 inches (3.8 to 5 cm) in the wall cloud. Note: the absence of return over Rota to the northeast of the radar is due to lowest elevation beams being blocked by Mount Barrigada. No products were received after these because the NEXRAD radar went into standby mode and could not be remotely reset from the Unit Control Position at Andersen AFB. (The radar site weathered the storm without major damage.)

- 2) The conventional FAA (Center-Radar Approach Control) CERAP radar located at Mount Santa Rosa proved invaluable for fixing Paka after the NEXRAD went into standby mode at 160721Z December. This support continued until the FAA radar failed at 161119Z.

IV IMPACT

Based on aerial and surface surveys, the following can be stated:

- 1) On Guam, as indicated by vegetation and crop blow downs and debris trails, the first wind (northwest through west) was less damaging than the second from the southwest through south . On Rota, the first wind (northeast through east) was less severe than the later second from the southeast. These observations support the fact that Paka was becoming more intense as it passed westward through the Rota Channel.
- 2) Moderate damage with pockets of heavy damage to private and commercial structures occurred on the northern half of Guam, which experienced outer wall cloud passage (Figure 3-05C-9). The slow passage (six hours) of the outer wall cloud across the center portion of the island allowed more time for high winds and rain to weaken structures.

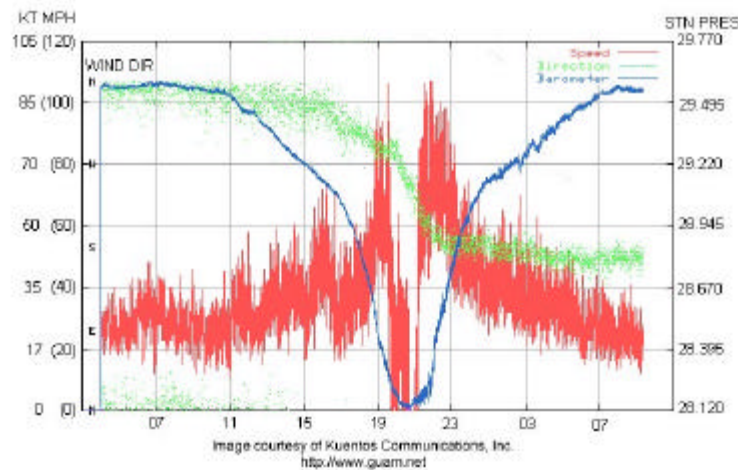


Figure 3-05C-4 This wind instrument, owned by Kuentos Communications, Inc, was the only one on Guam to recort the entire system passage.

- In general, the damage assessment of northern Guam indicated a mixture of tropical cyclone scale categories 3 and 4 (Saffir-Simpson Hurricane Scale as modified by Guard and Lander, 1995) depending upon the exposure sites. This provides a wide range of maximum sustained wind speeds from 96-115 kt (49-59 m/sec) for category 3 to 116-135 kt (59-69 m/sec) for category 4.

MICRO-BAROGRAPH
CHART NO. 5-1090-A
BELFORT INSTRUMENT COMPANY
BALTIMORE 2, MARYLAND, U.S.A.

INSTRUMENT NO. _____ DATE 15 Dec 97 STATION ANDERSEN AFB, GOMM

REMARKS _____

125

C.I. NUMBER	MAXIMUM WIND SPEED	T-NUMBER	MINIMUM SEA-LEVEL PRESSURE	
			(Atlantic)	(NW Pacific)
0	<25 kt			
0.5	25			
1	25	1		
1.5	25	1.5		
2	30	2	1009mb	1000mb
2.5	35	2.5	1005	997
3	45	3	1000	991
3.5	55	3.5	994	984
4	65	4	987	976
4.5	77	4.5	979	966
5	90	5	970	954
5.5	102	5.5	960	941
6	115	6	948	927
6.5	127	6.5	935	914
7	140	7	921	898
7.5	155	7.5	906	879
8	170	8	890	858

Figure 3-05C-6 Wind, pressure, and Dvorak relationship for both the Atlantic and Pacific.

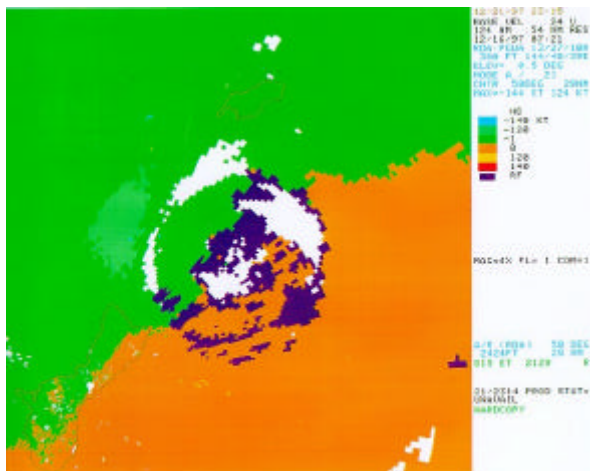


Figure 3-05C-7 NEXRAD radial velocity product for 0721Z on 16 December 97.

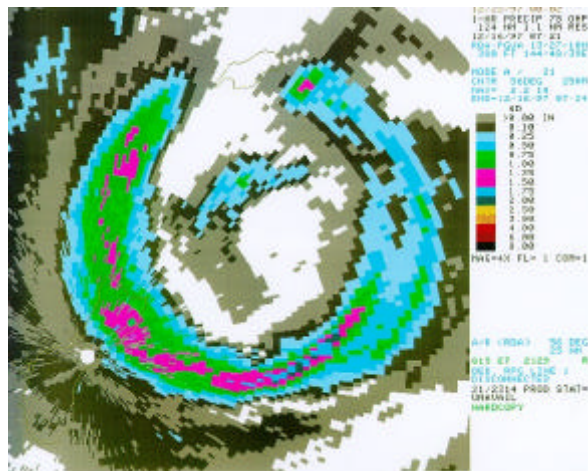


Figure 3-05C-8 NEXRAD one hour precipitation product for 0721Z on 16 December 97.

SUPER TYPHOON PAKA
GUAM AND ROTA, 16 DECEMBER 1997

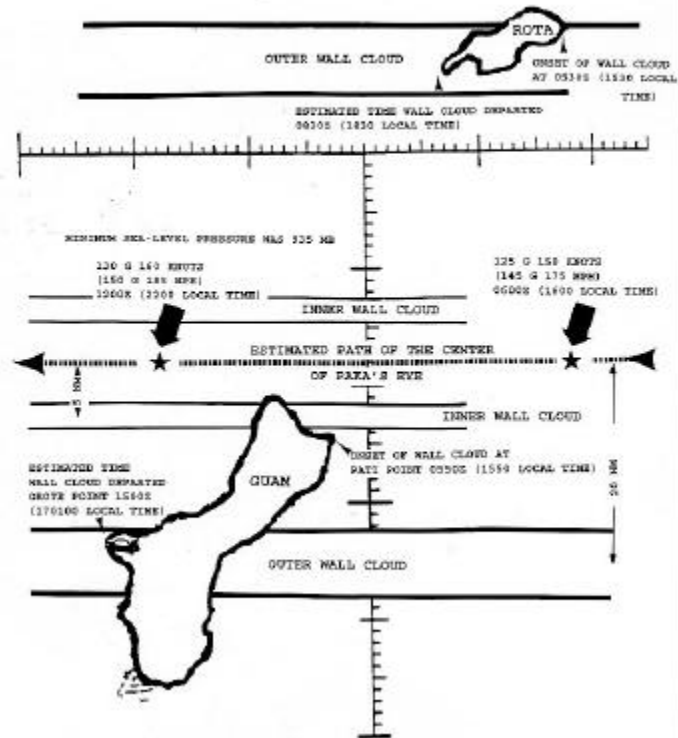


Figure 3-05C-9 Paka's (05C) track across Guam.

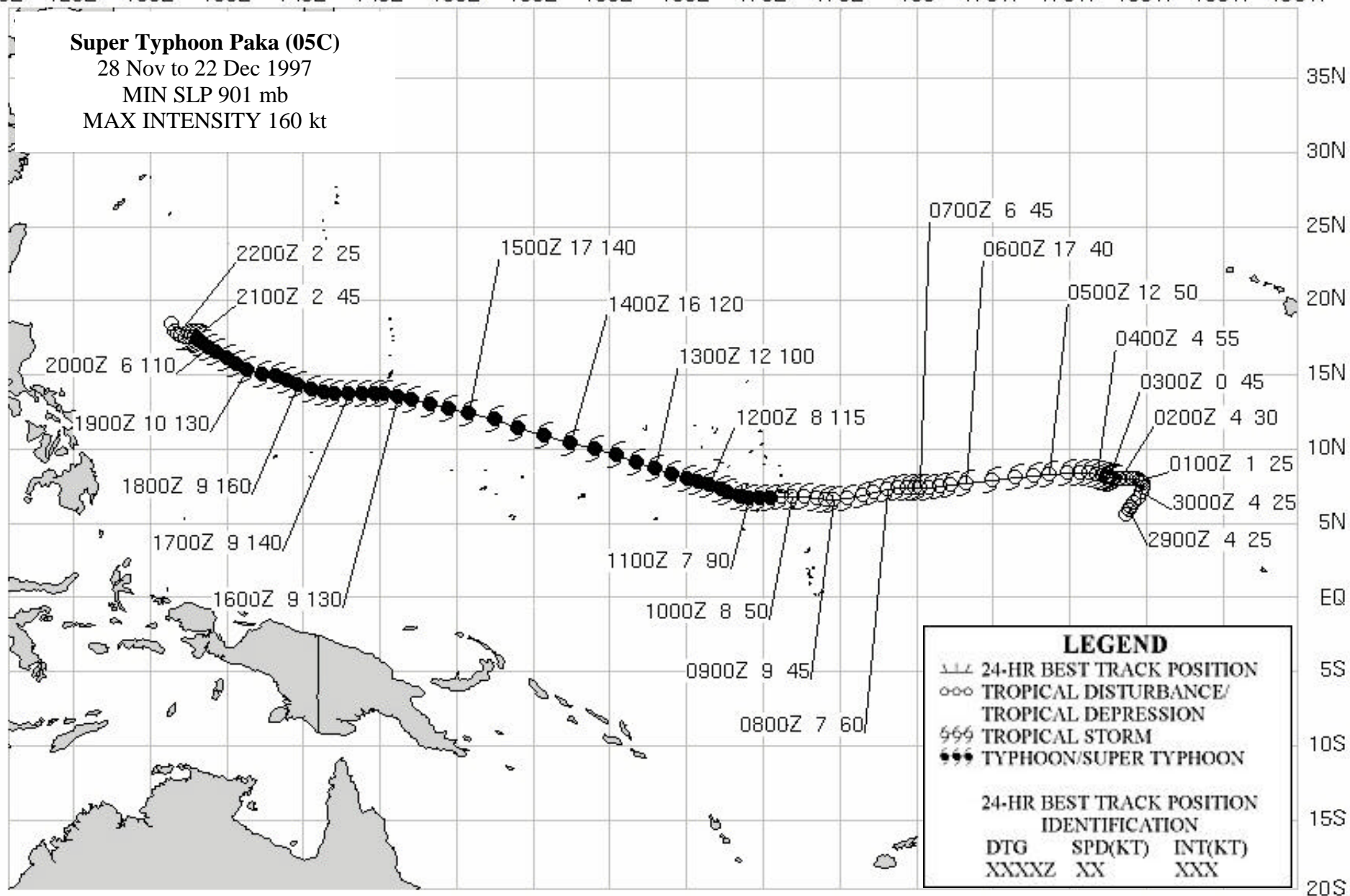
120E 125E 130E 135E 140E 145E 150E 155E 160E 165E 170E 175E 180 175W 170W 165W 160W 155W

Super Typhoon Paka (05C)

28 Nov to 22 Dec 1997

MIN SLP 901 mb

MAX INTENSITY 160 kt



TROPICAL CYCLONE 01B

Tropical Cyclone (TC) 01B emerged from a poorly organized area of convection embedded within the near-equatorial trough. It was first noted on the Significant Tropical Weather Advisory (ABIO) bulletin for the Indian Ocean valid 13 May. The system slowly developed as it drifted in a generally northward direction within the Bay of Bengal. The first warning was issued at 1800Z on 14 May based on a satellite derived intensity estimate of 25 kt (13 m/sec) and indications that the system was developing. The presence of equatorial westerlies and good upper level outflow meant that the cyclone should continue to intensify. Intensity estimates ranging from 35 to 40 kt (18-21 m/sec) were received less than six hours later. Beginning at 1200Z on the 15th, TC 01B slowed and veered toward the east, remaining at a constant intensity of 50 kt (26 m/sec) for approximately 24 hours. Afterwards the cyclone picked up speed and again tracked generally northward

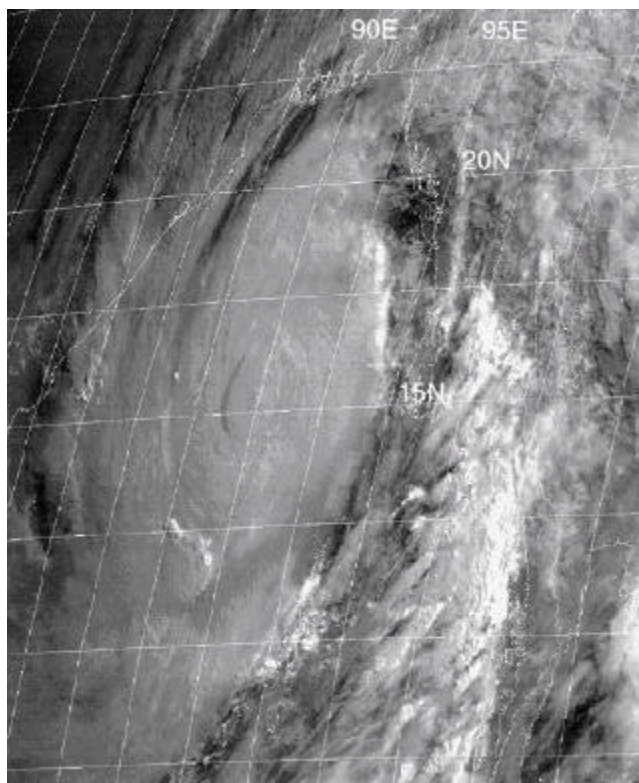
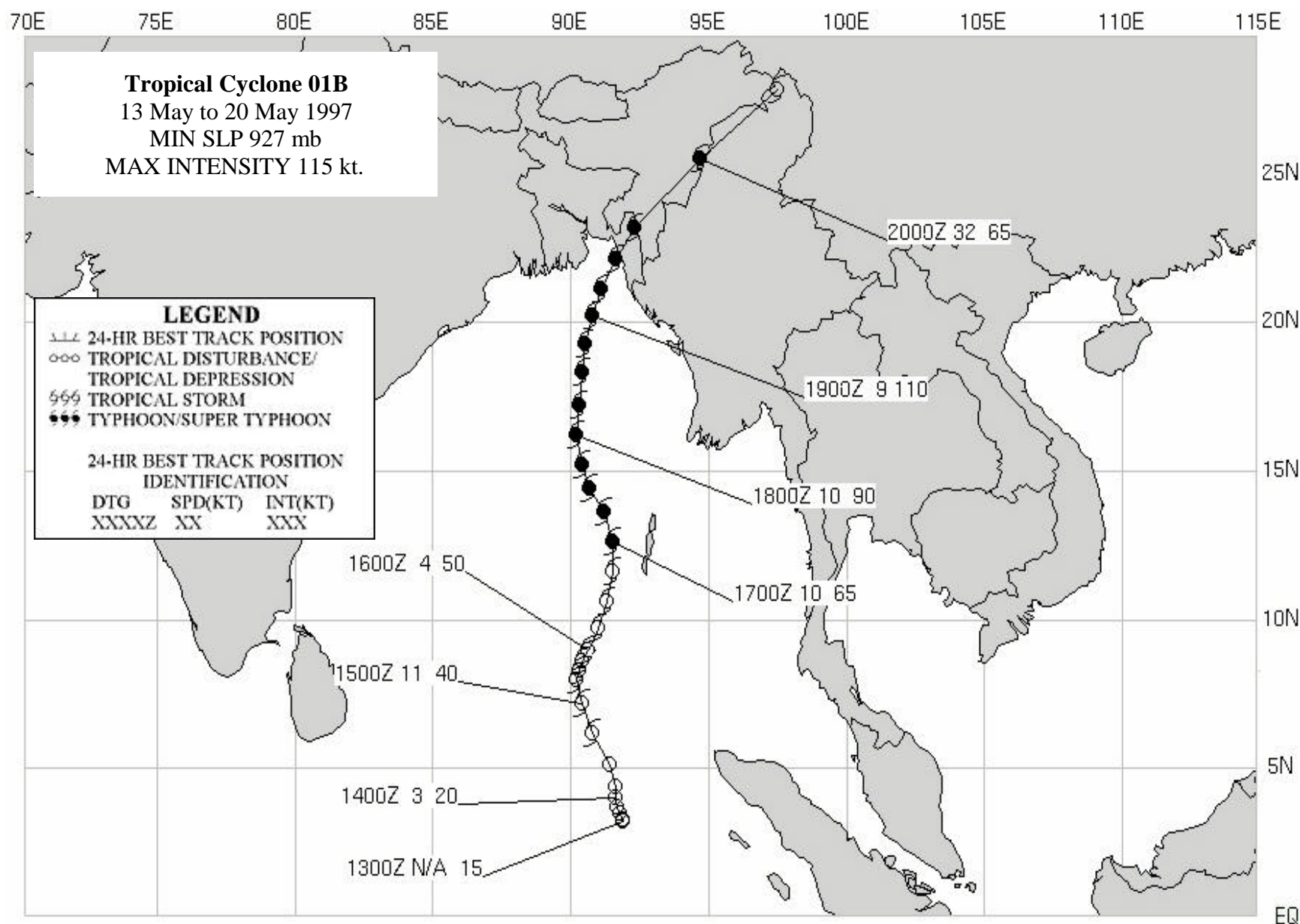


Figure 3-01B-1 Visible imagery of TC 01B from 180034Z May.

while further intensifying. By 0000Z on the 17th, TC 01B had reached 65 kt (33 m/sec). By 1800Z on the 18th the system developed an eye. Twelve hours later it peaked at 115 kt (59 m/sec). This intensity was maintained until landfall occurred in Bangladesh shortly after 1200Z on 19 May. Once over land, the system continued its north-northeastward track, increased its speed significantly north of the subtropical ridge axis, and dissipated due to land interaction as it neared China. TC 01B caused significant damage and several hundred casualties in Bangladesh.



TROPICAL CYCLONE 02B

Tropical Cyclone 02B began as an area of disturbed weather in the western Bay of Bengal and was first mentioned on the 19 September Significant Tropical Weather Advisory (ABIO). The disturbance continued to improve in organization through 21 September remaining quasi-stationary in the monsoon trough. After 21 September, the system began to move slowly northwestward until 24 September. On 24 September, the first warning was issued. At about this time, a developing mid-latitude trough northwest of the cyclone shifted the steering flow to southwesterly and by 26 September, the forward motion had increased from 6 kt (11 km/hr) to 14 kt (26 km/hr). Tropical Cyclone 02B increased in intensity as it tracked along the eastern coast of India.

The system reached a peak intensity of 65 kt (33 m/s) approximately 12 hours before making landfall in Bangladesh on 27 September. Forty-seven people were reported killed and more than 1000 injured as heavy surf, rain and wind gusts of 80 kt (40 m/s) swept the coastline. Tropical Cyclone 02B moved further inland where it eventually dissipated.

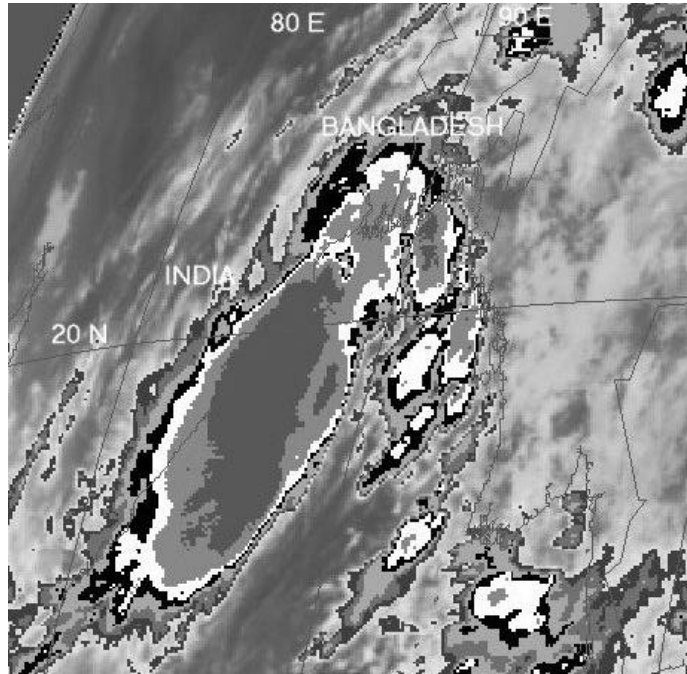
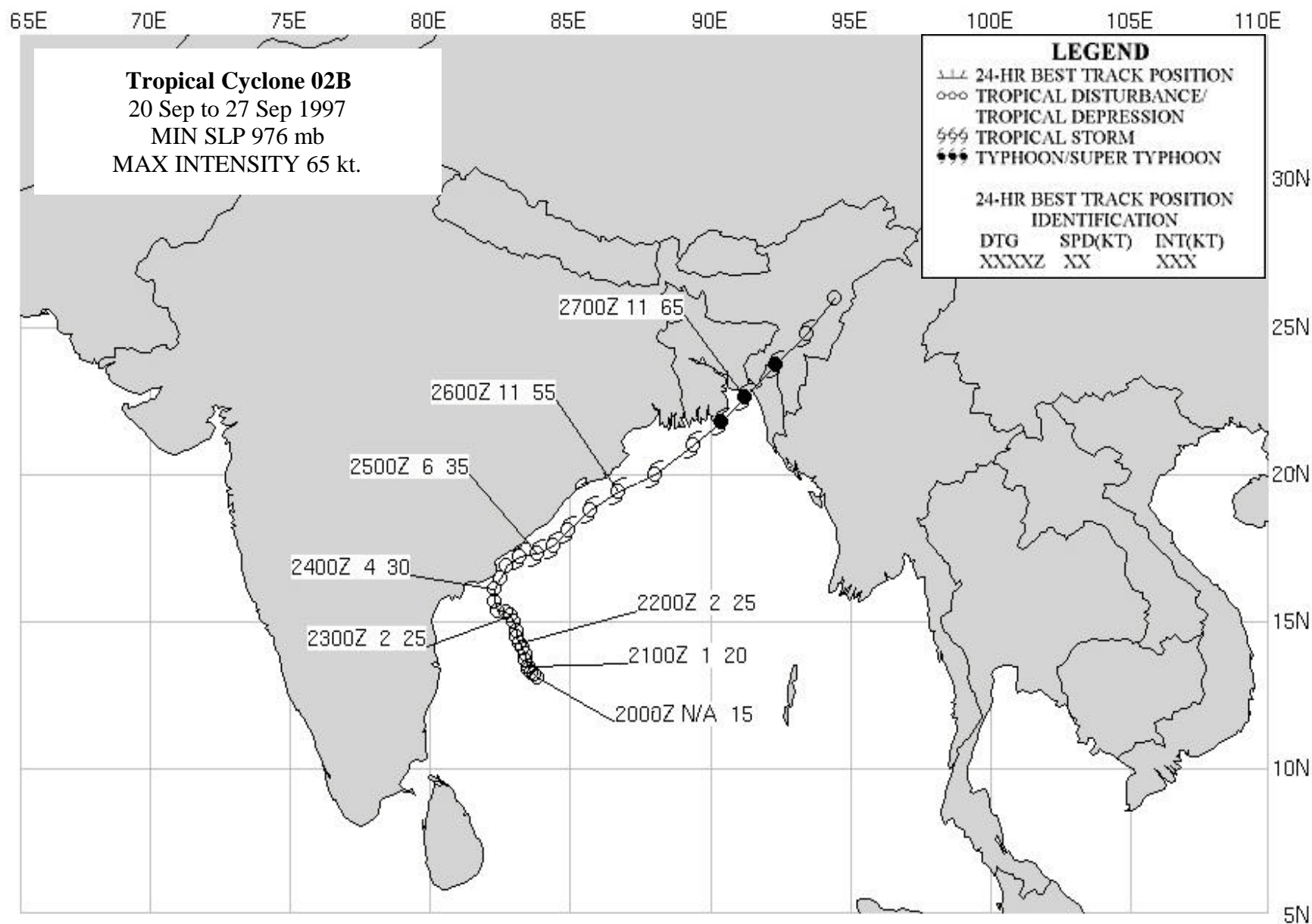


Figure 3-02B-1 Tropical Cyclone 02B as it skirts the eastern coast of India (242225Z September enhanced infrared GMS imagery).



TROPICAL CYCLONE 03A

The disturbance which became Tropical Cyclone (TC) 03A was first noted on the 07 November Significant Tropical Weather Advisory (ABIO) at 9N 54E. It was embedded within a widespread area of convection associated with broad troughing. The first warning was issued at 0600Z on 08 November. The system initially tracked northwestward at 6 kt (11 km/hr) towards the coast of Somalia with an intensity of 35 kt (18 m/sec). It maintained a 35 kt (18 m/sec) intensity over the next 18 hours despite the presence of moderate vertical wind shear as it approached the coast. By 0000Z on 09 November, TC 03A had made landfall over the northeast tip of Somalia. The partially exposed low-level center dissipated completely over land within the next 06 to 18 hours. No reports of damage were received by JTWC.

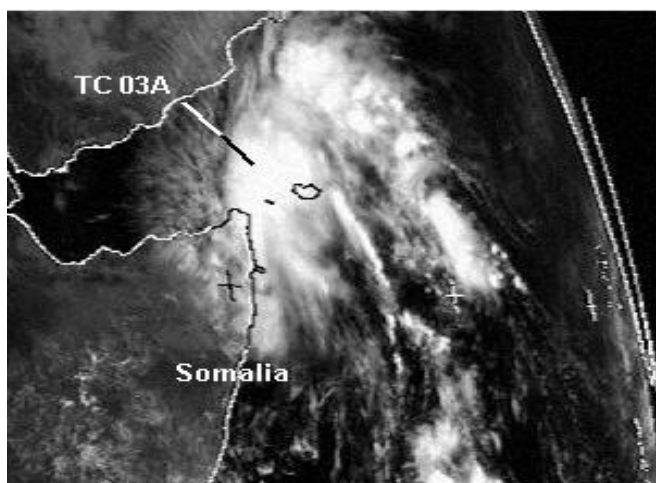
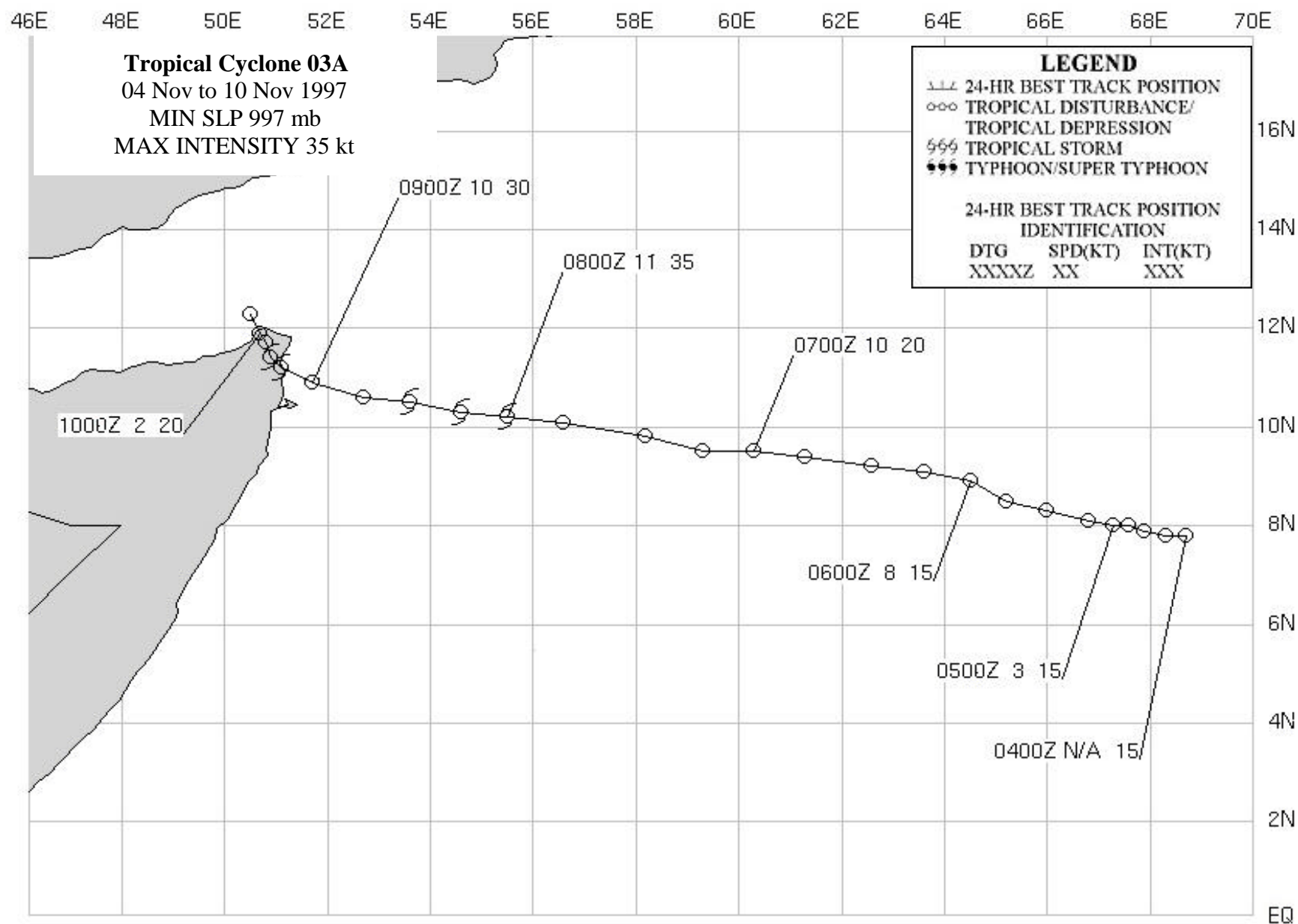


Figure 3-3A-1 TC 03A after reaching landfall (080830Z November visible Meteosat imagery).



TROPICAL CYCLONE 04A

Tropical Cyclone 04A started as a disturbance over Sri Lanka. It was first mentioned on the Indian Ocean Significant Tropical Weather Advisory (ABIO) at 1800Z on 6 November. Near 1200Z on the 7th, the circulation began moving to the north and then to the west over the lower tip of India. A Tropical Cyclone Formation Alert (TCFA) was issued at 1900Z on 9 November. The first warning was issued valid at 0000Z on 10 November. At 110600Z TC 04A reached its peak intensity of 55 kt (28 m/sec) while moving northwestward. It held this intensity for just over 24

hours, then began weakening under vertical wind shear. The remaining low-level circulation weakened, lost latitude, and dissipated over water. JTWC issued its final warning at 0000Z on the 14th. No reports of damage were received at JTWC.

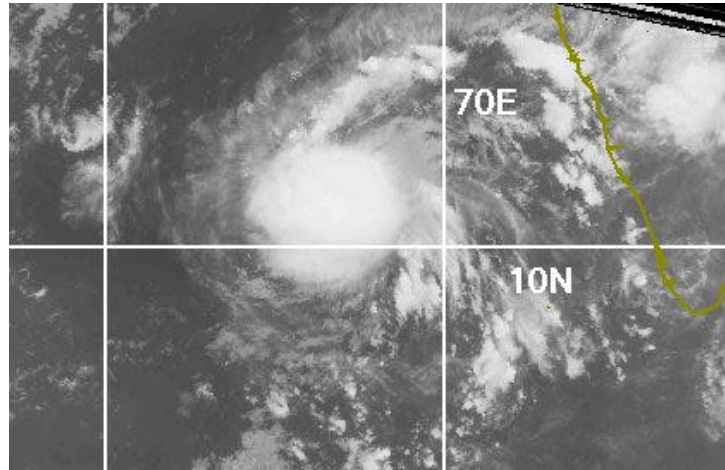


Figure 3-04A-1 Infrared imagery from 101200Z.

